



MONASH University

**FUNCTIONAL CHARACTERISATION OF
HEPATOCTE-LIKE CELLS GENERATED FROM
HUMAN AMNIOTIC EPITHELIAL CELLS**

Vijesh Vaghjiani

Supervisors: Professor Justin St. John and Dr. Ursula Manuelpillai

A thesis submitted in fulfilment of the requirement for the degree:

DOCTOR OF PHILOSOPHY

at the

Centre for Genetic Diseases

Hudson Institute of Medical Research

administered by

Monash University

2015

Copyright notice

© The author 2015. Except as provided in the Copyright Act 1968, this thesis may not be reproduced in any form without the written permission of the author. In particular no results or conclusions should be extracted from it, nor should be copied or closely paraphrased in whole or in part without the written consent of the author. Proper written acknowledgement should be made for any assistance obtained from this thesis.

Table of Contents

Acknowledgements.....	6
General Declaration.....	7
Abstract.....	8

Chapter 1.0 – Introduction, hypothesis and Aims

Declaration.....	11
Deriving Hepatocyte-like cells from placental cells for transplantation - <i>Current Stem Cell Research and Therapy</i>	12
Hypothesis and Aims.....	22

Chapter 2.0 – General Materials and Methods

2.1 Ethics Approval.....	24
2.2 Preparation of Growth factors and reagents	
2.2.1 Preparation of type I collagen.....	24
2.2.2 Collection of HepG2 conditioned media.....	24
2.2.3 Preparation of Epidermal Growth Factor.....	25
2.2.4 Preparation of Fibroblast Growth Factor-4.....	25
2.2.5 Preparation of Hepatocyte Growth Factor.....	25
2.2.6 Preparation of Dexamethasone.....	25
2.2.7 Preparation of 2'-3'-dideoxycytidine.....	26
2.2.8 Preparation of Uridine.....	26
2.3 Isolation of Human Amniotic Epithelial Cells.....	26
2.4 Differentiation of Hepatocyte-like cells.....	27
2.5 Extraction of Nucleic Acids	
2.5.1 RNA extraction.....	28
2.5.2 RNA quantification and purity.....	29

2.5.3 cDNA synthesis.....	29
2.5.4 Gene expression.....	30
2.5.5 DNA extraction.....	30
2.6 mtDNA copy number.....	31
2.7 Immunoprecipitation of methylated / hydroxymethylated DNA.....	32
2.8 Encapsulation of HLC and culture.....	33
2.9 Decapsulation.....	34
2.10 Statistical Analysis.....	34
Table 2.1 List of primers, conditions and product size for real-time PCR.....	36
2.11 References.....	37

Chapter 3.0 – Published Data

Declaration.....	39
Hepatocyte-Like Cells Derived from Human Amniotic Epithelial Cells Can be Encapsulated Without Loss of Viability or Function In Vitro – <i>Stem Cells and Development</i>	40

Chapter 4.0 – Role of Mitochondrial DNA Copy Number in Differentiation of Hepatocyte-Like Cells

4.1 Introduction.....	55
4.2 Materials and methods.....	61
4.3 Results.....	64
Table 4.1 Summary of expression levels from the glucose metabolism gene expression array.....	66
Table 4.2 Summary of expression levels from the mitochondrial metabolism gene expression array.....	69
Figure 4.1 MtDNA copy number and MeDIP in differentiated HLC.....	74
Figure 4.2 Gene expression of differentiated HLC.....	75
Figure 4.3 MtDNA copy number and MeDIP in HLC treated with 5-aza.....	77
Figure 4.4 Gene expression of differentiated HLC treated with 5-aza.....	78

Figure 4.5 MtDNA copy number and MeDIP in ddC depleted hAEC for 3 days and subsequent HLC differentiation.....	80
Figure 4.6 Gene expression of 3 day ddC depleted hAEC differentiated HLC for 7 and 14 days.....	81
Figure 4.7 MtDNA copy number and MeDIP in 7 day ddC depleted hAEC and differentiated HLC.....	83
Figure 4.8 Gene expression of 7 day ddC depleted hAEC differentiated HLC for 7 and 14 days.....	84
4.4 Discussion.....	86
4.5 References.....	94

Chapter 5.0 – Effects of Encapsulation on HLC mtDNA copy number, DNA methylation of POLGA and their transcriptomic profile

5.1 Introduction.....	103
5.2 Materials and Methods.....	107
5.3 Results	
5.3.1 MtDNA copy number and methylation of <i>POLGA</i> in encapsulated hAEC.....	110
Figure 5.1 Assessment of viability of encapsulated cells.....	111
Figure 5.2 MtDNA copy number and MeDIP of encapsulated cells.....	113
5.3.2 Changes in gene expression in differentiated HLC.....	114
Table 5.1 Top candidate differentially expressed genes in HLC compared to undifferentiated hAEC.....	115
Figure 5.3 ATM signalling pathway.....	116
Figure 5.4 Axonal guidance signalling pathway.....	118
Figure 5.5 Cell cycle control of the chromosomal replication pathway.....	119
Figure 5.6 Mitotic role of polo-like kinase pathway.....	120
Figure 5.7 Interferon signalling.....	121
Figure 5.8 Networks involved in differentiated HLC.....	124
Figure 5.9 Developmental and hepatic system development networks in HLC.....	125
Figure 5.10 The lipid, vitamin and mineral metabolism network in HLC.....	126
5.3.3 The effects of encapsulation on HLC differentiation and gene expression.....	127
Table 5.2 Top candidate genes differentially expressed in encapsulated HLC compared to undifferentiated hAEC.....	128

Figure 5.11	The Hepatic fibrosis and stellate cell activation pathway.....	130
Figure 5.12	The Mitotic role of polo-like kinase pathway.....	131
Figure 5.13	IL-1 mediated inhibition of RXR function.....	132
Figure 5.14	Top affected networks in encapsulated HLC.....	134
Figure 5.15	The developmental disorder and DNA replication and recombination networks in encapsulated HLC.....	135
Figure 5.16	Free radical scavenging and drug metabolism networks in encapsulated HLC.....	136
5.3.4	The effects of 3D HLC differentiation on gene expression.....	137
Table 5.3	Top candidate genes differentially expressed in encapsulated HLC compared to HLC.....	138
Figure 5.17	The interferon signalling pathway in encapsulated HLC.....	140
Figure 5.18	The pattern recognition pathway in encapsulated HLC.....	141
Figure 5.19	FXR/RXR activation in encapsulated HLC.....	142
Figure 5.20	Acute phase response pathway in encapsulated HLC.....	143
Figure 5.21	The organism injury and inflammatory response networks in encapsulated HLC.....	145
Figure 5.22	The organism development and cell signalling networks in encapsulated HLC.....	146
Figure 5.23	The cell death and survival and lipid metabolism networks in encapsulated HLC.....	147
5.4	Discussion.....	149
5.5	References.....	159

Chapter 6.0 – Summary, Implications and Future Perspectives

6.1	Summary.....	172
Figure 6.1	Summary of HLC differentiation compared to encapsulated HLC.....	177
6.2	Implications.....	178
6.3	Future Perspectives.....	180
6.4	References.....	182

Acknowledgements

I would first like to thank my PhD supervisors Professor Justin St. John and Dr. Ursula Manuelpillai for their help, guidance and support throughout my candidature. I have learnt much under their continued support and perseverance whilst I had to make changes to my thesis.

I would like to thank Professor Bernard Tuch and Dr. Vijay Vaithilingam at CSIRO, NSW for their tremendous help and expertise in encapsulation work. I would also like to thank staff and clinical nurses who helped collect placental tissue at odd hours of the day and night. In addition, I would like to thank staff and student at the Centre for Genetic Diseases. Particularly, Lynda Foulds for continual support in product ordering and general administrative support and Jacqui Johnson for laboratory support. Special mention goes to William Lee and Dr. Gael Cagnone for all their help in the lab in the initial stages and making this journey interesting. I would also like to acknowledge St. John lab members for thoughtful insights into mitochondrial genetics and interesting conversations. I would also like to acknowledge thought provoking questions from Dr. Patrick Western and Dr. Matthew McKenzie which inspired me to better address my thesis aims. I would also like to thank postdocs and students from the Centre for Genetic Diseases for their contribution to general discussions.

A special thank you also goes to Dr. Jason Cain and Samantha Jayasekara for help with injection of cells for tumour formation in mice.

I would also like to acknowledge generous Australian Postgraduate Award scholarship from the NHMRC.

A special thank you goes to my wife Priti, Mum, Dad, Harish Kaka, Ratan Kaki and my family. I would not have been able to complete my PhD without my wife Priti and brother Ashish for their continued love, support and encouragement. I would like to acknowledge their sacrifice to enable me to complete my PhD. I would also like to thank my friends and their partners for their continued support and keeping me sane.

I am sure there are many others to thank, and I will endeavour to do so at every opportunity.

Thanks,

Vijesh Vaghjiani

General Declaration

Monash University

Declaration for thesis based or partially based on conjointly published or unpublished work

In accordance with Monash University Doctorate Regulation 17.2 Doctor of Philosophy and Research Master's regulations the following declarations are made:

I hereby declare that this thesis contains no material which has been accepted for the award of any other degree or diploma at any university or equivalent institution and that, to the best of my knowledge and belief, this thesis contains no material previously published or written by another person, except where due reference is made in the text of the thesis.

This thesis includes 2 original papers published in peer reviewed journals and no unpublished publications. The core theme of the thesis is stem cells and differentiation. The ideas, development and writing up of all the papers in the thesis were the principal responsibility of myself, the candidate, working within the Centre for Genetic Diseases at Hudson Institute of Medical Research under the supervision of Professor Justin St. John.

In the case of Chapter 1 and Chapter 3 my contribution to the work involved the following:

Thesis Chapter	Publication title	Publication status	Nature and extent of candidate's contribution
1	Deriving Hepatocyte-like cells from placental cells for transplantation	Published	90% candidate contribution -authorship of publication 10% supervisory direction
3	Hepatocyte-Like Cells Derived from Human Amniotic Epithelial Cells Can be Encapsulated Without Loss of Viability or Function In Vitro	Published	90% candidate contribution -authorship of publication 10% supervisory direction

I have / have not (circle that which applies) renumbered sections of submitted or published papers in order to generate a consistent presentation within the thesis.

Signed:  Date: 12 May, 2016
Vijesh Vaghjani

Abstract

Chronic liver diseases and hepatocellular carcinoma are major global health burdens and liver transplantation is the only curative option currently available when these conditions become end stage liver diseases. Due to the severe shortage of suitable donor organs, hepatocyte transplantation is being trialled for patients with end stage disease as well as acute liver failure. However, obtaining sufficient numbers of human hepatocytes from liver re-sections, cadavers and aborted fetuses for transplantation is the principal limiting factor. Alternate sources of cells are being sought for transplant purposes, drug and toxicity screening, and seeding of bio-artificial liver devices. Human amniotic epithelial cells (hAEC) from term placenta are a good alternative source of stem cells to human hepatocytes.

In my studies, I show that differentiation of hAEC into hepatocyte like cells (HLC) results in expression of key hepatic transcription factors. Differentiated HLCs performed the hepatocytes functions including urea synthesis, drug metabolising cytochrome P450 (CYP)3A4 activity, indocyanine green(ICG) uptake, low-density lipoprotein (LDL) uptake and glutathione anti-oxidant capacity. A number of hepatocyte genes involved in fat, cholesterol, bile acid and xenobiotic metabolism were also expressed in the HLCs. When HLCs were encapsulated, they remained viable for 7 days *in-vitro* and continued to express genes involved in fat, cholesterol, bile acid and xenobiotic metabolism. Furthermore, encapsulated HLCs showed increased glutathione anti-oxidative capacity, CYP3A4 activity and urea synthesis

MtDNA copy did not increase with HLC differentiation, which, in turn, is marked by increased levels of DNA methylation at exon 2 of POLGA. Treatment with 5-azacytidine increased mtDNA copy number and reduced DNA methylation at exon 2 of POLGA compared to untreated controls. MtDNA depleted hAEC did not reconstitute their mtDNA copy number when they were allowed to recover for 7 and 14 days. The data were correlated with DNA methylation of POLGA at exon 2. Gene expression patterns indicated expression of some hepatocyte specific markers as well as pluripotency markers.

I performed RNAseq to evaluate the transcriptome profile of hAEC, HLC and encapsulated HLC. When I compared hAEC to HLC, I found 1722 differentially regulated genes, of which 695 genes were upregulated and 1027 genes down regulated. I performed network analysis of the differentially regulated genes and found that the top networks to be affected were cell cycle control and increased interferon signalling. When I compared hAEC to encapsulated HLC, I found 1325 differentially regulated genes with 705 genes upregulated and 620 genes down regulated. Analysis of HLC and

encapsulated HLC indicated 286 genes were differentially regulated of which 210 genes were upregulated and 76 genes were down regulated. Analysis of canonical pathway showed up regulation of FXR/RXR activation and down regulation of pattern recognition and interferon signalling. Network analysis exhibited increased cellular development, cellular movement and lipid metabolism. Overall, hAEC can be differentiated into functional HLC. However, hAEC are unable to synchronously modulate their mtDNA copy number during differentiation and become immunogenic. Encapsulation of HLC increases their functional capacity and reduces their inflammatory response, thus improved differentiation is achieved when HLC are encapsulated.

Chapter 1

Introduction, Hypothesis and Aims

Deriving Hepatocyte-like cells from placental cells for transplantation

Declaration for Thesis Chapter

Monash University

Declaration for Thesis Chapter 1

Declaration by candidate

In the case of Chapter 1, the nature and extent of my contribution to the work was the following:

Nature of contribution	Extent of contribution (%)
Authorship of publication	90%

The following co-authors contributed to the work. If co-authors are students at Monash University, the extent of their contribution in percentage terms must be stated:

Name	Nature of contribution	Extent of contribution (%) for student co-authors only
Dr Ursula Manuelpillai	Supervisory support, advice and editing	10%

The undersigned hereby certify that the above declaration correctly reflects the nature and extent of the candidate's and co-authors' contributions to this work.

Candidate's signature.....

..... **Date** 12 May 2016

Main supervisor's signature..

Date 12 May 2016



Deriving Hepatocyte-like Cells from Placental Cells for Transplantation

Vijesh Vaghjiani¹, Vijayaganapathy Vaithilingam², Bernard Tuch^{1,2}, William Sievert^{3,4} and Ursula Manuelpillai^{*1}

¹Centre for Reproduction & Development, Monash Institute of Medical Research, Monash University, Clayton, Victoria 3168, Australia; ²CSIRO Materials Science and Engineering, North Ryde, New South Wales 2113, Australia; ³Centre for Inflammatory Diseases, Department of Medicine, Monash University, Clayton, Victoria 3168, Australia; ⁴Gastroenterology and Hepatology Unit, Southern Health, Melbourne, Australia

Abstract: Human hepatocyte transplantation is being trialled *in lieu* of orthotopic liver transplants for patients with acute and chronic liver diseases. Stem cells that can be differentiated into hepatocyte-like cells may replace human hepatocytes that are difficult to source, culture and in critically short supply. Hepatocyte-like cells have been derived from embryonic and adult tissue stem cells using a combination of growth factors and chemical inducers. Stem cells derived from the human placenta have gained interest due to the unlimited supply of placental tissue, minimal issues associated with stem cell retrieval from placental tissue and the large yields of stem cells that can be obtained. Placental stem cells have been characterised and differentiated into hepatocyte-like cells. This review summarises the literature relating to the differentiation of human placental stem cells into hepatocyte-like cells, the characterisation of the differentiated cells, testing the functionality of the hepatocyte-like cells in pre-clinical animal models of liver disease and biomaterials used for culturing and transplantation of these cells into extra-hepatic sites.

Keywords: Amniotic epithelial cells, amniotic mesenchymal stromal cells, hepatocyte differentiation, hepatocyte characterisation, Wharton's Jelly mesenchymal stromal cells.

INTRODUCTION

The only currently available curative treatment for end stage liver disease arising from chronic exposure to viruses, excessive alcohol use, metabolic diseases and acute liver failure (ALF) is orthotopic liver transplantation. However, due to the severe shortage of suitable donor organs and the need for life-long immune suppression following transplantation, alternative therapies are being actively investigated. Human fetal and adult hepatocytes are being trialled to correct or compensate inherited metabolic disorders of the liver and to rescue patients with ALF [1-3]. In clinical trials, transplantation of adult hepatocytes has been reported to normalise serum albumin levels with short term clinical improvement of patients with ALF [1]. However, transplantation of human hepatocytes comes with its own challenges due to the limited supply of suitable livers for hepatocyte isolation, short term viability of the isolated hepatocytes in culture and constraints with cryopreservation.

Stem cells from different sources have been shown to differentiate into hepatocyte-like cells (HLC). Although there are concerns regarding the use of embryonic and induced pluripotent stem cells and subsequent formation of teratomas, mesenchymal stromal/stem cells (MSC) are less controversial and are being trialled clinically for a

variety of diseases [4]. MSC can be harvested from bone marrow (BM), adipose and other tissues such as dental pulp, endometrium and placenta. Harvesting BM-MSC is invasive and the quality and plasticity of these cells have been found to decline with increasing age of the donor [5]. Placental tissue is routinely discarded after birth and represents a good alternative source of MSC and also epithelial stem cells. This review summarises the differentiation and characterisation of HLC derived from placental stem cells and pre-clinical studies testing their efficacy.

PLACENTAL STEM CELLS

Placental stem cells have been isolated from the villous placenta, amniotic and chorionic fetal membranes, amniotic fluid and the umbilical cord (Fig. 1A). The types of stem cells sourced from the placenta include MSC, haematopoietic and epithelial stem cells.

PLACENTAL MSC

MSC are found in the villous placenta and other compartments and include amniotic membrane MSC (AM-MSC), chorionic membrane MSC (CM-MSC), amniotic fluid MSC (AF-MSC), umbilical cord blood MSC (UCB-MSC) and Wharton's Jelly MSC (WJ-MSC, Fig. 1B-C). Like adult bone marrow and adipose tissue derived MSC, placental MSC express CD73, CD90 and CD105 which is consistent with the criteria set by the International Society for Cellular Therapy to identify MSC [6]. Placental MSC express CD117, the c-kit receptor which has been reported to be absent in BM-MSC [7], although, Rebelatto *et al.*, re-

*Address correspondence to this author at the Monash Institute of Medical Research, Monash University, 27-31 Wright Street, Clayton, Victoria 3168, Australia; Tel: +61 3 9902-4803; Fax: +61 3 9594-7416; E-mail: ursula.manuelpillai@monash.edu

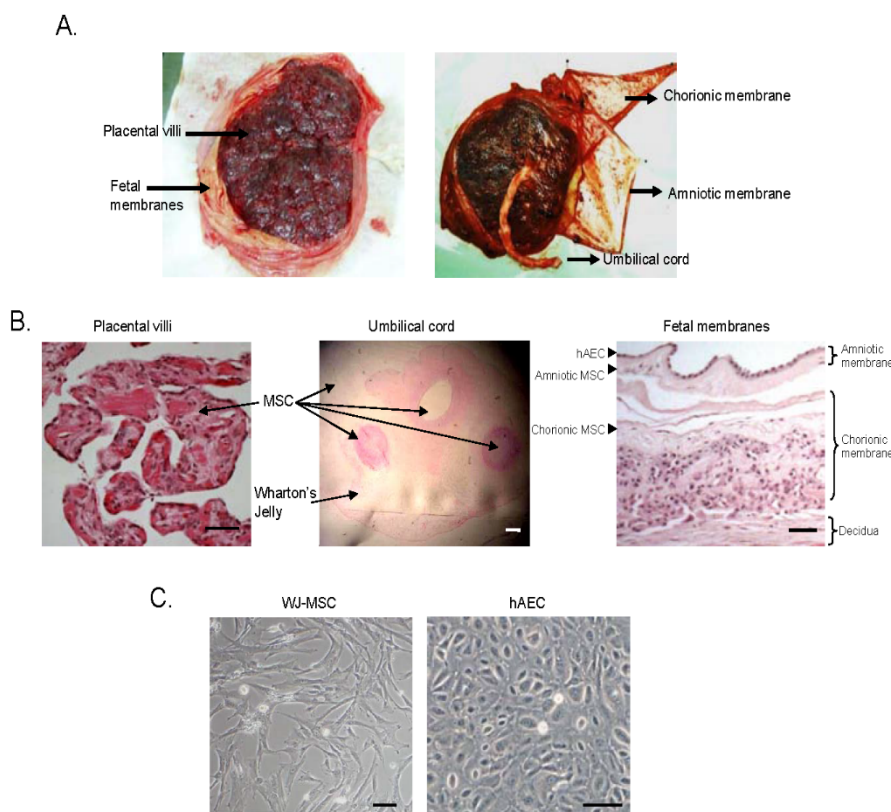


Fig. (1). (A) Term human placenta showing compartments that have been shown to harbour stem cell populations. (B) Cross section of the placental villi, fetal membranes and umbilical cord showing location of mesenchymal stromal/stem cells (MSC) and human amniotic epithelial cells (hAEC). (C) Wharton's Jelly MSC (WJ-MSC) and hAEC in culture. Scale bar = 100 μ m.

ported the presence of CD117 in BM-MSC [8]. Placental MSC express pluripotent stem cell associated markers SSEA-3, SSEA-4 and OCT-4, but the relative gene expression of these markers varies among MSC isolated from different placental compartments, gestational age of the placental tissue and isolation method [9, 10]. MSC isolated from the placenta conform to other defining criteria and adhere to plastic tissue culture plates, have a fibroblast-like appearance in culture and differentiate into adipocytes, chondrocytes and osteocytes *in vitro* [11-18]. These cells have also been reported to differentiate into ectodermal derived neurons and endodermal pancreatic and hepatic lineages [16, 19-23]. Differentiation into neuroectodermal and endodermal lineages may involve the process of de-differentiation. Like BM-MSC, placental MSC can be expanded up to 10 passages after which they undergo senescence [16]. However, WJ-MSC have been reported to expand up to 15 passages and maintain high levels of telomerase activity [24]. Other common and important features shared by both adult and placental MSC are the low level of HLA Class IA expression and absence of HLA Class II antigens and co-stimulatory molecules [23, 25-28] (Table 1). Therefore, placental MSC elicit a minimal proliferative response by peripheral blood mononuclear cells (PBMC) in mixed lymphocyte reactions *in vitro*. MSC from the placenta and BM secrete a number of immuno-modulatory substances including IL-10, HGF, HLA-G, PGE-2 and IL-6 [29-31]. The review by Anzalone *et al.*, [32] describes an extensive list of immuno-modulatory

factors that have been shown to be secreted by WJ-MSC and BM-MSC. Like their BM derived counterparts, low immunogenicity and immune modulation have facilitated transplantation of placental MSC both in xenogeneic and allogeneic settings and led to clinical trials for cardiomyopathy [33] and type-2 diabetes [34].

HUMAN AMNIOTIC EPITHELIAL CELLS (hAEC)

hAEC form a single layer of cells lining the amniotic membrane and are in continuous contact with the amniotic fluid during pregnancy (Fig. 1B-C). hAEC are fetal-derived cells and originate from the epiblast of the developing embryo 8-9 days post fertilization. Protocols have been developed to enzymatically digest the amniotic membrane and release the cells to yield about 150-200 million hAEC from each membrane [35, 36]. hAEC express typical epithelial markers, pluripotent stem cell markers and some CD antigens present in MSC (Table 1). Approximately 5-8% of hAEC express the pluripotent markers OCT-4 and SOX-2. SSEA proteins 3-4 are also expressed by hAEC [37, 38]. However, despite the expression of pluripotent markers hAEC do not form teratomas when grafted into immune deficient mice, unlike what occurs with embryonic stem cells [37, 38]. Differentiation of hAEC into different lineages derived from each of the primary germ layers has been reported *in vitro* including neurons (neuroectoderm); osteocytes, adipocytes, myocytes and cardiomyocytes (mesoderm) and hepatocyte and pancreatic-like cells (endoderm) [37, 38].

Table 1. Stem cell markers, cell surface antigens and other proteins present in placental mesenchymal stromal/stem cells (MSC) and human amniotic epithelial cells (hAEC).

	Markers*	Reference
Placental MSC	CD90+, CD73+ and CD105+ (MSC markers) CD13+, CD29+, CD166+, CD49d+, CD49e+, CD58+, CD44+ and CD117+ (other MSC markers) CD68+ (WJ-MSC) HLA-A+, -B+, -C+ (Class IA) and HLA-DR, -DP, -DQ negative- (Class II) CD34-, CD45- (haematopoietic) and CD31- (endothelial)	[9, 11-13, 16-19, 47, 76-78,79]
hAEC	CK-7+, CK-8/18+, EpCAM+, E-cadherin+ and CD49f+ (Epithelial markers) OCT-4+, SOX-2+, NANOG+, SSEA 1-4+ (Pluripotent stem cell markers) CD73+, CD105+ CD10+, CD13+, CD29+, CD49e+, CD117+, CD166+ (MSC markers) HLA-A+, -B+, -C+ (Class IA) and HLA-DQ, -DP, -DR negative (Class II) CD14-, CD45-, CD34- (haematopoietic), CD31- (endothelial) CD49d-, CD44- (adhesion molecules)	[12, 14, 16, 36-38, 80, 81]

*The percentage of positive cells is highly variable and depends on the gestational age of the placenta, isolation method and passage number.

The expression pattern of HLA Class IA, Class II and co-stimulatory molecules may make these cells less immunogenic while immuno-modulatory molecules secreted by hAEC enable these cells to modulate T cell and PBMC activity *in vitro* [10, 39-41].

IN VITRO DIFFERENTIATION OF PLACENTAL STEM CELLS INTO HLC

The immuno-modulatory properties of the placental stem cells together with their abundance, relative ease of access of placental tissue and minimal ethical constraints make placental stem cells an attractive source of cells for deriving HLC. A number of studies have investigated the differentiation of placental stem cells into HLC using protocols that vary from a single step cocktail of growth factors and hepatic inducers to multi step sequential exposure to growth factors and inducers. The overall aim has been to achieve rapid proliferation of stem cells followed by induction of hepatic progenitors and finally maturation and maintenance of HLC.

The most commonly used growth factors include epithelial growth factor (EGF), basic fibroblast growth factor (b-FGF), FGF-2 and FGF-4, bone morphogenetic protein-4 (BMP-4), hepatocyte growth factor (HGF) and oncostatin M. These growth factors have also been used to differentiate adult tissue derived stem cells into HLC. EGF and HGF induce proliferation [42], while FGF enriches for hepatic progenitors [43]. FGF, HGF and BMP-4 have been found to induce TGF- β family members which in turn induce hepatic progenitor genes such as FOX-A2, GATA-4, -6 and HHEX [42, 44]. Corticosteroids such as dexamethasone and hydrocortisone have been used to enhance hepatic gene induction and maturation of HLC [45] while oncostatin M has been found to suppress fetal liver function and induce tyrosine amino transferase (TAT) expression [46]. Table 2 lists the additives that have been used to differentiate placental stem cells into HLC.

Some of the placental MSC populations have been found to express genes present in hepatic progenitors suggesting that these cells would differentiate further along the hepatocyte lineage with stimulation. MSC from the amniotic mem-

brane, amniotic fluid and Wharton's Jelly express albumin, α -fetoprotein (α -FP) and cytokeratin (CK)-18 [27, 47]. Other genes expressed include alpha-antitrypsin (α 1-AT; AM-MSC and WJ-MSC); CK-19, tryptophan dioxygenase (TDO; WJ-MSC) and TAT and CCAAT enhancer binding protein (C/EBP; AF-MSC) [23, 28]. AM-MSC also express hepatocyte nuclear factor-4 α (HNF-4 α), a key transcription factor present in hepatic progenitors and mature cells [48].

HLC have been derived from both AM-MSC and WJ-MSC using single and multi-step protocols, respectively (Table 2). Although the supplements and duration needed for differentiation were variable, increased mRNA expression of α -FP, α 1-AT, CK-18, TAT, TDO and the drug metabolising enzyme CYP3A4 were found [25-27, 47]. Secretion of albumin and other key features such as glycogen storage, urea synthesis and uptake of low density lipoprotein (LDL) has also been reported [25-27, 48]. A single step protocol stimulating UCB-MSC with HGF and FGF-4 has demonstrated functional aspects of glycogen storage and LDL uptake [15, 49] while a two-step protocol reported HLC expressing albumin, TAT, α -FP, CK-18, HGF, proto-oncogene protein c-MET, phosphoenolpyruvate carboxykinase (PEPCK) and carbamoyl phosphate synthetase (CPS) [15, 49, 50]. Using a three-step protocol lasting 22-28 days, basal mRNA expression of albumin, α -FP, CK-18 and C/EBP α increased in AF-MSC and mRNA expression of mature hepatocyte markers HNF-1 α , CYP1A1 and HNF-4 α was initiated [20, 23, 28]. These and other studies outlined in Table 2 suggest that generating mature functional HLC may not necessarily require complex time consuming multi-step protocols. However, it would be important to examine the presence of HNF-4 α protein and transcriptional regulation of key hepatocyte genes such as CYP3A4 and ABCB1 by HNF-4 α in the HLC. Further, other important functional aspects such as drug metabolism by CYP enzymes, urea and bile salt secretion need to be investigated and compared with adult human hepatocytes.

As with placental MSC, hAEC express markers of endodermal lineage specification such as GATA-4 and HNF-3 β which suggests an intrinsic hepatic potential. GATA-4 and HNF-3 β bind to the enhancer region and activate albumin

Table 2. Differentiation of placental stem cells into hepatocyte-like cells.

Cell Type	Differentiation Protocol	Analysis	Reference
Placenta-derived multipotent cells	Plated on poly-L-lysine 60% DMEM-low glucose + 40% MCDB-201, 1x ITS, 4.7µg/ml linoleic acid, 1mg/ml BSA, 0.01µM dexamethasone, 0.1mM ascorbic acid, 10ng/ml EGF, 10ng/ml PDGF-BB, 20ng/ml HGF and 10ng/ml FGF-4 (28 days)	Albumin, α-FP and CYP3A4 mRNA LDL uptake, glycogen storage and human hepatocyte staining	[82]
AM-MSC	Plated on collagen I Alpha MEM + 10% FBS, 20ng/ml HGF, 10ng/ml FGF-2, 10ng/ml oncostatin M and 0.1mM dexamethasone (21 days)	Albumin, α-FP, CK-18, α1-AT and HNF4α by mRNA Albumin and α-FP protein and glycogen storage	[48]
WJ-MSC	Plated on collagen IV DMEM + 40% MCDB-201, 20ng/ml EGF, 10ng/ml b-FGF, 10ng/ml BMP4 (2 days) DMEM-LG + 40% MCDB-201, 2% FBS, 20ng/ml HGF, 10ng/ml b-FGF (7 days) DMEM-LG + 40% MCDB-201, 20ng/ml oncostatin M, 1µM dexamethasone and 1x ITS (7 days)	Albumin, HNF-1α, α1-AT and CYP3A4 mRNA Indocyanine green uptake	[25]
WJ-MSC	Iscove's modified DM + 1% FBS, 40ng/ml HGF and 10ng/ml FGF-4 (21 days)	Albumin, α-FP and CK-18 mRNA, ICC and Western blot Glycogen storage and LDL uptake	[26]
WJ-MSC	DMEM/F-12 + 50ng/ml HGF, 10ng/ml b-FGF, 10nM dexamethasone and 50mg/ml ITS (16 days) DMEM/F-12 + 20ng/ml oncostatin M, 1µM dexamethasone and 50mg/ml ITS (12 days)	Albumin, α-FP, CK-19, glucose-6-phosphatase and TDO mRNA LDL uptake, albumin secretion and urea synthesis	[27]
WJ-MSC	Plated on type I rat tail collagen DMEM-LG + 10% FBS, 20ng/ml EGF and 10ng/ml b-FGF (2 days) DMEM-LG + 10% FBS, 20ng/ml HGF, 10ng/ml b-FGF, 0.61g/L nicotine amide and 1% ITS (10 days) DMEM-LG + 10% FBS, 20ng/ml oncostatin M, 1µM dexamethasone and 1% ITS (10 days)	Albumin, α-FP, CK-18, CK-19, TAT and TDO mRNA CYP3A4 activity, urea synthesis and glycogen storage	[47]
AF-MSC	Plated on type I collagen gel Basal media: 60% DMEM + 40% MCDB-201, 2% FBS, 1mg/ml linoleic acid, 0.1mM L-ascorbic acid, 0.03mM nicotinamide, 0.25mM sodium pyruvate and 1.623mM glutamine Basal media + 10ng/ml FGF-4 (2 days) Basal media + 20ng/ml HGF (3 days) Basal media + 20ng/ml HGF, 1x ITS, 20µg/L dexamethasone and 1µM trichostatin A (23 days)	Albumin, α-FP, CK-18, HNF1α, C/EBPα and CYP1A1 mRNA Albumin, α-FP, CK-18, HNF1α, C/EBPα and CYP1A1 ICC Glycogen storage and urea synthesis	[28]
AF-MSC	Plated on fibronectin RPMI 1640 + 1% FBS, 1% DMSO and 10ng/ml EGF (2 days) RPMI 1640 + 10% FBS, 20ng/ml FGF-4 and 10ng/ml b-FGF (2 days) RPMI 1640 + 10% FBS and 30ng/ml HGF (8 days) RPMI 1640 + 10% FBS, 30ng/ml HGF, 1x ITS, 1µM dexamethasone and 10ng/ml oncostatin M (10 days)	Albumin, α-FP, CYP1B, CK-18 and HNF-4α mRNA Albumin and α-FP ICC Indocyanine green uptake and albumin secretion	[20]
AF-MSC	IMDM + 20ng/ml EGF and 10ng/ml b-FGF (2 days) IMDM + 20ng/ml HGF, 10ng/ml b-FGF and 0.1% DMSO (7 days) IMDM + 20ng/ml oncostatin M, 1µM dexamethasone and 50µg/ml ITS (14 days)	CK-7, CK-19, α-FP, TAT and albumin mRNA Glycogen storage, LDL uptake and urea synthesis	[23]
UCB-MSC	Plated on gelatine coated dishes DMEM + 15% FBS, 20ng/ml FGF-1, 10ng/ml FGF-2, 10ng/ml LIF, 10ng/ml SCF, 10ng/ml HGF and 10ng/ml oncostatin M (21 days)	Albumin, α-FP, GS and CK-18 mRNA Albumin, CK-18, CK-19 and PCNA ICC	[50]

Table 2. Contd....

Cell Type	Differentiation Protocol	Analysis	Reference
UCB-MSC	IMDM + 10% FBS, 20ng/ml HGF and 10ng/ml FGF-4 (28 days)	Albumin, α -FP and CK-18 mRNA Albumin and α -FP by radioimmunoassay Glycogen storage and urea synthesis	[15]
UCB-MSC	IMDM + 10% FBS, 0.5 μ M dexamethasone, 50mg/ml ITS and 50ng/ml HGF (14 days) IMDM + 10% FBS, 0.5 μ M dexamethasone, 50mg/ml ITS and 50ng/ml oncostatin M (14 days)	Albumin, α -FP, CK-18, GS, TAT, HGF, c-MET, PEPCK and CPS by mRNA Albumin, α -FP, CK-18 and CK-19 by Western blot and ICC LDL uptake	[49]
hAEC	Plated on collagen type IV DMEM/F-12 + 10% FBS, 0.1 μ M insulin and 0.1 μ M dexamethasone (28 days)	Albumin and HGF by ICC and FACS Electron microscopy	[37]
hAEC	Plated on collagen type I DMEM + 10% FBS, 20ng/ml HGF, 10ng/ml FGF-2 (with 10U/ml heparin sodium salt), 10ng/ml oncostatin M and 100nM dexamethasone (14 days)	Albumin, α -FP, α 1-AT, TTR, CK-18, GS, CPS-I, PEPCK, TAT, CYP2C9, CYP2D6 and CYP3A4 mRNA Albumin ICC, Albumin secretion and glycogen storage	[52]
hAEC	Plated on type I collagen DMEM + 10% FBS, 55 μ M 2-mercaptoethanol, 1mM sodium pyruvate, 10ng/ml EGF, 0.1 μ M dexamethasone and 0.1 μ M insulin (1mM phenobarbital for last 3 days) (21 days)	Albumin and α 1-AT mRNA Albumin and HNF-4 α ICC CYP1A1/2 activity	[38]
hAEC	Plated on type I collagen DMEM + 10% FBS and 10ng/ml EGF (2days) IMDM + 0.5% human albumin and 100ng/ml activin-A (3 days) IMDM + 10% FBS, 10ng/ml EGF and 0.1 μ M dexamethasone (20 days)	HNF-4 α , α 1-AT, albumin, C/EBP- α , CK-8, CK-18, CK-19, C-met, OATR, PXR, CAR, RAR, RXR, PRAR, CYP1A2, CYP2B6, CYP2C8, CYP2C9, CYP2C19, CYP2D6, CYP3A4, CYP3A7 and CYP7A1 mRNA	[45]
hAEC	DMEM + 10% FBS, 10ng/ml EGF (3 days) +/- 100ng/ml activin A pre-treatment 48 hr IMDM + 5% FBS, 10ng/ml EGF, 10ng/ml FGF-2, 10ng/ml HGF and 1 μ M dexamethasone (28 days) hAEC grown on mouse hepatocytes in IMDM + 5% FBS, 10ng/ml EGF and 1 μ M dexamethasone (2 days) Mouse hepatocyte + hAEC in MGM, 5% FBS, 10ng/ml EGF and 0.1 μ M dexamethasone (16 days) hAEC sandwiched in porcine liver-derived extracellular matrix or matrigel IMDM + 10% FBS, 10ng/ml EGF and 10ng/ml FGF-2 (2 days) IMDM + 10% FBS, 10ng/ml EGF, 10ng/ml FGF-2, 20ng/ml HGF, 1 μ M dexamethasone and 1x ITS (5 days) IMDM + 10% FBS, 10ng/ml EGF, 20ng/ml oncostatin M, 20ng/ml HGF, 1 μ M dexamethasone and 1x ITS (7 days)	Albumin, CYP3A4, CYP3A7, CYP2B6, OTC, α 1-AT and UGT1A1 mRNA Albumin, CYP3A4, CYP1A2, CYP2B6 and α 1-AT mRNA Testosterone metabolism Albumin, α 1-AT, CYP3A4, CYP3A7, CYP1A2, CYP2B6 and asialoglycoprotein receptor 1 by mRNA Urea synthesis and testosterone metabolism	[53] [53] [53]

transcription, which may explain the presence of albumin protein in undifferentiated hAEC [51]. Undifferentiated hAEC also express mRNA of genes which are present in hepatocytes including α 1-AT, CK-18, CPS-1 and PEPCK at basal levels [52]. Initial studies utilised a single step protocol with insulin/dexamethasone alone or in combination with FGF-2 and oncostatin M for periods of 14-28 days with hAEC being grown on a collagen matrix. The differentiated HLC showed increased gene expression of α 1-AT, CK-18, CPS-1, CYP3A4 and PEPCK and importantly increased HNF-4 α and CYP1A1 protein [38, 52].

A recent study found that culturing hAEC on mouse hepatocytes, matrigel or porcine liver derived extra-cellular matrix augmented the differentiation of hAEC into HLC [53] (Table 2). Marongiu *et al.*, showed increased mRNA expres-

sion of albumin and several CYP genes with porcine liver derived extra-cellular matrix being the most effective. The HLC had the functional fetal isoform CYP3A7 but CYP3A4 mRNA expression was not induced by phenobarbital unlike in adult hepatocytes [45, 53]. Interestingly, human hepatocytes grown on a biomimetic hydrogel (simulating liver extracellular matrix) containing type I collagen and hyaluronic acid have shown improved cell survival and function [54]. Culturing human hepatocytes on artificial and biological matrices and under 3 dimensional culture conditions including sandwich cultures has been shown to significantly augment the function and viability of these cells [53]. The matrices include poly N-p-vinylbenzyl-4-O- β -D-galactopyranosyl-D-gluconamide (PVLA), E-cadherin-IgG Fc (E-cad-Fc) and poly-L-lactic acid [55, 56]. Thus, it would

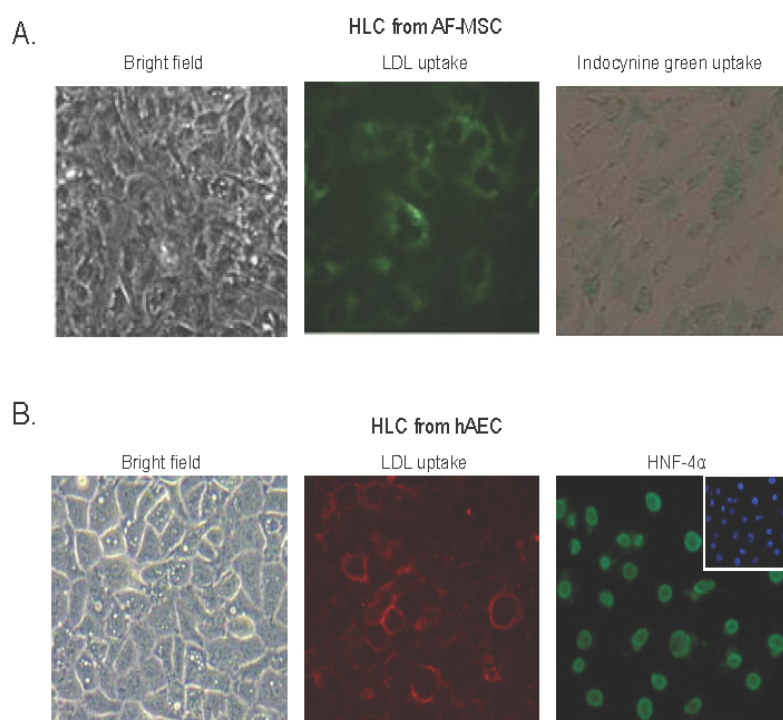


Fig. (2). (A) Hepatocyte-like cells (HLC) derived from amniotic fluid mesenchymal stromal/stem cells (AF-MSC) and (B) from human amniotic epithelial cells (hAEC). Low density lipoprotein (LDL) uptake demonstrates a functional feature of hepatocytes. Indocyanine green is a dye taken up specifically by hepatocytes. Hepatocyte nuclear factor-4 α (HNF-4 α), a key transcription factor is present in nuclei of HLC derived from hAEC; insert shows cell nuclei stained with DAPI. Magnification = 200x. AF-MSC from Zagoura *et al.*, [23] and Liu *et al.*, [20]. (For interpretation of the references to color in this figure legend, the reader is referred to the web version of this paper).

be important to differentiate and / or culture the HLC derived from placental cells under these conditions using materials compatible with clinical usage.

IN VIVO DIFFERENTIATION INTO HLC

Although placental stem cells were successfully differentiated into HLC *in vitro*, only few studies have investigated the ability of placental stem cells to differentiate into HLC *in vivo* or if the differentiated HLC could be transplanted. Undifferentiated placental stem cells have been transplanted to determine whether cues from the micro environment of the graft site would direct differentiation towards HLC and augment hepatic function. Human UCB-MSC have been tested in two models of liver disease. The fulminant hepatic failure (FHF) model induced by intraperitoneal injection of D-galactosamine and lipopolysaccharide is characterised by severe impairment of synthetic function and the development of hepatic encephalopathy. Half a million UCB-MSC were injected into the tail vein of 4-8 week old male SCID mice and monitored for up to four weeks [57]. In the Fas receptor mediated hepatocyte apoptosis and necrosis model, Nonome *et al.*, injected 5×10^4 CD34+ or CD34- UCB-MSC *via* the tail vein into SCID mice [58]. Although human MSC are thought to lack CD34, this group described a CD34+ population in UCB-MSC. The rationale for using CD34+/- cells was to examine which sub-population would engraft better in the diseased liver. These studies using UCB-MSC reported a significant improvement in liver function with reduction in serum alanine aminotransferase (ALT). The transplanted

UCB-MSC were positive for human α -FP and albumin after 4 weeks suggesting that the transplanted cells had differentiated into a mixture of mature and immature hepatocytes; α -FP being a marker of immature and albumin a mature hepatocyte marker. However, engrafted cells were <1% of the total hepatocyte population and sub-fractions of CD34+/- cells did not show significant differences in engraftment.

In vivo differentiation into HLC has also been observed with human AM-MSC following injection of the hepatotoxin carbon tetrachloride to induce hepatocyte apoptosis and necrosis in C57BL/6J mice [59]. Collectively, as these studies report that only a small number of infused cells were present in the liver. Strategies to improve engraftment such as over expression of migration and adhesion molecules or cytokines like tumor necrosis factor- α (TNF- α) and interleukin-6 (IL-6) should be tested [60]. Administration of TNF- α and IL-6 is thought to increase micro-vascular permeability and cause endothelial disruption to allow better access into the liver parenchyma [61]. However, TNF- α and IL-6 could increase inflammation and further damage the endogenous hepatocytes. In a study evaluating engraftment and differentiation Campard *et al.*, transplanted 3×10^6 WJ-MSC into SCID mice with ALF induced by partial hepatectomy [47]. WJ-MSC were injected into the spleen to test for direct and maximum engraftment in the liver. The WJ-MSC engrafted in the liver and were positive for α -FP and human albumin, indicating that the transplanted cells had acquired features of hepatocytes. However, whether the intra-splenic route increased engraftment compared to tail vein infusion was not reported

[47]. In contrast, WJ-MSC transplanted in a rat carbon tetrachloride model of liver fibrosis remained undifferentiated [62]. Differences in the differentiation of WJ-MSC into HLC may be due to differences between mice and rodents as well as differences within the liver in the different disease models.

Undifferentiated hAEC have some features of hepatocytes expressing α -FP and albumin but lack HNF-4 α [52]. In a recent study testing the anti-inflammatory and anti-fibrotic properties, we transplanted hAEC *via* the tail vein into C57BL/6 mice with fibrosis induced by carbon tetrachloride [63]. In addition to localising albumin positive hAEC in the liver, some of the hAEC expressed HNF-4 α , a mature hepatocyte marker, thus showing evidence of differentiation by hAEC into HLC. hAEC have also been transplanted *via* the spleen (0.5×10^6 cells) in the retrorsine model of liver repopulation with 60% partial hepatectomy. After 6 months, DNA-PCR for human Alu repeats showed approximately 0.1 - 1% human cells in the liver [53]. Using human specific primers, hAEC were found to express mRNA of mature hepatocyte markers such as cytochrome P450 CYP enzymes, UGT (transport of amino acids), GGT (drug detoxification and glutathione metabolism), albumin, HNF-4 α and membrane transporter proteins MRP2 and BSEP. Despite mRNA expression of these markers, there are no data to support functionality of the hAEC and indeed other placental MSC that have been infused. Improved delivery, cell engraftment and functionality will need to be established for hAEC and other placental stem cells prior to their clinical use. To do this, the cells could be retrieved from the liver and functional assays for drug metabolism, albumin secretion and urea metabolism could be tested and compared with mature human hepatocytes to verify that the placental cells have differentiated into functional HLC.

TRANSPLANTATION OF *IN VITRO* DIFFERENTIATED HLC

Transplantation of human adult and fetal hepatocytes has been trialled clinically [1-3], but few studies have examined the transplantation of *in vitro* differentiated placental stem cells with functional characteristics of HLC. A study by Zagoura *et al.*, evaluated engraftment of HLC and rescue of mice in the carbon tetrachloride model of ALF [23]. Human AF-MSC were injected as undifferentiated, partially differentiated hepatic progenitor (low LDL uptake, α -FP expression) or fully differentiated cells (glycogen storage, urea synthesis and high LDL uptake). The hepatic progenitors showed significant engraftment and rescued mice from ALF; whereas the differentiated cells were unable to engraft in the liver [23]. Interestingly, human fetal liver progenitors have shown better engraftment compared to mature hepatocytes in rats with ALF [64, 65]. In contrast, a study using urokinase plasminogen expressed under the albumin promoter which causes post-natal toxic liver injury in SCID mice showed that mature human hepatocytes repopulate liver far better than fetal hepatocytes [66]. Differences in engraftment could be due to cell-to-cell or cell-to-matrix interactions between partially differentiated / mature cells and endogenous liver cells and differences between the disease models. The native extracellular matrix has been found to be critical for hepatocyte engraftment and function. Further, it has been shown

that priming the diseased liver with HGF can make it more receptive to cell transplantation by disrupting tight junction protein complexes [67].

EXTRA HEPATIC TRANSPLANTATION OF HLC

While it is important to overcome the constraints associated with engraftment of mature HLC in the liver, it has been shown that hepatocytes can be transplanted into extra hepatic sites, such as beneath the renal capsule and still retain their function, provided supporting cells such as islets are also present [68]. Use of such extra hepatic sites with HLC may be important to overcome cell engraftment issues within the liver. In addition to low engraftment of undifferentiated and differentiated HLC, preventing immune rejection remains a major obstacle in cell transplantation. Although clinical studies suggest that allogeneic MSC may be tolerated the immunogenicity of cells has been shown to alter with differentiated cells relatively being more immunogenic than undifferentiated cells. Cell encapsulation in biocompatible microspheres is a strategy that may enable the delivery of large numbers of HLC needed to support liver function and avoidance of cellular and antibody mediated rejection of allogeneic HLC. Microcapsules made from alginate, chitosan, agarose and poly-ethylene glycol (PEG) have been utilized for cell encapsulation with capsule sizes ranging between 100-1000 μ m in diameter. The capsule membrane is porous and allows the entry of small molecules and oxygen diffusion but not large immunoglobulins [69]. Studies have shown that embryonic stem cells can be differentiated in poly-L-lysine microcapsules and that the 3 dimensional environment created within the capsule augments differentiation and function of HLC [70]. Although Penolazzi *et al.*, did not seek to differentiate WJ-MSC into HLC, surface CD antigen expression showed no change while secretion of macrophage migration inhibitory factor (MIF) and HGF increased in encapsulated WJ-MSC relative to monolayer cultures suggesting that encapsulation was not deleterious [71]. Importantly, growth factors can be incorporated into the capsular material that could direct differentiation of placental stem cells towards HLC. Thus, the differentiation of encapsulated placental stem cells into HLC may be worth investigating as a strategy to provide functional hepatocyte support in acute and chronic liver disease.

Others have shown that hepatocytes can be encapsulated and that large numbers of capsules can be grafted extra-hepatically into the peritoneal cavity and that these encapsulated cells can rescue animal models of ALF [72, 73]. Based on such studies, CD34+ umbilical cord blood mononuclear cells were initially differentiated into HLC expressing albumin, α -FP and GATA-4 mRNA. The HLC were then encapsulated and transplanted intraperitoneally into rats with ALF induced by D-galactosamine. The encapsulated HLC rescued rats with ALF that showed reduced aspartate aminotransferase, ALT and total bilirubin levels and improved survival compared to untreated controls [74]. In a preliminary study we have encapsulated HLC derived from hAEC and found that these cells remain viable (Fig. 3). A recent study found that co-encapsulation of human hepatocytes with mouse fibroblasts or liver endothelial cells in PEG-DA scaffolds enhanced the functionality of the hepatocytes [75]. Augmentation by fibroblasts may be due to the secretion of extracellu-

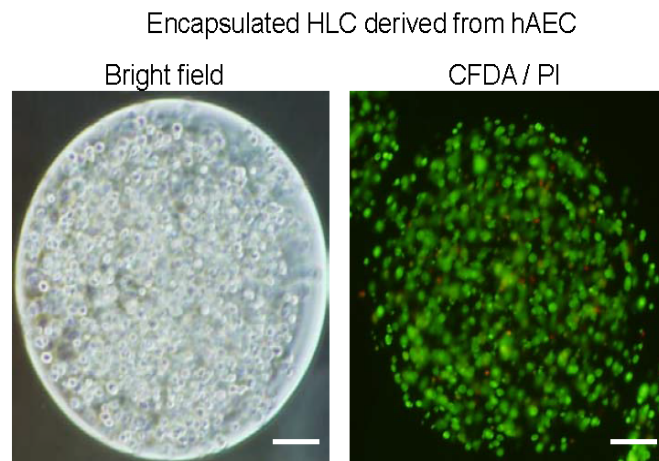


Fig. (3). Human amniotic epithelial cell (hAEC) derived hepatocyte-like cells (HLC) encapsulated in barium alginate micro-capsules (left panel). Capsules were cultured for 10 days and stained with 6-carboxyfluorescein diacetate (CFDA) and propidium iodide (PI). Viable cells stained green and dead cells stained red. Scale bars = 100 μ m. (For interpretation of the references to color in this figure legend, the reader is referred to the web version of this paper).

lar matrix that enhances hepatocyte function while endothelial cells may allow the encapsulated cells to adapt to the oxygen level in the capsules. Similar studies could be conducted with placental stem cells given that when hAEC were cultured on porcine liver extra cellular matrix, functional HLC were produced at least *in vitro* [53]. While these strategies appear to be promising, the short comings include an inflammatory response by the recipient leading to fibrosis around the capsules and scaffolds which in turn reduces oxygenation and increases necrosis of the encapsulated cells. In the case of microcapsules as they are too large to enter the capillary vasculature it would be feasible to retrieve the capsules from the peritoneum, if placed at single site, for example an omental pouch, and replenished with fresh encapsulated HLC. Thus, such strategies should be more widely explored with HLC derived from placental stem cells.

CONCLUSION

In summary although at an early stage, studies demonstrating the differentiation of placental stem cells into HLC show promise as an alternative to primary human hepatocytes. More stringent functional analyses for transporter proteins, metabolism of drugs, fat, cholesterol, glucose, urea synthesis and secretion of bile acids and albumin need to be carried out to determine how closely the HLC resemble mature human hepatocytes. Whether placental stem cells have better potential for *in vitro* derivation of HLC for transplantation rather than differentiation *in vivo* and efficacy of extra-hepatic vs hepatic transplantation needs to be investigated to determine the true clinical potential of HLC derived from placental stem cells.

CONFLICT OF INTEREST

The authors confirm that this article content has no conflicts of interest.

ACKNOWLEDGEMENTS

UM and WS supported by Australian National Health & Medical Research Council Project Grant #606473. Vijesh

Vaghjiani and UM supported by the Victorian Government's Operational Infrastructure Support Program.

REFERENCES

- [1] Bilir BM, Guinette D, Karrer F, *et al.* Hepatocyte transplantation in acute liver failure. *Liver Transpl* 2000; 6(1): 32-40.
- [2] Horslen SP, McCowan TC, Goertzen TC, *et al.* Isolated hepatocyte transplantation in an infant with a severe urea cycle disorder. *Pediatrics* 2003; 111(6 Pt 1): 1262-7.
- [3] Strom SC, Chowdhury JR, Fox IJ. Hepatocyte transplantation for the treatment of human disease. *Semin Liver Dis* 1999; 19(1): 39-48.
- [4] Connick P, Kolappan M, Patani R, *et al.* The mesenchymal stem cells in multiple sclerosis (MSCIMS) trial protocol and baseline cohort characteristics: an open-label pre-test: post-test study with blinded outcome assessments. *Trials* 2011; 12: 62.
- [5] Stolzing A, Jones E, McGonagle D, Scutt A. Age-related changes in human bone marrow-derived mesenchymal stem cells: consequences for cell therapies. *Mech Ageing Dev* 2008; 129(3): 163-73.
- [6] Dominici M, Le Blanc K, Mueller I, *et al.* Minimal criteria for defining multipotent mesenchymal stromal cells. The International Society for Cellular Therapy position statement. *Cytotherapy* 2006; 8(4): 315-7.
- [7] Lee RH, Kim B, Choi I, *et al.* Characterization and expression analysis of mesenchymal stem cells from human bone marrow and adipose tissue. *Cell Physiol Biochem* 2004; 14(4-6): 311-24.
- [8] Rebelatto CK, Aguiar AM, Moretao MP, *et al.* Dissimilar differentiation of mesenchymal stem cells from bone marrow, umbilical cord blood, and adipose tissue. *Exp Biol Med (Maywood)* 2008; 233(7): 901-13.
- [9] Soncini M, Vertua E, Gibelli L, *et al.* Isolation and characterization of mesenchymal cells from human fetal membranes. *J Tissue Eng Regen Med* 2007; 1(4): 296-305.
- [10] Wolbank S, Peterbauer A, Fahrner M, *et al.* Dose-dependent immunomodulatory effect of human stem cells from amniotic membrane: a comparison with human mesenchymal stem cells from adipose tissue. *Tissue Eng* 2007; 13(6): 1173-83.
- [11] Bailo M, Soncini M, Vertua E, *et al.* Engraftment potential of human amnion and chorion cells derived from term placenta. *Transplantation* 2004; 78(10): 1439-48.
- [12] Bilic G, Zeisberger SM, Mallik AS, Zimmermann R, Zisch AH. Comparative characterization of cultured human term amnion epithelial and mesenchymal stromal cells for application in cell therapy. *Cell Transplant* 2008; 17(8): 955-68.
- [13] De Coppi P, Bartsch G, Jr., Siddiqui MM, *et al.* Isolation of amniotic stem cell lines with potential for therapy. *Nat Biotechnol* 2007; 25(1): 100-6.

- [14] Diaz-Prado S, Muinos-Lopez E, Hermida-Gomez T, *et al.* Multi-lineage differentiation potential of cells isolated from the human amniotic membrane. *J Cell Biochem* 2010 Nov 1; 111(4): 846-57.
- [15] Kang XQ, Zang WJ, Bao LJ, Li DL, Xu XL, Yu XJ. Differentiating characterization of human umbilical cord blood-derived mesenchymal stem cells *in vitro*. *Cell Biol Int* 2006; 30(7): 569-75.
- [16] Parolini O, Alviano F, Bagnara GP, *et al.* Concise review: isolation and characterization of cells from human term placenta: outcome of the first international Workshop on Placenta Derived Stem Cells. *Stem Cells* 2008; 26(2): 300-11.
- [17] Roubelakis MG, Bitsika V, Zagoura D, *et al.* *In vitro* and *in vivo* properties of distinct populations of amniotic fluid mesenchymal progenitor cells. *J Cell Mol Med* 2011; 15(9): 1896-913.
- [18] Tsai MS, Lee JL, Chang YJ, Hwang SM. Isolation of human multipotent mesenchymal stem cells from second-trimester amniotic fluid using a novel two-stage culture protocol. *Hum Reprod* 2004; 19(6): 1450-6.
- [19] Diaz-Prado S, Muinos-Lopez E, Hermida-Gomez T, *et al.* Isolation and Characterization of Mesenchymal Stem Cells from Human Amniotic Membrane. *Tissue Eng Part C Methods*. 2010 Aug 30. [Epub ahead of print]
- [20] Liu H, Liu DQ, Li BW, *et al.* Human amniotic fluid-derived stem cells can differentiate into hepatocyte-like cells *in vitro* and *in vivo*. *In vitro Cell Dev Biol Anim* 2011; 47(9): 601-8.
- [21] Portmann-Lanz CB, Schoeberlein A, Huber A, *et al.* Placental mesenchymal stem cells as potential autologous graft for pre- and perinatal neuroregeneration. *Am J Obstet Gynecol*. 2006; 194(3): 664-73.
- [22] Wei JP, Zhang TS, Kawa S, *et al.* Human amnion-isolated cells normalize blood glucose in streptozotocin-induced diabetic mice. *Cell Transplant* 2003; 12(5): 545-52.
- [23] Zagoura DS, Roubelakis MG, Bitsika V, *et al.* Therapeutic potential of a distinct population of human amniotic fluid mesenchymal stem cells and their secreted molecules in mice with acute hepatic failure. *Gut* 2012; 61(6): 894-906.
- [24] La Rocca G, Anzalone R, Corrao S, *et al.* Isolation and characterization of Oct-4+/HLA-G+ mesenchymal stem cells from human umbilical cord matrix: differentiation potential and detection of new markers. *Histochem Cell Biol* 2009; 131(2): 267-82.
- [25] Kim MJ, Shin KS, Jeon JH, *et al.* Human chorionic-plate-derived mesenchymal stem cells and Wharton's jelly-derived mesenchymal stem cells: a comparative analysis of their potential as placenta-derived stem cells. *Cell Tissue Res* 2011; 346(1): 53-64.
- [26] Zhang YN, Lie PC, Wei X. Differentiation of mesenchymal stromal cells derived from umbilical cord Wharton's jelly into hepatocyte-like cells. *Cytotherapy* 2009; 11(5): 548-58.
- [27] Zhao Q, Ren H, Li X, *et al.* Differentiation of human umbilical cord mesenchymal stromal cells into low immunogenic hepatocyte-like cells. *Cytotherapy* 2009; 11(4): 414-26.
- [28] Zheng YB, Gao ZL, Xie C, *et al.* Characterization and hepatogenic differentiation of mesenchymal stem cells from human amniotic fluid and human bone marrow: a comparative study. *Cell Biol Int* 2008; 32(11): 1439-48.
- [29] Nasef A, Mathieu N, Chapel A, *et al.* Immunosuppressive effects of mesenchymal stem cells: involvement of HLA-G. *Transplantation* 2007; 84(2): 231-7.
- [30] Siegel G, Schafer R, Dazzi F. The immunosuppressive properties of mesenchymal stem cells. *Transplantation* 2009; 87(9 Suppl): S45-9.
- [31] Hwang JH, Lee MJ, Seok OS, *et al.* Cytokine expression in placenta-derived mesenchymal stem cells in patients with pre-eclampsia and normal pregnancies. *Cytokine* 2010; 49(1): 95-101.
- [32] Anzalone R, Lo Iacono M, Loria T, *et al.* Wharton's jelly mesenchymal stem cells as candidates for beta cells regeneration: extending the differentiative and immunomodulatory benefits of adult mesenchymal stem cells for the treatment of type 1 diabetes. *Stem Cell Rev* 2011; 7(2): 342-63.
- [33] Ichim TE, Solano F, Brenes R, *et al.* Placental mesenchymal and cord blood stem cell therapy for dilated cardiomyopathy. *Reprod Biomed Online* 2008; 16(6): 898-905.
- [34] Jiang R, Han Z, Zhuo G, *et al.* Transplantation of placenta-derived mesenchymal stem cells in type 2 diabetes: a pilot study. *Front Med* 2011; 5(1): 94-100.
- [35] Miki T, Marongiu F, Dorko K, Ellis EC, Strom SC. Isolation of amniotic epithelial stem cells. *Curr Protoc Stem Cell Biol*. 2010 Jan; Chapter 1: Unit 1E 3.
- [36] Murphy S, Rosli S, Acharya R, *et al.* Amnion epithelial cell isolation and characterization for clinical use. *Curr Protoc Stem Cell Biol*. 2010 Apr; Chapter 1: Unit 1E 6.
- [37] Ilancheran S, Michalska A, Peh G, Wallace EM, Pera M, Manuelpillai U. Stem cells derived from human fetal membranes display multilineage differentiation potential. *Biol Reprod* 2007; 77(3): 577-88.
- [38] Miki T, Lehmann T, Cai H, Stolz DB, Strom SC. Stem cell characteristics of amniotic epithelial cells. *Stem Cells* 2005; 23(10): 1549-59.
- [39] Banas RA, Trumpower C, Bentlejewski C, Marshall V, Sing G, Zeevi A. Immunogenicity and immunomodulatory effects of amnion-derived multipotent progenitor cells. *Hum Immunol* 2008; 69(6): 321-8.
- [40] Pratama G, Vaghjiani V, Tee JY, *et al.* Changes in culture expanded human amniotic epithelial cells: implications for potential therapeutic applications. *PLoS One* 2011; 6(11): e26136.
- [41] Manuelpillai U, Moodley Y, Borlongan CV, Parolini O. Amniotic membrane and amniotic cells: potential therapeutic tools to combat tissue inflammation and fibrosis? *Placenta* 2011; 32 Suppl 4: S320-5.
- [42] Michalopoulos GK, Bowen WC, Mule K, Luo J. HGF-, EGF-, and dexamethasone-induced gene expression patterns during formation of tissue in hepatic organoid cultures. *Gene Expr* 2003; 11(2): 55-75.
- [43] Sekhon SS, Tan X, Micsenyi A, Bowen WC, Monga SP. Fibroblast growth factor enriches the embryonic liver cultures for hepatic progenitors. *Am J Pathol* 2004; 164(6): 2229-40.
- [44] Rossi JM, Dunn NR, Hogan BL, Zaret KS. Distinct mesodermal signals, including BMPs from the septum transversum mesenchyme, are required in combination for hepatogenesis from the endoderm. *Genes Dev* 2001; 15(15): 1998-2009.
- [45] Miki T, Marongiu F, Ellis EC, *et al.* Production of hepatocyte-like cells from human amnion. *Methods Mol Biol* 2009; 481: 155-68.
- [46] Kamiya A, Kinoshita T, Ito Y, *et al.* Fetal liver development requires a paracrine action of oncostatin M through the gp130 signal transducer. *EMBO J* 1999; 18(8): 2127-36.
- [47] Campard D, Lysy PA, Najimi M, Sokal EM. Native umbilical cord matrix stem cells express hepatic markers and differentiate into hepatocyte-like cells. *Gastroenterology* 2008; 134(3): 833-48.
- [48] Tamagawa T, Oi S, Ishiwata I, Ishikawa H, Nakamura Y. Differentiation of mesenchymal cells derived from human amniotic membranes into hepatocyte-like cells *in vitro*. *Hum Cell* 2007; 20(3): 77-84.
- [49] Hong SH, Gang EJ, Jeong JA, *et al.* *In vitro* differentiation of human umbilical cord blood-derived mesenchymal stem cells into hepatocyte-like cells. *Biochem Biophys Res Commun* 2005; 330(4): 1153-61.
- [50] Kakinuma S, Tanaka Y, Chinzei R, *et al.* Human umbilical cord blood as a source of transplantable hepatic progenitor cells. *Stem Cells* 2003; 21(2): 217-27.
- [51] Bossard P, Zaret KS. GATA transcription factors as potentiators of gut endoderm differentiation. *Development* 1998; 125(24): 4909-17.
- [52] Takashima S, Ise H, Zhao P, Akaike T, Nikaido T. Human amniotic epithelial cells possess hepatocyte-like characteristics and functions. *Cell Struct Funct* 2004; 29(3): 73-84.
- [53] Marongiu F, Gramignoli R, Dorko K, *et al.* Hepatic differentiation of amniotic epithelial cells. *Hepatology* 2011; 53(5): 1719-29.
- [54] Skardal A, Smith L, Bharadwaj S, Atala A, Soker S, Zhang Y. Tissue specific synthetic ECM hydrogels for 3-D *in vitro* maintenance of hepatocyte function. *Biomaterials*. 2012; 33(18): 4565-75.
- [55] Adachi T, Goto M, Cho CS, Akaike T. Modulation of cytochrome P450 gene expression in primary hepatocytes on various artificial extracellular matrices. *Biochem Biophys Res Commun* 2011; 413(4): 577-81.
- [56] Torok E, Lutgehelmann M, Bierwolf J, *et al.* Primary human hepatocytes on biodegradable poly(l-lactic acid) matrices: a promising model for improving transplantation efficiency with tissue engineering. *Liver Transpl* 2011; 17(2): 104-14.
- [57] Yu J, Cao H, Yang J, *et al.* *In vivo* hepatic differentiation of mesenchymal stem cells from human umbilical cord blood after trans-

- plantation into mice with liver injury. *Biochem Biophys Res Commun.* 2012 Jun 15; 422(4): 539-45.
- [58] Nonome K, Li XK, Takahara T, *et al.* Human umbilical cord blood-derived cells differentiate into hepatocyte-like cells in the Fas-mediated liver injury model. *Am J Physiol Gastrointest Liver Physiol* 2005; 289(6): G1091-9.
- [59] Zhang D, Jiang M, Miao D. Transplanted human amniotic membrane-derived mesenchymal stem cells ameliorate carbon tetrachloride-induced liver cirrhosis in mouse. *PLoS One* 2011; 6(2): e16789.
- [60] Krohn N, Kapoor S, Enami Y, *et al.* Hepatocyte transplantation-induced liver inflammation is driven by cytokines-chemokines associated with neutrophils and Kupffer cells. *Gastroenterology* 2009; 136(5): 1806-17.
- [61] Johnson J, Meyrick B, Jesmok G, Brigham KL. Human recombinant tumor necrosis factor alpha infusion mimics endotoxemia in awake sheep. *J Appl Physiol* 1989; 66(3): 1448-54.
- [62] Tsai PC, Fu TW, Chen YM, *et al.* The therapeutic potential of human umbilical mesenchymal stem cells from Wharton's jelly in the treatment of rat liver fibrosis. *Liver Transpl* 2009; 15(5): 484-95.
- [63] Manuelpillai U, Lourenz D, Vaghjiani V, *et al.* Human amniotic epithelial cell transplantation induces markers of alternative macrophage activation and reduces established hepatic fibrosis. *PLoS One* 2012; 7(6): e38631.
- [64] Nierhoff D, Ogawa A, Oertel M, Chen YQ, Shafritz DA. Purification and characterization of mouse fetal liver epithelial cells with high *in vivo* repopulation capacity. *Hepatology* 2005; 42(1): 130-9.
- [65] Oertel M, Menthena A, Dabeva MD, Shafritz DA. Cell competition leads to a high level of normal liver reconstitution by transplanted fetal liver stem/progenitor cells. *Gastroenterology* 2006; 130(2): 507-20; quiz 90.
- [66] Haridass D, Yuan Q, Becker PD, *et al.* Repopulation efficiencies of adult hepatocytes, fetal liver progenitor cells, and embryonic stem cell-derived hepatic cells in albumin-promoter-enhancer urokinase-type plasminogen activator mice. *Am J Pathol* 2009; 175(4): 1483-92.
- [67] Delgado JP, Vanneaux V, Branger J, *et al.* The role of HGF on invasive properties and repopulation potential of human fetal hepatic progenitor cells. *Exp Cell Res* 2009; 315(19): 3396-405.
- [68] Ricordi C, Zeng Y, Tzakis A, *et al.* Evidence that canine pancreatic islets promote the survival of human hepatocytes in nude mice. *Transplantation* 1991; 52(4): 749-51.
- [69] de Vos P, Faas MM, Strand B, Calafiore R. Alginate-based microcapsules for immunoisolation of pancreatic islets. *Biomaterials* 2006; 27(32): 5603-17.
- [70] Maguire T, Novik E, Schloss R, Yarmush M. Alginate-PLL microencapsulation: effect on the differentiation of embryonic stem cells into hepatocytes. *Biotechnol Bioeng* 2006; 93(3): 581-91.
- [71] Penolazzi L, Tavanti E, Vecchiarelli R, *et al.* Encapsulation of mesenchymal stem cells from Wharton's jelly in alginate microbeads. *Tissue Eng Part C Methods* 2010; 16(1): 141-55.
- [72] Hamazaki K, Doi Y, Koide N. Microencapsulated multicellular spheroid of rat hepatocytes transplanted intraperitoneally after 90% hepatectomy. *HepatoGastroenterology* 2002; 49(48): 1514-6.
- [73] Mai G, Nguyen TH, Morel P, *et al.* Treatment of fulminant liver failure by transplantation of microencapsulated primary or immortalized xenogeneic hepatocytes. *Xenotransplantation* 2005; 12(6): 457-64.
- [74] Zhang FT, Wan HJ, Li MH, *et al.* Transplantation of microencapsulated umbilical-cord-blood-derived hepatic-like cells for treatment of hepatic failure. *World J Gastroenterol* 2011; 17(7): 938-45.
- [75] Chen AA, Thomas DK, Ong LL, Schwartz RE, Golub TR, Bhatia SN. Humanized mice with ectopic artificial liver tissues. *Proc Natl Acad Sci USA* 2011; 108(29): 11842-7.
- [76] Davydova DA, Vorotelyak EA, Smirnova YA, *et al.* Cell phenotypes in human amniotic fluid. *Acta Naturae* 2009; 1(2): 98-103.
- [77] Marongiu F, Gramignoli R, Sun Q, *et al.* Isolation of amniotic mesenchymal stem cells. *Curr Protoc Stem Cell Biol.* 2010 Mar; Chapter 1: Unit 1E 5.
- [78] Roubelakis MG, Pappa KI, Bitsika V, *et al.* Molecular and proteomic characterization of human mesenchymal stem cells derived from amniotic fluid: comparison to bone marrow mesenchymal stem cells. *Stem Cells Dev* 2007; 16(6): 931-52.
- [79] La Rocca G, Anzalone R, Farina F. The expression of CD68 in human umbilical cord mesenchymal stem cells: new evidences of presence in non-myeloid cell types. *Scand J Immunol* 2009; 70(2): 161-2.
- [80] Moodley Y, Ilancheran S, Samuel C, *et al.* Human amnion epithelial cell transplantation abrogates lung fibrosis and augments repair. *Am J Respir Crit Care Med* 2010; 182(5): 643-51.
- [81] Stadler G, Hennerbichler S, Lindenmair A, *et al.* Phenotypic shift of human amniotic epithelial cells in culture is associated with reduced osteogenic differentiation *in vitro*. *Cytherapy* 2008; 10(7): 743-52.
- [82] Chien CC, Yen BL, Lee FK, *et al.* *In vitro* differentiation of human placenta-derived multipotent cells into hepatocyte-like cells. *Stem Cells* 2006; 24(7): 1759-68.

Hypothesis

HAEC can be differentiated into functional HLCs which retain their functions post-encapsulation. HLC modulate their mtDNA copy number to achieve optimal functions, respiration and ATP generation. These parameters can be enhanced by encapsulation of HLC.

Aims

1. Differentiate and characterise HLCs derived from hAEC. Assess the effects of encapsulation on HLC functions and gene expression.
2. Evaluate changes in mtDNA copy number, DNA methylation of POLGA and gene expression patterns of differentiated HLCs.
3. Evaluate the effects of encapsulation on mtDNA copy number, DNA methylation of POLGA and their transcriptome profile.

Chapter 2

General Materials and Methods

2.1 Ethics approval

This study was approved by the Human Research Ethics Committees of Monash Medical Centre and The Royal Women's Hospital. Amniotic membranes were collected from healthy women with a normal singleton pregnancy delivered by Caesarean section at term (N = 20).

2.2 Preparation of growth factors and reagents

2.2.1 Preparation of type I collagen

Lyophilised 10 mg rat tail collagen type I (Roche, Mannheim, Germany) was dissolved in 10 ml of 0.2% acetic acid (Sigma Aldrich, St Louis, MO). Reconstituted collagen was allowed to fully dissolve for 18 hours at 4°C and stored at 4°C until further use. 1 ml of collagen was added per 10 cm² of tissue culture dish and incubated for 5 minutes. Excess collagen was aspirated and the culture dish was allowed to air dry. The culture dishes were rinsed twice with Dulbecco's phosphate buffer saline (DPBS; Sigma Aldrich) and once with DMEM/F12 media (Gibco, Grand Island, NY).

2.2.2 Collection of HepG2 conditioned media

Hepatocellular carcinoma cell line HepG2 (ATCC, HB-8065) was plated in T175 flasks (BD Biosciences, San Jose, CA) in DMEM/F12 with 10% fetal bovine serum (FBS; Gibco). Cell culture media was changed every alternate day. When cells reached 70% confluence, fresh culture media was added to HepG2 cells and conditioned media collected after 48 hours. Conditioned media was filter sterilised and 10 ml aliquots were stored at -20C until further use.

2.2.3 Preparation of epidermal growth factor (EGF)

100 µg of recombinant human EGF (Gibco) was reconstituted by adding 1 ml of DPBS to make a 100 µg/ml stock solution. 50 µl aliquots were stored at -20°C for further use. A final concentration of 10 ng/ml was used for cultures.

2.2.4 Preparation of fibroblast growth factor-4 (FGF)

10 µg of recombinant human FGF-4 was reconstituted with 1 ml of DPBS to make 10 µg/ml stock. The stock was aliquoted in 50 µl volume and stored at -20°C for further use. The final concentration for cell culture was 10 ng/ml of FGF-4.

2.2.5 Preparation of hepatocyte growth factor (HGF)

10 µg of recombinant human HGF was reconstituted with 1 ml of DPBS to make 10 µg/ml stock. 50 µl aliquots were stored at -20°C for further use. The final concentration for cell culture was 10 ng/ml of HGF.

2.2.6 Preparation of dexamethasone

1 mg of dexamethasone (Sigma Aldrich) was dissolved in 1 ml of absolute ethanol (Sigma Aldrich) to achieve 1 mg/ml solution (2.548 mM). Further 24.48 ml of DMEM/F12 was added to the solution to achieve 0.1 mM stock solution. Stock solution was aliquoted into 500 µl volume and stored at -20°C for further use. The final concentration for cell culture was 0.1 µM of dexamethasone.

2.2.7 Preparation of 2'-3'-dideoxycytidine (ddC)

A stock solution of 10 μ M was generated by dissolving 21.1 mg of ddC (Sigma Aldrich) in 10 ml of dH₂O. The stock solution was filter sterilised and 500 μ l aliquots were stored at -20°C for further use.

2.2.8 Preparation of Uridine

50 mg/ml stock solution was made by dissolving 250 mg of uridine (Sigma Aldrich) in 5 ml of dH₂O. The stock solution was filter sterilised and 250 μ l aliquots were stored at -20°C for further use.

2.3 Isolation of human amniotic epithelial cells (hAEC)

Amnion membranes were peeled from the chorionic membrane after delivery of the placenta. Each amnion membrane was placed in DMEM/F12 medium and transported on ice to the lab for isolation of hAEC. hAEC were isolated as previously described (1) with minor modifications. Under sterile conditions, the amniotic membranes were washed in DMEM/F12 medium twice to remove any blood clots. The amniotic membranes were cut into small pieces and washed twice in DPBS. The amniotic membranes were further washed three times in Hank's balanced salt solution (HBSS; Sigma Aldrich) and finally rinsed with 0.05% trypsin containing 0.05mM EDTA (Gibco). Stock trypsin (0.5%) was diluted to 0.05% in HBSS at PH 8.0 for digestion of the amniotic membrane.

Small pieces of amniotic membranes were distributed equally into two 50ml Falcon tubes each containing 15ml of 0.05% trypsin with the final volume being no more than 45ml. The amniotic membranes were digested for 10 minutes at 37°C with occasional shaking. Initial

digestion of cells containing trypsin was discarded which contained dead cells and debris. Amniotic membranes were transferred into two 50ml Falcon tubes containing 25 ml of 0.05% trypsin and digested for 40 minutes at 37°C with occasional shaking. Amniotic membranes were transferred into a second set of 50ml Falcon tubes containing 25ml of 0.05% trypsin for a further 40 minutes at 37°C. Trypsin was neutralised with two volumes of 10% newborn calf serum in DMEM/F12 (Gibco). Dissociated cells were centrifuged at 200 x g for 10 minutes, resuspended in DMEM/F12, strained through a 100µM filter and washed several times. Red blood cells were lysed with hypotonic solution for 7-8 minutes at 37°C. The cells were washed several times in DMEM/F12. To enrich for stage specific embryonic antigen, SSEA4, isolated cells were resuspended in HBSS solution at a concentration of 5 million/ml. 20 ml of cell suspension was gently cushioned onto 24ml of 24% Percoll (Sigma Aldrich) and centrifuged for 8 minutes at 150 x g at room temperature without rotor brakes. The cell pellet was collected and washed several times in DMEM/F12. Cell viability was assessed by trypan blue exclusion. Cells were cryopreserved in fetal bovine serum (FBS; Gibco) containing 10% dimethyl sulfoxide at a concentration of 3 million cells/ml.

2.4 Differentiation of hepatocyte-like cells

Cryopreserved hAEC were thawed and plated on type I collagen (Roche, Mannheim, Germany) coated dishes in DMEM/F12 with 20% FBS and 10 ng/ml epidermal growth factor (EGF) for 3-5 days. To induce differentiation, hAEC were cultured in DMEM/F12 supplemented with 10% FBS, 10% HepG2 cell conditioned medium, 10 ng/ml EGF, fibroblast growth factor-4 (FGF-4) and hepatocyte growth factor (HGF; growth factors purchased from Invitrogen, Camarillo, CA) and 0.1 µM insulin and dexamethasone (Sigma-Aldrich). After 14 days, cells were switched to DMEM/F12 supplemented with 10% FBS, 10% HepG2 cell

conditioned medium, 10 ng/ml HGF, 0.1 μ M dexamethasone and 1x insulin-transferrin-selenium (Invitrogen). Medium was replenished on alternate days. Cultures were maintained for a further 14 days.

2.5 Extraction of nucleic acids

2.5.1 RNA extraction

Total RNA was extracted from cells using RNeasy Mini Kit (Qiagen, Hilden, Germany) according to manufacturer's instructions. Briefly, cells were lysed in 350 μ l of RLT buffer with 1% β -mercaptoethanol. The cell lysate was passed through a 20 gauge needle in an RNase-free syringe several times to achieve optimal lysis. The lysate was loaded into the shredder columns (Qiagen) and centrifuged at 10,000 rpm for 2 minutes. Equal volume of 70% ethanol was added to the cell lysate recovered from the shredder columns and mixed thoroughly. Samples were transferred onto spin columns and centrifuged at 10,000 rpm for 15sec. Flow through was discarded and 700 μ l of buffer RW1 was added to the columns. The columns were centrifuged at 10,000 rpm for 15 sec and flow through was discarded. DNase I treatment was performed on the RNA columns to remove any DNA present. 10 units of DNase I (Qiagen) was diluted with 70 μ l of buffer RDD, loaded into the RNA columns and incubated at room temperature for 15 minutes. 350 μ l of buffer RW1 was added to the columns. The columns were centrifuged at 10,000 rpm for 15 sec and the flow through was discarded. 500 μ l of buffer RPE was added to the columns and centrifuged at 10,000 rpm for 15 sec. A further 500 μ l of buffer RPE was added to the columns and centrifuged at 10,000 rpm for 2 minutes. The columns were transferred to a new collection tube and centrifuged at 10,000 rpm for 1 minute. The columns were transferred into a collection tube and 50 μ l of

RNase free water was added to the column membrane. RNA was eluted by centrifugation of the columns at 10,000 rpm for 1 minute.

2.5.2 RNA quantification and purity

Total RNA was quantified using a NanoDrop 1000 spectrophotometer (Thermo Fisher, Wilmington, DE). The ratio of absorbance at 260nm to 280nm is used to assess purity of RNA, which is usually approximately 1.8. RNA that had a ratio of 1.7 - 1.9 in absorbance between 260nm to 280nm was used for cDNA synthesis. RNA purity was also confirmed with a ratio of absorbance between 260nm to 230nm, which was in the range of 2.0 – 2.2, as expected. RNA was concentrated for samples that were lower than 250 ng/µl. One tenth of a volume of 3 M sodium acetate (PH 5.2) was added to the RNA sample and was mixed well. An additional 2.2 volumes of 100% ice cold ethanol was added and samples were kept at -80°C for 30 mins. The precipitate was mixed and samples centrifuged at 14,000 rpm for 10 minutes. The supernatant was discarded and the RNA pellet was washed with 500 µl of 70% ice cold ethanol. The samples were centrifuged at 14,000 rpm for 2 minutes, the supernatant discarded and the RNA pellet allowed to air dry. The RNA pellet was resuspended in an appropriate volume of RNase free water.

2.5.3 cDNA synthesis

RNA was converted to cDNA using the SuperScript III first strand synthesis system (Invitrogen). 2µg of total RNA was added to 1 µl of random hexamers (stock 50 ng/µl) and 1 µl of 10 mM dNTP mix in a volume of 10 µl. The mix was incubated at 65°C for 5 minutes and chilled on ice for 2 minutes. An additional 10 µl of mix containing 2 µl RT buffer, 4 µl of 25 mM magnesium chloride, 2 µl of 0.1 mM DTT, 1 µl of RNase-out and 1 µl of Superscript

III enzyme was added. The samples were incubated at 25°C for 10 minutes followed by 50°C for 50 minutes and final extension at 85°C for 5 minutes. 1 µl of RNaseH was added to each reaction and incubated at 37°C for 20 minutes. Negative control reactions did not include the enzyme Superscript III. cDNA was stored at -20°C for further use.

2.5.4 Gene expression

Real-time quantitative PCR was performed on a Rotor-Gene 3000 (Qiagen) for pluripotent and hepatocyte specific genes. In a total volume of 20 µl, the reaction mixture consisted of 10 µl of 2x SensiMix SYBR[®] Hi-ROX (Bioline), 1 µl each of 5 µM forward and reverse primers (Table 2.1; Sigma Aldrich), 6 µl of H₂O and 2 µl of cDNA using conditions given in Table 2.1. Samples were run in triplicate. The list of genes assayed, primer sequences and annealing temperatures are given in Table 2.1.

Gene expression data were normalised to the housekeeping gene OAZ1 and expressed as fold change relative to undifferentiated hAEC calculated using the $2^{-\Delta\Delta CT}$ method (2).

2.5.5 DNA extraction

Genomic DNA was isolated using Isolate II Genomic DNA Kit (Bioline; London, United Kingdom). Frozen cell pellet (2-3 million cells) was resuspended in 200 µl of lysis buffer GL. 25 µl of proteinase K (Bioline) was added followed by 200 µl of lysis buffer G3. The lysate was incubated at 70°C for 15 minutes. After incubation, 4 µl of RNaseA (Qiagen) was added to the sample and incubated at room temperature for 10 minutes. Samples were briefly vortexed and 210 µl of 100% ethanol (Sigma Aldrich) was added followed by vigorous vortexing. The samples were loaded onto the genomic DNA spin columns and centrifuged at

13,000 rpm for 1 minute. Flow through was discarded and 500 µl of wash buffer GW1 was added to the columns. The columns were centrifuged at 13,000 rpm for 1 minute and the flow through discarded. 600 µl of wash buffer GW2 was added to the columns and centrifuged at 13,000 rpm for 1 minute and the flow through was discarded. The columns were further centrifuged at 13,000 rpm for 3 minutes to remove any residual ethanol. DNA was eluted in a fresh 1.5ml microcentrifuge tube by adding 100 µl of preheated (70°C) elution buffer G and incubated at room temperature for 1 minute followed by centrifugation at 13,000 rpm for 1 minute. DNA was quantified using a NanoDrop 1000 spectrophotometer.

2.6 mtDNA copy number

Nuclear DNA encoded β-globin and mtDNA were amplified by conventional PCR in a 50 µL volume which consisted of 5 µL of 10X NH₄ reaction buffer, 1.5 µL of 50 mM MgCl₂, 0.5 µL 50 mM dNTP mix, 0.5 µL BIOTAQTM DNA polymerase, 1 µL of 50 pmol/µL forward primer, 1 µL of 50 pmol/µL reverse primer, 2 µL (200ng) DNA template and 38.5 µL autoclaved Milli-Q water (see Table 2.1 for primer sequences and conditions). The PCR products were run on 2% agarose gels to confirm the amplified DNA template. The target bands were excised from the agarose gel and DNA purified using the Gel Purification Kit (Qiagen). Purified β-globin and mtDNA concentration were adjusted to 10 ng/µL to prepare stock for standards. Standards were prepared by tenfold serial dilution of purified DNA from range of 10⁻¹ to 10⁻⁸.

Real-time quantitative PCR was performed on a Rotor-Gene 3000 (Qiagen) for mtDNA and the nuclear encoded β-globin gene. In a total volume of 20 µl, the reaction mixture consisted of 10 µl of 2x SensiMix SYBR[®] Hi-ROX (Bioline), 1 µl each of 5 µM forward and reverse

primers (Table 2.1; Sigma Aldrich), 6 μ l of H₂O and 2 μ l of DNA (20 ng of DNA) using conditions given in Table 2.1. Samples were run in triplicate. Melt curve analysis was performed for each reaction to determine optimal melting temperatures for the second acquisition phase, which was 78°C. MtDNA copy number was calculated using the following formula:

$$N = ([\text{ng}/\mu\text{L}] \times 6.023 \times 10^{14}) / (N_{\text{bp}} \times 660) \text{ where:}$$

N is the number of molecules per reaction.

$\times 10^{14}$ is conversion of 1 mol to 1 nmol using Avogadro's constant, which states 1 mol contains 6.023×10^{23} .

N_{bp} is the product size of the amplicon.

660 is the mean molecular weight in Daltons of a nucleic acid base pairing.

MtDNA copy number (N) is calculated by dividing it by 2, as two copies of β -globin is present in diploid human cells.

2.7 Immunoprecipitation of methylated / hydroxymethylated DNA (MeDIP)

A total of 5 μ g genomic DNA was diluted in 100 μ L of Milli-Q water and 100 μ L of 2x TE buffer was added to a Covaris milliTUBE. Genomic DNA was sonicated to fragments of 200 to 1000 base pair using the Covaris Adaptive Focused Acoustics system. The temperature range was 4-8 °C, 105.0 peak power, 5.0 duty factor and 200 cycles/bursts. Sonicated DNA was divided into three tubes with 1.5 μ l of DNA in a total volume of 450 μ l adjusted with H₂O. DNA samples were denatured by incubating at 95 °C for 10 minutes and immediately chilled on ice for at least 5 minutes. 50 μ L of 10x IP buffer was added to bring the total volume to 500 μ L (final concentration is 1x IP buffer; 10 mM Na-Phosphate, pH 7.0, 140 mM NaCl and

0.05% Triton X-100). Samples were immunoprecipitated with 1 µg of antibody to 5mC or 5hmC (Active Motif, Carlsbad, CA), separately at 4 °C for 2 hours by rotation. Pre-washed 20 µl Protein G Dynabeads (Invitrogen) were added to the samples and incubated at 4°C for 16 hours by rotation. Samples were washed three times with 1 ml cold 1x IP buffer. The beads bound to DNA were resuspended in 250 µl of Proteinase K solution (5mM Tris, 1mM EDTA, pH8.0, 0.05% SDS) with 5 µl of Proteinase K (stock 20 µg/ml; Qiagen) and incubated at 50°C for 3 hours on a 1400 rpm shaker. The immunoprecipitated DNA was purified using PCR purification columns (Qiagen) and final DNA eluted in 50 µl of buffer EB.

QPCR was performed on captured DNA samples on a RotorGene 3000 for exon 2 of POLGA using primers and conditions listed in Table 2.1. qPCR was performed in a total volume of 20 µl consisting of 2x SensiMix SYBR[®] Hi-ROX, 1 µl of 5 µM forward and reverse primers, 6 µl of H₂O and 2 µl of MeDIP product. Samples were run in triplicate. Data were first normalised to input samples and enrichment levels were determined for 5mC and 5hmC. Data were expressed as fold change of 5mC relative to 5hmC.

2.8 Encapsulation of HLC and culture

Barium ions are cross-linked with alginate to make barium alginate microcapsules. HLC were encapsulated in barium alginate microcapsules, as described elsewhere (3). Briefly, HLC were trypsinized, washed three times in PBS and mixed with 2.2% ultra-pure alginate solution at a ratio of 1:6. The alginate solution was composed of a 60:40 mixture of guluronic acid : mannuronic acid (UP MVG Pronova, FMC Biopolymer, Sandvika, Norway). Under coaxial air flow, droplets are generated by ejecting liquid from the nozzle under a controlled air jet. Encapsulation was performed with an air driven droplet generator (Steinau, Berlin, Germany) at a pressure of 80 kPa with an air flow rate of 6 l/min. The liquid microcapsules

generated were solidified by incubation in a 20 mM barium chloride (BaCl₂) precipitation bath for 2 min. The polycations contained in BaCl₂ bind to guluronic and mannuronic acid components of alginate to form strong cross-links with polycations producing rigid microcapsules. The microcapsules are washed three times in 0.9% saline to remove excess barium. The average diameter of the microcapsules is 600 μm with approximately 1000 cells in each capsule. Similarly, transformed human hepatocyte HepG2 cells, were also encapsulated for comparison. Encapsulated cells were cultured *in vitro* for up to 28 days with media changed every alternate day.

2.9 Decapsulation of HLC

Decapsulation of encapsulated cells was carried out to extract DNA, RNA and other cell based assays. The decapsulation solution consists of 50 mM Ethylenediaminetetraacetic acid (EDTA; Sigma Aldrich) and 10 mM 4-(2-hydroxyethyl)-1-piperazineethanesulfonic acid (HEPES; Sigma Aldrich) in DBPS. Capsules were washed twice with 20 ml of DPBS and pre-warmed 15 ml of decapsulation solution was added to the capsules. Additional decapsulating solution was added to have enough EDTA to chelate Barium ions. The capsules with decapsulation solution were incubated at 37 °C for 15 minutes with gentle agitation. The solution was examined under a microscope to see whether the alginate was dissolving and cells were released from the capsules. After dissolving alginate capsules, the cells were mixed several times with a pipette to break the cell clusters. The solution was centrifuged at 3000 rpm for 5 mins to pellet the cells. Pelleted cells were further washed with DMEM/F12 and pelleted into an Eppendorf tube for DNA and RNA extraction.

2.10 Statistical analysis

Data are shown as the mean \pm SEM derived from a minimum of $n = 4-6$ hAEC cultures. Statistical significance was determined by one-way and two-way ANOVA followed by Bonferroni *post hoc* tests using GraphPad Prism V6.01 (Graph Pad Inc., San Diego, CA). Significance was accorded when $P < 0.05$; significance given as * $p < 0.05$, ** $p < 0.01$, *** $p < 0.001$ and **** $p < 0.0001$.

Table 2.1 List of primers, annealing temperature and product size for real-time qPCR.

Gene	Primer sequence	Annealing Temp (°C)	Product size (bp)
β-Globin	Forward - CAACTTCATCCACGTTTCACC Reverse - GAAGAGCCAAGGACAGGTAC	56	268
mtDNA	Forward - CGAAAGGACAAGAGAAATAAGG Reverse - CTGTAAAGTTTTAAGTTTTATGCG	53	152
POLG-Exon 2	Forward - CAGACCTCCACGTCGAACAC Reverse - GACAACCTGGACCAGCACTT	59	162
OAZ1	Forward - GGATCCTCAATAGCCACTGC Reverse - TACAGCAGTGGAGGGAGACC	60	150
Albumin	Forward - TTGGCACAATGAAGTGGGTA Reverse - AAAGGCAATCAACACCAAGG	60	161
Alpha-1 anti-trypsin	Forward - CCACCGCCATCTTCTTCCTGCCTGA Reverse - GAGCTTCAGGGGTGCCTCCTCTGTG	60	245
CYP3A4	Forward - TGTGCCTGAGAACACCAGAG Reverse - GTGGTGGAAATAGTCCCGTG	60	226
HNF4-alpha	Forward - CATGGCCAAGATTGACAACCT Reverse - TTCCCATATGTTTCCTGCATCAG	60	113
OCT-4	Forward - TCACCCTGGGGGTCTATTT Reverse - CTGGTTCGCTTTCTCTTTTCG	55	202
SOX-2	Forward - GGAGCTTTGCAGGAAGTTTG Reverse - GCAAGAAGCCTCTCCTTGAA	55	191
Nanog	Forward - TTAATAACCTTGGCTGCCGT Reverse - GCAGCAAATACGAGACCTCT	55	298
cMYC	Forward - ACAACACCCGAGCAAGGACGC Reverse - ACGGCTGCACCGAGTCGTAGT	55	180
hTERT	Forward - CACCAAGAAGTTCATCTCC Reverse - CAAGTGCTGTCTGATTCC	55	260

2.11 References

1. Miki T, Marongiu F, Ellis E, S CS. Isolation of amniotic epithelial stem cells. *Curr Protoc Stem Cell Biol.* 2007;Chapter 1:Unit 1E 3.
2. Livak KJ, Schmittgen TD. Analysis of relative gene expression data using real-time quantitative PCR and the $2^{-\Delta\Delta C(T)}$ Method. *Methods.* 2001;25(4):402-8.
3. Foster JL, Williams G, Williams LJ, Tuch BE. Differentiation of transplanted microencapsulated fetal pancreatic cells. *Transplantation.* 2007;83(11):1440-8.

Chapter 3 – Published data

Hepatocyte-Like Cells Derived from Human Amniotic Epithelial Cells Can be Encapsulated Without Loss of Viability or Function in Vitro

Declaration for Thesis Chapter

Monash University

Declaration for Thesis Chapter 3

Declaration by candidate

In the case of Chapter 1, the nature and extent of my contribution to the work was the following:

Nature of contribution	Extent of contribution (%)
Authorship of publication	90%

The following co-authors contributed to the work. If co-authors are students at Monash University, the extent of their contribution in percentage terms must be stated:

Name	Nature of contribution	Extent of contribution (%) for student co-authors only
Dr Ursula Manuelpillai	Supervisory support, advice and editing	10%

The undersigned hereby certify that the above declaration correctly reflects the nature and extent of the candidate's and co-authors' contributions to this work.

Candidate's signature..... **Date** 12 May 2016

Main supervisor's signature.....  **Date** 12 May 2016

Hepatocyte-Like Cells Derived from Human Amniotic Epithelial Cells Can Be Encapsulated Without Loss of Viability or Function In Vitro

Vijesh Vaghjiani,¹ Vijayaganapathy Vaithilingam,² Indah Saraswati,¹ Adnan Sali,¹ Padma Murthi,^{3,4} Bill Kalionis,^{3,4} Bernard E. Tuch,^{1,2} and Ursula Manuelpillai¹

Placenta derived human amniotic epithelial cells (hAEC) are an attractive source of stem cells for the generation of hepatocyte-like cells (HLC) for therapeutic applications to treat liver diseases. During hAEC differentiation into HLC, they become increasingly immunogenic, which may result in immune cell-mediated rejection upon transplantation into allogeneic recipients. Placing cells within devices such as alginate microcapsules can prevent immune cell-mediated rejection. The aim of this study was to investigate the characteristics of HLC generated from hAEC and to examine the effects of encapsulation on HLC viability, gene expression, and function. hAEC were differentiated for 4 weeks and evaluated for hepatocyte-specific gene expression and function. Differentiated cells were encapsulated in barium alginate microcapsules and cultured for 7 days and the effect of encapsulation on cell viability, function, and hepatocyte related gene expression was determined. Differentiated cells performed key functions of hepatocytes including urea synthesis, drug-metabolizing cytochrome P450 (CYP)3A4 activity, indocyanine green (ICG) uptake, low-density lipoprotein (LDL) uptake, and exhibited glutathione antioxidant capacity. A number of hepatocyte-related genes involved in fat, cholesterol, bile acid synthesis, and xenobiotic metabolism were also expressed showing that the hAEC had differentiated into HLC. Upon encapsulation, the HLC remained viable for at least 7 days in culture, continued to express genes involved in fat, cholesterol, bile acid, and xenobiotic metabolism and had glutathione antioxidant capacity. CYP3A4 activity and urea synthesis by the encapsulated HLC were higher than that of monolayer HLC cultures. Functional HLC can be derived from hAEC, and HLC can be encapsulated within alginate microcapsules without losing viability or function in vitro.

Introduction

LIVER FAILURE CAN ARISE from chronic or acute causes and inherited metabolic disorders. Chronic inflammation from many causes including alcohol abuse, obesity, and hepatotoxic viruses can lead to cirrhosis while acute liver failure can result from drug overdoses [1]. Inherited disorders such as ornithine transcarbamylase (OTC) enzyme deficiencies can lead to reduced urea output and to hyperammonia toxicity [2]. The common feature in these diseases is loss or defective hepatocyte function and the only curative therapy is orthotopic liver transplant. However, since there is a severe shortage of suitable donor organs, transplantation of human fetal and adult hepatocytes is being evaluated [3–6]. However, hepatocyte transplantation is limited by the severe

shortage of suitable liver resections for cell isolation, the large number of hepatocytes required for transplantation and difficulties associated with hepatocyte culture and cryopreservation [7]. Replacing hepatocytes with hepatocyte-like cells (HLC) generated from stem cells is an alternative strategy to overcome the shortage of hepatocytes.

HLC derived from both embryonic and induced pluripotent stem cells [8–10] have been shown to rescue fulminant hepatic failure when transplanted into the liver of non-obese diabetic, severe combined immune-deficient (SCID) mice [9,10]. There are ethical concerns regarding the use of embryonic stem cells and there is the risk of tumorigenesis with both embryonic and induced pluripotent stem cells. Mesenchymal stem/stromal cells (MSC) from various sources including bone marrow (BM), adipose, and placenta

¹Centre for Genetic Diseases, Monash Institute of Medical Research, Monash University, Clayton, Victoria, Australia.

²Materials Science and Engineering, Commonwealth Scientific and Industrial Research Organization, North Ryde, New South Wales, Australia.

³Department of Obstetrics and Gynecology, University of Melbourne, Parkville, Victoria, Australia.

⁴Department of Perinatal Medicine, Pregnancy Research Centre, Royal Women's Hospital, Parkville, Victoria, Australia.

can be used to derive HLC [11–15]. HLC generated from BM-MSC engraft in the livers of normal SCID mice [16] and contribute to regeneration in a murine liver regeneration model [17]. However, MSC from different sources have varied potential for differentiation into HLC [18] and they may fuse with other cells upon transplantation [19]. Thus, ethically acceptable, non-invasive, alternative cell sources are needed.

Human amniotic epithelial cells (hAEC) from the placenta are an important cell source for generating HLC. hAEC are very abundant, have stem cell-like features, and differentiate into the lineages from the three embryonic germ layers including HLC originating from the endoderm [20,21]. Naïve hAEC display some relevant features of hepatic progenitors such as the lineage specification transcription factors FoxA2 and GATA-4 [22]. hAEC also display characteristic expression of mature hepatocyte markers such as albumin, α 1-anti-trypsin, and OTC and also express various hepatocyte-related genes [22,23]. Upon differentiation, HLC derived from hAEC express mRNA of liver-enriched transcription factors such as *C/EBP- α* , *CAR*, *RAR*, and *PXR* [24], nuclear localization of the key transcription factor hepatocyte nuclear factor-4 alpha (HNF-4 α), cytochrome P450 (CYP)1A1/2, CYP3A4, and CYP3A7 activity [20,21,25]. These HLC can also synthesize urea and breakdown testosterone [25]. However, expression of genes involved in the metabolism of cholesterol, fat, urea, and xenobiotics and other important functional properties of hepatocytes, such as low-density lipoprotein (LDL) and indocyanine green (ICG) uptake, antioxidative capacity, and bile acid synthesis have not been reported for HLC derived from hAEC.

In a recent study, we found that interferon gamma, a cytokine that is markedly elevated in acute and chronic liver diseases, increased the expression of major histocompatibility complex class IA and II antigens and the costimulatory molecule CD40 when applied to HLC obtained from hAEC [22]. These findings suggest that following transplantation, HLC will be recognized by allogeneic T cells and be rejected. One strategy for preventing cell-mediated rejection is to place cells within immunoisolation devices such as microcapsules made from various polymers including agarose, polyethylene glycol, polyacrylates, and alginate [26]. Alginates are the most commonly used polymers for microencapsulation because of their biocompatibility and the ability to cross-link with Ca^{2+} / Ba^{2+} at physiological pH [27]. Barium alginate microcapsules have a diameter ranging from 100 to 700 μm and a pore size of \sim 250 kDa, thereby allowing the diffusion of nutrients and oxygen, but preventing the entry of immune cells and antibodies [28,29]. Further, microencapsulation creates a three-dimensional environment and this environment has been shown to enhance some hepatocyte-specific functions including detoxification and albumin and α 1-anti-trypsin production in human hepatocyte cell lines [30,31].

HLC derived from hAEC have not been encapsulated. Whether the HLC generated from any type of stem cells remain viable and functional following encapsulation has not been extensively evaluated. Here, we characterized HLC derived from hAEC and evaluated their viability, expression of genes associated with the urea cycle, cholesterol, fat, bile acid synthesis, and xenobiotic metabolism, and their ability

to function following encapsulation within barium alginate microcapsules.

Materials and Methods

Isolation of hAEC

This study was approved by the Human Research Ethics Committees of Monash Medical Center and The Royal Women's Hospital. Amniotic membranes were collected from healthy women with a normal singleton pregnancy delivered by caesarean section at term ($n=8$). hAEC were isolated as previously described [32] with minor modifications. Amniotic membranes were cut into small pieces, washed in Hank's Balanced Salt Solution, and digested twice in 0.05% trypsin containing 0.05 mM EDTA (Gibco, Grand Island, NY) for 40 min at 37°C. Trypsin was neutralized with 10% newborn calf serum in DMEM/F12 medium (Gibco). Dissociated cells were centrifuged at 200 g for 10 min, resuspended in DMEM/F12, strained through a 100 μm filter, and red blood cells lysed with hypotonic solution. The viable SSEA4+ population was recovered using a 24% Percoll (Sigma-Aldrich, St Louis, MO) gradient. Cells were washed several times in DMEM/F12 and viability assessed by trypan blue exclusion. Cells were cryopreserved in fetal bovine serum (FBS; Gibco) containing 10% dimethyl sulfoxide. Cells displaying typical cobble stone epithelial morphology in culture and >98% positive for the epithelial markers cytokeratin 7 and 8/18 (Dako, Glostrup, Denmark) were used in subsequent experiments [20,33].

Differentiation into HLC

Cryopreserved hAEC were thawed and plated on type I collagen (Roche, Mannheim, Germany)-coated dishes in DMEM/F12 with 20% FBS and 10 ng/mL epidermal growth factor (EGF) for 3–5 days. To induce differentiation, hAEC were cultured in DMEM/F12 supplemented with 10% FBS, 10% HepG2 cell-conditioned medium, 10 ng/mL EGF, fibroblast growth factor-4 (FGF-4) and hepatocyte growth factor (HGF; growth factors purchased from Invitrogen, Camarillo, CA), and 0.1 μM insulin and dexamethasone (Sigma-Aldrich). After 2 weeks cells were switched to DMEM/F12 supplemented with 10% FBS, 10% HepG2 cell-conditioned medium, 10 ng/mL HGF, 0.1 μM dexamethasone, and $1 \times$ insulin-transferrin-selenium (Invitrogen). Medium was replenished on alternate days. Cultures were maintained for a further 2 weeks.

Encapsulation of HLC and culture

HLC were encapsulated in barium alginate microcapsules as described elsewhere [34]. Briefly, HLC were trypsinized, washed thrice in PBS, and mixed with 2.2% ultra-pure alginate solution at a ratio of 1:6. The alginate solution was composed of 60:40 mixture of guluronic acid: manuronic acid (UP MVG Pronova; FMC Biopolymer, Sandvika, Norway). Encapsulation was performed with an air-driven droplet generator (Steinau, Berlin, Germany) at a pressure of 80 kPa with an air flow rate of 6 L/min. The microcapsules generated were incubated in a 20 mM barium chloride precipitation bath for 2 min followed by three washings in 0.9%

saline to remove excess barium. The average diameter of the microcapsules was 600 μm with $\sim 1,000$ HLC in each capsule. Similarly, transformed human hepatocyte HepG2 cells, were also encapsulated for comparison. Encapsulated cells were cultured for a further 7 days in parallel with monolayer HLC and HepG2 cultures that served as controls.

Cell viability assay

Viability of both non-encapsulated and encapsulated cells was determined using 6-carboxyfluorescein diacetate (CFDA, 4.6 $\mu\text{g}/\text{mL}$; Sigma-Aldrich) and propidium iodide (PI, 10 $\mu\text{g}/\text{mL}$; Sigma-Aldrich). Briefly, cells were rinsed with Dulbecco's phosphate-buffered saline (DPBS) and incubated with CFDA for 30 min at 37°C. After several washes with DPBS, PI was added and left for 5 min. Cultured cells were washed and detached from the culture plates using TripLE (Invitrogen). Encapsulated cells were decapsulated in 50 mM EDTA and 10 mM HEPES solution at 37°C for 15 min. Flow cytometry was used to quantitate the numbers of viable (green CFDA): dead (red PI) cells. Analysis was performed on a Canto II (BD Biosciences, San Jose, CA) flow cytometer and data analyzed using FlowJo v10 software (Tree Star Incorporation, Ashland, OR).

Immunocytochemistry

Non-encapsulated and decapsulated cells were fixed in 4% paraformaldehyde for 15 min (HNF-4 α) or 100% methanol for 8 min (albumin). Non-specific binding was blocked using CAS block (Invitrogen). Cells were incubated with rabbit anti-human HNF-4 α (1:6,000; Cell Signalling Technology, Danvers, MA) or rabbit anti-human albumin (1:500; Abcam, Cambridge, United Kingdom) at 4°C overnight. Cells were washed several times with DPBS and incubated with goat anti-rabbit Alexa Fluor-488 secondary antibody (1:1,000; Invitrogen) for 30 min at room temperature. Primary antibodies were omitted from negative controls. After several washes, cells were mounted in Vectashield with DAPI (Vector Laboratories, Burlingame, CA).

Periodic acid Schiff's stain

To assess glycogen accumulation, non-encapsulated and decapsulated cells were fixed in 100% ethanol for 8 min and rinsed several times with DPBS. Cells were incubated with periodic acid for 7 min and rinsed in water for 5 min followed by 7 min incubation with Schiff's reagent. Cells were counterstained with hematoxylin and mounted with DPX. Reagents were purchased from Sigma-Aldrich.

LDL uptake

LDL receptor and LDL uptake were analyzed using a commercial kit (Cayman Chemicals, Ann Arbor, MI). Non-encapsulated and encapsulated cells were grown in 96-well plates (1×10^4 cells/well). For LDL uptake, cells were washed in DMEM/F12 and incubated overnight at 37°C with LDL-Dylight 549 (1:100). After 24 h, Hoechst dye (5 $\mu\text{g}/\text{mL}$; Invitrogen) was added to stain the nuclei. LDL uptake is shown by red cytoplasmic staining. Cells were fixed for 10 min with the fixative from the kit. After several washes and blocking non-specific binding, cells were incubated with

rabbit anti-LDL receptor antibody (1:100) for 1 h at room temperature. Subsequently, cells were washed and incubated with DyLight 488 (green)-conjugated secondary antibody for 1 h. Secondary antibody was rinsed and the cells mounted with Vectashield (Vector Laboratories).

ICG uptake

ICG (Sigma-Aldrich) was dissolved in DMSO and added to cells at a final concentration of 0.5 mg/mL for 1 h at 37°C. Non-encapsulated and encapsulated HLC were rinsed several times with DPBS and visualized under bright field. Cells were then monitored for a period of 24 h to study the efflux of ICG.

CYP3A4 activity

Non-encapsulated and encapsulated cells were treated with 20 μM rifampicin for 48 h to induce CYP3A4 activity [35] and enzyme activity measured using the P450-Glo assay (Promega, Madison, WI) with 3 μM luciferin-IPA (CYP3A4 specific) as the substrate. An equal volume of detection reagent from the kit was added and readings taken on a luminometer (BMG Labtech, Offenburg, Germany) as per manufacturer's instructions.

Urea synthesis

Non-encapsulated and encapsulated cells were treated with 10 mM ammonium chloride in serum-free DMEM/F12 for 18 h. Media were collected and urea measured by the Quantichrome urea assay kit (Bioassay Systems; Hayward, CA) according to the manufacturer's instructions. Optical density readings were taken at 420 nm using a plate reader (Labsystems, Franklin, MA).

Glutathione

Non-encapsulated and decapsulated cells were plated on 96-well plates (1×10^4 cells/well). Total and oxidized glutathione were measured using the GSH/GSSG-Glo assay (Promega) according to the manufacturer's instructions. Briefly, cells were lysed with luciferin NT (total glutathione) or luciferin NT with 25 mM NEM buffer (oxidized glutathione) and gently shaken for 5 min. An equal volume of luciferin generation reagent was added and incubated for a further 30 min. Luciferin detection reagent was added and luminescence allowed to stabilize for 20 min and readings taken on a luminometer (BMG Labtech).

Expression of genes associated with urea, fat, cholesterol, and xenobiotic metabolism

Total RNA was extracted using RNeasy mini columns (Qiagen, Hilden, Germany) and quantitated using the NanoDrop1000 spectrophotometer (Thermo Fisher, Wilmington, DE). For urea cycle and CYP3A4 gene expression, HLC were stimulated with ammonium chloride or rifampicin, respectively as described previously. Briefly, 2 μg of total RNA was converted to cDNA using Superscript III (Invitrogen). cDNA was diluted 1:20 and mixed with 250 nM TaqMan probes (Applied Biosystems, Foster City, CA; Supplementary Table S1; Supplementary Data are

available online at www.liebertpub.com/scd) and amplified according to parameters given by the supplier. Samples were assayed in duplicate on a 7900HT realtime PCR machine (Applied Biosystems).

Forward and reverse primers for *CYP3A4* are also shown in Supplementary Table S1. The annealing temperature for *CYP3A4* was 58°C for 30 s and extension at 72°C for 30 s. Data were normalized to 18S rRNA, expressed as a fold change relative to naive hAEC or HLC monolayers grown for a further week and calculated by the $2^{-\Delta\Delta Ct}$ method [36].

Statistical analysis

Data are shown as the mean \pm SEM from HLC derived from a minimum of $n=4-6$ hAEC cultures. Cultures were set up in duplicate or triplicate wells for each assay. Comparisons were made using the unpaired *t*-test (GraphPad

Prism V5.04, San Diego, CA) and multiple comparisons by ANOVA followed by Tukey’s post hoc test. Significance was accorded when $P < 0.05$.

Results

Characterization of the differentiated cells

hAEC were stimulated with a combination of growth factors (EGF, FGF, and HGF), hepatic inducers (insulin and dexamethasone) and HepG2-conditioned medium in a two-step protocol over a 4-week period and the resulting cells were examined. Hepatocytes synthesize albumin and store glycogen. Albumin protein was present in naive hAEC and increased amounts detected in the differentiated cells (Fig. 1A). Like albumin, glycogen was also detected in naive hAEC by periodic acid Schiff staining, however, the differentiated cells showed intense violet staining indicative of

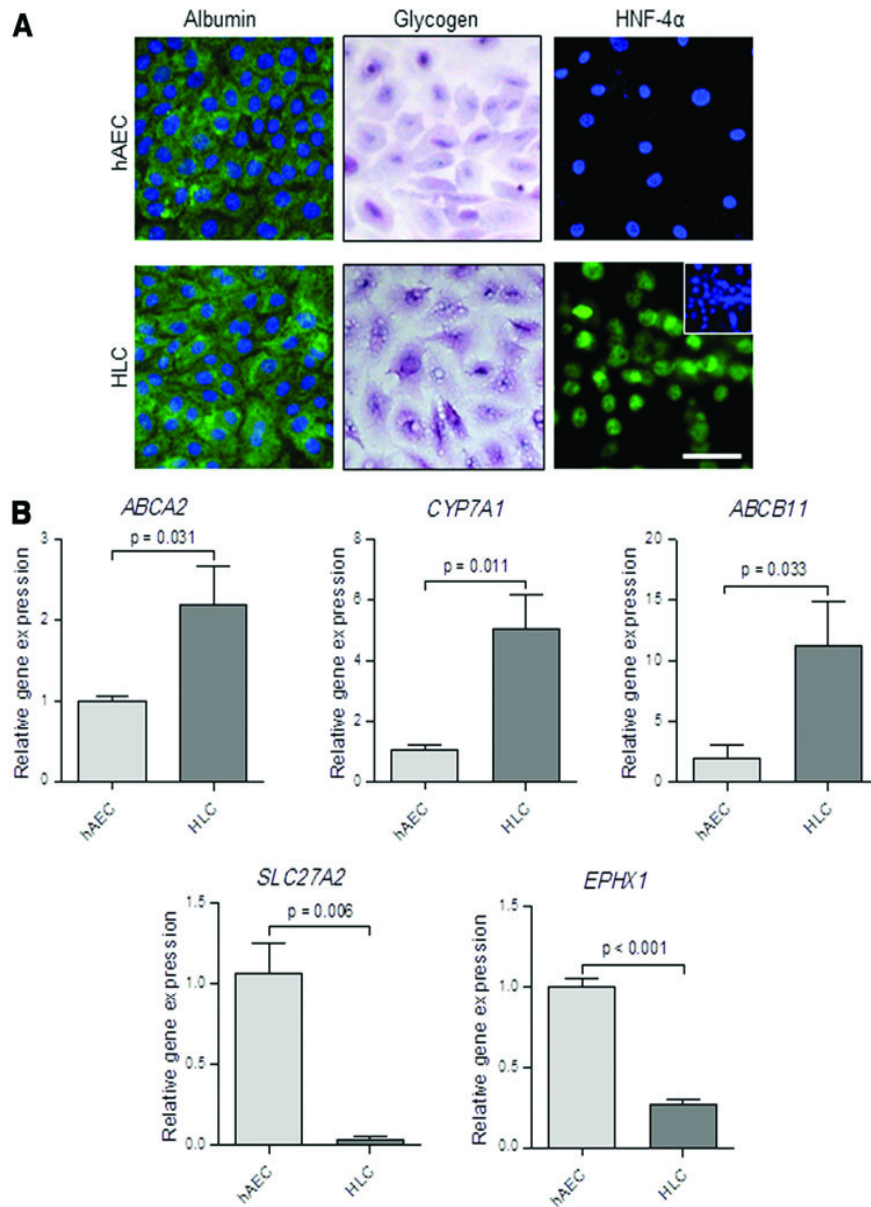


FIG. 1. Characterization of differentiated human amniotic epithelial cells (hAEC). hAEC were differentiated over a 4-week period. Albumin and glycogen continued to be accumulated while the transcription factor hepatocyte nuclear factor-4 alpha (HNF-4 α) was found only in the nuclei of stimulated cells; nuclei stained with DAPI is shown in the inset (A). Compared with hAEC, the differentiated cells showed increased expression of *ABCA2*, *CYP7A1* involved in cholesterol metabolism, and *ABCB11*, encoding a bile acid export pump. Expression of genes involved in fat (*SLC27A2*) and xenobiotic metabolism (*EPHX1*) were reduced relative to hAEC. Data were normalized to 18S rRNA, expressed as $2^{-\Delta\Delta Ct}$ relative to naive hAEC and analyzed by the unpaired *t*-test (B). Scale bar=100 μ m. Color images available online at www.liebertpub.com/scd

increased glycogen storage. Unlike the naïve hAEC, which do not express HNF-4 α , the HLC showed strong nuclear localization of the transcription factor HNF-4 α , which regulates the expression of many hepatocyte-specific genes (Fig. 1A).

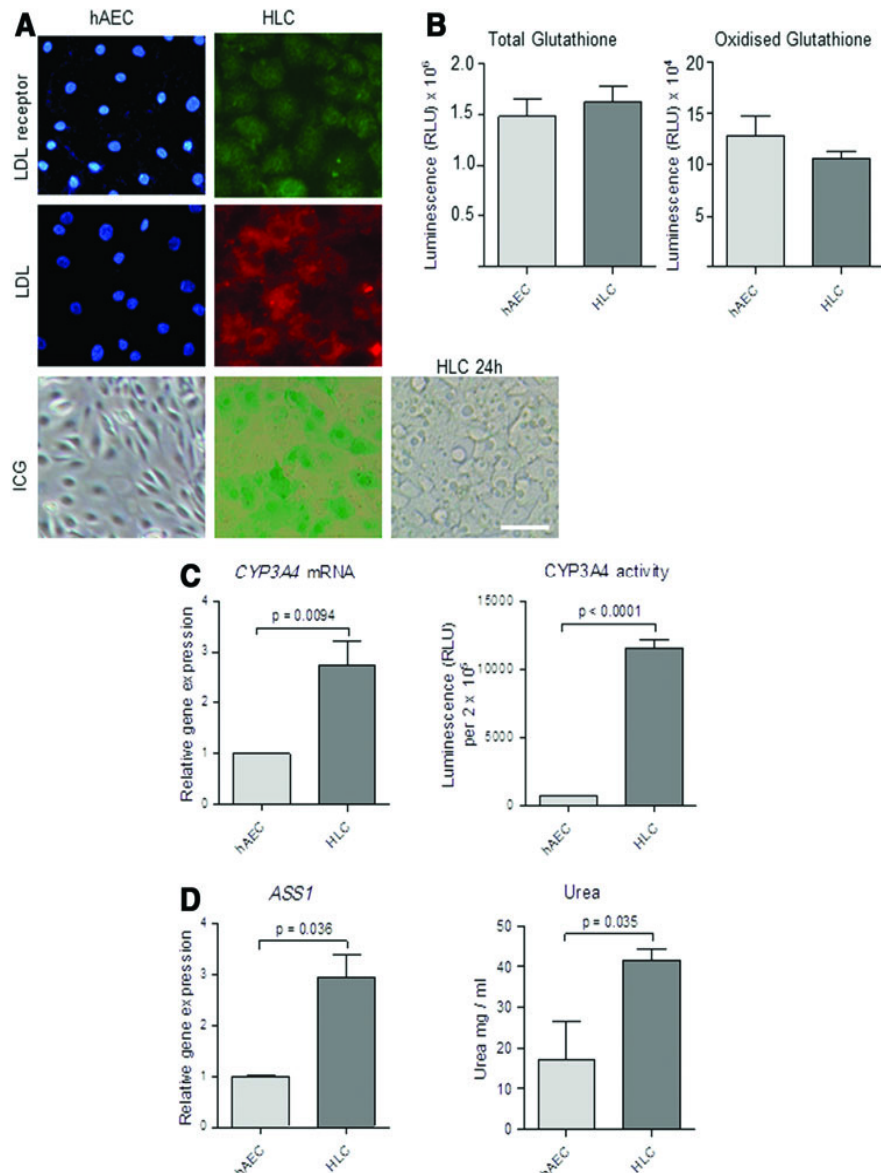
We then examined whether the differentiated cells expressed genes linked to cholesterol, fat, and xenobiotic metabolism that are known to be present in mature hepatocytes. Expression of *ABCA2* associated with cholesterol transport and *CYP7A1* encoding an enzyme that catalyses the first step in the cholesterol catabolic pathway were elevated compared with naïve hAEC ($P < 0.05$ and $P < 0.01$, respectively; Fig. 1B). The membrane transporter *ABCA1* was expressed by hAEC but its expression did not alter with differentiation (Supplementary Fig. S1) while *APOF* that is implicated in cholesterol metabolism was absent in naïve and stimulated hAEC. *HSD3B7* and *ABCB11/BSEP* are involved in the bile acid synthesis pathway that utilizes cholesterol and bile acid export, respectively. *HSD3B7* was expressed in naïve and differentiated cells while *ABCB11/*

BSEP expression was elevated compared with naïve hAEC ($P < 0.05$). *ACOX2*, *BAAT*, and *SCL27A2* regulate fat metabolism. There were no significant changes in *ACOX2* and *BAAT* expression following differentiation (Supplementary Fig. S1) while *SCL27A2* was highly suppressed in the differentiated cells ($P < 0.01$). Genes associated with xenobiotic metabolism *AKR1C3* and *HAMP* were elevated but not significantly, whereas *EPHX1* mRNA was decreased in the stimulated cells ($P < 0.001$; Fig. 1B).

Functional characterization of the differentiated cells

Next, we examined whether the differentiated cells were able to perform some of the key functions of hepatocytes. LDL receptors were evident in the differentiated cells and these cells were able to take up LDL, whereas the hAEC neither expressed LDL receptors nor showed LDL uptake (Fig. 2A). ICG is taken up by hepatocytes and effluxed unchanged with the bile acids. Differentiated cells showed

FIG. 2. Functional characteristics of the differentiated cells. Differentiated cells were positive for low-density lipoprotein (LDL) receptors and LDL was present in the cytoplasm in contrast to naïve hAEC. Only differentiated cells took up indocyanine green (ICG) and effluxed the dye (A). Total and oxidized glutathione levels remained similar (B). Differentiated cells showed increased mRNA expression of the drug metabolizing enzyme *CYP3A4* and had elevated *CYP3A4* enzymatic activity after rifampicin stimulation compared with hAEC (C). Upon stimulation with ammonium chloride, there was increased mRNA expression of the urea cycle gene *ASS1* and increased urea synthesis in the differentiated cells relative to naïve hAEC. Data were analyzed by the unpaired *t*-test (D). Scale bar = 100 μ m. Color images available online at www.liebertpub.com/scd



uptake of ICG unlike the naïve hAEC and ICG was effluxed within 24 h. Glutathione levels are indicative of the ability of cells to eliminate free radicals while levels of oxidized glutathione show effective scavenging of free radicals. The differentiated cells had high levels of total glutathione and oxidized glutathione; but these levels were similar to those of hAEC (Fig. 2B). CYP3A4 is a major class of P450 enzymes responsible for drug metabolism in hepatocytes. Following stimulation with the specific inducer rifampicin, CYP3A4 mRNA expression was significantly increased in the differentiated cells compared with naïve hAEC ($P < 0.01$), and CYP3A4 enzyme activity increased concurrently ($P < 0.0001$ vs. hAEC; Fig. 2C). Another important function of hepatocytes is detoxification. We examined the expression of enzymes associated with the removal of ammonia via the urea cycle. Upon stimulation with ammonium chloride, mRNA of the urea cycle enzyme *ASS1* was elevated in the differentiated cells compared with naïve hAEC ($P < 0.05$; Fig. 2D). However, there was no significant change in *ARG1* and *CPS1* expression (Supplementary Fig. S1). Consistent with these findings, hAEC showed some ability to synthesize urea following stimulation with ammonium chloride, whereas the differentiated cells produced higher amounts of urea ($P < 0.05$; Fig. 2D). Collectively, these findings confirm that the hAEC had differentiated into HLC.

We also examined the functional competency of the differentiated cells compared to the transformed human hepatocyte cell line HepG2. ICG was taken up by HepG2 cells and effluxed within 24 h. Total and oxidized glutathione levels were similar. However, CYP3A4 activity in the HepG2 cells was nearly twofold greater while urea production was three times higher (Table 1).

Viability and gene expression of encapsulated HLC

Next, we examined the effects of encapsulation on viability and gene expression in the HLC. HLC encapsulated in barium alginate microcapsules were maintained for 7 days in culture. Initially, we evaluated the viability of monolayer and encapsulated HLC at day 0 using CFDA/PI staining followed by flow cytometry. The percentage of viable cells in monolayer HLC was 86.9 ± 1.0 (mean \pm SEM) and there was no significant loss of viability immediately following encapsulation (84.1 ± 2.8 ; Fig. 3A). Similar to monolayer HLC, the encapsulated HLC were viable after 7 days (85.1 ± 1.3). Representative photomicrographs and flow cytometry plots of cells stained with CFDA/PI are shown in Figure 3A. Encapsulated HLC continued to have HNF-4 α

protein localized in the nuclei after 7 days in culture (Fig. 3B). Similarly, cytoplasmic albumin was abundant and glycogen staining showed intense, cytoplasmic violet coloration in the encapsulated HLC cultures (Fig. 3B).

We also assessed changes in gene expression in the encapsulated HLC after 7 days in culture. Initially, we determined whether the extended culture period altered the mRNA expression in monolayer cultures. There were no significant changes in the expression of genes linked to fat, cholesterol, and xenobiotic metabolism between monolayer HLC grown for ± 1 week except for *ACO2* and *BAAT* ($P < 0.05$ by ANOVA; Supplementary Fig. S2). Following encapsulation, expression of *ACO2* and *BAAT* remained low, while *ABCA1* declined in the encapsulated HLC ($P < 0.05$ vs. extended HLC) and *SLC27A2*, which was absent in the extended HLC was expressed in the encapsulated HLC ($P < 0.001$; Fig. 3C).

Functional properties of encapsulated HLC

Like the monolayer cultures, the encapsulated HLC showed LDL uptake as shown by the red fluorescence in the cytoplasm. The encapsulated HLC took up ICG (Fig. 4A) and effluxed the dye within 24 h similar to monolayer HLC (data not shown). While total glutathione levels remained unchanged with extended culture, levels declined with encapsulation ($P < 0.05$; Fig. 4B). Oxidized glutathione levels were lower in the encapsulated HLC compared with the extended HLC cultures ($P < 0.01$).

The encapsulated and extended monolayer HLC responded to rifampicin stimulation showing increased CYP3A4 mRNA expression with the encapsulated HLC having the highest expression levels ($P < 0.05$; Fig. 4C). We then investigated the expression of HNF-4 α , one of the main regulators of CYP3A4 expression, and likewise found highly increased HNF-4 α mRNA expression in the encapsulated HLC treated with rifampicin ($P < 0.001$; Fig. 4C). Analyzing CYP3A4 activity, the highest levels were seen in the encapsulated HLC ($P < 0.01$ vs. extended monolayer HLC cultures; Fig. 4C).

There was no difference in the mRNA expression of urea cycle enzymes *ASS1*, *ARG1*, and *CPS1* between HLC monolayer cultures ± 1 week. While there were changes in mRNA expression with encapsulation (*ARG1* decreased while *CPS1* was elevated), the relative changes were minor. Urea output was elevated in the encapsulated HLC compared with the extended monolayer cultures ($P < 0.05$ by ANOVA; Fig. 4D).

We then compared the functional aspects of encapsulated HLC with encapsulated HepG2 cells. CYP3A4 activity, urea secretion, and oxidized glutathione levels of encapsulated HLC were similar to encapsulated HepG2 (Table 1). Overall, the encapsulated HLC were functionally closer to the HepG2 cells, suggesting that encapsulation augmented some HLC functions.

Discussion

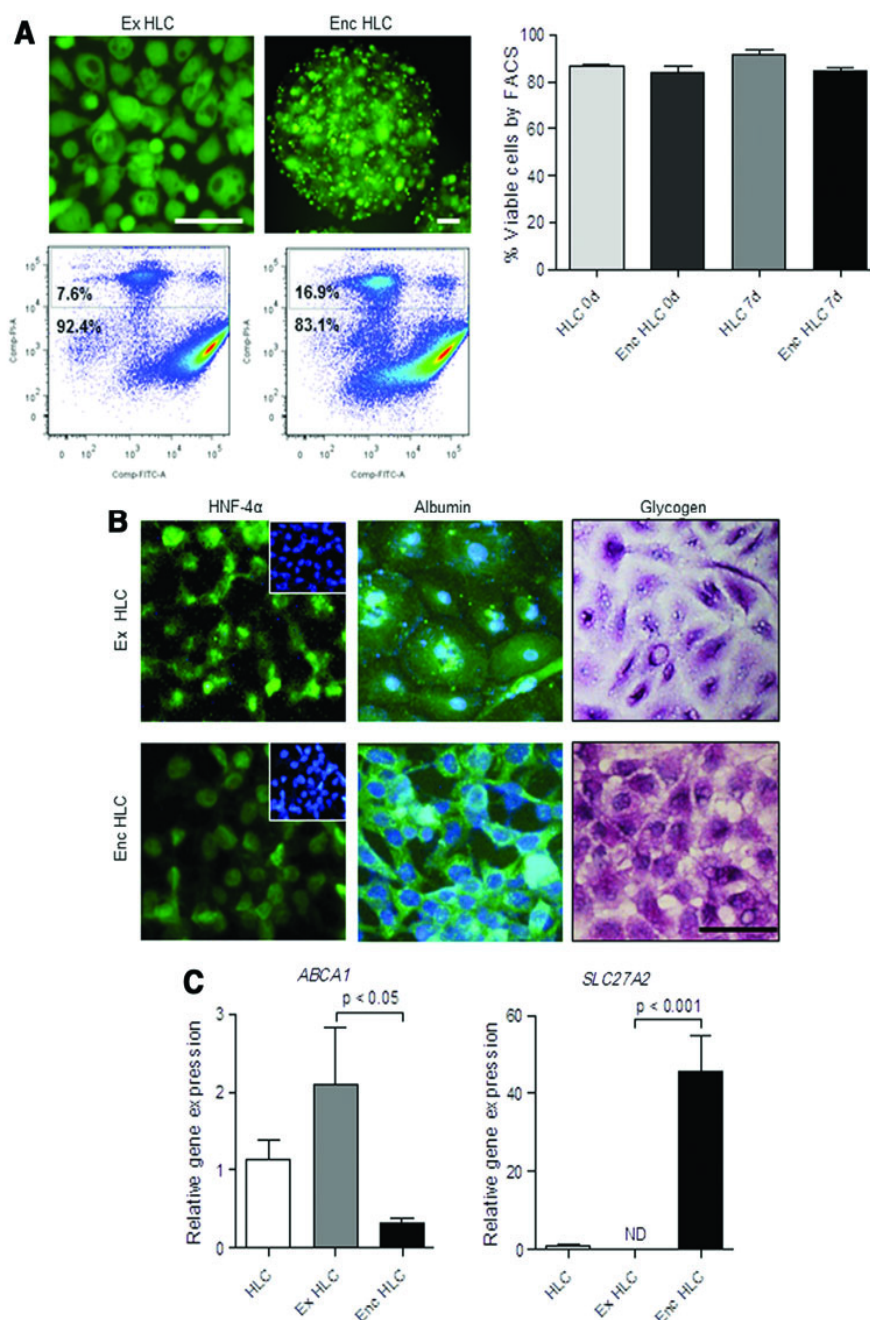
We showed that hAEC differentiate into HLC, that these HLC remain viable and functional following encapsulation in barium alginate microspheres, and that there was a significant increase in urea output and CYP3A4 activity

TABLE 1. COMPARISON OF FUNCTIONAL PROPERTIES OF HLC AND HepG2 CELLS

Assay	HepG2:HLC	Enc-HepG2: Enc-HLC
Total glutathione	1.063	0.634
Oxidized glutathione	0.869	1.105
CYP3A4 activity	1.878	1.246
Urea synthesis	3.247	1.310

Enc, encapsulation; HLC, hepatocyte-like cells.

FIG. 3. Characterization of encapsulated hepatocyte-like cells (enc HLC). HLC were encapsulated and cultured for 7 days to determine effects on viability and function. Comparisons were made with monolayer cultures extended for 7 days (ex HLC). Enc HLC remained viable as shown by 6-carboxyfluorescein diacetate (CFDA)/propidium iodide (PI) staining and quantitated by flow cytometry (A). HNF-4 α localized to the nuclei of enc HLC; DAPI-stained nuclei shown in the *inset*. Enc HLC had stored albumin and glycogen after 7 days in culture (B). Scale bar=100 μ m. Relative to ex HLC, mRNA expression of *ABCA1* decreased while *SLC27A2* increased in enc HLC; data were analyzed by ANOVA followed by Tukey's post hoc test (C). Color images available online at www.liebertpub.com/scd



following encapsulation. HLC were differentiated from hAEC in a similar manner as previously reported [20,22], except for the addition of HepG2-conditioned medium. Studies have shown that when hAEC were co-cultured with mouse hepatocytes expression of albumin, α 1 anti-trypsin, and cytochrome P450 enzyme was increased [25]. Conditioned medium from human HepG2 cells, a non-xenogenic cell source, was also effective since HLC expressed albumin, glycogen, and HNF-4 α . The HLC also expressed several mRNAs present in hepatocytes and were able to carry out hepatocyte-specific functions.

The HLC expressed genes linked with cholesterol, fat, and xenobiotic metabolism and importantly, encapsulation did not inhibit their expression. An important functional test

was to determine whether the HLC would take up cholesterol and convert it into bile acids. The HLC had abundant LDL receptors and took up LDL. Further, the expression of *CYP7A1*, which encodes the rate-limiting enzyme in the first step of cholesterol breakdown and *ABCA2*, a membrane transporter, increased with differentiation, and the expression remained unaltered with culture following encapsulation. *CYP7A1* mRNA expression is regulated by HNF-4 α [37]. HNF-4 α protein was localized to the nuclei of the HLC and it appears that downstream target genes of HNF-4 α are being transcribed in the HLC. Moreover, high expression level of *ABCB11/BSEP*, the bile acid export pump, was maintained in the HLC following encapsulation. In a previous study, we detected bile canaliculi like structures in the

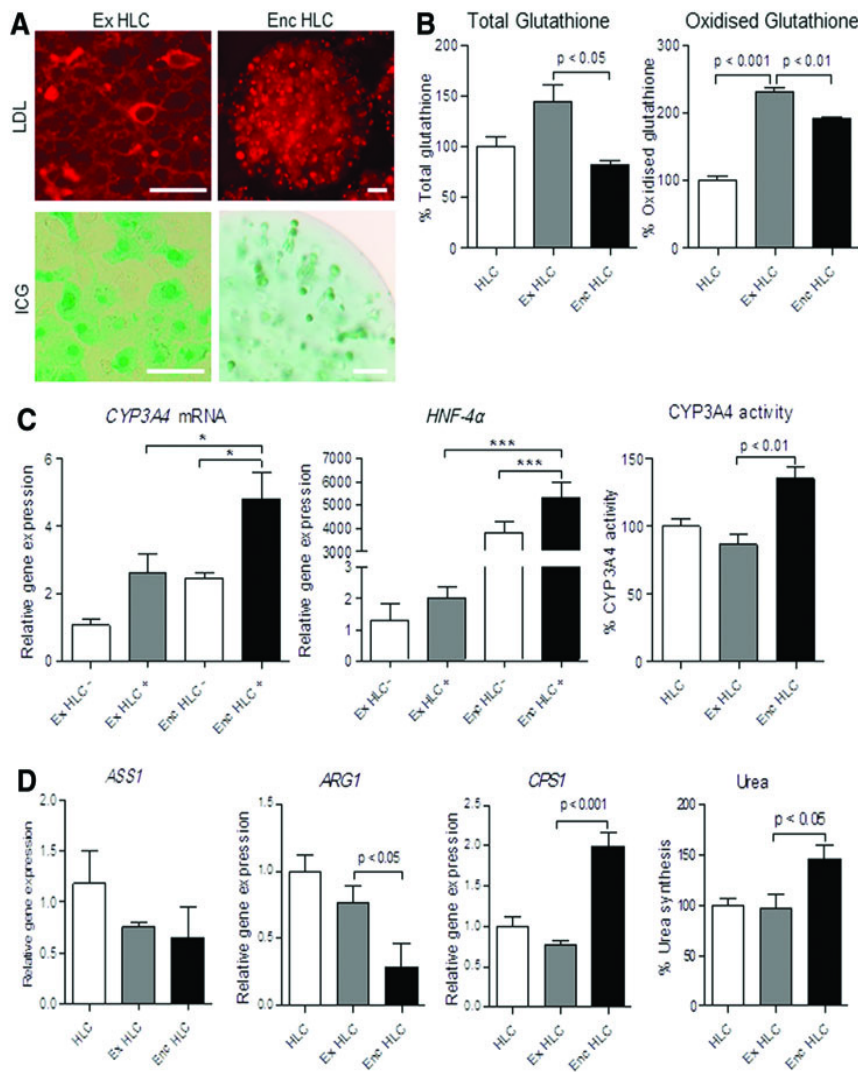


FIG. 4. Functional characteristics of enc HLC. Enc HLC cultured for 7 days took up LDL and ICG (A). Both total and oxidized glutathione levels in enc HLC grown for 7 days were lower than monolayer HLC cultures extended for 7 days (ex HLC) (B). Rifampicin stimulation (+) and encapsulation led to increased *CYP3A4* mRNA expression. *HNF-4α*, which regulates *CYP3A4* mRNA expression was highly elevated in the enc HLC. *CYP3A4* enzymatic activity was highest in the enc HLC. **P* < 0.05 and ****P* < 0.001, respectively (C). Despite some changes in the mRNA expression of the urea cycle genes *ARG1* and *CPS1*, urea output increased in enc HLC (D). mRNA expression data were normalized to *18S* rRNA, expressed as $2^{-\Delta\Delta Ct}$ relative to HLC. Comparisons were made by ANOVA. Scale bar = 100 μ m. Color images available online at www.liebertpub.com/scd

HLC derived from hAEC [20]. Collectively, while these data suggest that bile acid is synthesized and secreted, it would be important to confirm the presence of bile acids via HPLC analysis.

Uptake and efflux of ICG is clinically used to evaluate liver functions [38,39]. The monolayer HLC showed uptake of ICG and complete efflux occurred within 24 h. A similar profile in the uptake and efflux of ICG was also seen with the encapsulated HLC. ICG is removed from the liver together with the bile acids, suggesting that functional bile canaliculi may be present in the HLC.

Inflammation and breakdown of drugs and xenobiotics via cytochrome P450 enzymes generate reactive oxygen species (ROS) such as superoxide and hydrogen peroxide. To prevent ROS-mediated damage to hepatocytes, cytoplasmic superoxide, and hydrogen peroxide are inactivated producing oxidized glutathione [40]. The HLC had high levels of oxidized glutathione suggesting that they can efficiently eliminate ROS. Importantly, glutathione incorporates cysteine and prevents cysteine toxicity and generation of lethal ROS [41]. Although not significant, encapsulated

HLC had a higher ratio of oxidized glutathione to total glutathione relative to non-encapsulated HLC. This implies that the encapsulated HLC were generating higher levels of ROS and utilizing glutathione to mop-up the ROS. Interestingly, in addition to *CYP3A4* activity, higher levels of ROS are generated via urea synthesis and notably both of these functions were elevated in the encapsulated HLC.

One of the important functions of hepatocytes is xenobiotic metabolism and the cytochrome P450 family members are the major phase I enzymes implicated in the process. Studies have shown that HLC derived from hAEC have functional *CYP1A2* and *CYP3A7* enzymes [21,22,25]. *CYP3A4* is highly expressed in the liver and is thought to breakdown almost 50% of all therapeutic drugs [42]. Although *CYP3A4* activity significantly increased with differentiation, enzyme activity in the monolayer cultures was only half that of HepG2 cells. These findings are consistent with earlier reports showing that *CYP3A4* activity in cultured HLC derived from hAEC does not reach levels seen in the transformed HepG2 cell line or human hepatocytes [22,24,25]. Although not ideal HepG2 cells are commonly

used for comparison in lieu of human hepatocytes, which are difficult to source and culture. The underlying cause of low CYP3A4 activity is unclear but it may be partly attributed to lower expression of CYP3A4 mRNA due to epigenetic regulation. However, CYP3A4 mRNA expression was responsive to rifampicin stimulation with encapsulated HLC showing the strongest upregulation of CYP3A4 mRNA. HLC derived from hAEC express transcription factors such as PXR, CAR, and RAR [24], which regulate CYP3A4 expression. CYP3A4 is also a downstream target of the transcription factor HNF-4 α [43]. As reported in the encapsulated, transformed human hepatocyte cell line Huh7 [44], we found highly elevated HNF-4 α mRNA levels in the encapsulated HLC and nuclear HNF-4 α protein, which may have contributed toward increased CYP3A4 mRNA expression and subsequently CYP3A4 protein and activity. Indeed, CYP3A4 activity in the encapsulated HLC was close to that of encapsulated HepG2 cells. Previous studies reported elevated CYP3A4 activity in hepatocytes grown on matrices or encapsulated to create a three-dimensional environment [45–47], and that the increase in CYP3A4 activity could be due to increased cell to cell contact, additional extracellular matrix and recovery of cell polarity within in the microcapsule [44,48]. Thus, encapsulated HLC may also be suitable as an in vitro drug screening tool.

Earlier studies revealed the presence of OTC, an important enzyme of the urea cycle in HLC derived from hAEC, and that urea was produced [22,25]. Encapsulated HLC had significantly enhanced levels of urea synthesis relative to monolayer HLC. Similar findings have been observed in human hepatocytes, which showed significant increases in urea synthesis upon encapsulation [46]; however, the mechanism underlying increased urea synthesis with encapsulation remains to be elucidated.

Collectively, our data suggest that gene expression and the functional properties of the HLC were retained following encapsulation and their culture for at least 7 days. Microencapsulation is a strategy used to prevent the rejection of grafted tissues [49]. Transplantation of encapsulated islet cells to treat type 1 diabetes is currently being evaluated clinically [50]. Evaluating the effects of encapsulation on HLC function is an important first step in assessing whether encapsulated HLC could provide an alternative approach to the transplantation of naïve stem cells into the liver or spleen, which would subsequently differentiate into HLC. Studies have shown that hAEC delivered into the murine liver differentiated into HLC expressing HNF-4 α , CYP genes, hepatocyte-enriched transcription factors, and hepatic transporter proteins and could rescue a murine retrosine model of liver regeneration [25]. hAEC also rescued mice with intermediate maple syrup urine disease with improvement in peripheral metabolites [51,52]. Unlike naïve hAEC transplantation, it may be feasible to graft encapsulated HLC into an extra hepatic site such as the peritoneal cavity. This would allow the delivery of large numbers of HLC, which may be able to provide immediate support to liver function. Indeed, a recent study showed that encapsulated HLC generated from umbilical cord blood cells and grafted into the peritoneal cavity was able to rescue rats with acute hepatic failure [53]. HLC derived from hAEC secrete some of the immunomodulatory factors produced by the parental

cells, but soluble HLA-G was significantly lower [22]. In addition to reduced immunomodulation, it may be important to prevent cell–cell contact-mediated interactions with allogeneic immune cells by means such as encapsulation. The HLC were found to have increased HLA Class IA and II antigens and co-stimulatory molecules compared with naïve hAEC and directly interacted with allogeneic T cells stimulating their proliferation in vitro [22]. Such interaction in vivo would lead to cytotoxic outcomes for the HLC.

However, the diffusion of nutrients and oxygen to the core of the microcapsule remains a key challenge in cell encapsulation. Insufficient nutrient and oxygen diffusion to the core of the capsules can activate hypoxia-inducible factor-1 alpha (HIF-1 α) and lead to eventual necrotic cell death [54]. In this study, we found that encapsulated HLC remained viable for a week in culture suggesting sufficient diffusion of nutrients and oxygen to the core of the microcapsules. However, the effects of longer term in vitro culture and importantly the effects in vivo on viability, gene expression, and function need careful assessment. In conclusion, we have shown that HLC derived from hAEC can be encapsulated within alginate microcapsules without loss of viability and with improvement to key functions such as CYP3A4 activity and urea synthesis suggesting that further evaluation in animal models is warranted.

Acknowledgments

Study funded by a SMART grant from the Australian Regenerative Medicine Institute. U.M. is supported by a Researcher Accelerator Award from Monash University and B.K. by NHMRC grant no. 509178, KAIMRC grant no. RC08/114, and KACST grant no. ARP-29-186. V. Vaghjiani and U.M. are supported by the Victorian Government's Operational Infrastructure Support Program.

Author Disclosure Statement

The authors have no conflicts of interest financial or otherwise.

References

1. Lee WM. (2012). Acute liver failure. *Semin Respir Crit Care Med* 33:36–45.
2. Hansen K and S Horslen. (2008). Metabolic liver disease in children. *Liver Transpl* 14:713–733.
3. Bilir BM, D Guinette, F Karrer, DA Kumpe, J Krysl, J Stephens, L McGavran, A Ostrowska and J Durham. (2000). Hepatocyte transplantation in acute liver failure. *Liver Transpl* 6:32–40.
4. Strom SC, JR Chowdhury and IJ Fox. (1999). Hepatocyte transplantation for the treatment of human disease. *Semin Liver Dis* 19:39–48.
5. Habibullah CM, IH Syed, A Qamar and Z Taher-Uz. (1994). Human fetal hepatocyte transplantation in patients with fulminant hepatic failure. *Transplantation* 58:951–952.
6. Horslen SP, TC McCowan, TC Goertzen, PI Warkentin, HB Cai, SC Strom and IJ Fox. (2003). Isolated hepatocyte transplantation in an infant with a severe urea cycle disorder. *Pediatrics* 111:1262–1267.
7. Soltys KA, A Soto-Gutierrez, M Nagaya, KM Baskin, M Deutsch, R Ito, BL Shneider, R Squires, J Vockley, et al. (2010). Barriers to the successful treatment of liver disease by hepatocyte transplantation. *J Hepatol* 53:769–774.

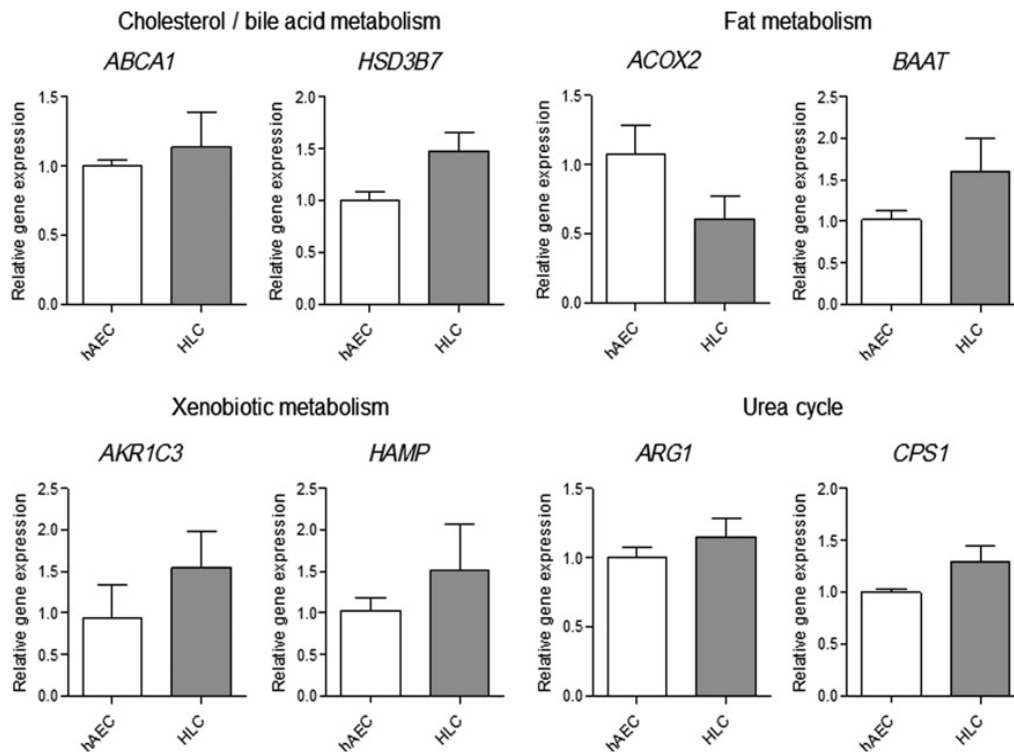
8. Hannan NR, CP Segeritz, T Touboul and L Vallier. (2013). Production of hepatocyte-like cells from human pluripotent stem cells. *Nat Protoc* 8:430–437.
9. Touboul T, NR Hannan, S Corbineau, A Martinez, C Martinet, S Branchereau, S Mainot, H Strick-Marchand, R Pedersen, et al. (2010). Generation of functional hepatocytes from human embryonic stem cells under chemically defined conditions that recapitulate liver development. *Hepatology* 51:1754–1765.
10. Basma H, A Soto-Gutierrez, GR Yannam, L Liu, R Ito, T Yamamoto, E Ellis, SD Carson, S Sato, et al. (2009). Differentiation and transplantation of human embryonic stem cell-derived hepatocytes. *Gastroenterology* 136:990–999.
11. Alison MR, R Poulosom, R Jeffery, AP Dhillon, A Quaglia, J Jacob, M Novelli, G Prentice, J Williamson and NA Wright. (2000). Hepatocytes from non-hepatic adult stem cells. *Nature* 406:257.
12. Banas A, T Teratani, Y Yamamoto, M Tokuhara, F Take-shita, G Quinn, H Okochi and T Ochiya. (2007). Adipose tissue-derived mesenchymal stem cells as a source of human hepatocytes. *Hepatology* 46:219–228.
13. Tamagawa T, S Oi, I Ishiwata, H Ishikawa and Y Nakamura. (2007). Differentiation of mesenchymal cells derived from human amniotic membranes into hepatocyte-like cells in vitro. *Hum Cell* 20:77–84.
14. Anzalone R, M Lo Iacono, S Corrao, F Magno, T Loria, F Cappello, G Zummo, F Farina and G La Rocca. (2010). New emerging potentials for human Wharton's jelly mesenchymal stem cells: immunological features and hepatocyte-like differentiative capacity. *Stem Cells Dev* 19:423–438.
15. Vaghjiani V, V Vaithilingam, B Tuch, W Sievert and U Manuelpillai. (2013). Deriving hepatocyte-like cells from placental cells for transplantation. *Curr Stem Cell Res Ther* 8:15–24.
16. Stock P, S Bruckner, S Ebensing, M Hempel, MM Dollinger and B Christ. (2010). The generation of hepatocytes from mesenchymal stem cells and engraftment into murine liver. *Nat Protoc* 5:617–627.
17. Aurich I, LP Mueller, H Aurich, J Luetzkendorf, K Tisljar, MM Dollinger, W Schormann, J Walldorf, JG Hengstler, WE Fleig and B Christ. (2007). Functional integration of hepatocytes derived from human mesenchymal stem cells into mouse livers. *Gut* 56:405–415.
18. Wu XB and R Tao. (2012). Hepatocyte differentiation of mesenchymal stem cells. *Hepatobiliary Pancreat Dis Int* 11:360–371.
19. Charbord P. (2010). Bone marrow mesenchymal stem cells: historical overview and concepts. *Hum Gene Ther* 21:1045–1056.
20. Ilancheran S, A Michalska, G Peh, EM Wallace, M Pera and U Manuelpillai. (2007). Stem cells derived from human fetal membranes display multilineage differentiation potential. *Biol Reprod* 77:577–588.
21. Miki T, T Lehmann, H Cai, DB Stolz and SC Strom. (2005). Stem cell characteristics of amniotic epithelial cells. *Stem Cells* 23:1549–1559.
22. Tee JY, V Vaghjiani, YH Liu, P Murthi, J Chan and U Manuelpillai. (2013). Immunogenicity and immunomodulatory properties of hepatocyte-like cells derived from human amniotic epithelial cells. *Curr Stem Cell Res Ther* 8:91–99.
23. Takashima S, H Ise, P Zhao, T Akaike and T Nikaïdo. (2004). Human amniotic epithelial cells possess hepatocyte-like characteristics and functions. *Cell Struct Funct* 29:73–84.
24. Miki T, F Marongiu, EC Ellis, K Dorko, K Mitamura, A Ranade, R Gramignoli, J Davila and SC Strom. (2009). Production of hepatocyte-like cells from human amnion. *Methods Mol Biol* 481:155–168.
25. Marongiu F, R Gramignoli, K Dorko, T Miki, AR Ranade, M Paola Serra, S Doratiotto, M Sini, S Sharma, et al. (2011). Hepatic differentiation of amniotic epithelial cells. *Hepatology* 53:1719–1729.
26. Opara EC and WF Kendall Jr. (2002). Immunoisolation techniques for islet cell transplantation. *Expert Opin Biol Ther* 2:503–511.
27. Santos E, J Zarate, G Orive, RM Hernandez and JL Pedraz. (2010). Biomaterials in cell microencapsulation. *Adv Exp Med Biol* 670:5–21.
28. de Vos P, MM Faas, B Strand and R Calafiore. (2006). Alginate-based microcapsules for immunoisolation of pancreatic islets. *Biomaterials* 27:5603–5617.
29. Vaithilingam V, G Kollarikova, M Qi, I Lacik, J Oberholzer, GJ Guillemin and BE Tuch. (2011). Effect of prolonged gelling time on the intrinsic properties of barium alginate microcapsules and its biocompatibility. *J Microencapsul* 28:499–507.
30. Nakamura K, R Mizutani, A Sanbe, S Enosawa, M Kasahara, A Nakagawa, Y Ejiri, N Murayama, Y Miyamoto, et al. (2011). Evaluation of drug toxicity with hepatocytes cultured in a micro-space cell culture system. *J Biosci Bioeng* 111:78–84.
31. Selden C, A Shariat, P McCloskey, T Ryder, E Roberts and H Hodgson. (1999). Three-dimensional in vitro cell culture leads to a marked upregulation of cell function in human hepatocyte cell lines—an important tool for the development of a bioartificial liver machine. *Ann N Y Acad Sci* 875:353–363.
32. Miki T, F Marongiu, E Ellis and CS S. (2007). Isolation of amniotic epithelial stem cells. *Curr Protoc Stem Cell Biol* Chapter 1:Unit 1E 3.
33. Pratama G, V Vaghjiani, JY Tee, YH Liu, J Chan, C Tan, P Murthi, C Gargett and U Manuelpillai. (2011). Changes in culture expanded human amniotic epithelial cells: implications for potential therapeutic applications. *PLoS One* 6:e26136.
34. Foster JL, G Williams, LJ Williams and BE Tuch. (2007). Differentiation of transplanted microencapsulated fetal pancreatic cells. *Transplantation* 83:1440–1448.
35. Rae JM, MD Johnson, ME Lippman and DA Flockhart. (2001). Rifampin is a selective, pleiotropic inducer of drug metabolism genes in human hepatocytes: studies with cDNA and oligonucleotide expression arrays. *J Pharmacol Exp Ther* 299:849–857.
36. Livak KJ and TD Schmittgen. (2001). Analysis of relative gene expression data using real-time quantitative PCR and the 2⁻(-Delta Delta C(T)) Method. *Methods* 25:402–408.
37. Crestani M, A Sadeghpour, D Stroup, G Galli and JY Chiang. (1998). Transcriptional activation of the cholesterol 7alpha-hydroxylase gene (CYP7A) by nuclear hormone receptors. *J Lipid Res* 39:2192–2200.
38. Faybik P and H Hetz. (2006). Plasma disappearance rate of indocyanine green in liver dysfunction. *Transplant Proc* 38:801–802.
39. Tsubono T, S Todo, N Jabbour, A Mizoe, V Warty, AJ Demetris and TE Starzl. (1996). Indocyanine green elimination test in orthotopic liver recipients. *Hepatology* 24:1165–1171.

40. Sies H. (1999). Glutathione and its role in cellular functions. *Free Radic Biol Med* 27:916–921.
41. Garcia-Ruiz C and JC Fernandez-Checa. (2007). Redox regulation of hepatocyte apoptosis. *J Gastroenterol Hepatol* 22 (Suppl 1):S38–S42.
42. Nebert DW and DW Russell. (2002). Clinical importance of the cytochromes P450. *Lancet* 360:1155–1162.
43. Lim YP, SC Kuo, ML Lai and JD Huang. (2009). Inhibition of CYP3A4 expression by ketoconazole is mediated by the disruption of pregnane X receptor, steroid receptor coactivator-1, and hepatocyte nuclear factor 4alpha interaction. *Pharmacogenet Genomics* 19:11–24.
44. Sainz B, Jr., V TenCate and SL Uprichard. (2009). Three-dimensional Huh7 cell culture system for the study of Hepatitis C virus infection. *Virol J* 6:103.
45. Cheng N, E Wauthier and LM Reid. (2008). Mature human hepatocytes from ex vivo differentiation of alginate-encapsulated hepatoblasts. *Tissue Eng Part A* 14:1–7.
46. Miranda JP, A Rodrigues, RM Tostoes, S Leite, H Zimmerman, MJ Carrondo and PM Alves. (2010). Extending hepatocyte functionality for drug-testing applications using high-viscosity alginate-encapsulated three-dimensional cultures in bioreactors. *Tissue Eng Part C Methods* 16:1223–1232.
47. Chia SM, KW Leong, J Li, X Xu, K Zeng, PN Er, S Gao and H Yu. (2000). Hepatocyte encapsulation for enhanced cellular functions. *Tissue Eng* 6:481–495.
48. Elkayam T, S Amitay-Shaprut, M Dvir-Ginzberg, T Harel and S Cohen. (2006). Enhancing the drug metabolism activities of C3A—a human hepatocyte cell line—by tissue engineering within alginate scaffolds. *Tissue Eng* 12:1357–1368.
49. Krishnamurthy NV and B Gimi. (2011). Encapsulated cell grafts to treat cellular deficiencies and dysfunction. *Crit Rev Biomed Eng* 39:473–491.
50. Tuch BE, GW Keogh, LJ Williams, W Wu, JL Foster, V Vaithilingam and R Philips. (2009). Safety and viability of microencapsulated human islets transplanted into diabetic humans. *Diabetes Care* 32:1887–1889.
51. Skvorak KJ, K Dorko, F Marongiu, V Tahan, MC Hansel, R Gramignoli, E Arming, T Bottiglieri, KM Gibson and SC Strom. (2013). Improved amino acid, bioenergetic metabolite and neurotransmitter profiles following human amnion epithelial cell transplant in intermediate maple syrup urine disease mice. *Mol Genet Metab* 109:132–138.
52. Skvorak KJ, K Dorko, F Marongiu, V Tahan, MC Hansel, R Gramignoli, KM Gibson and SC Strom. (2013). Placental stem cell correction of murine intermediate maple syrup urine disease. *Hepatology* 57:1017–1023.
53. Zhang FT, HJ Wan, MH Li, J Ye, MJ Yin, CQ Huang and J Yu. (2011). Transplantation of microencapsulated umbilical-cord-blood-derived hepatic-like cells for treatment of hepatic failure. *World J Gastroenterol* 17:938–945.
54. Sahai S, R McFarland, ML Skiles, D Sullivan, A Williams and JO Blanchette. (2012). Tracking hypoxic signaling in encapsulated stem cells. *Tissue Eng Part C Methods* 18:557–565.

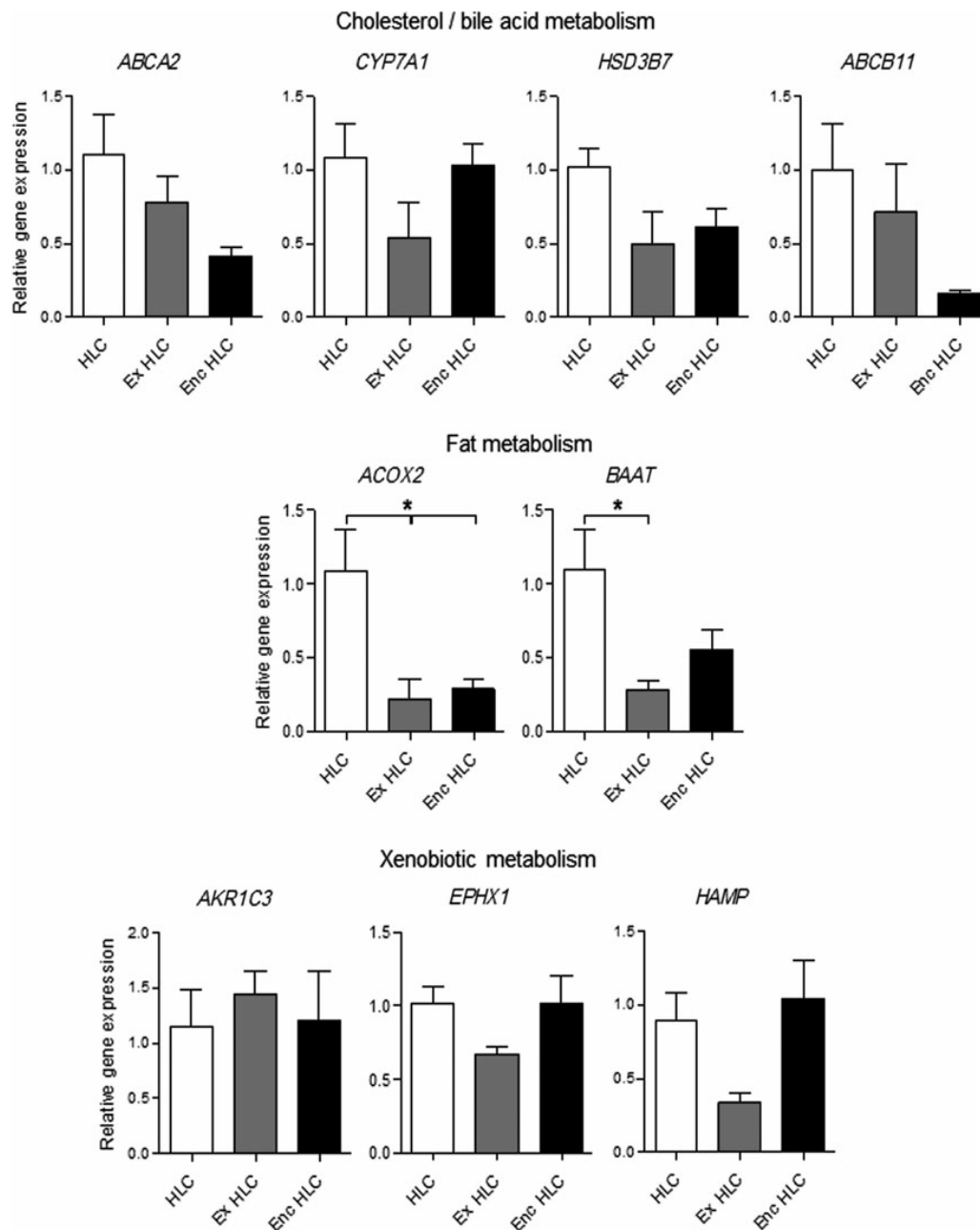
Address correspondence to:
Dr. Ursula Manuepillai
Centre for Genetic Diseases
Monash Institute of Medical Research
Monash University
27-31 Wright Street
Clayton
Victoria 3168
Australia

E-mail: ursula.manuepillai@monash.edu
ucmanuepillai@gmail.com

Received for publication October 6, 2013
Accepted after revision November 28, 2013
Republished on Liebert Instant Online December 2, 2013



SUPPLEMENTARY FIG. S1. Gene expression in human amniotic epithelial cells (hAEC) and hepatocyte-like cells (HLC). hAEC were differentiated into HLC and gene expression was examined. No significant changes in cholesterol (*ABCA1* and *HSD3B7*), fat (*ACOX2* and *BAAT*), xenobiotic (*AKR1C3* and *HAMP*) metabolism, and urea cycle genes (*ARG1* and *CPS1*) were found in HLC compared to naïve hAEC. Expression was normalized to 18S rRNA, expressed as $2^{-\Delta\Delta Ct}$ relative to naïve hAEC and analyzed by the unpaired *t*-test.



SUPPLEMENTARY FIG. S2. Gene expression in HLC, extended HLC (ex HLC), and encapsulated HLC (enc HLC). Expression in genes associated with cholesterol/bile acid (*ABCA2*, *CYP7A1*, *HSD3B7*, and *ABCB11*), fat (*ACOX2* and *BAAT*), and xenobiotic (*EPHX1* and *HAMP*) metabolism is shown. *ACOX2* and *BAAT* mRNA expression was lower in ex HLC and enc HLC compared with HLC (* $P < 0.05$), otherwise no changes in expression between HLC, ex HLC, and enc HLC were found. Expression was normalized to *18S* rRNA, expressed as $2^{-\Delta\Delta Ct}$ relative to HLC. Data were analyzed by one-way ANOVA and Tukey's post hoc test.

SUPPLEMENTARY TABLE S1. LIST OF GENES ANALYZED

<i>Gene</i>	<i>Gene name</i>	<i>TaqMan ID</i>
Cholesterol metabolism		
<i>ABCA1</i>	ATP-binding cassette, subfamily A, member 1	Hs01059118_m1
<i>CYP7A1</i>	Cytochrome P450, family 7, subfamily A, polypeptide 1	Hs00167982_m1
<i>APOF</i>	Apolipoprotein F	Hs00155750_m1
<i>ABCA2</i>	ATP-binding cassette, subfamily A, member 2	Hs00242232_m1
<i>HSD3B7</i>	Hydroxy-delta-5-steroid dehydrogenase, 3 beta- and steroid delta-isomerase 7	Hs00228639_m1
<i>ABCB11</i>	ATP-binding cassette, subfamily B, member 11	Hs00184824_m1
Fat metabolism		
<i>ACOX2</i>	Acyl-CoA oxidase 2	Hs00185873_m1
<i>SLC27A2</i>	Solute carrier family 27, subfamily A, member 2	Hs00186324_m1
<i>BAAT</i>	Bile acid CoA: amino acid <i>N</i> -acyltransferase	Hs00156051_m1
Xenobiotic metabolism		
<i>AKRIC3</i>	Aldo-keto reductase family 1, member C3	Hs00366267_m1
<i>EPHX1</i>	Epoxide hydrolase 1	Hs01116806_m1
<i>HAMP</i>	Hepcidin antimicrobial peptide	Hs00221783_m1
Drug metabolism		
<i>CYP3A4</i>	F' TGTATGAACTGGCCACTCACC R' TAGCTTGGAATCATCACCACC	
Urea cycle enzymes		
<i>CPS1</i>	Carbamoyl-phosphate synthetase 1	Hs00157048_m1
<i>ASS1</i>	Argininosuccinate synthetase 1	Hs00540723_m1
<i>ARG1</i>	Arginase 1	Hs00968979_m1
Transcription factor		
<i>HNF-4α</i>	Hepatocyte nuclear factor-4 alpha	Hs00230853_m1
Housekeeping gene		
<i>18S</i>	18S ribosomal RNA	Hs03003631_g1

Chapter 4

Role of mitochondrial DNA copy number in differentiation of hepatocyte-like cells

4.1 Introduction

Mitochondria are the powerhouse of the cell and generate the majority of energy required for cell function. Mitochondria have their own genome, which is about 1% of DNA compared to the nuclear genome. Each cell contains a specific number of mitochondria and each mitochondrion has between 1-9 copies of mitochondrial DNA (mtDNA). MtDNA copy number is directly correlated with the ATP requirement of the cell. Cells with a low adenosine triphosphate (ATP) requirement such as endothelial cells have low mtDNA copy number whilst cells with a high ATP requirement such as hepatocytes and neurons have high mtDNA copy number. During differentiation, mtDNA copy number is synchronously increased to promote differentiation and achieve optimal ATP production in terminally differentiated cells. During hepatic differentiation of embryonic cells, induced pluripotent cells and bone marrow MSC, there is increased mtDNA copy number and ATP production. Human amniotic epithelial cells (hAEC) have been shown to express hepatocyte specific genes and function and should also be able to increase their mtDNA copy number to meet functional ATP needs. Here, I evaluate the role of mtDNA copy number in hepatocyte-like cells derived from hAEC.

Human Amniotic Epithelial cells

HAEC are derived from inner amniotic membrane of the placental membranes. The placental membrane consists of a chorionic membrane and an amniotic membrane, which are lightly fused. Amniotic membranes are of foetal origin and consist of a basal collagen layer that harbours amniotic mesenchymal cells and a top single layer of amniotic epithelial cells that are directly in contact with the amniotic fluid. HAEC are derived from the inner cell mass and they possess pluripotency markers such as octamer binding protein 4 (OCT4), SOX-2 and NANOG (1, 2). They also express stem cell markers SSEA-3, SSEA-4, TRA 1-60 and

TRA 1-81 (2) and have been shown to differentiate into endoderm, mesoderm and ectoderm lineages (1). Interestingly, they do not form teratomas in NOD/SCID mice when injected in under the testes capsule (1, 2). It has previously been demonstrated that mtDNA copy number plays a critical role in the initiation of tumorigenesis. However, the tumorigenic capacity of mtDNA deleted hAEC has not been evaluated.

HAEC have been shown to differentiate into hepatic lineages with variable success. Earlier studies showed expression of albumin, hepatocyte nuclear factor 4 (HNF4 α) (2) and Hepatocyte growth factor (HGF) (1). HAEC have a unique immunologic profile; they express high HLA class 1A, no HLA class II and no expression of the co-stimulatory molecules CD80 and CD86 and high CD40 (3). They also express high levels of HLA-G, which is thought to be one of the immune-suppression proteins (3, 4). These properties of low immunogenicity in hAEC make them ideal candidates for cell therapies. In addition to the wide plasticity of hAEC, what makes them particularly suitable for hepatocyte differentiation is expression of hepatocyte specific genes and proteins in naïve hAEC. Freshly isolated hAEC produce albumin, express α 1 anti-trypsin, GATA4 and HNF3 β (3).

Differentiation of hAEC into HLC may represent a default pathway as naïve hAEC already express hepatic progenitor markers GATA4 and HNF3 β (3). In addition, they also secrete albumin, a carrier protein secreted by hepatocytes. During differentiation of HLC, I evaluated if there was a further increase in expression of α 1 anti-trypsin and albumin. I also evaluated expression of the key hepatocyte transcription factor HNF4 α and the major cytochrome P450 enzyme CYP3A4. Since, naïve hAEC express some of the pluripotency markers, I set out to determine if pluripotency genes were down regulated with hepatic differentiation. We evaluated the gene expression of pluripotency markers OCT4, SOX2 and NANOG as well as oncogene cMYC and the human telomerase reverse transcriptase (hTERT) in differentiating HLC.

Mitochondrial DNA

Human mitochondria contain a double stranded circular genome which is 16 569 base pair in size (5). MtDNA encodes 13 polypeptides of the electron transport chain (ETC), 22 transfer RNAs and 2 ribosomal RNAs. It also contains the non-coding D-loop which contains two hyper variable region D-loop and sites where nuclear encoded mtDNA replication factors interact (5). Replication of mtDNA is driven by both nuclear and mitochondrial encoded factors. Mitochondrial transcription factor A (TFAM) initiates replication of mtDNA (6). Human mitochondrial Polymerase Gamma is a heterotrimer enzyme which consists of a catalytic subunit Polymerase Gamma A (POLGA) and two accessory subunit Polymerase Gamma B (POLGB) (7). In addition, mtDNA replication is supported by mtDNA single strand-binding protein (MTSSB), which stabilises single stranded DNA, and the mtDNA-specific helicase TWINKLE, which unwinds DNA during the replication process.

The role of mitochondria in stem cell fate

Differentiation of stem cells into functional hepatocytes is associated with a metabolic shift from glycolysis to OXPHOS which is dependent on mitochondria. Mitochondrial morphology in human pluripotent stem cells is globular with perinuclear localisation (8, 9). Whereas differentiated cells display elongated mitochondria with numerous extended cristae distributed as networks in the cytoplasm (9). In addition, there is increased mitochondrial content, mitochondrial mass and mtDNA copy number during differentiation. Stem cells generate ATP primarily through glycolysis, whereas, mature differentiated cells generate ATP primarily through OXPHOS. Inhibition of OXPHOS hinders stem cell differentiation and promotes maintenance of the pluripotent state. Increased mitochondrial biogenesis promotes OXPHOS and stimulates differentiation. I propose that increased mitochondrial

mass and copy number are the drivers of the differentiation and specification rather than these events being the hall mark of differentiation.

Role of mitochondria in hepatocytes

The liver performs essential functions of carbohydrate homeostasis, drug metabolism, lipid metabolism and protein synthesis. Insulin plays a key role in regulating blood glucose and glycogen synthesis in hepatocytes (10). Hepatocytes also produce the carrier protein albumin and detoxify ammonia via the urea cycle. Genes involved in ammonia detoxification and urea synthesis (glutamate dehydrogenase, CPS1 and OTC) are exclusively expressed in hepatocyte mitochondria. Non-alcoholic fatty liver disease (NAFLD) is defined as excessive fat in hepatocytes and may result in the compromised capacity of mitochondria to oxidise fatty acids. Increased ROS production due to defects in ETC, plays an important role in progression of NAFLD (11). Disruptions in mitochondrial metabolism can also be induced by chronic alcohol consumption resulting in reduced ATP synthase thus placing hepatocytes under bioenergetic stress. Breakdown of ethanol results in reduced activity of complex I and III of ETC and increased ROS production. Increased ROS production leads to DNA damage and is known to play a role in the activation of apoptosis. A study comparing mtDNA copy number in hepatocellular carcinoma (HCC) found that male patients had lower mtDNA copy number compared to female patients in non-cancerous liver tissue (12). These findings suggest that mtDNA copy number is essential for maintenance of liver function and perturbed mtDNA copy number results in HCC.

Mitochondrial biogenesis is primarily driven by nuclear encoded transcription factors (PPARs, NRF1 and GABP) and co-activators (PGC-1 α and β) (11). Increased mitochondrial biogenesis leads to increased ATP production through OXPHOS and fatty acid metabolism (lipid metabolism). The latter is more important for hepatocytes to produce bile acid via the

cholesterol metabolism super pathway. Mitochondrial biogenesis defects lead to cellular homeostasis imbalance resulting in increased reactive oxygen species (ROS) and incidents of HCC (11). Mitochondrial encoded cytochrome aa3, b and c1 are suppressed in liver cancer (13). Furthermore, lower cytochrome oxidase activity results in decreased respiration and disturbed ETC, thus allowing leakage of electrons and generation of ROS.

DNA methylation of POLGA

DNA methylation is a process whereby a methyl group is added to a cytosine, which results in silencing of gene expression. The process of DNA methylation is catalysed by DNA methyltransferase (DNMT) enzymes. The DNMT family of enzymes consists of DNMT1 which maintains DNA methylation, whereas, DNMT3A and DNMT3B act as *de novo* methyltransferases (14). 2-deoxycytidine is catalysed to 5-methylcytosine by the DNMT enzymes with S-adenosylmethionine acting as a methyl donor (15). Ten-eleven translocation (TET) enzymes can oxidise 5-methylcytosine (5mC) to 5-hydroxymethylcytosine (5hmC) (16, 17). TET enzymes are α -ketoglutarate dependent deoxygenases; α -ketoglutarate being a product of the citric acid (TCA) cycle and may have direct implications in ATP production via the TCA cycle and DNA methylation. The highest levels of 5hmC are found in various stem cells, suggesting potential demethylation and subsequent activation of gene transcription (18).

Transcription of POLGA is regulated by DNA methylation at exon 2 of POLGA. In human, increased levels of 5-methylcytosine at exon 2 of POLGA suppresses its transcription thus leading to little or no replication of mtDNA (19). MtDNA copy number is regulated in a tissue specific manner in mouse (20). POLGA expression is negatively correlated with DNA methylation at exon 2 of POLGA and mtDNA copy number. Liver tissue has been shown to have high mtDNA copy number and DNA methylation of exon 2 of POLGA with low

expression of POLGA (20). However, in human, hyper methylation of exon 2 of POLGA results in low mtDNA copy number and low expression of POLGA (19). Thus, there is positive inverse correlation of methylation of POLGA and mtDNA copy number in stem cells and differentiated cells.

Modulating mtDNA copy number

Genome wide demethylation can be induced by treatment with agents such as 5-azacytidine (5aza). 5aza, which has anti-metabolic activity, was first developed and used against acute myelogenous leukemia (21). 5aza is a chemical analogue of cytidine, once converted to 5-aza-2'-deoxycytidine-triphosphate, it is incorporated into DNA as a substitute for cytosine. The azacytidine-guanine base pair is recognised by DNMT1, which results in formation of a covalent bond between cytosine and DNMT1, making it unavailable for DNA methylation (22). Discovery of 5aza incorporation into DNA inhibited DNA methylation and activation of gene expression led to its use as a cancer therapeutic (23). Treating cells with 5-aza causes demethylation at exon 2 of POLGA and thus results in increased POLGA expression to increase mtDNA copy number. Alternatively, depleting mtDNA using agents such as dideoxycytidine (ddC) (24), the cell is reset to more naive state, thus allowing cells to fully differentiate towards HLC. ddC is a DNA nucleotide analogue that was used as an anti-retroviral that inhibited viral replication; but it also inhibited replication of mtDNA (25). Depleting mtDNA assimilates an embryonic stem cell-like state, which has low mtDNA copy number and results in the cells being highly proliferative. This establishes the mtDNA set point, from where they are able to increase their mtDNA copy number depending on the functional needs as they differentiate (7). I depleted mtDNA in hAEC and differentiated them for 14 days to evaluate their potential to replenish mtDNA, DNA methylation levels for POLGA at exon 2 and gene expression patterns for both hepatocyte specific and pluripotency genes.

4.2 Materials and Methods

HAEC isolation

HAEC were isolated, as previously described in the General Materials and Methods Section 2.3 and frozen in DMEM/F12 with 10% DMSO in liquid nitrogen until further use.

MtDNA depletion

HAEC were cultured for 3-5 days until they achieved epithelial morphology. To deplete mtDNA, cells were then treated with 10 μ M ddC supplemented with 50 μ g/ml Uridine (Sigma Aldrich) in DMEM/F12 with 10% FBS. The media was changed every 24 hours for 3 and 7 days.

HLC differentiation

Upon encapsulation, hAEC were differentiated into HLC, as described in section 2.4 of the General Materials and Methods. Encapsulated hAEC were differentiated into HLC for 14 and 28 days with media changed every alternate day.

5-azacytidine treatment

HAEC were plated on a collagen coated flask in DMEM/F12 with 20% FBS and 10 ng/ml of EGF. Once hAEC had attained epithelial morphology, they were treated with 0.5 μ M 5-azacytidine (Sigma Aldrich) for 48 hours in DMEM/F12 media with 10% FBS and 10 ng/ml EGF with media changed every day. 0.5 μ M 5-azacytidine was added to HLC differentiation media and hAEC were differentiated into HLC for 14 and 28 days with media changed every day. At the end of the differentiation time point, the cells were trypsinised and collected for DNA and RNA extraction.

Nucleic acid purification

DNA was extracted from cell pellets, as described in the General Materials and Methods, Section 2.5.4. RNA was extracted from cell pellets, as described in the General Materials and Methods, Section 2.5.1.

Qiagen real-time PCR gene expression array (RT² profiler)

Total RNA was extracted, as described in the General Materials and Methods Section 2.5.1 with on column DNase I digest to eliminate contaminating DNA. An additional genomic DNA elimination step was performed by adding 2 μ l of 5x genomic DNA elimination buffer (Qiagen, Hilden, Germany) to 1 μ g of RNA to a total of 10 μ l and incubated at 42°C for 10 minutes. cDNA was synthesized using the RT² First Strand Kit (Qiagen), according to the manufacturer's instructions. Each reaction consisted of 1 μ g RNA in 10 μ l, 4 μ l of 5x RT buffer, 1 μ l primers, 2 μ l RT enzyme mix and 3 μ l of autoclaved H₂O in a total volume of 20 μ l. The reactions were incubated on a thermal cycler (Hybaid Px2, Thermo Fisher) at 42°C for 15 minutes followed by 95°C for 5 minutes. 91 μ l of autoclaved H₂O was added to each sample cDNA and mixed gently.

We performed the Glucose Metabolism Array (Qiagen #PAHS-006Z) and the Mitochondrial metabolism Array (Qiagen #PAHS-008Z). The samples run on the arrays were hAEC, HLC 14d and HLC 28 days and HepG2 cells from three independent patients. The real-time PCR reactions were performed in 384 well optical reaction plates with a probe for each gene on the plate. A master mix was prepared by adding 550 μ l RT² SYBR green/ROX, 448 μ l of sterile autoclaved H₂O and 102 μ l of diluted cDNA was prepared for each replicate and time point. 10 μ l of master mix was added to each tube on the plate and run on an ABI 7900HT Real Time PCR machine (Applied Bioscience). Thermal cycling conditions were; 95°C for 5 minutes

followed by 40 cycles at 95°C for 10 seconds and annealing and extension at 60°C for 1 minute. Data were generated as cycle threshold (Ct) for each target gene. Five housekeeping genes (GUSB, HPRT1, HSP90AB1, GAPDH and β -ACTIN) were used to normalise the data. Relative gene expression was calculated using $\Delta\Delta$ CT method and expressed as fold change relative to undifferentiated hAEC.

MtDNA copy number and MeDIP

MtDNA copy number was evaluated for encapsulated HLC as described in the General Materials and Methods, Section 2.6. Immunoprecipitation for 5-methylcytosine and 5-hydroxymethylcytosine was performed on encapsulated HLC, as described in the General Materials and Methods, Section 2.7.

Gene expression

Total RNA was converted to cDNA as described in the General Materials and Methods, Section 2.5.3 and gene expression was analysed, as described in Section 2.5.4.

Statistical analysis

Data are shown as the mean \pm SEM derived from a minimum of n = 4-6 hAEC cultures. Statistical significance was determined by one-way and two-way ANOVA followed by Bonferroni *post hoc* tests using GraphPad Prism V6.01 (Graph Pad Inc., San Diego, CA). Significance was accorded when $P < 0.05$; significance given as * $p < 0.05$, ** $p < 0.01$, *** $p < 0.001$ and **** $p < 0.0001$.

4.3 Results

Glucose and mitochondrial metabolism arrays

To evaluate the metabolic capacity of HLC with regards to glucose consumption and mitochondrial metabolism, we performed gene expression arrays. As hAEC differentiate towards HLC, it is anticipated that there would be increased demand for ATP and glucose consumption. To evaluate whether there was increased glucose consumption in differentiated HLC, we analysed gene expression using real time PCR array for glucose metabolism in hAEC, HLC 14 days, HLC 28 days and HepG2 cells. There were 80 genes associated with glucose metabolism on the array plate.

There were a total of 54 genes differentially regulated in 14 day differentiated HLC compared to hAEC (Table 4.1). There were 27 genes differentially regulated genes in 28 day differentiated HLC compared to hAEC. In addition, there were 24 genes that were up regulated in both 14 day and 28 day differentiated HLC compared to hAEC (Table 4.1). The majority of the genes in differentiated HLC were up regulated compared to hAEC. Genes involved in the glycolysis pathway were up regulated in 14 and 28 day differentiated HLC (Table 4.1). Particularly, Aldolase A, B and C and Enolase 2 and 3 were significantly up regulated, thus resulting in increased glycolysis (Table 4.1). Tricarboxylic acid cycle (TCA cycle) associated genes showed up regulation in 14 day differentiated HLC and TCA cycle associated gene expression declined in 28 day differentiated HLC (Table 4.1). Similarly, increased gene expression patterns were observed in the pentose pathway in 14 day differentiated HLC and declined in 28 day differentiated HLC (Table 4.1). Glucose is converted to glycogen in the liver, which is mediated by GBE1, GYS1, GYS2 and UGP2 which were significantly up regulated in 14 and 28 day differentiated HLC (Table 4.1). PDK1, PDK2, PDK3 and PDK4, which are involved in glucose regulation, were also up

regulated in 14 and 28 day differentiated HLC (Table 4.1). Interestingly, expression of PGM1, PGM2 and PGM3, which are associated with glycogen degradation, were up regulated in 14 day HLC, however, their expression declined in 28 day differentiated HLC (Table 4.1). The summary of differentially regulated genes in the glucose metabolism array is given in Table 4.1 and expressed as fold change relative to undifferentiated hAEC. Gene expression patterns of HepG2 cells are also compared to differentiated HLC which showed similar patterns of gene expression. These results indicate that there is increased gene expression of glucose metabolism associated genes in 14 day and 28 day differentiated HLC; however, there were some genes that were down regulated to levels similar to hAEC in 28 day differentiated HLC.

Table 4.1 Summary of expression levels from the glucose metabolism gene expression array. Gene expression of 14 day and 28 day differentiated HLC shown as fold change relative to undifferentiated hAEC. Statistical significance $P < 0.05$; red indicates increased expression and blue indicates decreased expression.

Symbol	Gene Name	HLC 14d Fold Change	HLC 28d Fold Change	HepG2 Fold Change
ACO2	Aconitase 2, mitochondrial	3.9754	1.0438	3.3364
ALDOA	Aldolase A, fructose-bisphosphate	2.9679	1.3194	3.9699
ALDOB	Aldolase B, fructose-bisphosphate	42.5534	3.9678	67.4404
ALDOC	Aldolase C, fructose-bisphosphate	4.1626	1.2928	6.7213
BPGM	2,3-bisphosphoglycerate mutase	2.0996	1.9611	0.4565
ENO2	Enolase 2 (gamma, neuronal)	11.2204	3.7222	53.0153
ENO3	Enolase 3 (beta, muscle)	5.9281	1.6076	7.2705
FBP1	Fructose-1,6-bisphosphatase 1	16.7863	1.8013	26.3035
FBP2	Fructose-1,6-bisphosphatase 2	20.0989	2.1645	272.3411
G6PC	Glucose-6-phosphatase, catalytic subunit	43.9166	4.7295	120.8355
GALM	Galactose mutarotase (aldose 1-epimerase)	2.5186	1.432	7.9757
GBE1	Glucan (1,4-alpha-), branching enzyme 1	3.87	1.6985	2.4974
GCK	Glucokinase (hexokinase 4)	43.9166	4.7295	21.4326
GSK3A	Glycogen synthase kinase 3 alpha	2.5964	1.617	0.9153
GSK3B	Glycogen synthase kinase 3 beta	2.1559	0.843	0.4165
GYS1	Glycogen synthase 1 (muscle)	4.0546	1.1268	0.8163
GYS2	Glycogen synthase 2 (liver)	48.5491	6.6279	15.3014
H6PD	Hexose-6-phosphate dehydrogenase (glucose 1-dehydrogenase)	5.1576	1.9313	1.8536
HK3	Hexokinase 3 (white cell)	37.8309	3.4054	10.218
IDH2	Isocitrate dehydrogenase 2 (NADP+)	2.153	2.1081	1.8513
IDH3A	Isocitrate dehydrogenase 3 (NAD+) alpha	2.0588	1.3262	1.2157
IDH3G	Isocitrate dehydrogenase 3 (NAD+) gamma	2.381	1.1178	0.5034
MDH1B	Malate dehydrogenase 1B, NAD (soluble)	63.903	14.6068	0.5254
PCK1	Phosphoenolpyruvate carboxykinase 1 (soluble)	43.9166	4.7295	4441.8062
PDHA1	Pyruvate dehydrogenase (lipoamide) alpha 1	2.9801	1.3169	2.3032
PDK1	Pyruvate dehydrogenase kinase, isozyme 1	8.6938	2.1109	2.8677
PDK2	Pyruvate dehydrogenase kinase, isozyme 2	2.6335	1.5235	0.4731
PDK3	Pyruvate dehydrogenase kinase, isozyme 3	5.1886	2.8385	4.4894
PDK4	Pyruvate dehydrogenase kinase, isozyme 4	62.2129	6.8726	42.4392
PDPR	Pyruvate dehydrogenase phosphatase regulatory	3.9112	1.5256	2.548
PFKL	Phosphofructokinase, liver	6.1214	1.2954	2.3107
PGAM2	Phosphoglycerate mutase 2 (muscle)	5.738	1.6505	1.721
PGK1	Phosphoglycerate kinase 1	2.6948	1.342	2.3436
PGK2	Phosphoglycerate kinase 2	43.9166	4.7295	16.9808
PGLS	6-phosphogluconolactonase	3.9336	2.6628	1.1344
PGM1	Phosphoglucomutase 1	2.99	2.2483	0.6396
PGM3	Phosphoglucomutase 3	2.1497	0.6593	1.4898

Continued on next page

Table 4.1 continued from previous page

Symbol	Gene Name	HLC 14d Fold Change	HLC 28d Fold Change	HepG2 Fold Change
PHKA1	Phosphorylase kinase, alpha 1 (muscle)	3.8198	1.1534	0.621
PHKB	Phosphorylase kinase, beta	2.1939	1.4533	2.2284
PHKG1	Phosphorylase kinase, gamma 1 (muscle)	13.5634	2.4619	7.1102
PHKG2	Phosphorylase kinase, gamma 2 (testis)	4.185	1.4605	1.2353
PKLR	Pyruvate kinase, liver and RBC	8.0039	1.0936	355.7093
PRPS1	Phosphoribosyl pyrophosphate synthetase 1	0.5016	0.3421	0.6039
PRPS1L1	Phosphoribosyl pyrophosphate synthetase 1-like 1	37.3489	4.0222	14.4413
PYGL	Phosphorylase, glycogen, liver	2.5029	2.2907	0.9433
PYGM	Phosphorylase, glycogen, muscle	14.5054	4.3915	7.7563
RBKS	Ribokinase	12.3696	5.1343	28.0413
RPE	Ribulose-5-phosphate-3-epimerase	2.3177	1.6928	3.8638
RPIA	Ribose 5-phosphate isomerase A	3.1964	2.3035	2.5301
SDHA	Succinate dehydrogenase complex, subunit A, flavoprotein (Fp)	2.5179	1.148	2.8824
SDHB	Succinate dehydrogenase complex, subunit B, iron sulfur (Ip)	36.2567	27.5823	29.1625
SDHC	Succinate dehydrogenase complex, subunit C	2.5854	1.7998	3.771
SUCLA2	Succinate-CoA ligase, ADP-forming, beta subunit	2.0702	1.3424	0.9954
SUCLG2	Succinate-CoA ligase, GDP-forming, beta subunit	4.8208	2.4367	2.464
UGP2	UDP-glucose pyrophosphorylase 2	1.9803	2.5385	1.3218

To determine the extent that genes associated with mitochondrial metabolism were upregulated, we analysed 80 genes associated with mitochondrial metabolism in undifferentiated hAEC, 14 day HLC, 28 day HLC and HepG2 cells. There were a total of 64 genes up regulated in 14 day differentiated HLC and 44 genes up regulated in 28 day differentiated HLC. There were 41 genes that were up regulated in both 14 day and 28 day HLC compared to hAEC, however, there were no genes that were down regulated on the mitochondrial metabolism panel. Genes involved in complex I of electron transport chain (NDUFA, NDUFB, NDUFC, NDUFS and NDUFV family of genes) were up regulated in 14 and 28 day differentiated HLC compared to hAEC (Table 4.2). Interestingly, genes involved in ETC complex I had the highest expression at 14 day of differentiation. Similarly, genes involved in complex II of the ETC (SDHA, SDHB and SDHD) were also up regulated in 14 day differentiated HLC compared to hAEC (Table 4.2). The UQCR family of genes, which are involved in complex III of ETC, were also up regulated in 14 and 28 day differentiated HLC (Table 4.2). In addition, COX4-8 genes which are involved in complex IV of ETC were significantly upregulated in both 14 and 28 differentiated HLC and so were the genes of complex V (ATP family of genes; Table 4.2). These findings indicate that 14 day differentiated cells up regulate mitochondrial associated genes, thus driving increased reliance on OXPHOS for the generation of ATP. However, some of these genes were down regulated in 28 day differentiated HLC, thus suggesting a partial block in OXPHOS in ATP generation.

Table 4.2 Summary of expression levels from the mitochondrial metabolism gene expression array. Gene expression of 14 day and 28 day differentiated HLC shown as fold change relative to undifferentiated hAEC. Statistical significance $P < 0.05$; red indicates increased expression and blue indicates decreased expression.

Symbol	Description	HLC 14d Fold Change	HLC 28d Fold Change	HepG2 Fold Change
ATP12A	ATPase, H+/K+ transporting, nongastric, alpha polypeptide	5.8331	0.6461	0.6698
ATP4A	ATPase, H+/K+ exchanging, alpha polypeptide	47.2827	2.3364	32.1487
ATP4B	ATPase, H+/K+ exchanging, beta polypeptide	32.4997	1.1373	4.8352
ATP5C1	ATP synthase, H+ transporting, mitochondrial F1 complex, gamma polypeptide 1	3.0743	1.8996	2.5018
ATP5G2	ATP synthase, H+ transporting, mitochondrial Fo complex, subunit C2 (subunit 9)	17.4485	6.4385	0.281
ATP5H	ATP synthase, H+ transporting, mitochondrial Fo complex, subunit d	2.291	2.2743	1.7984
ATP5I	ATP synthase, H+ transporting, mitochondrial Fo complex, subunit E	6.4313	2.8721	4.2605
ATP5J	ATP synthase, H+ transporting, mitochondrial Fo complex, subunit F6	2.0027	2.6394	1.3553
ATP5J2	ATP synthase, H+ transporting, mitochondrial Fo complex, subunit F2	7.5035	1.3371	5.5857
ATP5L	ATP synthase, H+ transporting, mitochondrial Fo complex, subunit G	5.5744	1.654	1.3095
ATP5O	ATP synthase, H+ transporting, mitochondrial F1 complex, O subunit	2.3779	2.3779	2.5872
ATP6V0A2	ATPase, H+ transporting, lysosomal V0 subunit a2	2.325	0.6795	0.9661
ATP6V0D2	ATPase, H+ transporting, lysosomal 38kDa, V0 subunit d2	49.8815	2.4648	23.5752
ATP6V1C2	ATPase, H+ transporting, lysosomal 42kDa, V1 subunit C2	40.7231	1.3222	21.7195
ATP6V1E2	ATPase, H+ transporting, lysosomal 31kDa, V1 subunit E2	5.3578	2.2319	0.723
ATP6V1G3	ATPase, H+ transporting, lysosomal 13kDa, V1 subunit G3	17.5355	2.0029	2.674
COX4I1	Cytochrome c oxidase subunit IV isoform 1	3.0854	2.3637	7.2862
COX4I2	Cytochrome c oxidase subunit IV isoform 2 (lung)	37.1567	3.5644	49.2051
COX5B	Cytochrome c oxidase subunit Vb	3.24	2.2916	8.6289
COX6A2	Cytochrome c oxidase subunit VIa polypeptide 2	49.1534	5.3787	10.1163
COX6B1	Cytochrome c oxidase subunit Vib polypeptide 1 (ubiquitous)	2.2973	3.3742	1.3462
COX6B2	Cytochrome c oxidase subunit VIb polypeptide 2 (testis)	55.6384	2.3335	8.3993
COX6C	Cytochrome c oxidase subunit VIc	56.5151	3.2334	12.2016
COX7A2L	Cytochrome c oxidase subunit VIIa polypeptide 2 like	2.5054	3.6201	2.1101
COX7B	Cytochrome c oxidase subunit VIIb	3.2072	2.3381	3.1408
COX8C	Cytochrome c oxidase subunit VIIC	46.1501	11.2001	2.8142
LHPP	Phospholysine phosphohistidine inorganic pyrophosphate phosphatase	5.7181	3.0656	0.8956

Continued on next page

Table 4.2 continued from previous page

NDUFA1	NADH dehydrogenase (ubiquinone) 1 alpha subcomplex, 1, 7.5kDa	2.8016	2.1973	1.2402
NDUFA10	NADH dehydrogenase (ubiquinone) 1 alpha subcomplex, 10, 42kDa	4.6942	1.5524	1.7897
NDUFA11	NADH dehydrogenase (ubiquinone) 1 alpha subcomplex, 11, 14.7kDa	5.7587	2.0777	2.2416
NDUFA2	NADH dehydrogenase (ubiquinone) 1 alpha subcomplex, 2, 8kDa	3.5335	2.3351	2.9064
NDUFA3	NADH dehydrogenase (ubiquinone) 1 alpha subcomplex, 3, 9kDa	6.6224	2.6318	3.3732
NDUFA4	NADH dehydrogenase (ubiquinone) 1 alpha subcomplex, 4, 9kDa	14.206	42.240	18.0833
NDUFA5	NADH dehydrogenase (ubiquinone) 1 alpha subcomplex, 5, 13kDa	15.38	8.8999	1.652
NDUFA6	NADH dehydrogenase (ubiquinone) 1 alpha subcomplex, 6, 14kDa	3.0697	2.532	0.6921
NDUFA7	NADH dehydrogenase (ubiquinone) 1 alpha subcomplex, 7, 14.5kDa	2.5407	1.9457	5.0063
NDUFAB1	NADH dehydrogenase (ubiquinone) 1, alpha/beta subcomplex, 1, 8kDa	2.0699	1.5605	2.7562
NDUFB10	NADH dehydrogenase (ubiquinone) 1 beta subcomplex, 10, 22kDa	3.137	2.0156	1.8388
NDUFB2	NADH dehydrogenase (ubiquinone) 1 beta subcomplex, 2, 8kDa	1.4799	2.1472	0.3377
NDUFB3	NADH dehydrogenase (ubiquinone) 1 beta subcomplex, 3, 12kDa	2.0339	2.3326	0.7777
NDUFB4	NADH dehydrogenase (ubiquinone) 1 beta subcomplex, 4, 15kDa	2.07	2.1995	1.0197
NDUFB5	NADH dehydrogenase (ubiquinone) 1 beta subcomplex, 5, 16kDa	2.6366	2.8922	1.229
NDUFB6	NADH dehydrogenase (ubiquinone) 1 beta subcomplex, 6, 17kDa	2.1901	2.1424	0.6319
NDUFB7	NADH dehydrogenase (ubiquinone) 1 beta subcomplex, 7, 18kDa	3.7283	1.6991	1.3446
NDUFB8	NADH dehydrogenase (ubiquinone) 1 beta subcomplex, 8, 19kDa	2.9276	1.9095	3.4149
NDUFB9	NADH dehydrogenase (ubiquinone) 1 beta subcomplex, 9, 22kDa	2.4652	1.353	4.427
NDUFC1	NADH dehydrogenase (ubiquinone) 1, subcomplex unknown, 1, 6kDa	3.1228	2.7787	2.8487
NDUFC2	NADH dehydrogenase (ubiquinone) 1, subcomplex unknown, 2, 14.5kDa	3.0591	2.0391	1.1162
NDUFS1	NADH dehydrogenase (ubiquinone) Fe-S protein 1, 75kDa (NADH-coenzyme Q reductase)	2.4498	1.0806	2.1628
NDUFS2	NADH dehydrogenase (ubiquinone) Fe-S protein 2, 49kDa (NADH-coenzyme Q reductase)	2.9708	1.4346	2.1976
NDUFS3	NADH dehydrogenase (ubiquinone) Fe-S protein 3, 30kDa (NADH-coenzyme Q reductase)	3.365	1.8537	2.8874
NDUFS4	NADH dehydrogenase (ubiquinone) Fe-S protein 4, 18kDa (NADH-coenzyme Q reductase)	3.6757	3.0553	2.3014
NDUFS6	NADH dehydrogenase (ubiquinone) Fe-S protein 6, 13kDa (NADH-coenzyme Q reductase)	2.1746	1.849	1.6877
NDUFS8	NADH dehydrogenase (ubiquinone) Fe-S protein 8, 23kDa (NADH-coenzyme Q reductase)	2.391	1.4624	5.2571
NDUFV1	NADH dehydrogenase (ubiquinone) flavoprotein 1, 51kDa	3.0864	1.5836	1.0202
NDUFV2	NADH dehydrogenase (ubiquinone) flavoprotein 2, 24kDa	3.6255	1.9832	3.4866

Table 4.2 Continued from previous page

NDUFV3	NADH dehydrogenase (ubiquinone) flavoprotein 3, 10kDa	3.9737	1.8392	6.7194
OXA1L	Oxidase (cytochrome c) assembly 1-like	4.528	3.3933	8.726
PPA2	Pyrophosphatase (inorganic) 2	3.6556	2.1789	1.0801
SDHA	Succinate dehydrogenase complex, subunit A, flavoprotein (Fp)	3.6688	1.3296	3.1002

SDHC	Succinate dehydrogenase complex, subunit C, integral membrane protein, 15kDa	3.122	2.701	4.0831
SDHD	Succinate dehydrogenase complex, subunit D, integral membrane protein	2.362	1.4533	1.1073
UQCR11	Ubiquinol-cytochrome c reductase, complex III subunit XI	3.1813	2.6713	1.9246
UQCRC2	Ubiquinol-cytochrome c reductase core protein II	3.2746	2.1458	5.1465
UQCRH	Ubiquinol-cytochrome c reductase hinge protein	2.5376	3.1307	2.8601
UQCRCQ	Ubiquinol-cytochrome c reductase, complex III subunit VII, 9.5kDa	1.843	2.3139	2.084

Regulation of mtDNA copy number during differentiation of HLC.

As cells are specified and differentiate into specific lineages, they increase their mtDNA copy number in accordance with their energy requirements as mature cell types (20, 26). We evaluated whether this was also the case for the differentiation of hAEC into mature hepatocytes. Undifferentiated hAEC had low numbers of mtDNA copy per cell (Fig. 4.1), which is consistent with pluripotent and multipotent stem cells (19). However, mtDNA copy number was significantly down regulated at 14 and 28 days of differentiation (Fig. 4.1). In contrast, bone marrow mesenchymal stem cells (BM-MSc) possessed ~1000 copies of mtDNA and, as they underwent differentiation, there were significant increases in mtDNA copy number (Fig. 4.1).

As mtDNA replication is primarily driven by POLGA, which is DNA methylated at exon 2, we performed MeDIP to evaluate the levels of enrichment for 5mC and 5hmC in both BM-MSc and hAEC. We expressed mtDNA copy number relative to 5mC:5hmC to determine their respective levels of mtDNA replication efficiency. Undifferentiated hAEC had significantly lower levels of mtDNA replication efficiency than BM-MSc (Fig. 4.1). Due to increased 5mC:5hmC enrichment at exon 2 of POLGA. During differentiation, hAEC mtDNA replication efficiency did not increase and remained significantly lower at days 14 and 28 (Fig. 4.1). In contrast, mtDNA replication efficiency increased with differentiation in BM-MSc compared to their undifferentiated counterparts (Fig. 4.1).

When we evaluated hepatocyte specific gene expression, there was increased expression of Albumin in day 28 hAEC derived HLC but Albumin was not detected in day 28 BM-MSc. Expression of α 1-AT in undifferentiated and day 14 and 28 differentiated BM-MSc remained unchanged. However, expression levels of α 1-AT in 14 and 28 day HLC were significantly lower than hAEC (Fig. 4.2). Expression of the cytochrome enzyme CYP3A4

remained unchanged in undifferentiated and differentiated BM-MSC whilst, CYP3A4 levels were significantly increased in 14 and 28 day differentiated hAEC (Fig. 4.2). Expression of the transcription factor HNF4 α remained unchanged in BM-MSC, whilst 28 day differentiated hAEC showed lower expression but was not statistically significant (Fig. 4.2).

BM-MSC showed no significant change in expression of hTERT, whereas, cMYC was significantly increased in 14 and 28 day differentiated BM-MSC (Fig. 4.2). However 14 and 28 day differentiated hAEC showed significant increases in expression of cMYC and hTERT (Fig. 4.2).

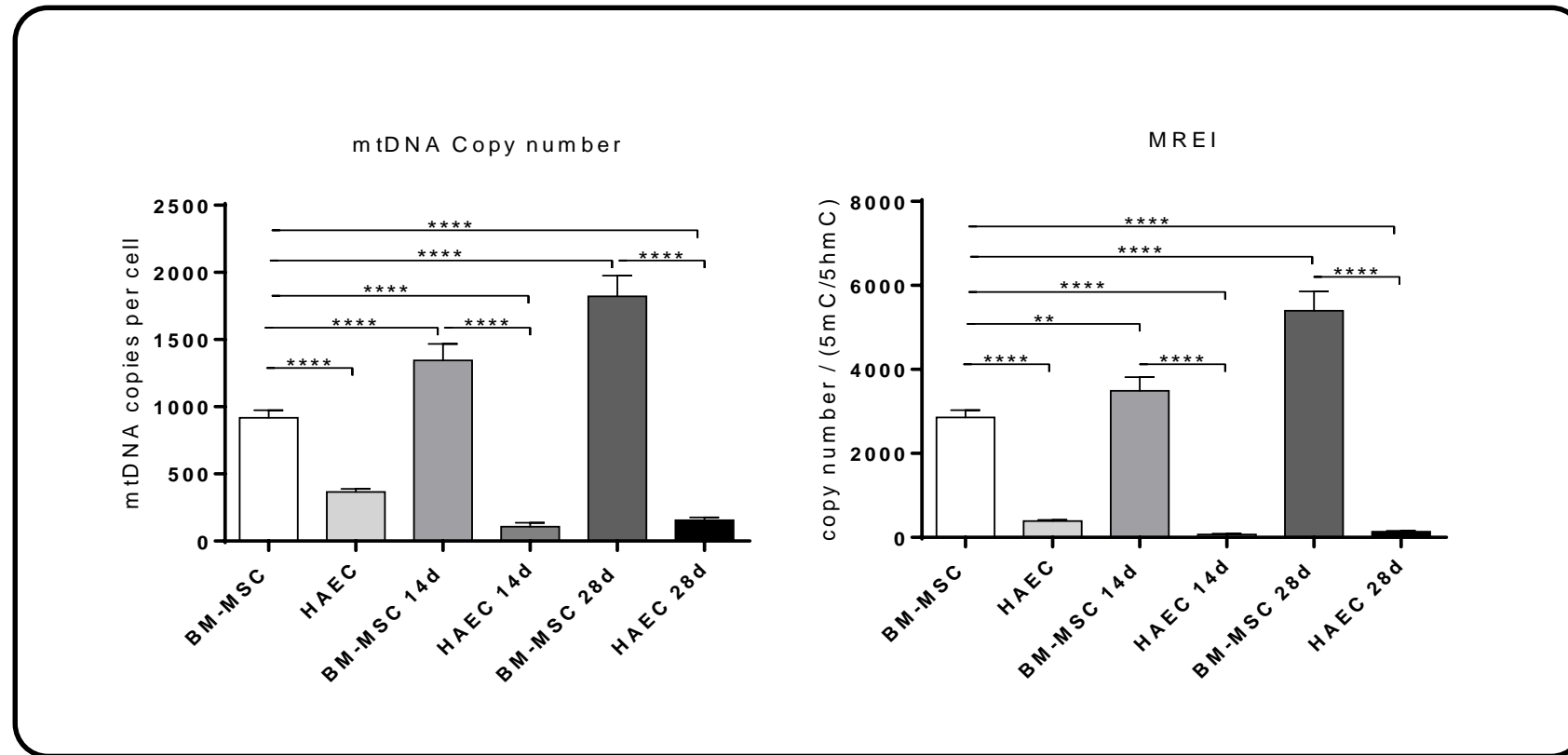


Figure 4.1. MtDNA copy number and MeDIP in differentiated HLC. (A) MtDNA copy number and the mitochondrial replication efficiency index (MREI) of BM-MSC and hAEC in undifferentiated, 14 day and 28 day differentiated HLC. Data presented as mean \pm SEM of $n = 4$. * $P < 0.05$, ** $P < 0.01$, *** $P < 0.001$ and **** $P < 0.0001$ compared to BM-MSC using Two-way ANOVA.

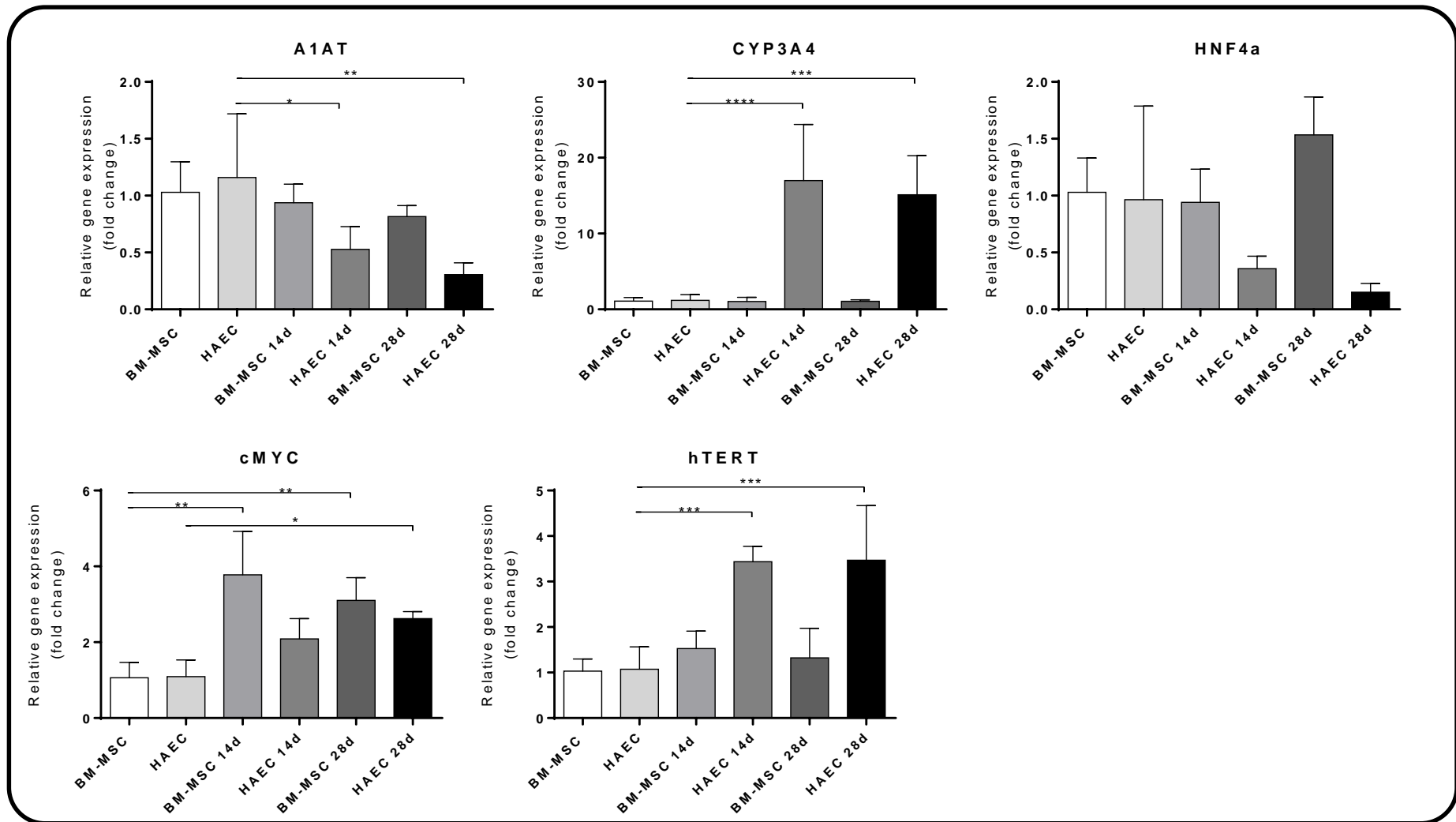


Figure 4.2. Gene expression of differentiated HLC. Gene expression of the hepatocyte markers A1AT, CYP3A4 and HNF4A; the oncogene cMYC and the proliferative marker hTERT in undifferentiated BM-MSC and hAEC and during HLC differentiation at 14 and 28 days. Data presented as mean \pm SEM of $n = 4$. * $P < 0.05$, ** $P < 0.01$, *** $P < 0.001$ and **** $P < 0.0001$ compared to BM-MSC using two-way ANOVA.

The effects of DNA demethylation on hAEC mtDNA copy number and the potential to differentiate.

To determine whether mtDNA copy number could be modulated in hAEC, we treated cells with the global DNA demethylation agent 5-azacytidine (5-aza). Enrichment of 5mC was reduced in undifferentiated hAEC, which was maintained through HLC differentiation (Fig. 4.3). This resulted in an increase in mtDNA copy number in undifferentiated hAEC, which was maintained at similar levels during differentiation and was reflected in respective levels of mtDNA replication efficiency (Fig. 4.3). Assessment of gene expression patterns of hepatocyte specific genes showed aberrant patterns. With differentiation, there were increased levels of expression for CYP3A4 whereas levels of expression for $\alpha 1$ antitripsin were significantly reduced, expression of albumin was lost and there was no change for HNF4 α (Fig. 4.3 and 4.4). There were significant increases in expression of NANOG and OCT4 in 5-aza treated undifferentiated hAEC and differentiated HLC (Fig. 4.4). 5-aza treatment resulted in DNA demethylation at exon 2 of POLGA, increased mtDNA copy number and increased expression of pluripotency genes.

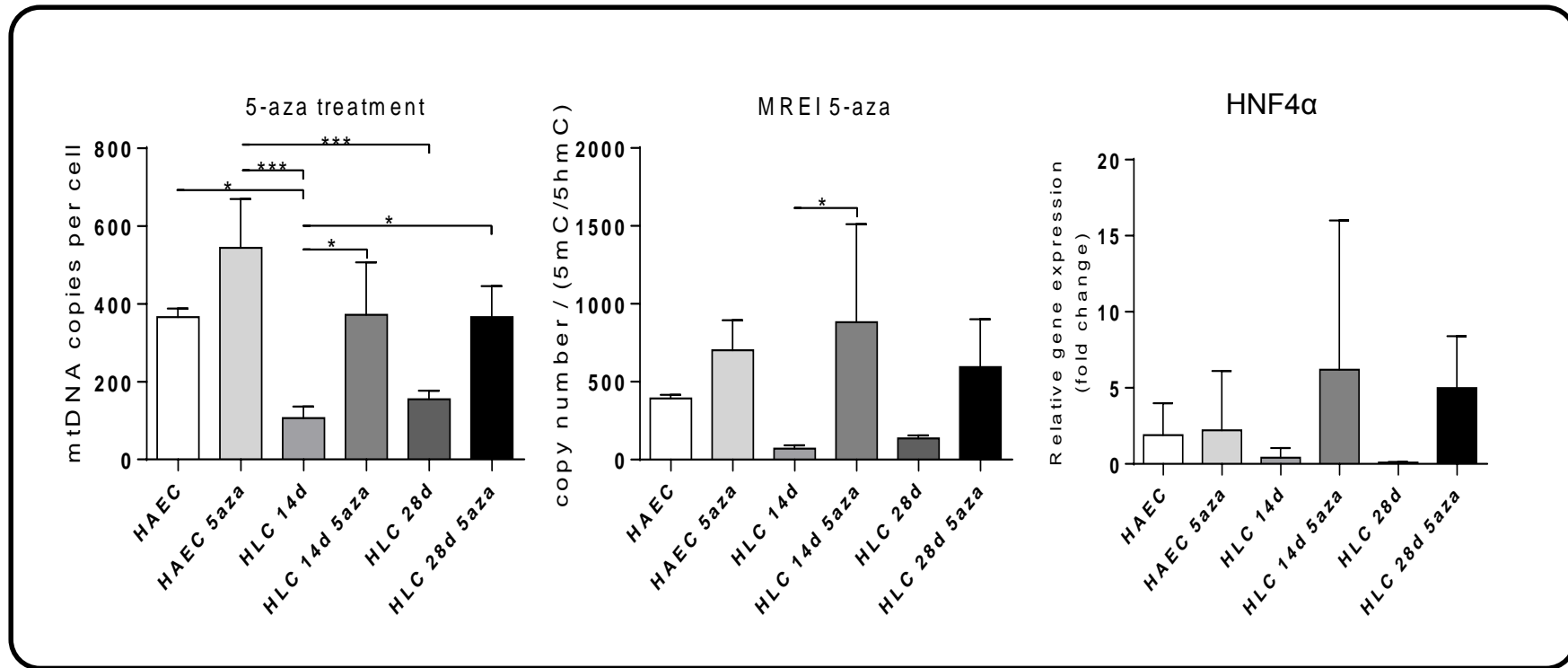


Figure 4.3. MtDNA copy number and MeDIP in differentiated HLC treated with 5-aza. MtDNA copy number and replication efficiency of 5-aza treated BM-MSC and hAEC in undifferentiated, 14 day and 28 day differentiated HLC. Changes in gene expression for transcription factor HNF4 α in 5-aza treated undifferentiated BM-MSC and hAEC and during HLC differentiation at 14 and 28 days. Data presented as mean \pm SEM of n = 4. * P < 0.05, ** P < 0.01 and *** P < 0.001 compared to hAEC using one-way ANOVA.

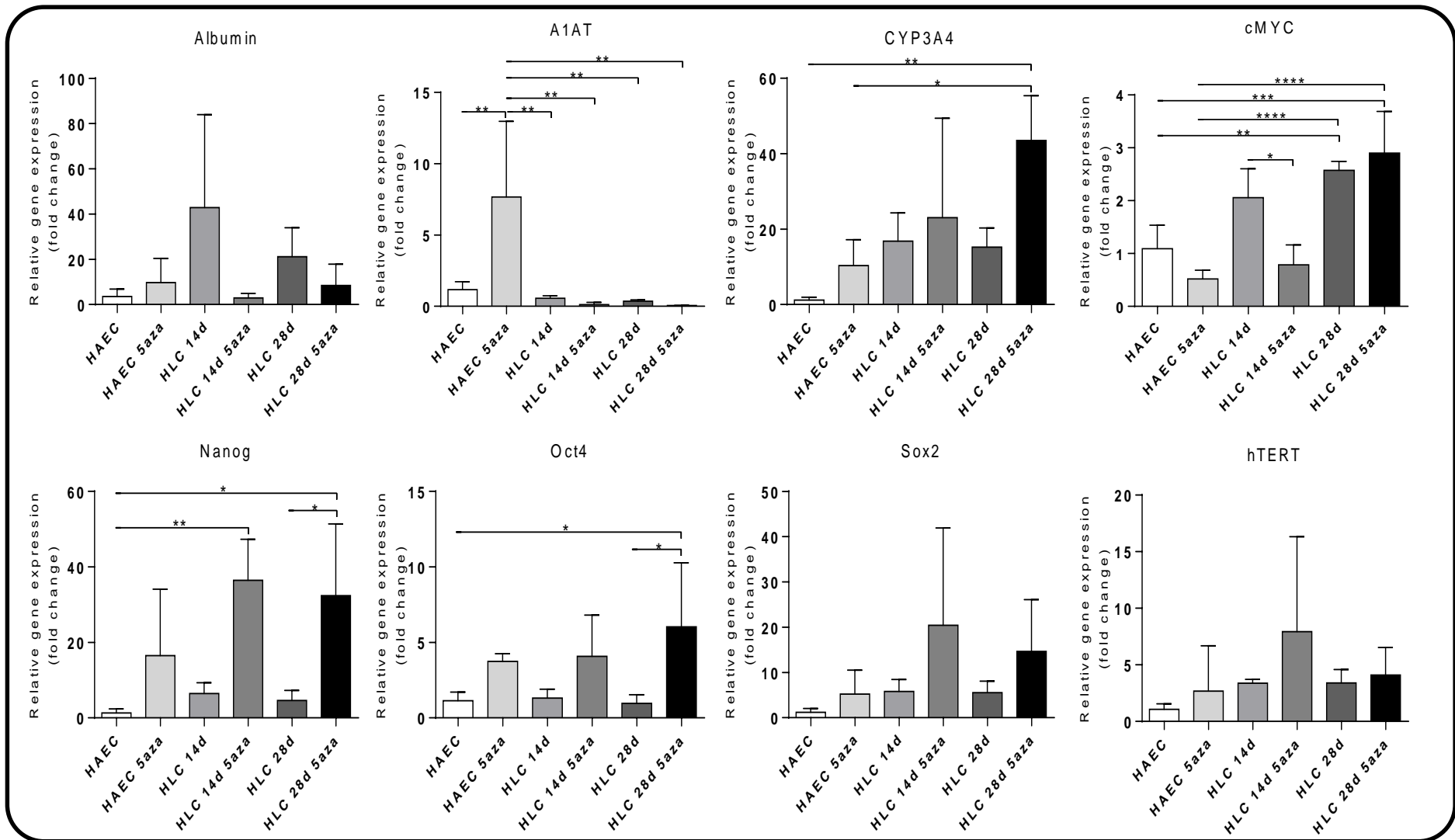


Figure 4.4. Gene expression of differentiated HLC treated with 5-aza. Gene expression of the hepatocyte specific genes Albumin, A1AT and CYP3A4; the pluripotency genes NANOG, OCT4 and SOX2; the oncogene cMYC; and the proliferative marker hTERT in undifferentiated BM-MSC and hAEC and during HLC differentiation at 14 and 28 days. Data presented as mean \pm SEM of $n = 4$. * $P < 0.05$, ** $P < 0.01$, *** $P < 0.001$ and **** $P < 0.0001$ compared to hAEC using one-way ANOVA.

The effects of mtDNA depletion on the differentiation potential of hAEC.

Partial depletion of mtDNA can also reset the cells to a more undifferentiated state, which then allows differentiation to ensue (19, 27). Treating hAEC with ddC for 3 days depleted mtDNA copy number to 30% of their original mtDNA content (Fig. 4.5). However, when mtDNA depleted cells were allowed to recover in HLC differentiation media for 7 and 14 days, they failed to increase mtDNA copy number (Fig. 4.5). When we evaluated DNA methylation at exon 2 of POLGA in day 3 mtDNA depleted hAEC, 5mC enrichment and, thus, replication efficiency was reduced compared to non-depleted hAEC but was not statistically significant (Fig. 4.5). Whilst DNA methylation at exon 2 of POLGA remained steady at day 7 of differentiation, it increased at day 14 when compared to day 3 mtDNA depleted hAEC (Fig. 4.5). The levels of enrichment for 5mC at day 14 of differentiation returned to similar levels as undifferentiated hAEC (Fig. 4.5).

The hepatocyte specific gene α 1-AT showed a significant increase in gene expression with mtDNA depletion and at day 7 of differentiation but declined to similar levels to undifferentiated cells by day 14 of differentiation (Fig. 4.6). Albumin gene expression significantly decreased with mtDNA depletion and differentiation (Fig. 4.6). CYP3A4 and HNF4 α gene expression increased significantly and peaked at day 7 of differentiation. However, the expression of these genes was reduced at day 14 of differentiation (Fig. 4.6). Although there was no change in expression of cMYC, there were significant increases in expression of the pluripotency genes in mtDNA depleted hAEC and differentiated hAEC (Fig. 4.6). Expression of NANOG and OCT4 increased significantly in mtDNA depleted hAEC at 7 and 14 days of differentiation (Fig. 4.6). However, SOX2 expression was increased significantly in mtDNA depleted cells at day 7 of differentiation only (Fig. 4.6).

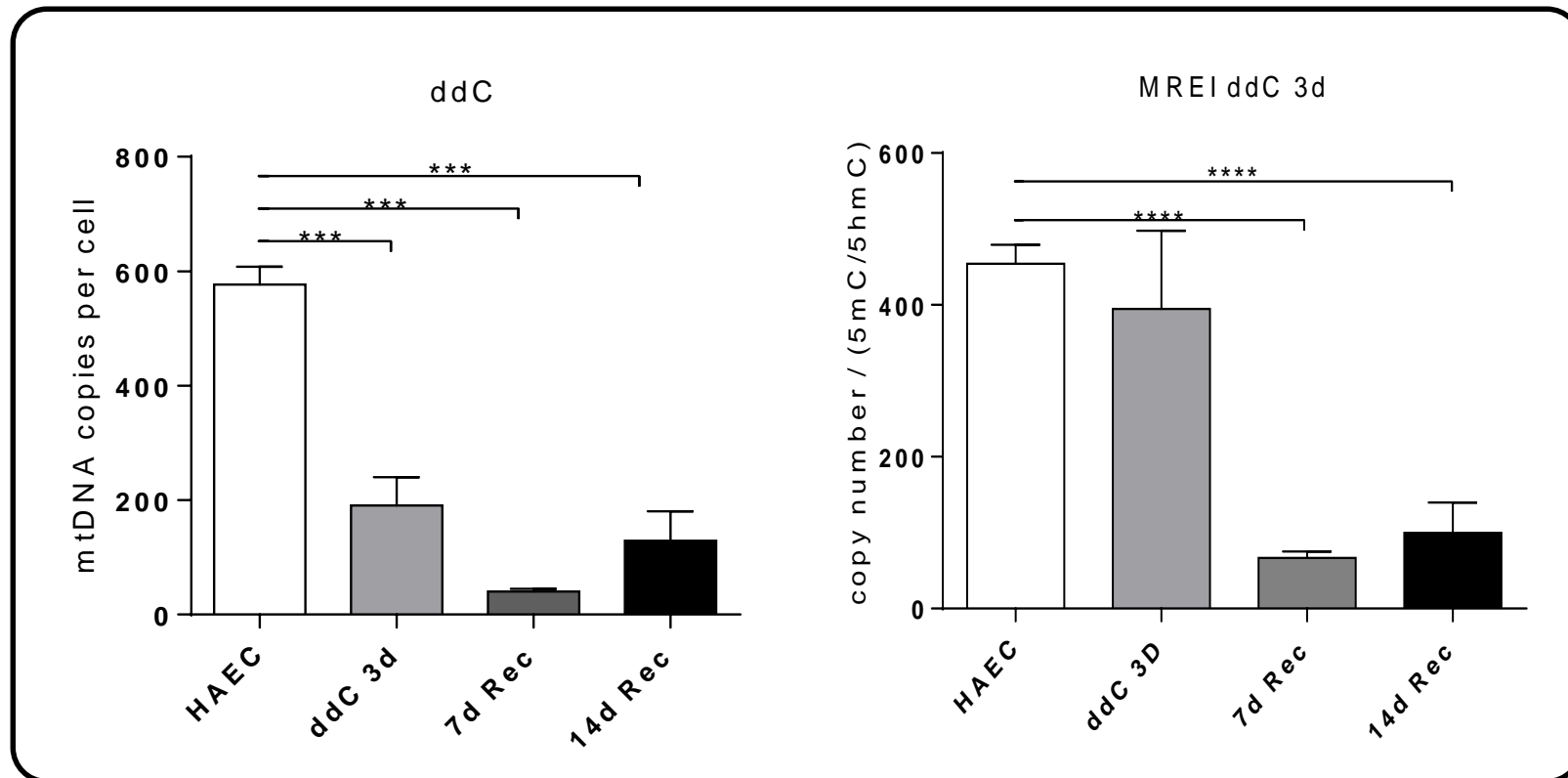


Figure 4.5. MtDNA copy number and MeDIP in ddC depleted hAEC for 3 days and subsequent HLC differentiation. MtDNA copy number and mitochondrial replication efficiency index (MREI) of 3 day ddC depleted hAEC and day 7 and 14 recovered HLC compared to hAEC. Data presented as mean \pm SEM of $n = 4$. *** $P < 0.001$ and **** $P < 0.0001$ compared to hAEC using one-way ANOVA.

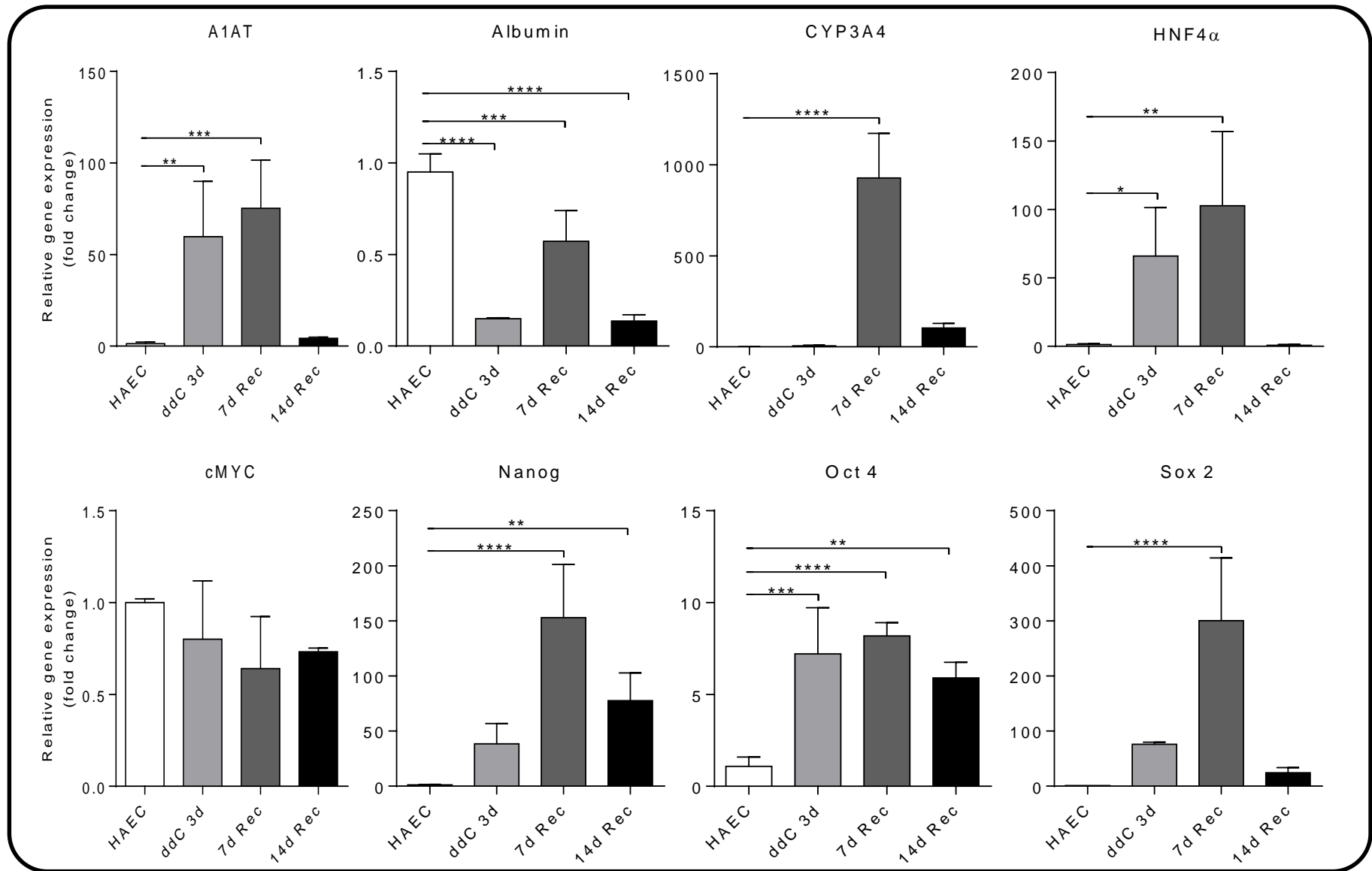


Figure 4.6. Gene expression of 3 day ddC depleted hAEC differentiated HLC for 7 and 14 days. Gene expression of the hepatocyte specific genes A1AT, Albumin, CYP3A4 and HNF4 α ; the pluripotency genes NANOG, OCT4 and SOX2; and the oncogene cMYC in 3 day ddC depleted hAEC and 7 and 14 day recovered HLC compared to hAEC. Data presented as mean \pm SEM of n = 4. * P < 0.05, ** P < 0.01, *** P < 0.001 and **** P < 0.0001 compared to hAEC using one-way ANOVA.

Depleting mtDNA for 7 days reduced mtDNA copy number to ~2% of its original content. Furthermore, mtDNA copy number did not increase following 7 and 14 days of differentiation and remained at < 2% of its original content (Fig. 4.7). Evaluation of 5mC:5hmC enrichment at exon 2 of POLGA showed a reduction in 5mC enrichment for mtDNA depleted hAEC, which was maintained in day 7 and 14 differentiated cells (Fig. 4.7).

Levels of gene expression for albumin decreased significantly in mtDNA depleted hAEC and day 7 differentiated cells (Fig. 4.8) whilst expression of HNF4 α remained unchanged (Fig. 4.7). However, gene expression of α 1-AT significantly increased in mtDNA depleted hAEC and there were further significant increases in gene expression at days 7 and 14 of differentiation (Fig. 4.8). Furthermore, expression of CYP3A4 increased with mtDNA depletion and further significant increases were observed at days 7 and 14 of differentiation (Fig. 4.8). Expression of the oncogene cMYC increased significantly in mtDNA depleted hAEC as well as at days 7 and 14 of differentiation (Fig. 4.8). The pluripotent genes OCT4, SOX2 and NANOG showed significant increases in gene expression in mtDNA depleted hAEC (Fig. 4.8). The significant increase in OCT4 gene expression was maintained whereas, SOX2 and NANOG expression continued to increase at days 7 and 14 of differentiation (Fig. 4.8). Likewise, expression of hTERT, a marker of proliferation, was significantly increased in mtDNA depleted hAEC at days 7 days and 14 of differentiation (Fig. 4.8). Overall, hAEC failed to regulate their mtDNA copy number during HLC differentiation due to higher levels of DNA methylation at exon 2 of POLGA. This is the case for both 5-aza treatment and partial depletion of mtDNA.

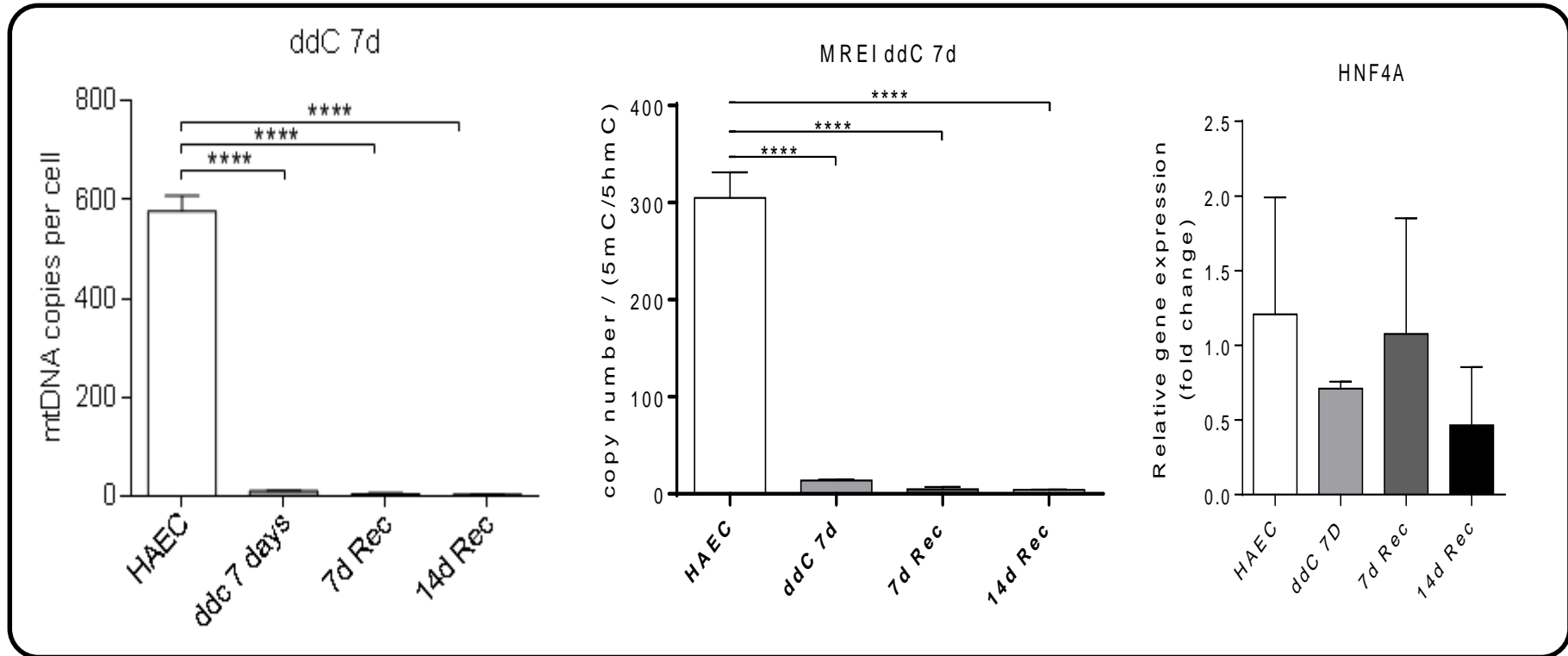


Figure 4.7. MtDNA copy number and MeDIP in 7 day ddC depleted hAEC and differentiated HLC. MtDNA copy number and mitochondrial replication efficiency index (MREI) of 7 day ddC depleted hAEC and 7 and 14 day recovered HLC compared to hAEC. Gene expression of the hepatic transcription factor HNF4 α in 7 day ddC depleted hAEC and 7 and 14 day recovered HLC compared to hAEC. Data presented as mean \pm SEM of n = 4. **** P < 0.0001 compared to hAEC using one-way ANOVA.

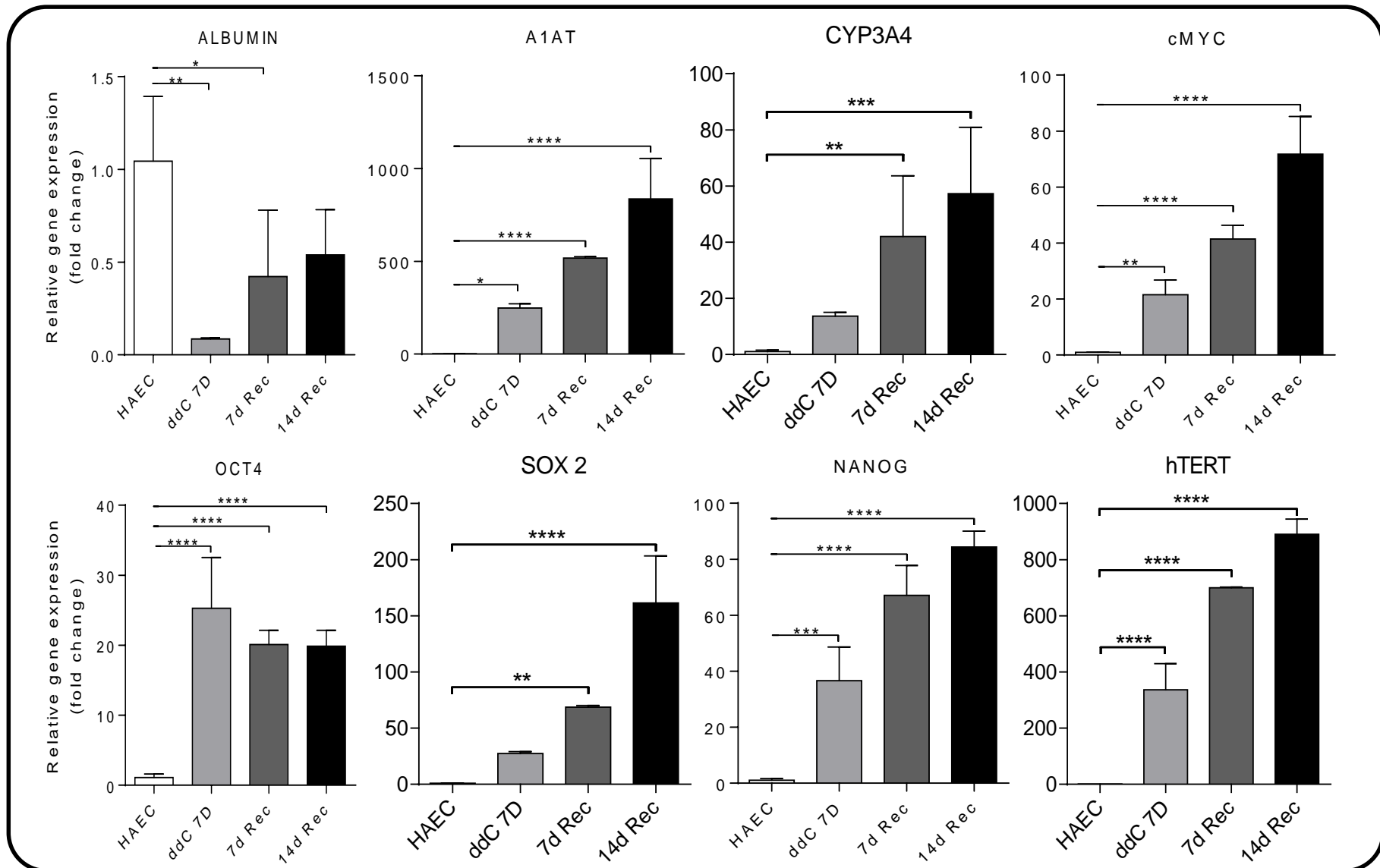


Figure 4.8. Gene expression of 7 day ddC depleted hAEC differentiated HLC for 7 and 14 days. Gene expression of the hepatocyte specific genes Albumin, A1AT and CYP3A4; the oncogene cMYC; the pluripotency gene OCT4, SOX2 and NANOG; and the proliferative marker hTERT in 7 day ddC depleted hAEC and 7 and 14 day recovered HLC compared to hAEC. Data presented as mean \pm SEM of $n = 4$. * $P < 0.05$, ** $P < 0.01$, *** $P < 0.001$ and **** $P < 0.0001$ compared to hAEC using one-way ANOVA.

The tumorigenic potential of mtDNA depleted hAEC

As depleted and non-depleted hAEC expressed high levels of pluripotent genes, the oncogene cMYC and the proliferation factor hTERT, we evaluated the tumorigenic capacity of hAEC and hAEC depleted to 60, 30 and 5% of their original mtDNA content. We injected 2 million cells into NOD/SCID mice. However, the depleted and non-depleted cell types failed to form tumours over 6 months, which was the ethical end point for these experiments.

4.4 Discussion

Differentiation of hAEC to HLC requires a switch from glycolysis to OXPHOS in order to meet the ATP needs for functional output. The glucose metabolism gene expression array indicated that day 14 and 28 differentiated HLC showed higher levels of gene expression than hAEC. These results imply a switch from glycolysis to OXPHOS, a key hallmark of differentiation. The three fructose biphosphotase aldolases (ALDOA, ALDOB and ALDOC) are involved in glycolysis (28). Down regulation of ALDOA, which catalyses fructose 1, 6-biphosphate to glyceraldehyde 3-phosphate and dihydroxyacetone phosphate, in day 28 differentiated HLC indicates an exit from glycolysis. Expression of ALDOA is repressed in human liver with higher expression of ALDOB (29). In addition, down regulation of ALDOB and ALDOC was more significant in day 28 differentiated HLC, indicating the shutdown of glycolysis. Enolase enzymes act further downstream from aldolase enzymes. Enolase catalyses the conversion of phosphoglycerate to phosphoenolpyruvate in the glycolytic pathway. Enolase 2 (ENO2) is ubiquitously expressed in all tissues whereas Enolase 3 (ENO3) is muscle specific (30). These enzymes were increased at day 14 of differentiation indicating increased glycolysis and repressed in day 28 differentiated HLC indicating reduced glycolysis. Similarly, genes associated with the TCA cycle were upregulated in day 14 differentiated HLC showing higher ATP production through aerobic respiration. However, gene expression was down regulated in day 28 differentiated HLC, indicating these cells had switched to ATP production other than the TCA cycle.

The pentose phosphate pathway which acts in parallel to glycolysis for the generation of ATP is upregulated in day 14 differentiated HLC. However, expression of these genes decreased in day 28 differentiated HLC. Taken together, these results show increased anaerobic ATP generation through glycolysis, the TCA cycle and the pentose phosphate pathway in day 14 differentiated HLC but in day 28 differentiated HLC had shut down these pathways for ATP

generation. Interestingly, α -ketoglutarate which is generated in TCA cycle is also known to play a role in DNA methylation; thus the metabolic profile of a cell may enhance maintenance of pluripotency or lead to lineage commitment (31). These data suggest ATP generation through OXPHOS is a probable dominant pathway in day 28 differentiated HLC. Moreover, genes associated with glycogen synthesis from glucose showed marked upregulation in day 14 and 28 differentiated HLC demonstrate functional capacity to synthesise and store glycogen. There are studies suggesting increased glycogen synthesis observed in differentiated hepatocytes (3, 4, 32). Importantly, glycogen degradation genes were down regulated in day 28 differentiated HLC indicating active promotion of increased glycogen synthesis and storage.

Mitochondria produce the vast majority of ATP required for cell function, particularly, hepatocytes have a high demand for ATP. Evaluation of mitochondrial metabolism showed high gene expression in day 14 and 28 differentiated HLC. Genes involved in the five complexes of ETC were all upregulated in day 14 differentiated HLC. Electrons are transferred from electron donors to acceptors through redox reactions, generating a proton gradient that drives ATP synthesis. Complex I, which consists of at least 45 polypeptides, transfers electrons from NADH to coenzyme Q. Increased expression of complex I genes suggest increased OXPHOS. Complex I of ETC is also a primary site of electron leakage that results in generation of ROS (33). Complex II, which consists of 4 subunits, reduces coenzyme Q and oxidises succinate; reduced coenzyme Q transfers electrons to cytochrome C in complex III which comprises of 10 nuclear and 1 mitochondrial encoded subunits (33). Both complex II and III were upregulated in day 14 and 28 differentiated HLC indicating increased OXPHOS activity. Complex IV of ETC consists of 13 subunits that transfer electrons from cytochrome C to oxygen to reduce it to H₂O. Complex V consists of 14 nuclear and 2 mitochondrial encoded subunits that convert ADP to ATP and water (34).

Genes associated with all five complexes of ETC were upregulated in day 14 and 28 differentiated HLC indicating increased ATP generation through OXPHOS. There are no reports of comparison of 14 and 28 day differentiated HLC in literature. However, we noted that gene expression was highest in day 14 differentiated HLC suggesting that OXPHOS would have peaked between 20-28 days post-differentiation.

Pluripotent and multipotent stem cells have low mtDNA copy number, and as cells differentiate, mtDNA copy number is synchronously increased (20, 26, 35). My data show that BM-MSC follow this process robustly, however, hAEC are unable to increase their mtDNA copy number. It has previously been shown that BM-MSC differentiate into hepatocyte-like cells (36-39). However, the differentiation efficiency of BM-MSC has not been reported. Our findings are in line with previous reports of low mtDNA copy number in undifferentiated pluripotent cells (20, 26). Differentiated cells have increased mitochondrial content, mass and mtDNA copy number (7, 40). The inability of hAEC to modulate their mtDNA copy number is due to higher ratio of 5mC: 5hmC at exon 2 of POLGA in day 14 and 28 differentiated HLC. POLGA is the catalytic subunit of mitochondria specific polymerase gamma (7). DNA methylation at exon 2 of POLGA is known to modulate mtDNA copy number in a tissue specific manner (19, 20). My results show that increased DNA methylation on exon 2 of POLGA prevents the synchronous increase in mtDNA copy number in HLC derived from hAEC. However, reduced DNA methylation at exon 2 of POLGA results in increased mtDNA copy number in BM-MSC differentiated HLC. DNA methylation of POLGA suppresses its transcription, thus resulting in blocked mtDNA replication machinery (41). ATP levels are sensitive to inhibition of glycolysis in pluripotent stem cells whereas differentiated cells are sensitive to inhibition of OXPHOS (42). My data conclusively show that differentiation of BM-MSC into HLC results in an increase in

mtDNA copy number and reduced DNA methylation at exon 2 of POLGA but not in hAEC. This suggests a potential blockage in differentiation of hAEC into HLC.

Surprisingly, a block in mtDNA copy number does not prevent gene expression associated HLC differentiation. Cytochrome 3A4 (43), which is a major drug metabolising enzyme and HNF4 α , which is major hepatic transcription factor (44), were expressed in hAEC differentiated HLC. These data suggest that differentiated HLC had acquired some of the hepatic phenotype. In contrast, though there were no changes in mature hepatic gene expression in BM-MSC derived HLC, and hepatic gene expression was significantly higher in hAEC derived HLC compared to BM-MSC. My finding shows that BM-MSc are better able to regulate their mtDNA copy number and express some genes of hepatic lineages.. Cell to cell signalling mediates suppression of pluripotency genes by epigenetic silencing and enhanced expression of lineage specific genes (45) during differentiation. However, this does not occur either in HLC derived from BM-MSC or hAEC, resulting in incomplete shutdown of the pluripotency pathway. Remarkably, HLC derived from hAEC had very low gene expression with and without differentiation. The oncogene cMYC was highly expressed in BM-MSC derived HLC indicating deregulation and promotion of tumorigenic capacity (46). In addition, both hAEC and BM-MSC derived HLC were highly proliferative and expressed hTERT. The combination of cMYC and hTERT, in which the former is known to activate later (47, 48), may have an implication in clinical use of these cells as they may result in tumours.

Treatment of hAEC with 5aza increased levels of 5hmC and reduced 5mC levels of POLGA. It has been well known that the addition of a hydroxyl group to 5mC by TET1 marks DNA methylation as an active conducive for gene transcription (49). Here, I showed that increased 5hmC at exon 2 of POLGA resulted in increased mtDNA copy number in hAEC and day 14 and 28 differentiated HLC. Since 5aza is not gene specific, it has aberrant effects on gene

expression patterns (50) resulting in uncharacteristic hepatic gene expression in differentiated HLC. Increased expression of CYP3A4 in differentiated HLC indicates the capacity for drug metabolism and this can be attributed to 5aza treatment. HepG2 cells have also been shown to respond to 5aza treatment with increased CYP3A4 and CCAAT element-binding protein(C/EBP) (51). C/EBP and HNF4 α are co-expressed and interact (52) in the liver tissue may explain increased expression of HNF4 α in 5aza treated day 14 and 28 differentiated HLC. Treatment with 5aza leads to DNA hypo-methylation and results in increased expression of pluripotency genes (53) demonstrating increased pluripotency gene expression (OCT4 and NANOG) in 5aza treated HLC that were differentiated for 14 and 28 days. hAEC are also easily reprogrammed into induced pluripotent stem cells compared to fibroblasts indicating potential epigenetic memory and increased pluripotent gene expression (54). My results show that mtDNA copy number can be modulated by 5aza treatment, but it also results in expression of some hepatic and pluripotency genes.

Resetting of the pluripotency state by mtDNA depletion has been shown to enhance differentiation potential (27). Depletion of mtDNA promotes conversion of 5mC to 5hmC, thus making mitochondrial replication efficiency higher. Increased gene expression for pluripotency markers in depleted hAEC demonstrates the resetting of the pluripotency ground state (55). I had proposed that, better differentiation can be achieved when a cell is reset to its ground state. My results show that, depleted hAEC do not replenish their mtDNA copy number when allowed to differentiate. This finding may be due to an inherent block in replication of mtDNA due to the origin of the tissue. Once the depleted hAEC are allowed to differentiate, they regain DNA methylation at exon 2 of POLGA preventing replication of mtDNA, which may be due to repression of POLGA because of the increased activity of the DNMTs (56).

Whilst, there was no increase in mtDNA copy number in day 7 and 14 recovered HLC, increased gene expression was observed in 3 day depleted cells after day 7 recovery. Hepatocyte specific α 1-AT, albumin, CYP3A4 and HNF4 α showed increased expression after day 7 of differentiation. This indicates that, after short term depletion, hAEC are committed and differentiate into hepatic lineages. Though expression of α 1-AT, which is mainly expressed by hepatocytes, is consistent with hepatic lineage commitment (57), surprisingly other mature hepatic markers were also expressed. Expression of HNF4 α , which is a key transcription factor and expressed in mature liver (44), was unexpected considering, 3 day depleted hAEC were only differentiated for 7 days. Expression of CYP3A4 was unexpected at day 7 of recovery, this may be due to expression of the transcription factor HNF4 α . CYP3A4 is one of the targets of HNF4 α , where it binds to the promoter and activates transcription (32, 58). However, hepatocyte specific gene expression was shut down in day 14 recovered HLC. This may be due to the inability of these cells to modulate mtDNA copy number and increased DNA methylation that resulted in suppression of gene expression (59).

My results confirm that upon 3 day depletion of mtDNA, there is increased gene expression of pluripotency factors OCT4, SOX2 and NANOG. These data support our hypothesis of resetting ground state pluripotency with depletion of mtDNA. Remarkably, expression of OCT4, SOX2 and NANOG was further increased at day 7 of HLC differentiation. These results indicate that day 7 differentiated HLC are in the process of establishing the pluripotent state. Epigenetic memory is erased during reprogramming of induced pluripotent cells (60-63). This may explain persistent expression of pluripotency genes as well as mature hepatic genes in early stages of differentiation. Expression of OCT4, SOX2 and NANOG had decreased at 14 days of HLC differentiation compared to 7 days, indicating potential shut down of pluripotency genes. I also note that hepatic gene expression was also reduced in day

14 differentiated HLC. This suggests that there is possible global shut down of both hepatic and pluripotency associated genes.

Depletion of mtDNA for 7 days reduced mtDNA copy number to less than 2% of their original mtDNA copy number. When 7 day mtDNA depleted hAEC are allowed to recover, they do not increase their mtDNA copy number. This may be due to the fact that mtDNA had been depleted below their capacity to recover. It has been previously reported that depletion of mtDNA copy number can only recover up to 1% depletion (27). However, hAEC do not recover their mtDNA copy number when depleted to less than 2%. Exon 2 of POLGA remains hypermethylated, which would prevent mtDNA replication. Depletion of mtDNA also has implications for the tumorigenic capacity of these cells (27). My results show that cMYC, an oncogene involved in many cancers (48, 64), was highly expressed in day 7 and 14 differentiated HLC after 7 days of mtDNA depletion. Though it has been reported that hAEC are not tumorigenic, my results suggest potential tumorigenic capacity in mtDNA depleted hAEC. In addition, expression of hTERT was also highly expressed in 7 and 14 day differentiated HLC after depletion. CMYC directly activates hTERT which is expressed in rapidly proliferating and cancerous cells (65).

Hepatic gene α 1-AT and CYP3A4 showed increased expression in 7 and 14 day differentiated HLC after 7 days of mtDNA depletion. Hepatic gene expression peaked at day 14 of differentiation, however, there was no change in expression of HNF4 α which indicated incomplete differentiation. In addition, pluripotency persisted in 7 day depleted hAEC and differentiated HLC. Though OCT4 was consistently expressed in 7 day depleted and 7 and 14 day differentiated HLC, SOX2 and NANOG showed a different profile of expression. Both SOX2 and NANOG were highly expressed after 7 day depletion in day 7 and 14 differentiated HLC. These results show that depleted hAEC remain in a pluripotent state even after day 14 of differentiation. My results show that depletion of mtDNA resets the

pluripotent state by up regulating OCT4, SOX2 and NANOG. Upon differentiation, persistence of both hepatic and pluripotency genes is observed after 14 days of differentiation.

Evaluation of tumorigenesis in hAEC and mtDNA depleted hAEC shows that the cells did not form tumours. Nevertheless these cells show high levels of expression of oncogene CMYC and telomerase enzyme hTERT which promotes proliferation. The inability of hAEC to form tumours may be due to relatively low levels of cMYC compared to BM-MSc, which are not tumorigenic. BM-MSc possess similar levels of cMYC expression to placental derived MSc and higher than hAEC (66). Though, expression of the pluripotency genes OCT4, SOX 2 and NANOG was high in mtDNA depleted hAEC, they failed to initiate tumorigenesis. The failure of tumour formation despite high expression of the pluripotency genes and cMYC might be due to suppression of other genes. Cancer associated P53 and PTEN are well known genes associated with tumorigenesis (67), however, their expression in hAEC and mtDNA depleted hAEC remains unknown. Suppression of P53 and PTEN or other cancer associated genes could prevent tumorigenesis in hAEC. Additional genes, such as E2F1, which is known to negatively regulate CMYC induced hTERT (68) may suppress tumorigenesis.

Overall, my results indicate that hAEC are unable to modulate their mtDNA copy number which correlates with DNA methylation at exon 2 of POLGA. Differentiated HLC express some hepatic markers, however, there is persisted expression of pluripotency genes. Modulation of mtDNA using 5aza increases mtDNA copy number and reduces DNA methylation, however, there is aberrant gene expression. Depletion of mtDNA to reset the pluripotent state results in increased pluripotent gene expression. However, it does not modulate an increase in mtDNA copy number to enhance HLC differentiation. Though this creates more pluripotent cells, they are not tumorigenic.

4.5 References

1. Ilancheran S, Michalska A, Peh G, Wallace EM, Pera M, Manuelpillai U. Stem cells derived from human fetal membranes display multilineage differentiation potential. *Biology of reproduction*. 2007;77(3):577-88.
2. Miki T, Lehmann T, Cai H, Stolz DB, Strom SC. Stem cell characteristics of amniotic epithelial cells. *Stem cells*. 2005;23(10):1549-59.
3. Tee JY, Vaghjiani V, Liu YH, Murthi P, Chan J, Manuelpillai U. Immunogenicity and immunomodulatory properties of hepatocyte-like cells derived from human amniotic epithelial cells. *Current stem cell research & therapy*. 2013;8(1):91-9.
4. Pratama G, Vaghjiani V, Tee JY, Liu YH, Chan J, Tan C, et al. Changes in culture expanded human amniotic epithelial cells: implications for potential therapeutic applications. *PloS one*. 2011;6(11):e26136.
5. Anderson S, Bankier AT, Barrell BG, de Bruijn MH, Coulson AR, Drouin J, et al. Sequence and organization of the human mitochondrial genome. *Nature*. 1981;290(5806):457-65.
6. Parisi MA, Clayton DA. Similarity of human mitochondrial transcription factor 1 to high mobility group proteins. *Science*. 1991;252(5008):965-9.
7. Facucho-Oliveira JM, Alderson J, Spikings EC, Egginton S, St John JC. Mitochondrial DNA replication during differentiation of murine embryonic stem cells. *Journal of cell science*. 2007;120(Pt 22):4025-34.
8. Mandal S, Lindgren AG, Srivastava AS, Clark AT, Banerjee U. Mitochondrial function controls proliferation and early differentiation potential of embryonic stem cells. *Stem cells*. 2011;29(3):486-95.

9. St John JC, Ramalho-Santos J, Gray HL, Petrosko P, Rawe VY, Navara CS, et al. The expression of mitochondrial DNA transcription factors during early cardiomyocyte in vitro differentiation from human embryonic stem cells. *Cloning and stem cells*. 2005;7(3):141-53.
10. Bugianesi E, McCullough AJ, Marchesini G. Insulin resistance: a metabolic pathway to chronic liver disease. *Hepatology*. 2005;42(5):987-1000.
11. Yamashina S, Sato N, Kon K, Ikejima K, Watanabe S. Role of mitochondria in liver pathophysiology. *Drug Discovery Today: Disease Mechanisms*. 2009;6(1–4):e25-e30.
12. Yin PH, Lee HC, Chau GY, Wu YT, Li SH, Lui WY, et al. Alteration of the copy number and deletion of mitochondrial DNA in human hepatocellular carcinoma. *British journal of cancer*. 2004;90(12):2390-6.
13. Oyanagui Y, Sato N, Hagihara B. Spectrophotometric analysis of cytochromes in rat liver during carcinogenesis. *Cancer research*. 1974;34(3):458-62.
14. Pradhan S, Esteve PO. Mammalian DNA (cytosine-5) methyltransferases and their expression. *Clinical immunology*. 2003;109(1):6-16.
15. Okano M, Xie S, Li E. Cloning and characterization of a family of novel mammalian DNA (cytosine-5) methyltransferases. *Nature genetics*. 1998;19(3):219-20.
16. Ito S, Shen L, Dai Q, Wu SC, Collins LB, Swenberg JA, et al. Tet proteins can convert 5-methylcytosine to 5-formylcytosine and 5-carboxylcytosine. *Science*. 2011;333(6047):1300-3.
17. Tahiliani M, Koh KP, Shen Y, Pastor WA, Bandukwala H, Brudno Y, et al. Conversion of 5-methylcytosine to 5-hydroxymethylcytosine in mammalian DNA by MLL partner TET1. *Science*. 2009;324(5929):930-5.
18. Vasanthakumar A, Godley LA. 5-hydroxymethylcytosine in cancer: significance in diagnosis and therapy. *Cancer genetics*. 2015;208(5):167-77.

19. Lee W, Johnson J, Gough DJ, Donoghue J, Cagnone GL, Vaghjiani V, et al. Mitochondrial DNA copy number is regulated by DNA methylation and demethylation of POLGA in stem and cancer cells and their differentiated progeny. *Cell death & disease*. 2015;6:e1664.
20. Kelly RD, Mahmud A, McKenzie M, Trounce IA, St John JC. Mitochondrial DNA copy number is regulated in a tissue specific manner by DNA methylation of the nuclear-encoded DNA polymerase gamma A. *Nucleic acids research*. 2012;40(20):10124-38.
21. Cihak A. Biological effects of 5-azacytidine in eukaryotes. *Oncology*. 1974;30(5):405-22.
22. Stresemann C, Lyko F. Modes of action of the DNA methyltransferase inhibitors azacytidine and decitabine. *International journal of cancer Journal international du cancer*. 2008;123(1):8-13.
23. Christman JK. 5-Azacytidine and 5-aza-2'-deoxycytidine as inhibitors of DNA methylation: mechanistic studies and their implications for cancer therapy. *Oncogene*. 2002;21(35):5483-95.
24. Brown TA, Clayton DA. Release of replication termination controls mitochondrial DNA copy number after depletion with 2',3'-dideoxycytidine. *Nucleic acids research*. 2002;30(9):2004-10.
25. Martin JL, Brown CE, Matthews-Davis N, Reardon JE. Effects of antiviral nucleoside analogs on human DNA polymerases and mitochondrial DNA synthesis. *Antimicrobial agents and chemotherapy*. 1994;38(12):2743-9.
26. Facucho-Oliveira JM, St John JC. The relationship between pluripotency and mitochondrial DNA proliferation during early embryo development and embryonic stem cell differentiation. *Stem cell reviews*. 2009;5(2):140-58.

27. Dickinson A, Yeung KY, Donoghue J, Baker MJ, Kelly RD, McKenzie M, et al. The regulation of mitochondrial DNA copy number in glioblastoma cells. *Cell death and differentiation*. 2013;20(12):1644-53.
28. Kukita A, Yoshida MC, Fukushige S, Sakakibara M, Joh K, Mukai T, et al. Molecular gene mapping of human aldolase A (ALDOA) gene to chromosome 16. *Human genetics*. 1987;76(1):20-6.
29. Rottmann WH, Tolan DR, Penhoet EE. Complete amino acid sequence for human aldolase B derived from cDNA and genomic clones. *Proceedings of the National Academy of Sciences of the United States of America*. 1984;81(9):2738-42.
30. Oliva D, Cali L, Feo S, Giallongo A. Complete structure of the human gene encoding neuron-specific enolase. *Genomics*. 1991;10(1):157-65.
31. Carey BW, Finley LW, Cross JR, Allis CD, Thompson CB. Intracellular alpha-ketoglutarate maintains the pluripotency of embryonic stem cells. *Nature*. 2015;518(7539):413-6.
32. Vaghjiani V, Vaithilingam V, Saraswati I, Sali A, Murthi P, Kalionis B, et al. Hepatocyte-like cells derived from human amniotic epithelial cells can be encapsulated without loss of viability or function in vitro. *Stem cells and development*. 2014;23(8):866-76.
33. Garrett R, Grisham CM. *Biochemistry*. 4th ed. Belmont, CA: Brooks/Cole, Cengage Learning; 2010. xxxiii, 1059, 48, 34 p. p.
34. Baker BM, Haynes CM. Mitochondrial protein quality control during biogenesis and aging. *Trends in biochemical sciences*. 2011;36(5):254-61.
35. Kelly RD, St John JC. Role of mitochondrial DNA replication during differentiation of reprogrammed stem cells. *The International journal of developmental biology*. 2010;54(11-12):1659-70.

36. Aurich I, Mueller LP, Aurich H, Luetzkendorf J, Tisljar K, Dollinger MM, et al. Functional integration of hepatocytes derived from human mesenchymal stem cells into mouse livers. *Gut*. 2007;56(3):405-15.
37. Lysy PA, Campard D, Smets F, Malaise J, Mourad M, Najimi M, et al. Persistence of a chimerical phenotype after hepatocyte differentiation of human bone marrow mesenchymal stem cells. *Cell proliferation*. 2008;41(1):36-58.
38. Lysy PA, Smets F, Najimi M, Sokal EM. Leukemia inhibitory factor contributes to hepatocyte-like differentiation of human bone marrow mesenchymal stem cells. *Differentiation; research in biological diversity*. 2008;76(10):1057-67.
39. Wang PP, Wang JH, Yan ZP, Hu MY, Lau GK, Fan ST, et al. Expression of hepatocyte-like phenotypes in bone marrow stromal cells after HGF induction. *Biochemical and biophysical research communications*. 2004;320(3):712-6.
40. Cho YM, Kwon S, Pak YK, Seol HW, Choi YM, Park do J, et al. Dynamic changes in mitochondrial biogenesis and antioxidant enzymes during the spontaneous differentiation of human embryonic stem cells. *Biochemical and biophysical research communications*. 2006;348(4):1472-8.
41. Falkenberg M, Larsson NG, Gustafsson CM. DNA replication and transcription in mammalian mitochondria. *Annual review of biochemistry*. 2007;76:679-99.
42. Zhang J, Khvorostov I, Hong JS, Oktay Y, Vergnes L, Nuebel E, et al. UCP2 regulates energy metabolism and differentiation potential of human pluripotent stem cells. *The EMBO journal*. 2011;30(24):4860-73.
43. Watkins PB, Wrighton SA, Maurel P, Schuetz EG, Mendez-Picon G, Parker GA, et al. Identification of an inducible form of cytochrome P-450 in human liver. *Proceedings of the National Academy of Sciences of the United States of America*. 1985;82(18):6310-4.

44. Chandra V, Huang P, Potluri N, Wu D, Kim Y, Rastinejad F. Multidomain integration in the structure of the HNF-4 α nuclear receptor complex. *Nature*. 2013;495(7441):394-8.
45. Mohammad HP, Baylin SB. Linking cell signaling and the epigenetic machinery. *Nature biotechnology*. 2010;28(10):1033-8.
46. Dominguez-Sola D, Ying CY, Grandori C, Ruggiero L, Chen B, Li M, et al. Non-transcriptional control of DNA replication by c-Myc. *Nature*. 2007;448(7152):445-51.
47. Hahn WC, Counter CM, Lundberg AS, Beijersbergen RL, Brooks MW, Weinberg RA. Creation of human tumour cells with defined genetic elements. *Nature*. 1999;400(6743):464-8.
48. Latil A, Vidaud D, Valeri A, Fournier G, Vidaud M, Lidereau R, et al. htert expression correlates with MYC over-expression in human prostate cancer. *International journal of cancer Journal international du cancer*. 2000;89(2):172-6.
49. Moore LD, Le T, Fan GP. DNA Methylation and Its Basic Function. *Neuropsychopharmacol*. 2013;38(1):23-38.
50. Yuan BZ, Jefferson AM, Popescu NC, Reynolds SH. Aberrant gene expression in human non small cell lung carcinoma cells exposed to demethylating agent 5-aza-2'-deoxycytidine. *Neoplasia*. 2004;6(4):412-9.
51. Dannenberg LO, Edenberg HJ. Epigenetics of gene expression in human hepatoma cells: expression profiling the response to inhibition of DNA methylation and histone deacetylation. *BMC genomics*. 2006;7:181.
52. Wallerman O, Motallebipour M, Enroth S, Patra K, Bysani MS, Komorowski J, et al. Molecular interactions between HNF4a, FOXA2 and GABP identified at regulatory DNA elements through ChIP-sequencing. *Nucleic acids research*. 2009;37(22):7498-508.
53. De Carvalho DD, You JS, Jones PA. DNA methylation and cellular reprogramming. *Trends Cell Biol*. 2010;20(10):609-17.

54. Easley CA, Miki T, Castro CA, Ozolek JA, Minervini CF, Ben-Yehudah A, et al. Human amniotic epithelial cells are reprogrammed more efficiently by induced pluripotency than adult fibroblasts. *Cellular reprogramming*. 2012;14(3):193-203.
55. Takashima Y, Guo G, Loos R, Nichols J, Ficz G, Krueger F, et al. Resetting transcription factor control circuitry toward ground-state pluripotency in human. *Cell*. 2014;158(6):1254-69.
56. Smallwood A, Esteve PO, Pradhan S, Carey M. Functional cooperation between HP1 and DNMT1 mediates gene silencing. *Genes & development*. 2007;21(10):1169-78.
57. Kelsey GD, Povey S, Bygrave AE, Lovell-Badge RH. Species- and tissue-specific expression of human alpha 1-antitrypsin in transgenic mice. *Genes & development*. 1987;1(2):161-71.
58. Tirona RG, Lee W, Leake BF, Lan LB, Cline CB, Lamba V, et al. The orphan nuclear receptor HNF4alpha determines PXR- and CAR-mediated xenobiotic induction of CYP3A4. *Nature medicine*. 2003;9(2):220-4.
59. Goffin J, Eisenhauer E. DNA methyltransferase inhibitors-state of the art. *Annals of oncology : official journal of the European Society for Medical Oncology / ESMO*. 2002;13(11):1699-716.
60. Gafni O, Weinberger L, Mansour AA, Manor YS, Chomsky E, Ben-Yosef D, et al. Derivation of novel human ground state naive pluripotent stem cells. *Nature*. 2013;504(7479):282-6.
61. Koyanagi-Aoi M, Ohnuki M, Takahashi K, Okita K, Noma H, Sawamura Y, et al. Differentiation-defective phenotypes revealed by large-scale analyses of human pluripotent stem cells. *Proceedings of the National Academy of Sciences of the United States of America*. 2013;110(51):20569-74.

62. Ma H, Morey R, O'Neil RC, He Y, Daughtry B, Schultz MD, et al. Abnormalities in human pluripotent cells due to reprogramming mechanisms. *Nature*. 2014;511(7508):177-83.
63. Polo JM, Anderssen E, Walsh RM, Schwarz BA, Nefzger CM, Lim SM, et al. A molecular roadmap of reprogramming somatic cells into iPS cells. *Cell*. 2012;151(7):1617-32.
64. Prochownik EV. c-Myc: linking transformation and genomic instability. *Current molecular medicine*. 2008;8(6):446-58.
65. Wang J, Hannon GJ, Beach DH. Risky immortalization by telomerase. *Nature*. 2000;405(6788):755-6.
66. Roson-Burgo B, Sanchez-Guijo F, Del Canizo C, De Las Rivas J. Transcriptomic portrait of human Mesenchymal Stromal/Stem Cells isolated from bone marrow and placenta. *BMC genomics*. 2014;15:910.
67. Lawrence MS, Stojanov P, Polak P, Kryukov GV, Cibulskis K, Sivachenko A, et al. Mutational heterogeneity in cancer and the search for new cancer-associated genes. *Nature*. 2013;499(7457):214-8.
68. Zhang Y, Zhang A, Shen C, Zhang B, Rao Z, Wang R, et al. E2F1 acts as a negative feedback regulator of c-Mycinduced hTERT transcription during tumorigenesis. *Oncology reports*. 2014;32(3):1273-80.

Chapter 5

Effects of Encapsulation on HLC mtDNA copy number, DNA methylation of POLGA and their transcriptomic profile

5.1 Introduction

Deriving functional hepatocytes will pave the way for treating liver disease and drug screening. Due to the scarcity of human hepatocytes available for transplantation, hepatocyte-like cells have been derived from various stem cell types with varied success (1-3). Cells grown under laboratory conditions are often on hard plastic or glass surfaces that do not represent true *in vivo* conditions. Cells within the organs are generally supported by extracellular matrix and in contact with other cells. Culturing cells in 3D closely mimics physiological conditions better than 2D culture. We have reported changes in gene expression and the metabolic profile of 3D cultured cells compared to 2D cultured cells (4). Culturing hepatocyte-like cells in 3D may represent a novel tool for toxicity and metabolic drug screening assays (5). I seek to establish whether encapsulation and differentiation of hAEC generates functionally mature hepatocytes. Here, I evaluate global changes in gene expression with hepatic differentiation and encapsulation using RNAseq.

Encapsulation of hAEC

Various methods have been used to create a 3D environment that mimics *in vivo* conditions. Cell encapsulation in biocompatible microcapsules is a good alternative strategy for preventing immune rejection and delivering large number of cells. Use of hydrogels and synthetic biomaterials is a common approach in culturing cells in 3D (6, 7). A variety of biomaterials have been used including alginate (6, 8, 9), chitosan (10-12), agarose (13) and poly-ethylene-glycol (PEG) (14) for cell encapsulation; Of these, Barium alginate as a capsular material is most widely used for hepatocyte encapsulation studies (15). Barium alginate microcapsules have been used in human clinical trials and its safety has been evaluated in both animals and humans (16, 17). The choice of material influences foreign body response (FBR) from host immune cells when encapsulated cells are transplanted. The

standard assessment post-transplantation of encapsulated cells is the viability of the encapsulated cells and fibrotic cellular overgrowth around the capsule (16, 18). Although barium alginate is an inert material, there is passive FBR to the capsules. In addition, there have been reports of FBR to encapsulated islet cells which is mediated by macrophages that results in fibrosis and eventual death of encapsulated cells. However, this can be overcome by using a purer grade of alginate in the composition of microcapsules to reduce FBR (19).

Since initial conception of immune-isolation of the graft by encapsulation (20), further efforts have been made to deliver cells for various diseases. Transplantation of encapsulated islet cells has been the most widely used application of this technology. Both allogenic and xenogeneic cells have been transplanted in various models (21). Recent studies have shown that hepatocytes can also be encapsulated; a large number of capsules grafted to the extra hepatic site and the transplanted cells can rescue animal models of ALF (22, 23). Transplantation of encapsulated hepatocytes overcomes the need for systemic immune suppression and the low rate of engraftment.

The microcapsules are 200-700 μM in diameter, have a porous membrane that allow small molecules and oxygen to diffuse but not large immunoglobulins. Furthermore, encapsulation creates a three dimensional (3D) environment which enhances the function of HLC. In fact, recent studies have shown that the 3D environment augments the function of hepatocytes by secretion of extracellular matrixes (24). A 3D culture system allows cell-to-cell and cell-to-matrix interactions that are important for cell functions. Both induced pluripotent cells (25) and embryonic stem cells (26) show improved differentiation potential in 3D culture. We have also shown that barium alginate encapsulated HLC have enhanced gene expression and metabolic functions (4). Encapsulating HLC for cell transplantation purposes would be a good alternative strategy but the effects of encapsulation on mtDNA copy number, DNA methylation of POLGA and their transcriptome remains largely unexplored.

MtDNA copy number and DNA methylation.

Mitochondrial DNA copy number increases with lineage commitment and differentiation (27, 28). The role of mitochondria in encapsulated HLC would also be important due to lack of sufficient oxygen to the core of the capsule. The encapsulated HLC at the core of the capsule are often prone to oxygen and nutrient deprivation due to the limit of passive diffusion. Encapsulating HLC at a rate of 1000 cells per capsule with an average diameter of 600 μm maintains viability at more than 90% (4). Continual replication of mtDNA is required to generate ATP via OXPHOS to meet the functional needs of HLC. Provided there is a limited supply of oxygen, it would be important to evaluate mtDNA copy number in encapsulated hAEC and HLC. My previous findings showed that partial depletion of mtDNA with ddC promotes induction of pluripotent genes. I also sought to determine mtDNA copy number in encapsulated hAEC and HLC depleted of mtDNA for one and three days.

MtDNA replication is primarily driven by POLGA, which has been shown to be differentially methylated at exon 2 (27, 28). DNA methylation at exon 2 of POLGA results in low mtDNA copy number; whereas demethylation results in transcription of POLGA and a subsequent increase in mtDNA copy number. However, DNA methylation at exon 2 of POLGA has not been evaluated in encapsulated hAEC and HLC. I set out to evaluate mtDNA copy number and DNA methylation of POLGA in encapsulated hAEC and HLC in non-depleted cells and 1 and 3 day mtDNA depleted cells.

Gene expression Patterns for encapsulated HLC

Encapsulation provides 3D culture conditions where there are cell-to cell and cell-to-matrix interactions that mimic *in vivo* conditions and impact gene expression (29). Encapsulation and differentiation of hAEC allows secretion of extracellular matrix, which has been shown to enhance hepatocyte functions (30, 31). HAEC cultured in 2D are also cultured on collagen

coated flasks to promote better differentiation and function. Mechanical properties of secreted collagen within the capsules would be different compared to a collagen coated flask, which would in turn affect gene expression. There is evidence that changes in the extracellular matrix impact on ERK and RHO signalling in cultured breast cancer cells (32). Culturing neuroblastoma cells in a 3D collagen matrix increases gene expression of cytoskeleton, extracellular matrix and neurite outgrowth associated genes (33). Integrins interact with extracellular matrix and activate kinase and MAPK signalling. These interactions also dictate formations of tight junctions and cell adhesion molecules in 3D environment (34). Culturing human hepatocytes in 3D aggregates increases gene expression of lipid, organic acid and amino acid metabolism. In addition, there was increased expression of transcription factor HNF4 α and its target genes (30). Interestingly, HepG2 cells cultured in spheroids also showed increased expression of E-cadherin, VEGF and KDR (35). Cell-to-cell contact in 3D cultures allows for increased expression of cell adhesion and tight junction proteins claudin-1, ZO-1, occluding, β -catenin and E-cadherin in the hepatoma cell line Huh7 (36). These studies suggest that anchor proteins and maintenance of proliferation are enhanced in 3D culture.

Metabolic functions of hepatocytes are also impacted when culture in 3D compared to 2D. The primary driver of enhanced metabolic functions is the ability of hepatocyte to become polarised (37). A key step in attaining polarity is accompanied by increased OXPHOS, changes in mitochondrial mass and their distribution in the cytoplasm (38). Polarisation of hepatocytes requires increased ATP production, which is generated from lipid metabolism. There is increased production of albumin and urea when hepatocytes are cultured in 3D and polarised (39). These findings suggest that culture and differentiation of hepatocytes in 3D barium alginate microcapsules enhance their metabolic functions and gene expression patterns. Here, I evaluate transcriptome changes when hAEC are induced to differentiate into HLC and with encapsulation of HLC.

5.2 Materials and Methods

hAEC isolation

hAEC were isolated, as previously described in the General Materials and Methods, Section 2.3 and frozen in DMEM/F12 with 10% DMSO in liquid nitrogen until further use.

MtDNA depletion

hAEC were cultured for 3-5 days until they achieved epithelial morphology. To deplete mtDNA, cells were then treated with 10 μ M ddC supplemented with 50 μ g/ml Uridine (Sigma Aldrich) in DMEM/F12 with 10% FBS. The media was changed every 24 hours for 1 (20% mtDNA depletion) and 3 days (50% mtDNA depletion).

Encapsulation of hAEC

Upon mtDNA depletion, cells were encapsulated in barium alginate microcapsules, as described in the General Materials and Methods, Section 2.8.

HLC differentiation

Upon encapsulation, hAEC were differentiated into HLC, as described in Section 2.4 of the General Materials and Methods. Encapsulated hAEC were differentiated into HLC for 14 and 28 days with media changed every alternate day.

Cell viability of encapsulated cells

Viability of encapsulated cells was determined at 0 days post-encapsulation and at 14 and 28 post-encapsulation in differentiating HLC. Encapsulated cells were stained with 6-carboxyfluorescein diacetate (CFDA, 4.6 μ g/mL; Sigma Aldrich) and propidium iodide (PI, 10 μ g/ml; Sigma Aldrich). The encapsulated cells were rinsed three times in warm DPBS and incubated with CFDA at 37°C for 30 minutes. Encapsulated cells were washed three times

with DPBS to remove excess CFDA and PI was added for 10 minutes. Encapsulated cells were rinsed in DPBS and visualised under a fluorescence microscope under blue filter. The live cells were stained green and dead cells were stained red.

Decapsulation of HLC

Upon completion of HLC differentiation, encapsulated cells were decapsulated, as described in the General Materials and Methods, Section 2.9.

Nucleic acid purification

After decapsulation of HLC, DNA was extracted from the cell pellets, as described in the General Materials and Methods, Section 2.5.4. RNA was extracted from cell pellets, as described in the General Materials and Methods, Section 2.5.1.

MtDNA copy number and MeDIP

MtDNA copy number was evaluated for encapsulated HLC, as described in the General Materials and Methods, Section 2.6. Immunoprecipitation for 5-methylcytosine and 5-hydroxymethylcytosine was performed on encapsulated HLC, as described in the General Materials and Methods, Section 2.7.

RNA-seq

RNA was extracted using the RNA Mini Kit (Qiagen). On column DNase I digest was performed to eliminate contaminating DNA. Quality control was performed on all RNA samples using Agilent Bioanalyser Nanochip (Agilent Technologies). RNAseq was performed at the Australian Genomic Research Facility (AGRF) at Walter and Eliza Hall Institute of Medical Research (WEHI). cDNA libraries were prepared using the Illumina TrueSeq stranded mRNA Kit (Illumina), according to the manufacturer's instructions. RNA libraries were sequenced using Illumina HiSeq 2000 (Illumina) with 100 base pair single end reads

with 20 million reads per sample. Data were generated with the Illumina CASAVA pipeline version 1.8.2 (Illumina). Data analysis was performed using R package. HLC were compared with hAEC, encapsulated HLC with hAEC, and encapsulated HLC with HLC.

Ingenuity Pathway Analysis

Normalised gene expression data generated from RNA-seq were uploaded into Ingenuity Pathway Analysis software (IPA; Qiagen). Pathway and network analysis was performed with IPA by applying a minimum of 2 fold change in gene expression, P value of <0.05 and false discovery rate of <0.05 (q value). The selected genes were mapped against the inbuilt KEGG pathway for selection of the top five canonical pathways and top five networks, which showed differential gene expression.

Statistical analysis

Data are shown as the mean \pm SEM derived from a minimum of n = 4-6 hAEC cultures. Comparisons were made using One-Way Anova using GraphPad Prism V6.01 (Graph Pad, San Diego, CA). Significance was accorded when $P < 0.05$; significance given as * $p < 0.05$, ** $p < 0.01$, *** $p < 0.001$ and **** $p < 0.0001$.

5.3 Results

5.3.1 MtDNA copy number and methylation of *POLGA* in encapsulated hAEC.

I performed encapsulation of hAEC to differentiate hAEC in a 3-dimensional environment. The encapsulation of hAEC was performed on cells depleted of their mtDNA for 1 day (20% depletion of mtDNA), 3 days (50% depletion of mtDNA) and non-depleted hAEC. Both mtDNA depleted and non-depleted hAEC retained viability at more than 95% post-encapsulation. The viability of encapsulated cells remained more than 90% after 14 and 28 days post-encapsulation (Figure 5.1).

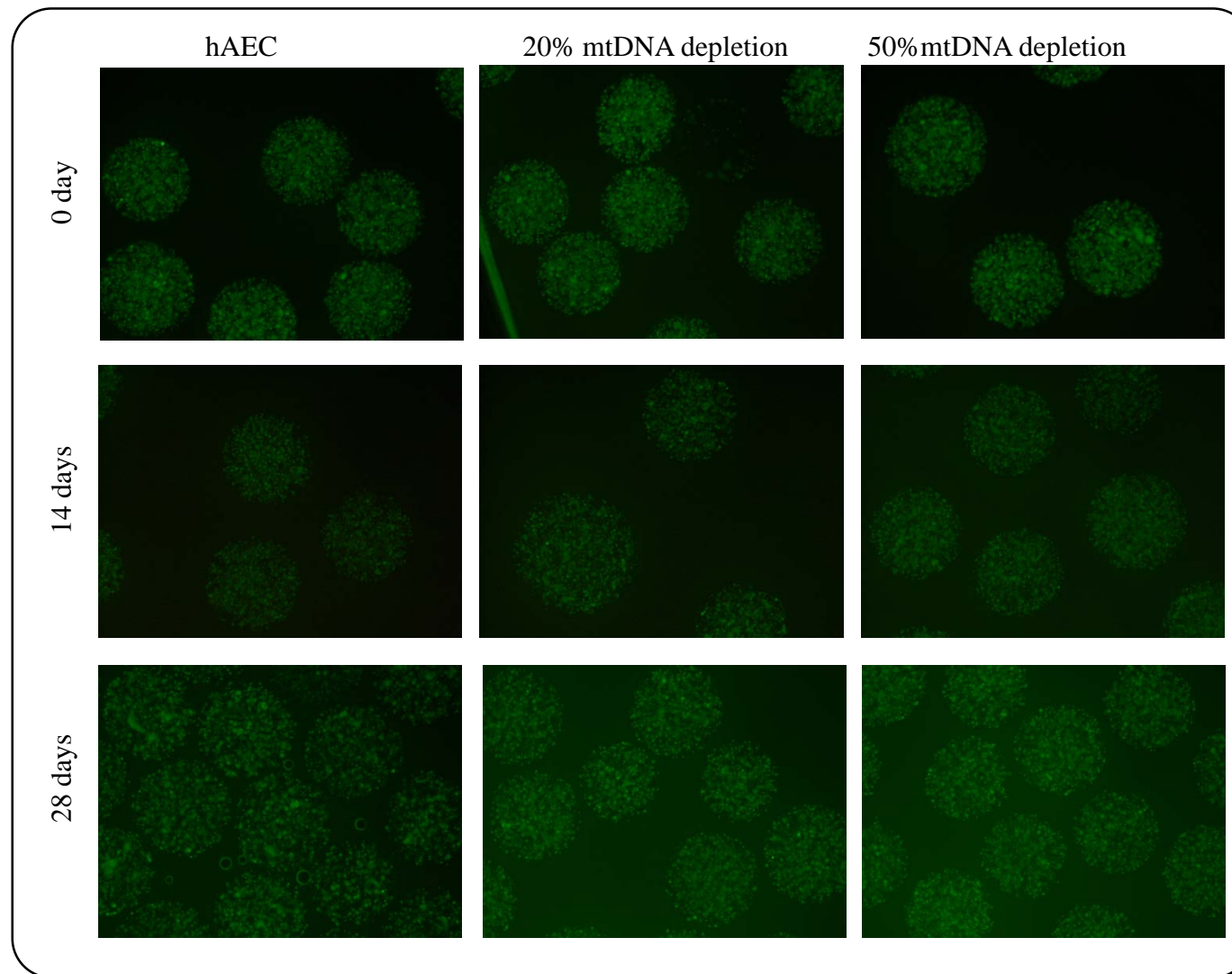


Figure 5.1. Assessment of viability of encapsulated cells. Encapsulated cells were stained with CFDA (green) and propidium iodide (red) to evaluate viability of the encapsulated cells at 0 days, 14 days and 28 days in hAEC, 20% mtDNA depleted cells and 50% mtDNA depleted cells respectively. Average capsule size was 600 μ M.

Assessment of mtDNA copy number showed encapsulated 2wk HLC and HLC had significantly reduced mtDNA copy number with differentiation (Figure 5.2A). In addition, the levels of 5mC enrichment were also significantly lower in encapsulated 2wk HLC and encapsulated HLC (Figure 5.2A). These results show that encapsulated HLC are unable to increase their mtDNA copy number despite having low DNA methylation at exon 2 of *POLGA*. Whereas 20% mtDNA depleted hAEC showed decreased mtDNA copy number in 2wk encapsulated HLC, mtDNA copy number in encapsulated HLC returned to similar levels as undifferentiated hAEC (Figure 5.2B). Analysis of the level of enrichment for 5mC in 20% mtDNA depleted hAEC showed high levels of enrichment for DNA methylation at exon 2 of *POLGA*, whereas 5mC enrichment was significantly reduced in 2wk encapsulated HLC and encapsulated HLC (Figure 5.2B).

Upon encapsulation and differentiation, mtDNA copy number was further significantly decreased in 2wk encapsulated HLC but mtDNA copy number in encapsulated HLC returned to their original levels (Figure 5.2C). However, analysis of 5mC enrichment showed very low DNA methylation in 50% mtDNA depleted hAEC and 2wk encapsulated HLC (Figure 5.2C). Contrary to that, 5mC enrichment levels were increased in 50% mtDNA depleted encapsulated HLC, however, the changes were not statistically significant (Figure 2C). Overall, mtDNA copy number was significantly reduced at 14 days of encapsulated differentiation and there was increased mtDNA copy number in encapsulated HLC in both depleted and non-depleted hAEC. The ratio of 5mC:5hmC showed a significant reduction in DNA methylation at exon 2 of *POLGA* with encapsulation, however, there were no increases in mtDNA copy number in encapsulated cells.

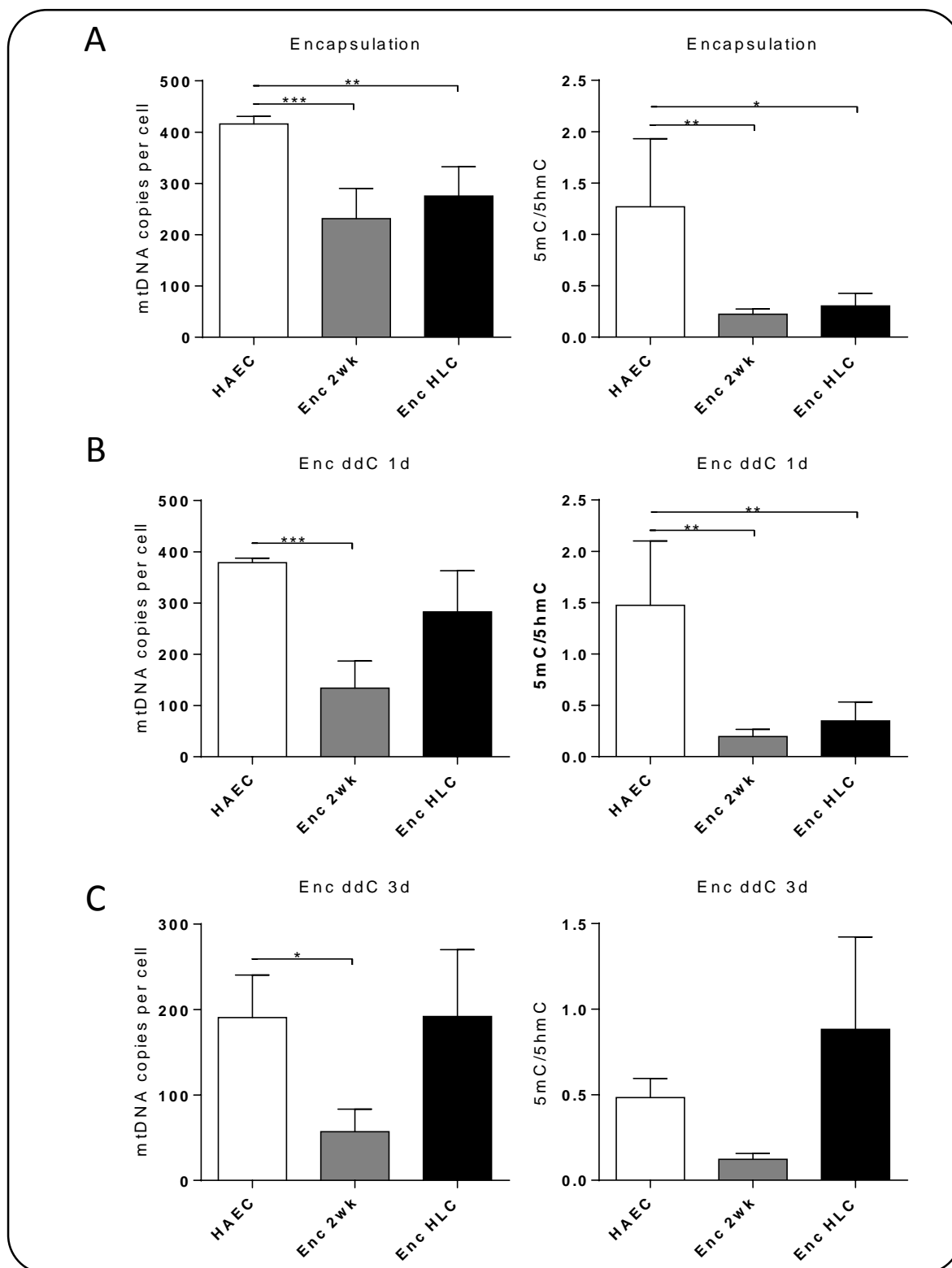


Figure 5.2. MtdNA copy number and MeDIP of encapsulated cells. MtdNA copy number and DNA methylation of *POLGA* at exon 2 in (A) hAEC encapsulated 2wk HLC and encapsulated HLC. (B) MtdNA copy number and methylation of *POLGA* at exon 2 in 20% mtdNA depleted hAEC, 2wk encapsulated HLC post-depletion and encapsulated HLC post-depletion. (C) MtdNA copy number and DNA methylation of *POLGA* at exon 2 in 50% mtdNA depleted hAEC, 2wk encapsulated HLC post-depletion and encapsulated HLC post-depletion. Data presented as mean \pm SEM of $n = 4$. * $P < 0.05$, ** $P < 0.01$ and *** $P < 0.001$ compared to hAEC using one-way ANOVA.

5.3.2 Changes in gene expression in differentiated HLC.

I performed RNA-seq on differentiated HLC and compared them to undifferentiated hAEC to evaluate changes in gene expression with HLC differentiation. There were 1722 differentially regulated genes in HLC with 695 genes being up regulated and 1027 genes being down regulated. The top candidate genes up regulated in HLC include *MIR612*, which inhibits hepatocellular carcinoma proliferation, migration and metastasis (Table 5.1) (40). *KDR*, which functions as a *VEGF*-inducer of proliferation and tubular morphology (41), was also up regulated. A *WNT-2* family inhibitor *DKK1* was highly expressed in HLC, which is known to inhibit *WNT-2* mediated cell growth (42) and may promote differentiation. In addition, *OASL* was also upregulated, which regulates cytokine-mediated signalling pathway (43) and glutathione enzyme *GGT5* (Table 5.1). Other notable genes that were up regulated in HLC include complement factor B, follistatin and cytochrome P450 enzyme *CYP1B1*. Increased expression of *CYP1B1*, which is responsible for Phase I metabolism by inserting one atom of oxygen (44), creates substrates for other P450 cytochrome enzymes. Top candidate genes that were down regulated include *LICAM* and *PODXL*, which are involved in cell adhesion and migration (Table 5.1). Lipoprotein receptor *LDLR* and *LIPG*, genes involved in lipoprotein metabolism were also down regulated (Table 5.1). *LDLR* binding is thought to suppress cholesterol synthesis (45). Other notable genes that were down regulated include *SOX9*, *RASGRF1* and *SLCO2A1* (Table 5.1).

The top Canonical pathways affected were ATM signalling, axonal guidance signalling, cell cycle control of chromosomal replication, mitotic role of polo-like kinases and interferon signalling. The ATM signalling pathway was largely down regulated with only four genes, *GADD45B*, *GADD45G*, *JUN* and *NFKB* being up regulated. Upregulation of *GADD45* inhibits *CDK1* and *Cyclin B*, which, in turn, controls G2/M transition (Figure 5.3). Genes that control G2-M phase progression, *CDC25C* and *CDC2*, were also down regulated (Figure 5.3).

Table 5.1. Top candidate differentially expressed genes in HLC compared to undifferentiated hAEC. Up and down regulation is shown as fold change and its function.

Genes	Fold change	Function
MIR3936	261	No known function (may be implicated in cancer)
MIR612	241	Inhibition of HCC proliferation, migration, invasion, and metastasis
WDR86	178	No known function
KDR	144	Main mediator of VEGF-induced endothelial proliferation, survival, migration, tubular morphogenesis
CHST2	131	Transfer of sulfate to position 6 of non-reducing N-acetylglucosamine (GlcNAc) residues within keratan-like structures on N-linked glycans
DKK1	127	Secreted protein with two cysteine rich regions and is involved in embryonic development through its inhibition of the WNT signaling pathway
SCNN1A	93	Nonvoltage-gated, amiloride-sensitive, sodium channels control fluid and electrolyte transport across epithelia
GGT5	83	Convert leukotriene C4 to leukotriene D4. The enzyme is capable of cleaving the gamma-glutamyl moiety of glutathione.
EBF3	81	DNA binding transcription factor. EBF proteins are involved in B-cell differentiation, bone development and neurogenesis
OASL	73	Cytokine-mediated signalling pathway; defence response to virus; immune response
L1CAM	-497	Cell adhesion molecule, plays an important role in nervous system development, including neuronal migration and differentiation
PODXL	-320	Cell adhesion; cell migration; epithelial tube formation
SOX9	-199	Acts during chondrocyte differentiation and, with steroidogenic factor 1, regulates transcription of the anti-Muellerian hormone (AMH) gene.
RASGRF1	-159	A guanine nucleotide exchange factor (GEF), stimulates the dissociation of GDP from RAS protein
LDLR	-156	Low density lipoprotein (LDL) is normally bound at the cell membrane and taken into the cell. Has a role in homeostasis of cholesterol
PRRT4	-146	Proline-rich transmembrane protein 4
MYEOV	-139	Myeloma overexpressed
LIPG	-132	Has substantial phospholipase activity and may be involved in lipoprotein metabolism and vascular biology
KRT80	-130	Involved in cell differentiation, localizing near desmosomal plaques in earlier stages of differentiation but then dispersing throughout the cytoplasm in terminally differentiating cells
SLCO2A1	-121	Mediates the uptake and clearance of prostaglandins in numerous tissues

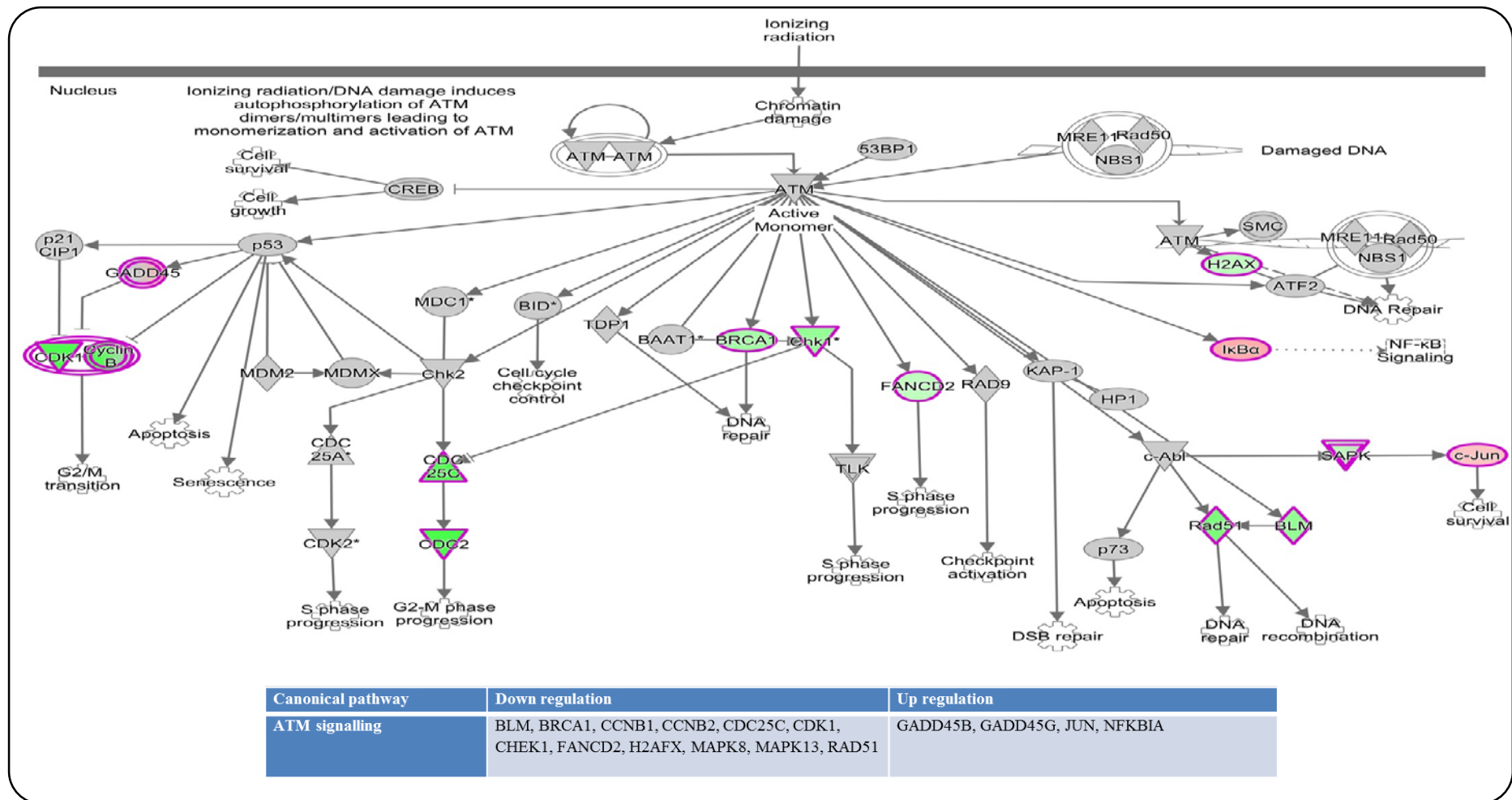


Figure 5.3. ATM signalling pathway. ATM signalling was the top canonical pathway affected in differentiated HLC compared to hAEC. Genes in the ATM signalling pathway were mainly down regulated except for GADD, JUN and NFKBIA. Red indicates up regulation in HLC and green indicates down regulation in HLC with $P < 0.05$ and $Q < 0.05$ and fold change ≥ 2 from $n = 4$.

Whereas there were a large number of genes down regulated in axonal guidance signalling, there were still 20 genes that were up regulated which included members of membrane anchored proteins and *WNT* genes (Figure 5.4). Though *EPHA2* and *EPHB2* were down regulated, their downstream targets *KALRN* and *SDC2* were up regulated which control cytoskeletal reorganisation in a cascade of genes (Figure 5.4). The cell cycle control of chromosomal replication pathway was down regulated which involved genes of cell division control protein *CDC6*, *CDC45* and DNA replication factor *MCM3*, 4, 5 and 6 (Figure 5.5). *ORC1* and *ORC6*, which are part of origin recognition complex (*ORC*) that control centriole and centrosome copy number, were also down regulated in HLC (Figure 5.5). Gene involved mitotic role of polo-like kinase, *KIF* and *PLK* were down regulated. *CDC2* and *Cyclin B* which are central to centrosome separation and mitotic entry, were also down regulated (Figure 5.6). More interestingly, the interferon signalling pathway was significantly up regulated with high expression of *IFIT* genes as well as *STAT* genes in HLC (Table 3). *JAK1* and *JAK2*, which activate *STAT1*, were up regulated. *STAT1* can be phosphorylated and form homodimers to activate Interferon type II signalling, whereas, phosphorylated *STAT1* and *STAT2* form heterodimers to activate type I interferon signalling (46) (Figure 5.7). Overall, these results indicate that HLC have exited proliferation and initiated differentiation, however, they also become highly immunogenic by up regulating interferon signalling.

I also performed network analysis on differentiated HLC. The top networks affected were cell cycle and cellular assembly, DNA replication, recombination and repair, developmental and hereditary disorders, hepatic system development and lipid, vitamin and mineral metabolism. Cell cycle, cellular assembly and organisation had four genes, *AURKB*, *BUB1*, *NDC80* and *SGOL1*, which were central to the network that were down regulated (Figure 5.8).

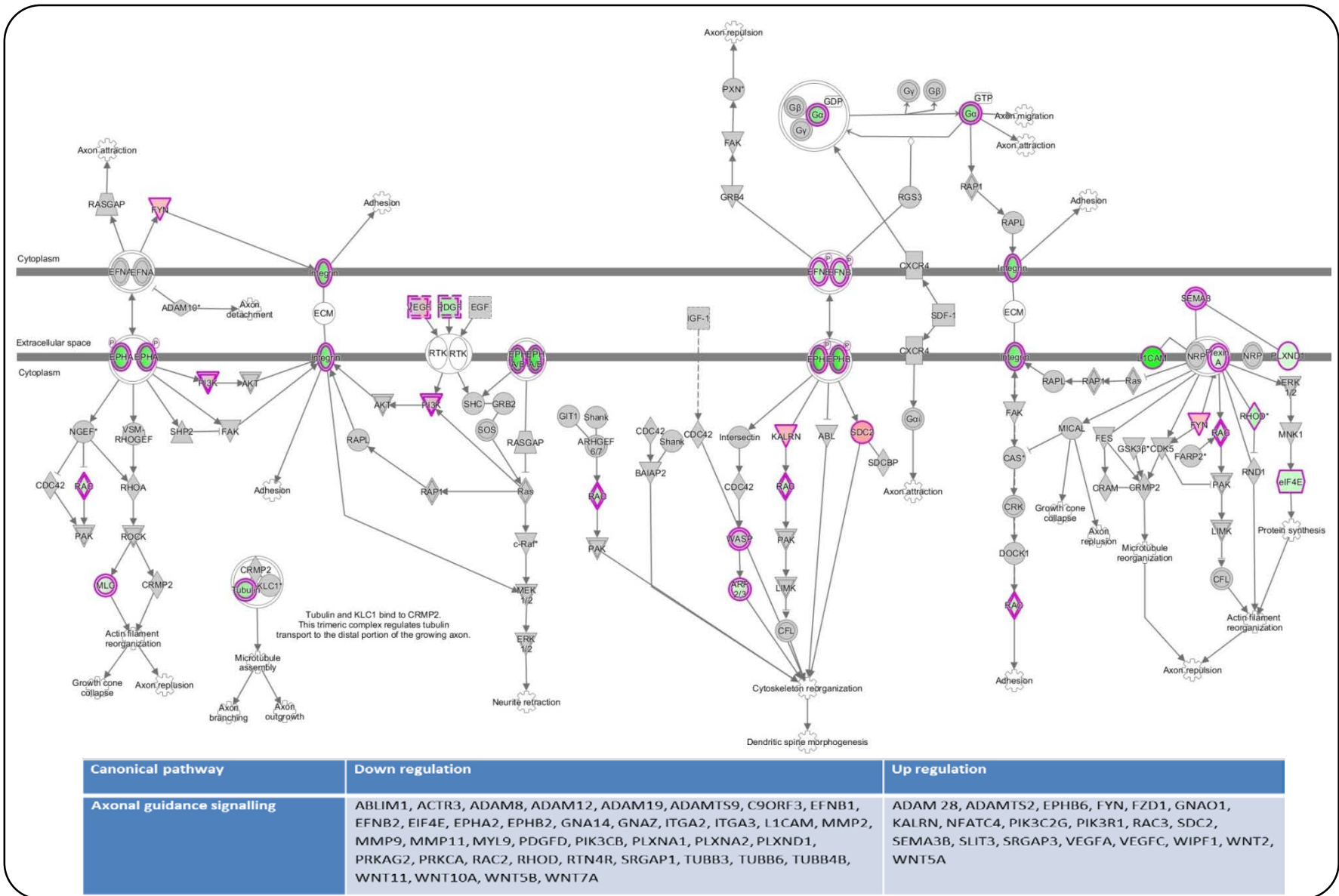


Figure 5.4. Axonal guidance signalling pathway. The top canonical pathway affected in differentiated HLC compared to hAEC. Genes in the axonal guidance signalling pathway showed equal number of genes up and regulated in HLC. Red indicates up regulation in HLC and green indicates down regulation in HLC with $P < 0.05$ and $Q < 0.05$ and fold change ≥ 2 from $n = 4$.

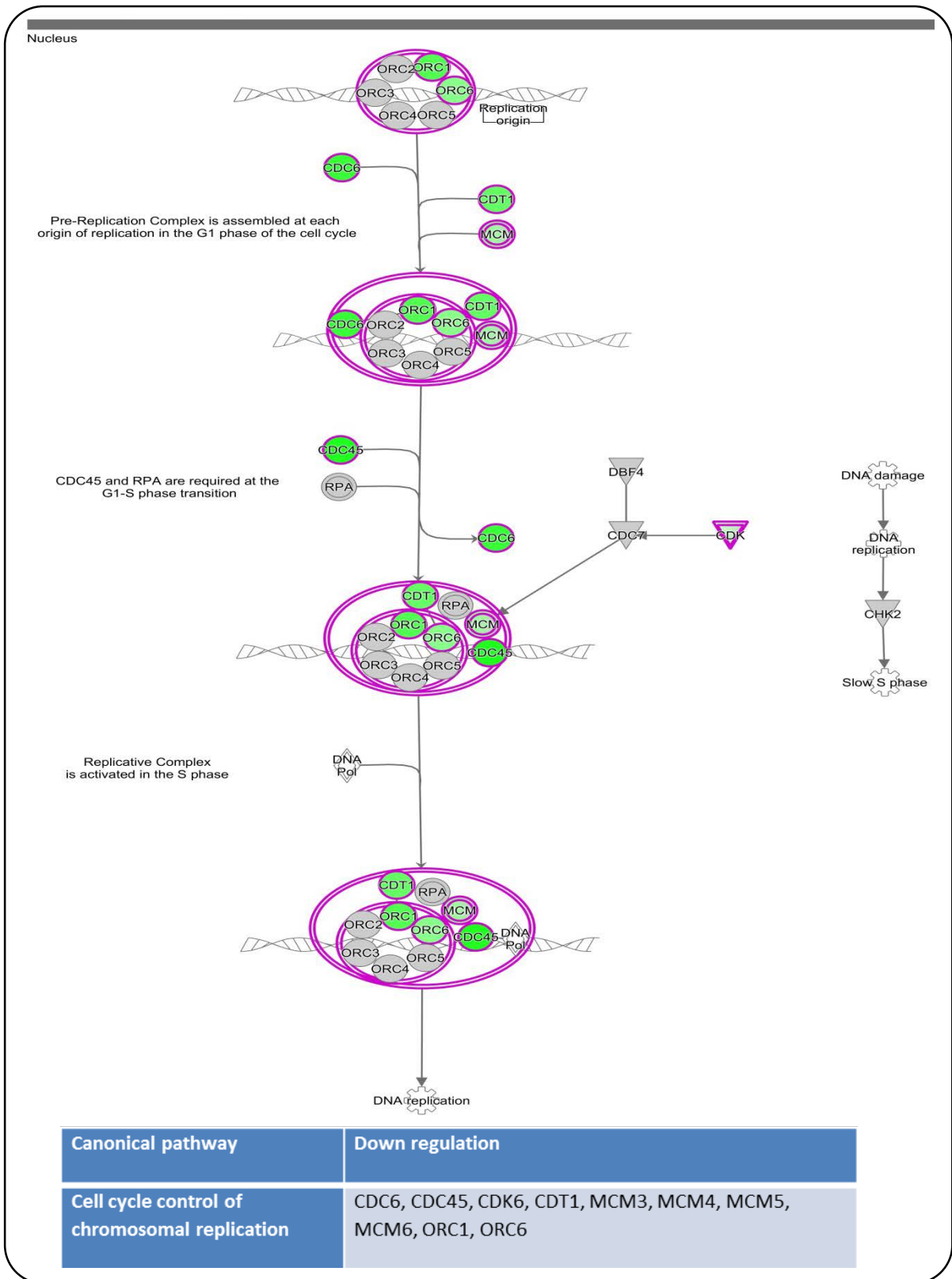


Figure 5.5. Cell cycle control of the chromosomal replication pathway. Cell cycle control and replication was among the canonical pathways affected in differentiated HLC compared to hAEC. Genes in the cell cycle control and chromosomal replication pathway were all down regulated in HLC. Red indicates up regulation in HLC and green indicates down regulation in HLC with $P < 0.05$ and $Q < 0.05$ and fold change ≥ 2 from $n = 4$.

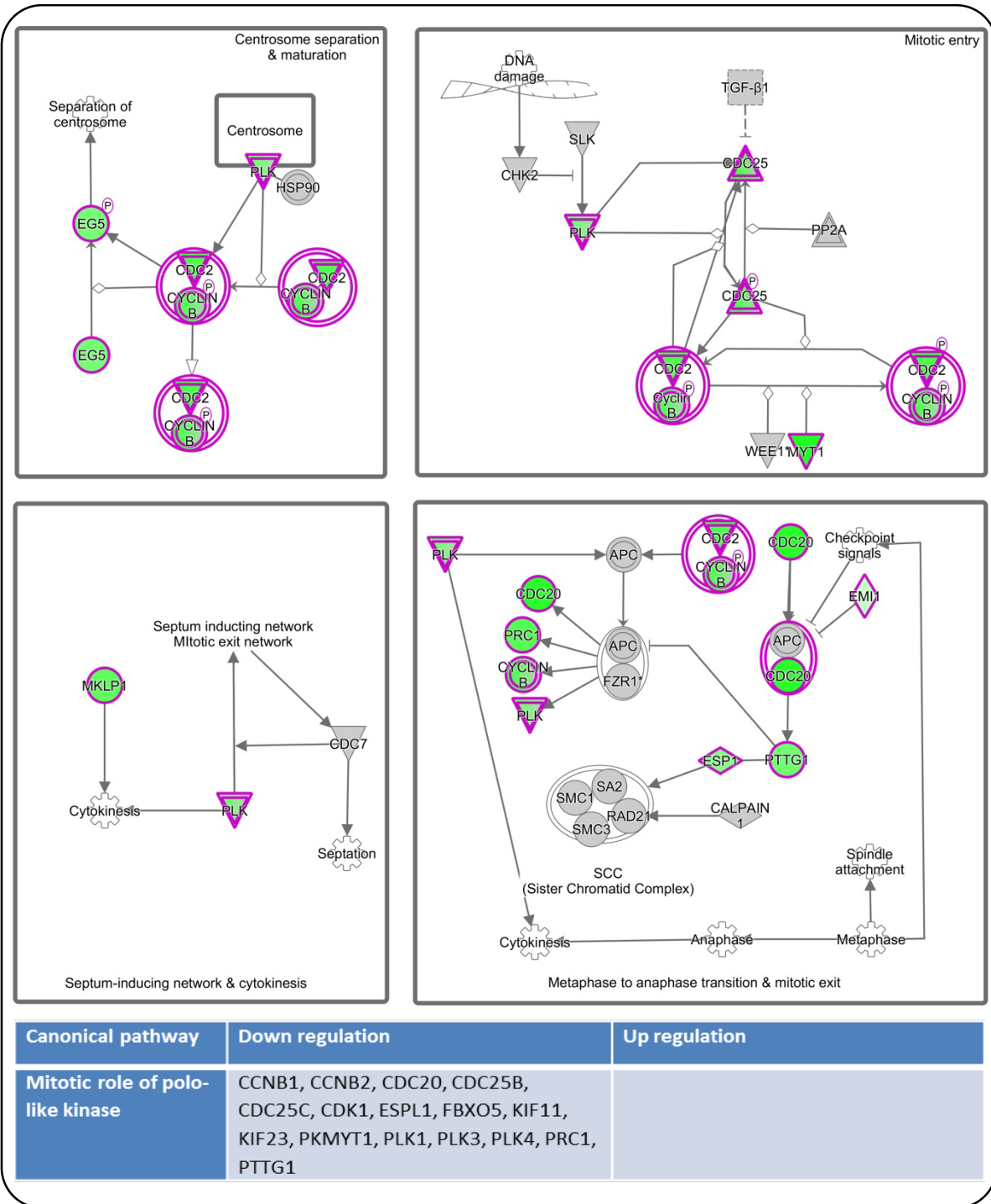


Figure 5.6. Mitotic role of polo-like kinase pathway. The mitotic role of polo-like kinase pathway was among the canonical pathways affected in differentiated HLC compared to hAEC. Genes in the mitotic role of polo-like kinase pathway were all down regulated in HLC. Red indicates up regulation in HLC and green indicates down regulation in HLC with $P < 0.05$ and $Q < 0.05$ and fold change ≥ 2 from $n = 4$.

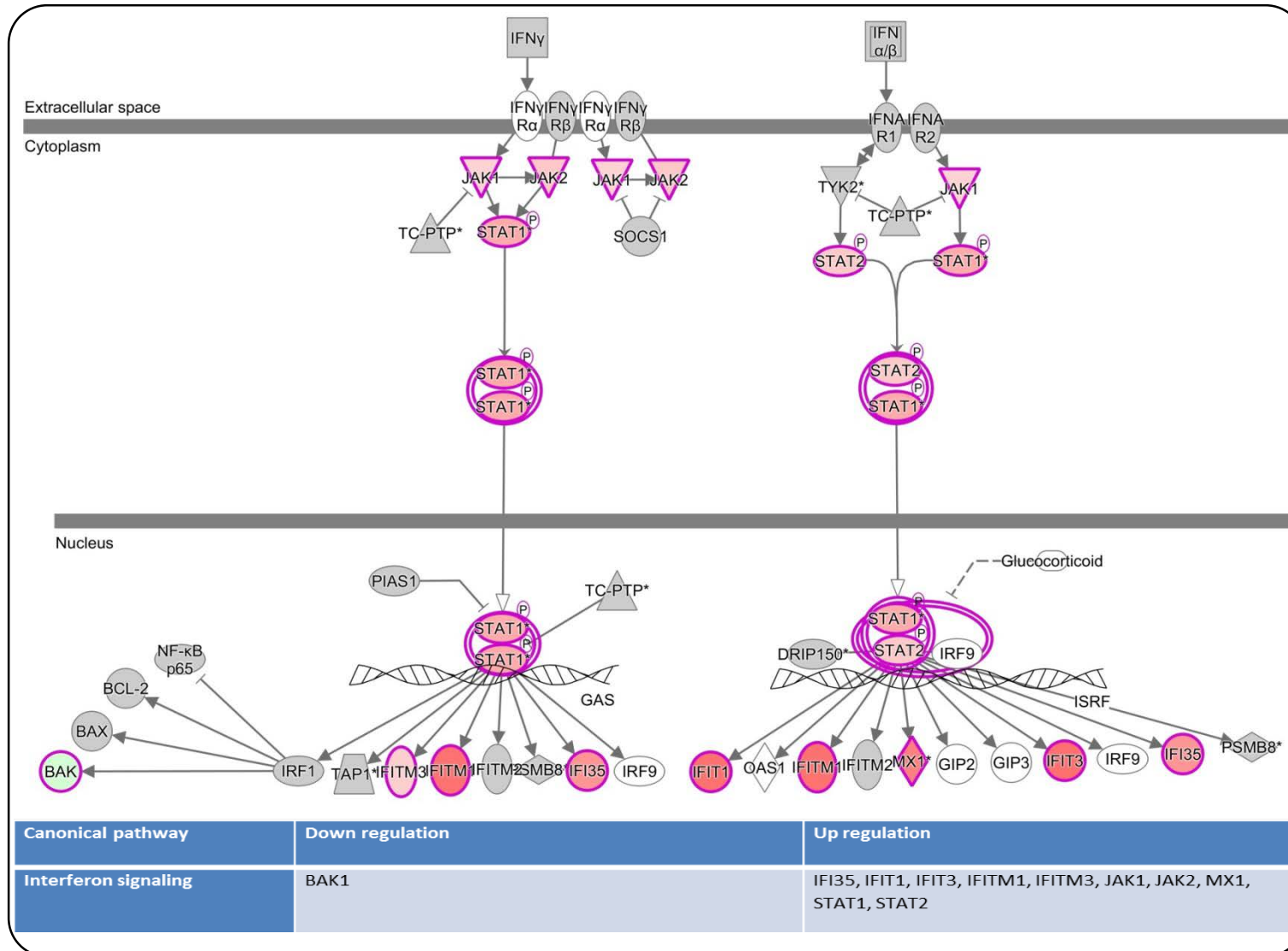


Figure 5.7. Interferon signalling. Interferon signalling was among the canonical pathways highly affected in differentiated HLC compared to hAEC. Genes in the interferon signalling pathway were all up regulated in HLC. Red indicates up regulation in HLC and green indicates down regulation in HLC with $P < 0.05$ and $Q < 0.05$ and fold change ≥ 2 from $n = 4$.

AURKB participates in chromosomal segregation during mitosis, *BUB1* is required in spindle assembly, *NDC80* is involved in correct segregation of chromosome during mitosis and *SGOL1* also participates in cell division. Some of the genes associated with *SGOL1*, *PPP2R2D* and *PPME1*, were upregulated in the network (Figure 5.8A). *CNN2*, *UACA* and *SPRED1* and *SPRED2* were all down regulated, however, they did not affect *ERK* expression even though they target *ERK* directly (Figure 5.8A). The DNA replication, recombination and repair network showed similar distribution of both up regulated and down regulated genes, with up regulation of *PLSCR1* and *CALCOCO2*, which were central to the network (Figure 5.8B). The other network involved in differentiated HLC was development and hereditary disorders. The majority of the genes in the network were down regulated with *BARD1*, *SRPK1* and *PCNA* central to regulating other genes in the network (Figure 5.9A). *BARD1*, which regulates cell growth and acts as a tumour suppressor, had an inhibitory effect on the target genes (Figure 5.9A). *SRPK1* and *PCNA*, which are involved with cell cycle and proliferation also had mainly inhibitory effects on gene expression of the target genes (Figure 5.9A).

Involvement of the hepatic system development network shows that hAEC are differentiating into HLC (Figure 5.9B). However, most genes involved were down regulated with only 6 genes up regulated. *NFκB* complex expression was unchanged, however, *B3GNT9* and *ARHGAP28*, which act directly on *NFκB* were up regulated in HLC. In addition, other genes in the hepatic system development network that act on *NFκB* were down regulated (Figure 5.9B). *GALK1* and *CRIPAK* which are directly associated with *ECT2* were also up regulated (Figure 5.9B). Moreover, genes involved in lipid, vitamin and mineral metabolism were also up regulated in differentiated HLC. *CA12*, a zinc metalloenzyme that catalyses hydration of carbon dioxide, which is also associated with *RDH11* and *SGSM2*, was highly expressed (Figure 5.10). *NADP-retinol dehydrogenase* was highly expressed and it is associated with

RDH10 and *DHRS3*, which were also highly expressed in HLC (Figure 5.10). These results indicate that HLC may also be able to perform some of the hepatocyte functions.

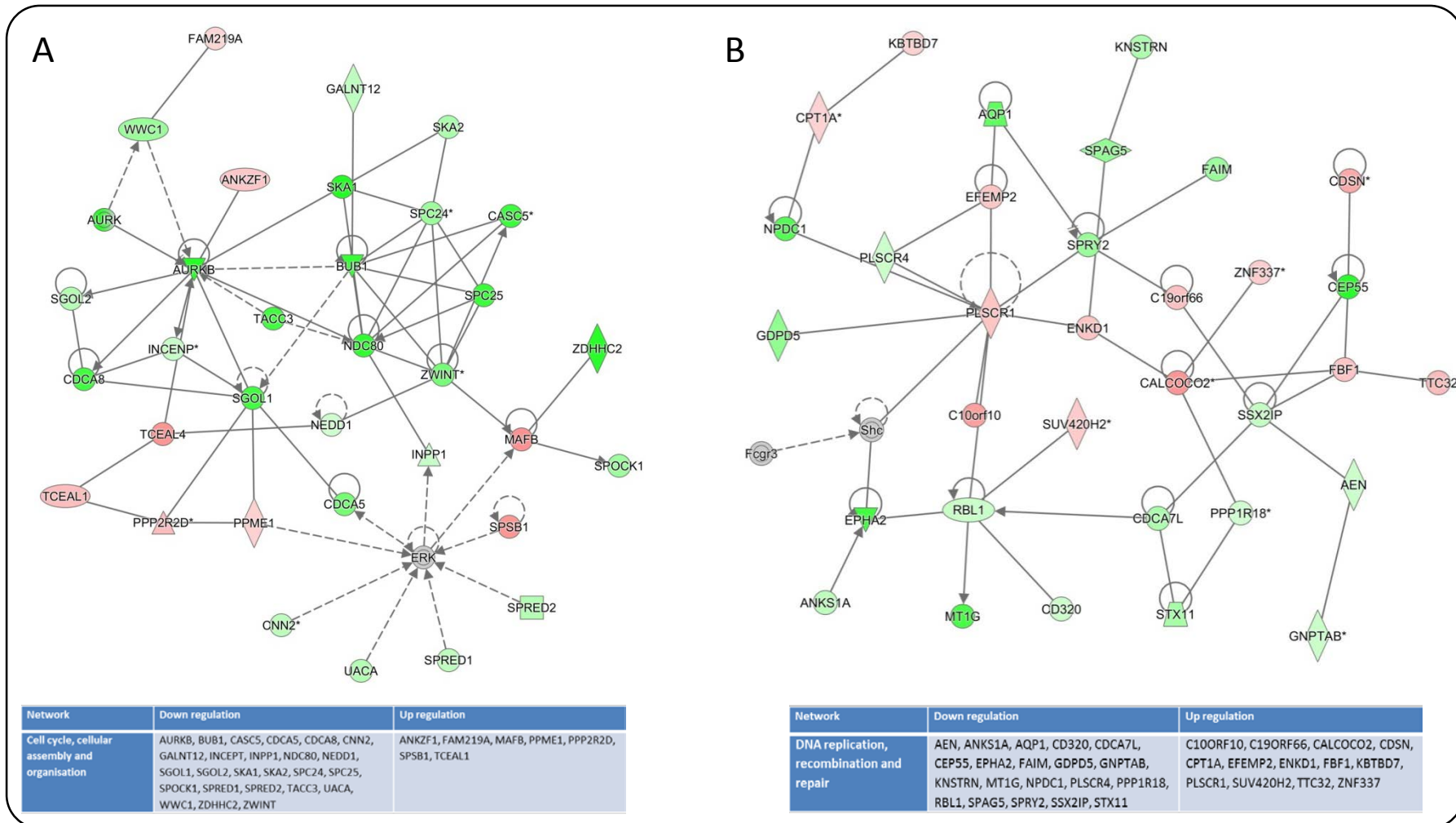


Figure 5.8. Networks involved in differentiated HLC. The top networks involved in differentiated HLC were (A) cell cycle, cellular assembly and organisation and (B) DNA replication, recombination and repair. (A) The cell cycle and cellular assembly network showed down regulation of the majority of genes in HLC compared to hAEC, but there were few genes up regulated in HLC. The DNA replication and repair network showed an equal number of genes up regulated and down regulated in HLC compared to hAEC. Red indicates up regulation in HLC and green indicates down regulation in HLC with $P < 0.05$ and $Q < 0.05$ and fold change ≥ 2 from $n = 4$.

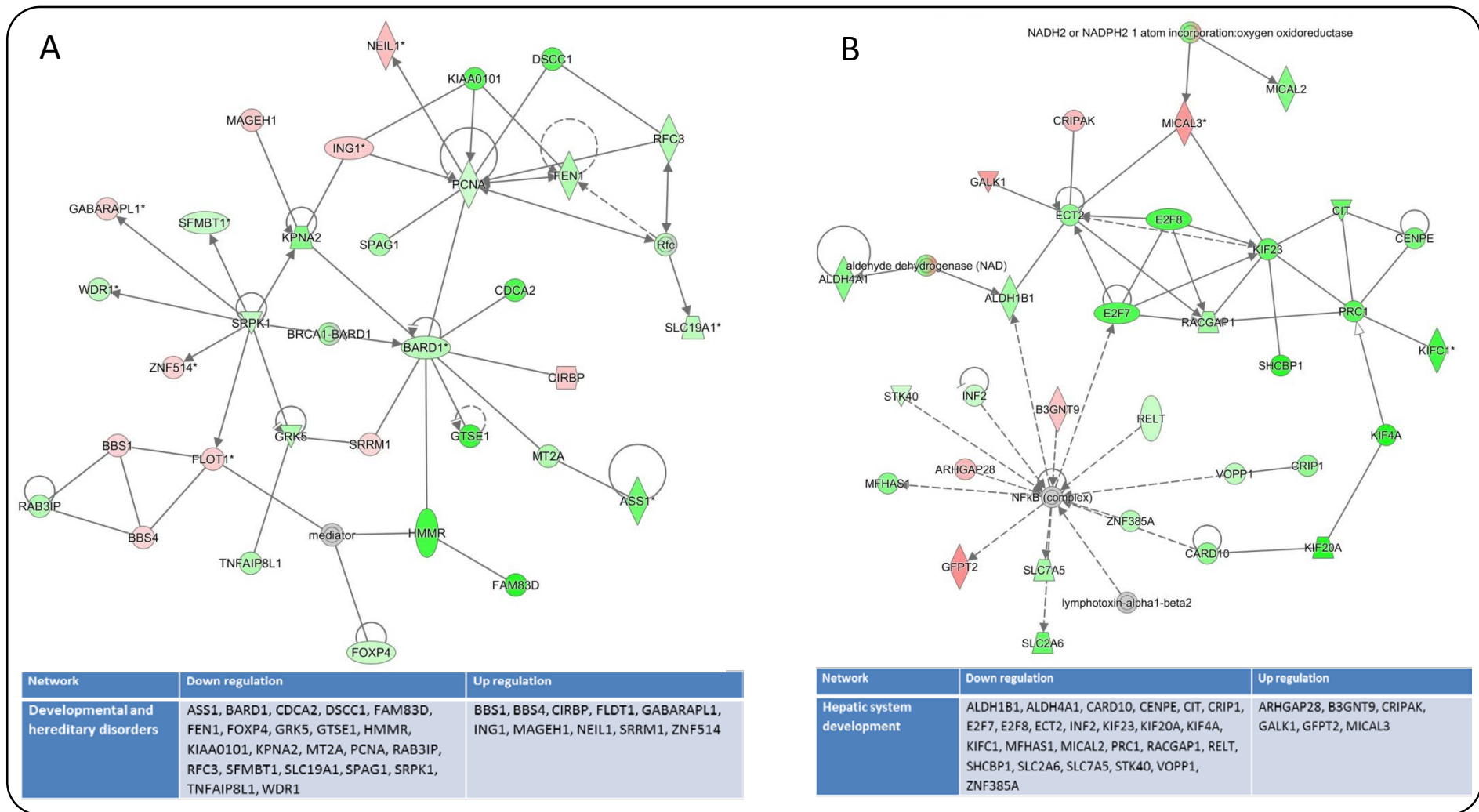


Figure 5.9. Developmental and hepatic system development networks in HLC. Additional networks involved in differentiated HLC were (A) developmental and hereditary disorder and (B) Hepatic system development. (A) The developmental and hereditary network showed down regulation of the majority of genes in HLC compared to hAEC, but there were few genes up regulated in HLC. (B) The hepatic system development network showed major down regulation of genes with few genes up regulated in HLC compared to hAEC. Red indicates up regulation in HLC and green indicates down regulation in HLC with $P < 0.05$ and $Q < 0.05$ and fold change ≥ 2 from $n = 4$.

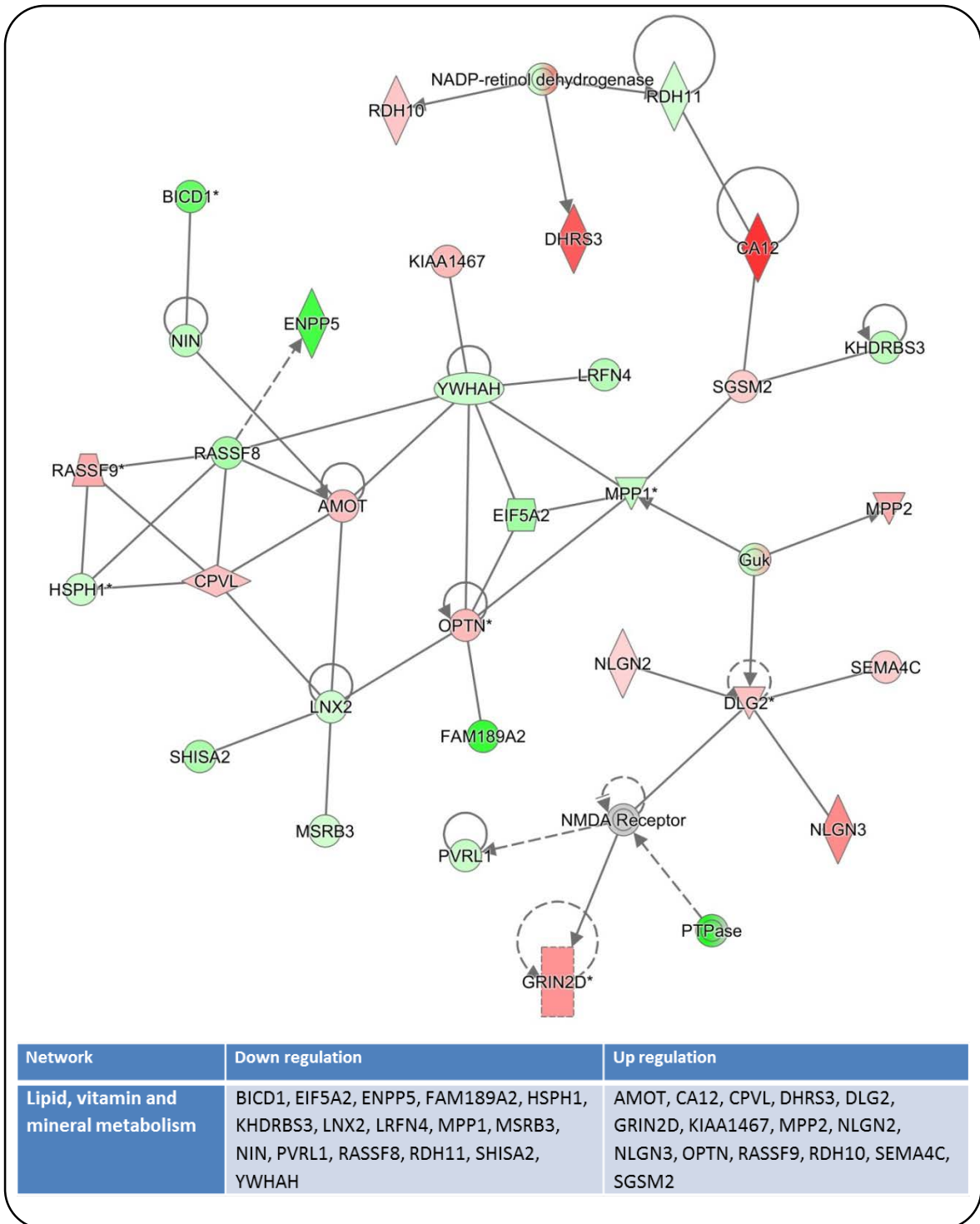


Figure 5.10. The lipid, vitamin and mineral metabolism network in HLC.

Involvement of the lipid, vitamin and mineral network showed similar distribution of both up regulated and down regulated genes in HLC compared to hAEC. Some of the genes like CA12 and DHRS3 were highly expressed in HLC compared to hAEC. Red indicates up regulation in HLC and green indicates down regulation in HLC with $P < 0.05$ and $Q < 0.05$ and fold change ≥ 2 from $n = 4$.

5.3.3 The effects of encapsulation on HLC differentiation and gene expression.

I compared encapsulated HLC to hAEC to evaluate changes in gene expression during differentiation in encapsulated HLC. There were total of 1325 differentially regulated genes, with 705 genes up regulated and 620 genes down regulated. The top candidate genes that were upregulated include *MIR203*, which directly targets *CDK6*, *Vimentin* and *SET* (47) (Table 5.2). Increased levels of *MIR203* down regulates *SOCS3* in hepatocytes, thus allowing *STAT3* driven expression of *cyclin A* and *D1* which promote proliferation (48). *Follistatin*, which binds and activates the *TGF- β* superfamily, was also highly expressed in encapsulated HLC. Genes involved in cell adhesion and extracellular matrix organisation, *COL18A1* and *CD248*, a cell adhesion trans-membrane receptor, were also highly expressed in encapsulated HLC compared to hAEC (Table 5.2). Forkhead box protein A3 (*FOXA3* also known as *HNF3G*), which is involved in activation of liver specific transcripts of albumin and plays a role in liver differentiation increased 17 fold in encapsulated HLC. Other notable genes that were up regulated include acyl-CoA synthetase *ACSL5*, collagen *COL27A1* and solute carrier *SLC43A1*. The top candidate genes that were down regulated include *CLDN11*, membrane protein and component of tight junction strands, and *TNFSF15*, which mediates activation of *NF κ B* (48)(Table 5.2). *TGF- α* , which binds to *EGF*-receptor and promotes proliferation and differentiation, was also down regulated in encapsulated HLC (Table 5.2). *LIPG* and *SEMA3D*, which are involved in lipid metabolism and cell differentiation, respectively, were also down regulated in encapsulated HLC compared to hAEC (Table 5.2). Other notable genes that were down regulated in encapsulated HLC were *integrin β 4*, *L1* cell adhesion molecule and *inhibin β A*.

When I performed canonical pathway analysis, I found that the stellate cell activation pathway was the top affected pathway in encapsulated HLC compared to hAEC (Figure 5.11).

Table 5.2. Top candidate genes differentially expressed in encapsulated HLC compared to undifferentiated hAEC. Up and down regulation of genes is shown as fold change as are gene functions.

Genes	Fold change	Function
MIR203	700	Inhibit cell growth and directly target CDK6, Vimentin, SET and SMYD3
MLXIPL	185	Cellular response to carbohydrate stimulus; cellular response to glucose stimulus; energy reserve metabolic process
FST	143	Binds to activating and TGF- β superfamily, specifically inhibits follicle-stimulating hormone release
ACSL5	133	Convert free long-chain fatty acids into fatty acyl-CoA esters, and play a key role in lipid biosynthesis and fatty acid degradation
CHST2	113	Transfer of sulfate to position 6 of non-reducing N-acetylglucosamine (GlcNAc) residues within keratan-like structures on N-linked glycans
PNMT	104	Catalyses the last step of the catecholamine biosynthesis pathway, which methylates norepinephrine to form epinephrine (adrenaline)
COL18A1	102	Cell adhesion and extracellular matrix organization
SCNN1A	93	Nonvoltage-gated, amiloride-sensitive, sodium channels control fluid and electrolyte transport across epithelia
CD248	77	Family of C-type lectin transmembrane receptors which play a role in cell-cell adhesion processes and host defence
CA12	71	Zinc metallo-enzymes that catalyse the reversible hydration of carbon dioxide. Participate in calcification, acid-base balance, bone resorption, and the formation of saliva, and gastric acid
CLDN11	-418	Membrane protein and components of tight junction strands. playS critical roles in maintaining cell polarity and signal transductions
PODXL	-205	Cell adhesion; cell migration; epithelial tube formation
TNFSF15	-107	Mediates activation of NF-kappa-B. Inhibits vascular endothelial growth and angiogenesis (in vitro). Promotes activation of caspases and apoptosis
CDH3	-99	The encoded protein is a calcium-dependent cell-cell adhesion glycoprotein comprised of five extracellular cadherin repeats
PRRT4	-68	Proline-rich transmembrane protein 4
TNC	-61	Cell adhesion; cellular response to prostaglandin D stimulus; cellular response to retinoic acid; cellular response to vitamin D; extracellular matrix organisation
TGFA	-47	Ligand for the EGF receptor, which activates a signalling pathway for cell proliferation, differentiation and development
LIPG	-46	Has phospholipase activity and may be involved in lipoprotein metabolism and vascular biology
PSG1	-46	Pregnancy specific beta-1-glycoprotein 1
SEMA3D	-44	Cell differentiation; multicellular organismal development.

Collagen genes (*11A2*, *16A1*, *18A1*, *27A1* and *9A3*) and growth factor vascular endothelial growth factor (*VEGF*) were specifically upregulated in encapsulated HLC. Genes that were down regulated in the stellate cell activation pathway included matrix metalloproteinase (*MMP*) and tissue inhibitors of metalloproteinase (*TIMP*) (Figure 5.11). The results suggest that there is increased collagen synthesis and reduced breakdown of matrix proteins in encapsulated HLC. The mitotic role of polo-like kinase pathway was completely down regulated, including *cyclins* involved in centromere separation and cell division cycle protein involved in mitotic entry (Figure 5.12). *IL-1* mediated inhibition of *RXR* function showed marked upregulation. The genes that were up regulated include *APOE*, *APOC1* and *SCARB1* which are involved in cholesterol and lipid metabolism (Figure 5.13). Phase III transporters *MRP2* and *MRP3* were also activated in the pathway (Figure 5.13). Genes involved in fatty acid metabolism (*ACOX*, *CPT*, *FABP* and *ACS*) were also activated in the pathway (Figure 5.13). Canonical pathways for P53 and PTEN signalling were also impacted, with genes in these pathways both up and down regulated in encapsulated HLC. P53 and PTEN signalling pathways mainly activated genes involved in apoptosis and cell cycle progression. Upstream analysis showed activation of TGF- β 1, dexamethasone and oncostatin M, which are involved in hepatocyte differentiation.

We also performed network analysis on encapsulated HLC relative to undifferentiated hAEC. The top network affected was cell cycle and DNA repair and replication, which showed that the majority of the genes were down regulated (Figure 5.14A). Key genes in the network (*BUB1*, *SGOL1* and *NDC80*) were all down regulated. Expression of *ERK* remained unchanged, however, up regulation of *MAFB*, a leucine zipper transcription factor caused down regulation of *SPOCK1*, *ZDHHC2* and *BACH2* (Figure 5.14A). The cellular assembly and cell cycle networks showed equal distribution of both up and down regulated genes.

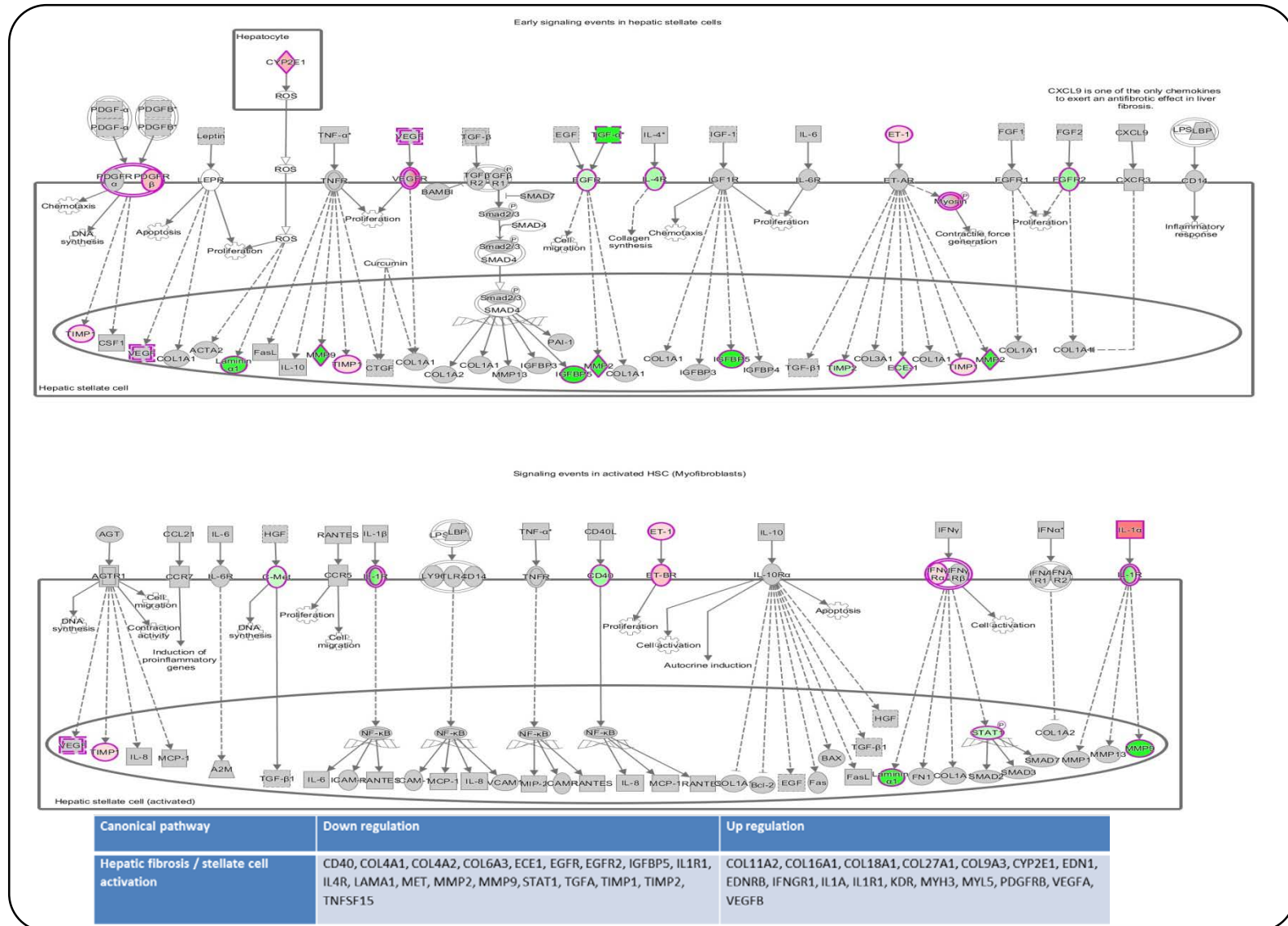


Figure 5.11. The Hepatic fibrosis and stellate cell activation pathway. The top canonical pathway affected in encapsulated HLC compared to hAEC. Genes in the hepatic fibrosis and stellate cell activation pathway showed up regulation in a family of collagen genes and down regulation of EGRF and matrix metalloproteins in encapsulated HLC compared to hAEC. Red indicates up regulation in encapsulated HLC and green indicates down regulation in encapsulated HLC with $P < 0.05$ and $Q < 0.05$ and fold change ≥ 2 from $n = 4$.

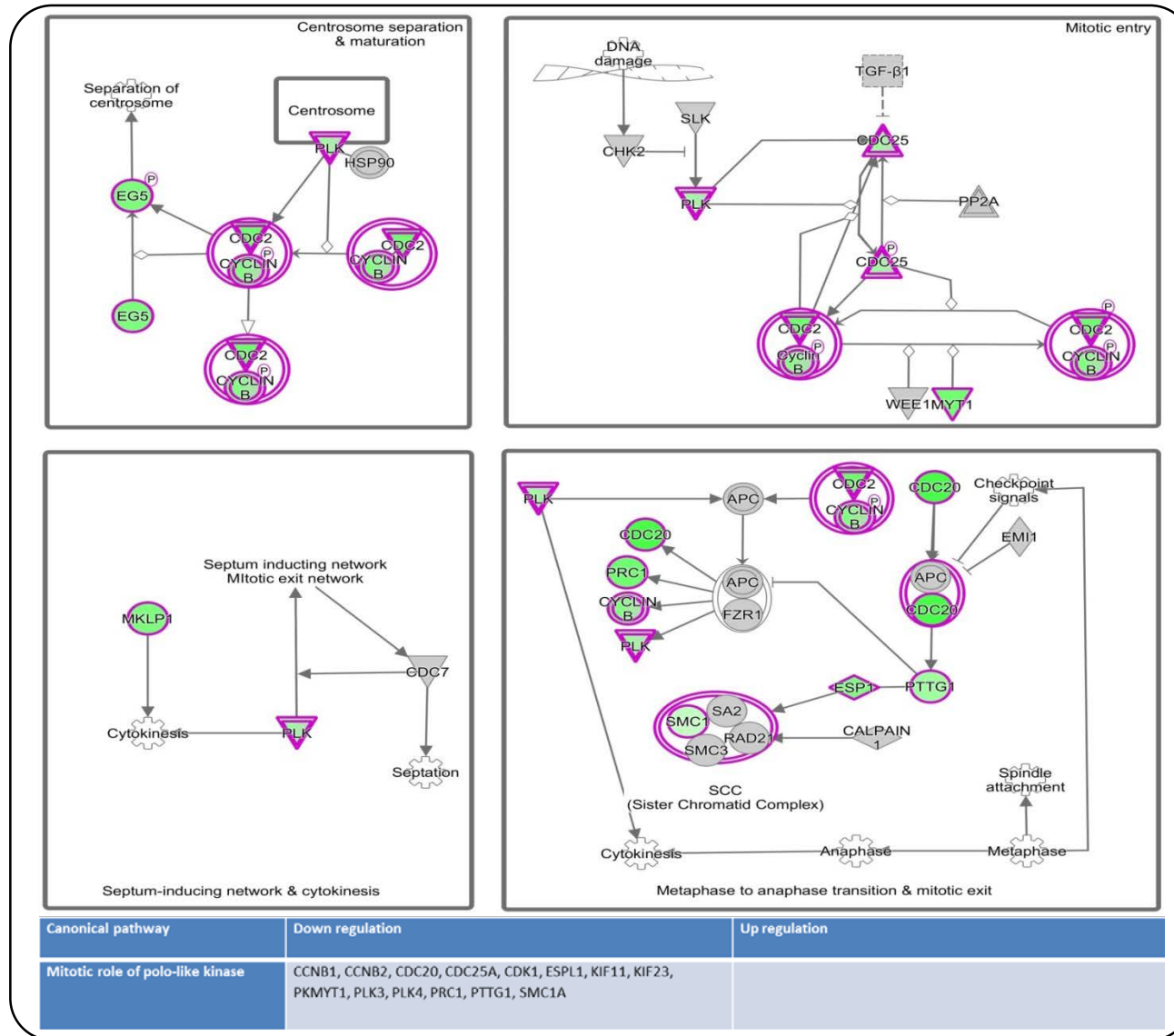


Figure 5.12. The mitotic role of polo-like kinase pathway. The mitotic role of polo-like kinase pathway was affected in encapsulated HLC compared to hAEC. Genes in the mitotic role of polo-like kinase pathway showed major down regulation of cyclin genes in encapsulated HLC compared to hAEC. Red indicates up regulation in encapsulated HLC and green indicates down regulation in encapsulated HLC with $P_{131} < 0.05$ and $Q < 0.05$ and fold change ≥ 2 from $n = 4$.

Up regulation of *WNT2*, *CEL*, *CSAD*, *TRIM29* and *NAT9* led to down regulation of *GSK3B*, a protein kinase that phosphorylates the rate limiting enzyme of glycogen synthesis (49) (Figure 5.14B). There was major down regulation of the developmental disorder network. The key molecules in the network, *ETV5*, *PTPase*, *cytokeratin*, *EPS15* and *TEAD1* were all down regulated in encapsulated HLC compared to hAEC (Figure 5.15A). The DNA replication, recombination and repair network showed up regulation of *NXF1*, which facilitates mRNA export from the nucleus to the cytoplasm (50) showed both inhibition and expression of the target genes. More interestingly, though *CD3* remained unchanged, most of the target genes were up regulated including *ZNF133*, *ZNF76*, *BTG1*, *NKTR*, *NLGN3* and *MST1* (Figure 5.15B).

There was a significant increase in gene expression of free radical scavenging and cell-to-cell signalling network. Up regulation of *TRAF1*, a factor that interacts with the cytoplasmic domain of TNF receptor-1 also up regulated its target genes (Figure 5.16A). Up regulation of *60S ribosomal subunit* resulted in up regulation of ribosomal protein *RPL29*, *RPL38*, *RPL39* and *RPL27A* (Figure 5.16A). *MIR-210* was highly expressed in encapsulated HLC which had inhibitory effects on its target genes *SCARA3*, *PTPB3* and *BHLHE41* (Figure 5.16A). The drug metabolism network was also affected in encapsulated HLC with upregulation of cytochrome P450 genes *CYP1B1*, *CYP2D6* and *CYP2E1* (Figure 5.16B). *ETC2*, a transforming protein that interacts with RHO-like proteins and acts as an oncogene (51), was down regulated and its target genes were also down regulated (Figure 5.16B). These results show that not only have encapsulated hAEC differentiated into HLC, the encapsulated HLC have capacity to perform hepatocyte functions.

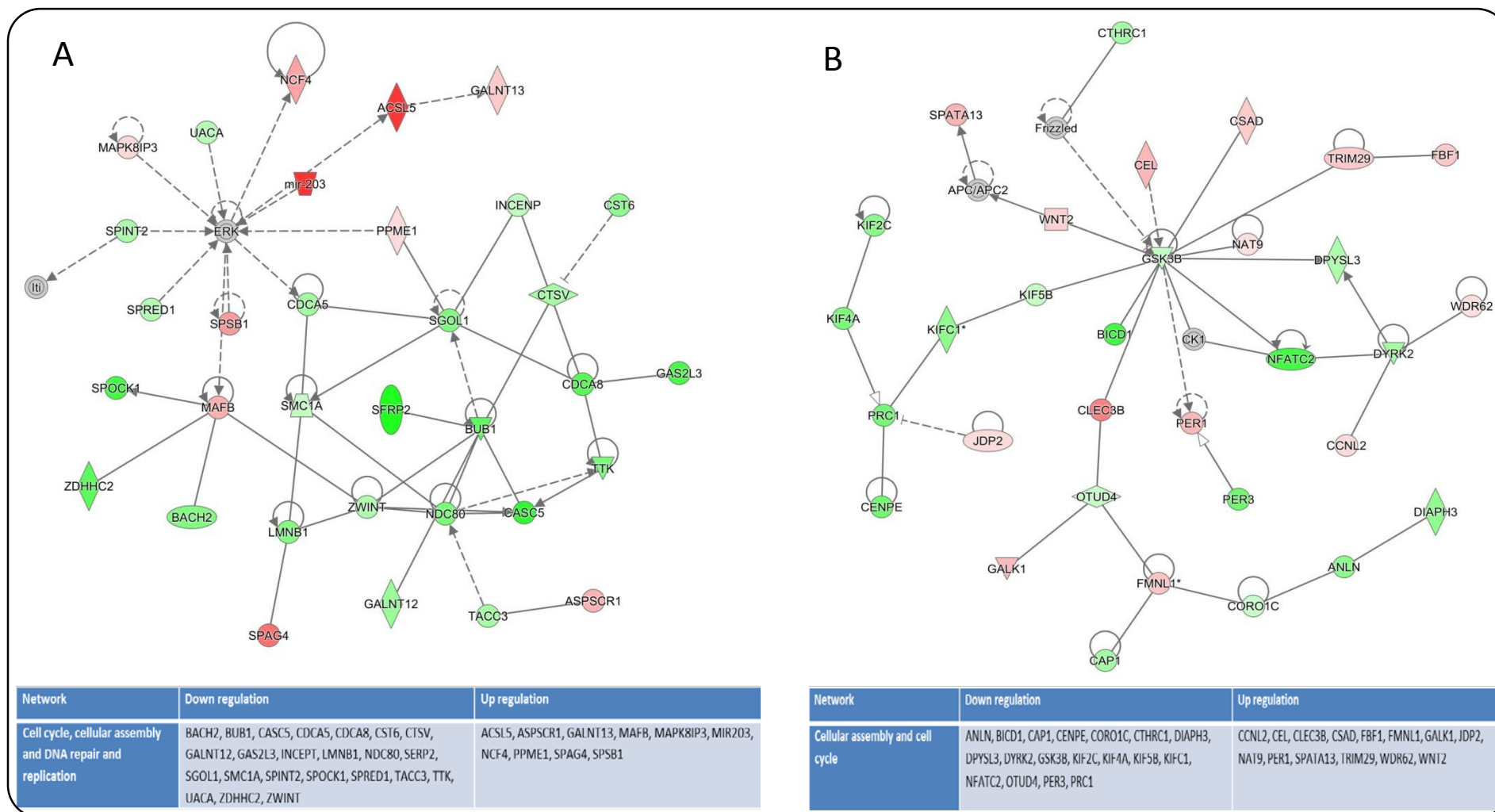


Figure 5.14. Top affected networks in encapsulated HLC. The top networks affected in encapsulated HLC compared to hAEC were (A) Cell cycle, cellular assembly and DNA repair and replication and (B) cellular assembly and cell cycle. (A) The majority of the genes in the cell cycle, cellular assembly and DNA repair and replication networks were down regulated in encapsulated HLC compared to hAEC. However, there were few genes (ACSL5 and MIR203), were highly expressed in encapsulated HLC. (B) The cellular assembly and cell cycle network showed similar distribution of both up regulated and down regulated genes with GSK3B being central to the network in encapsulated HLC compared to hAEC. Red indicates up regulation in encapsulated HLC and green indicates down regulation in encapsulated HLC with $P < 0.05$ and $Q < 0.05$ and fold change ≥ 2 from $n = 4$.

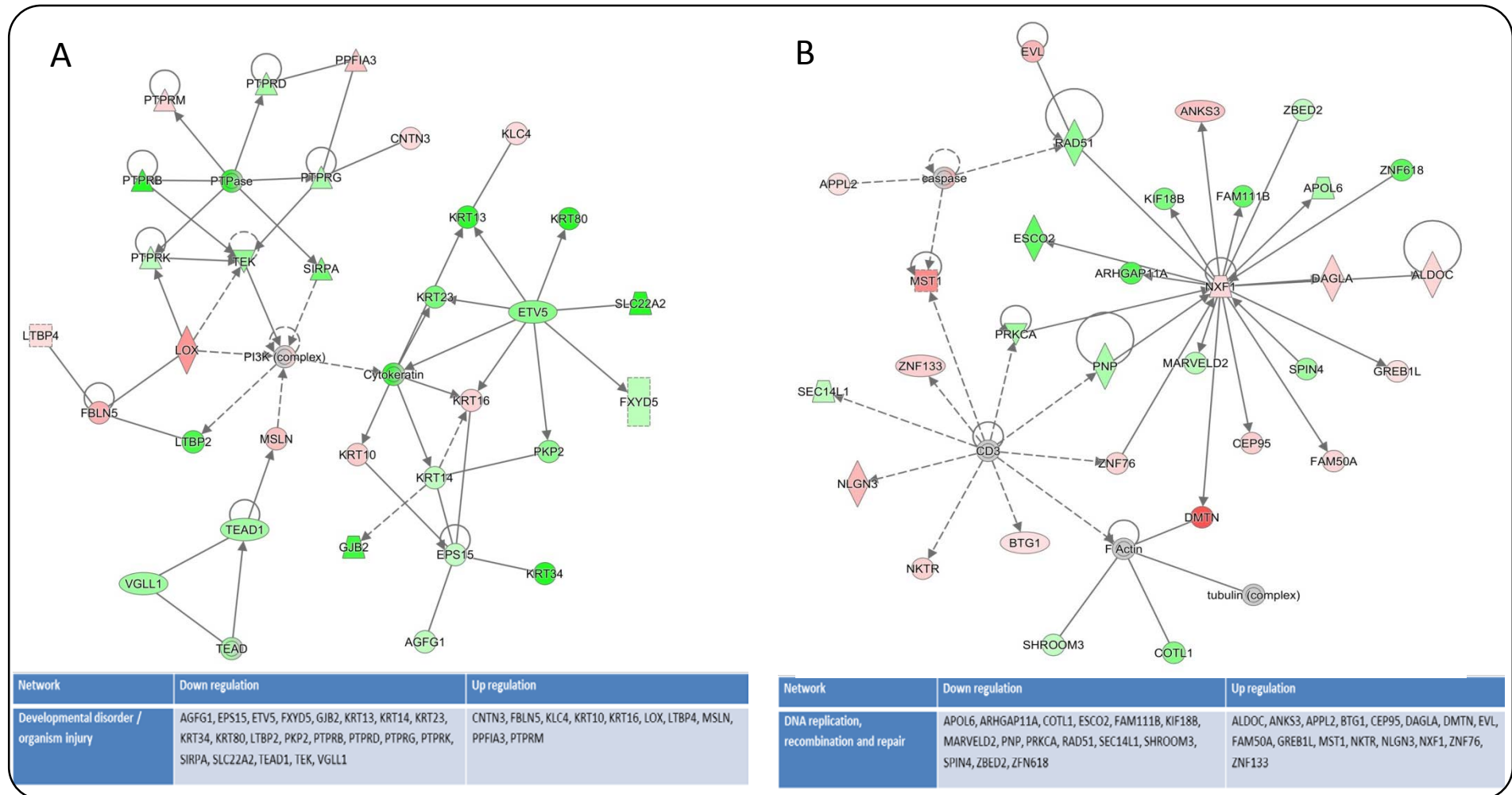


Figure 5.15. The Developmental disorder and DNA replication and recombination networks in encapsulated HLC. The top networks affected in encapsulated HLC compared to hAEC were (A) Developmental disorder and organism injury and (B) DNA replication, recombination and repair. (A) The majority of the genes in the developmental disorder and organism injury network were down regulated in encapsulated HLC compared to hAEC. However LOX, KRT10 and a few other genes were also up regulated in encapsulated HLC. (B) The DNA replication , recombination and repair network showed similar distribution of both up regulated and down regulated genes with NXF1 being central to the network in encapsulated HLC compared to hAEC. Red indicates up regulation in encapsulated HLC and green indicates down regulation in encapsulated HLC with $P < 0.05$ and $Q < 0.05$ and fold change ≥ 2 from $n = 4$.

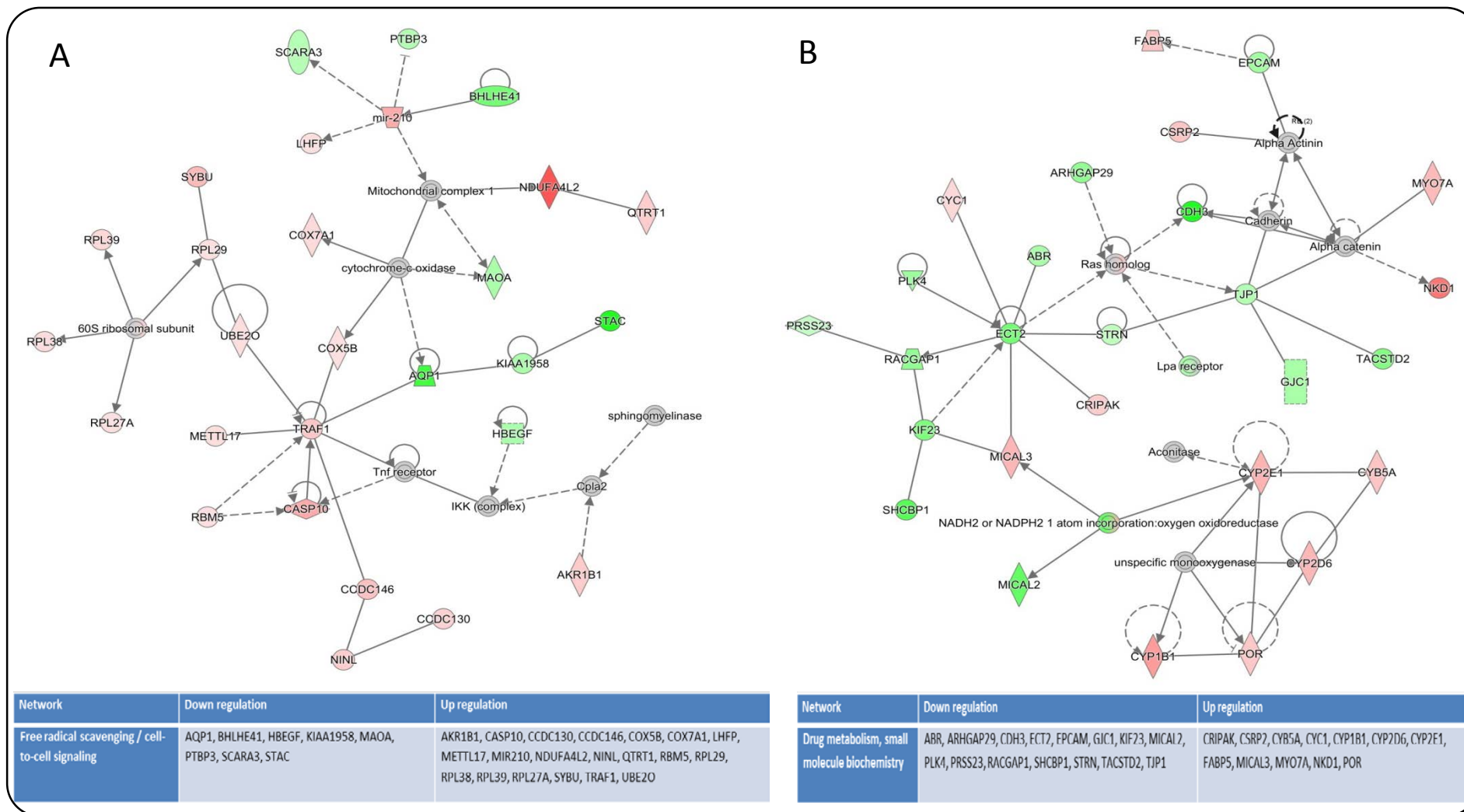


Figure 5.16. Free radical scavenging and drug metabolism networks in encapsulated HLC. The top networks affected in encapsulated HLC compared to hAEC were (A) Free radical scavenging and cell-to-cell signalling and (B) Drug metabolism and small molecule biochemistry. (A) The majority of the genes in the free radical scavenging and cell-to-cell signalling network were up regulated in encapsulated HLC compared to hAEC. The two major genes in the network were TRAF1 and MIR210, which were up regulated in encapsulated HLC compared to hAEC. (B) The drug metabolism and small molecule biochemistry network showed similar distribution of both up regulated and down regulated genes in encapsulated HLC compared to hAEC. Cytochrome P450 genes showed significant up regulation in encapsulated HLC compared to hAEC. Red indicates up regulation in encapsulated HLC and green indicates down regulation in encapsulated HLC with $P < 0.05$ and $Q < 0.05$ and fold change ≥ 2 from $n = 4$. 136

5.3.4 The effects of 3D HLC differentiation on gene expression.

Comparing encapsulated HLC to HLC showed the effects of differentiation in the 3D environment compared to 2D. There were 286 differentially regulated genes with 210 genes up regulated and 76 genes down regulated. Top candidate genes that were upregulated include ferric iron transmembrane transporter transferrin (*TF*) and asialoglycoprotein receptor.

ASGR1 (Table 5.3). *SERPINF2*, which regulates cell-cell adhesion mediated by cadherins and *COL18A1*, which is involved in cell adhesion and extracellular matrix organisation primarily in liver (52), were up regulated in encapsulated HLC (Table 5.3). Serine protease converter of hepatocyte growth factor *HGFAC* and *FGFR4*, which acts in the cascade of mitogenesis and differentiation, were also up regulated in encapsulated HLC compared to HLC (Table 5.3). Other notable genes that were up regulated include *APOE*, involved in catabolism of triglyceride-rich lipoproteins, *MIR-203*, which targets *P63* and regulates stem cell maintenance and members of ATP-binding cassette (*ABC*).

The top candidate genes that were down regulated include *OAS1*, an essential protein involved in the innate immune response to viral infection (53) and *MXI*, which participates in cellular antiviral response (Table 5.3). The key genes involved in interferon signalling, *IFITM1*, *IFIT1*, *IFIT3* and *IFI27*, were all down regulated in encapsulated HLC but not in HLC (Table 5.3). *MIR612*, which regulates hepatocellular carcinoma proliferation, migration and metastasis (40), was also down regulated in encapsulated HLC. The down regulation of interferon genes in encapsulated HLC suggest that there is less immunogenic response from encapsulated HLC compared to non-encapsulated HLC. *OAS3*, an enzyme that inhibits cellular protein synthesis and viral infection resistance (53) was also down regulated in encapsulated HLC (Table 5.3). Other notable genes that were down regulated include *STAT1* and toll-like receptor 3 (*TLR3*), which recognises double stranded RNA.

Table 5.3. Top candidate genes differentially expressed in encapsulated HLC compared to HLC. Up and down regulation of genes is shown as fold change and its function.

Genes	Fold change	Function
TF	787	Ferric iron binding; ferric iron transmembrane transporter activity
ASGR1	281	Asialoglycoprotein receptor activity; cellular response to extracellular stimulus
SERPINF2	242	Regulation of cell-cell adhesion mediated by cadherin; positive regulation of cell differentiation; positive regulation of collagen biosynthetic process
HGFAC	145	Acts as serine protease that converts hepatocyte growth factor to the active form
FGFR4	100	Interaction with fibroblast growth factor, cascade of mitogenesis and differentiation
APOE	86	Binds to a specific liver and peripheral cell receptor, and is essential for the normal catabolism of triglyceride-rich lipoprotein constituents. Cholesterol transport activity
ST6GAL1	84	Glycosyltransferase type II membrane protein that catalyses the transfer of sialic acid from CMP-sialic acid to galactose-containing substrates
COL18A1	76	Cell adhesion and extracellular matrix organization
SPOCK2	76	Extracellular matrix organization; peptide cross-linking via chondroitin 4-sulfate glycosaminoglycan
FTCD	75	Cellular metabolic process; cellular nitrogen compound metabolic process
OAS1	-137	Essential proteins involved in the innate immune response to viral infection. The encoded protein is induced by interferons
MX1	-97	A guanosine triphosphate (GTP)-metabolizing protein that participates in the cellular antiviral response. The encoded protein is induced by type I and type II interferons and antagonizes the replication process of several different RNA and DNA viruses
IFITM1	-84	Protein binding; receptor signalling protein activity
IFIT1	-76	The encoded protein may inhibit viral replication and translational initiation
IFIT3	-63	Identical protein binding, protein binding, tetratricopeptide repeat
MIR612	-49	Regulation of Hepatocellular carcinoma proliferation, migration and metastasis
OAS3	-40	This enzyme family plays a significant role in the inhibition of cellular protein synthesis and viral infection resistance
LAMP3	-35	Cell proliferation; immune system process
DDX60	-34	Positive regulation of MDA-5 signalling pathway; positive regulation of RIG-I signalling pathway; response to virus
IFI27	-23	Activation of cysteine-type endopeptidase activity involved in apoptosis; apoptotic signalling pathway; cytokine-mediated signalling pathway.

When I performed canonical pathway analysis of encapsulated HLC with HLC, the major pathways affected were interferon signalling and pattern recognition. The interferon signalling pathway, which included major interferon genes *IFI35*, *IFIT1*, *IFIT3*, *IFITM1* and *IFITM3* and signal transducers and activators of transcription genes *STAT1* and *STAT2*, were down regulated in encapsulated HLC (Figure 5.17). Phosphorylated *STAT1* homodimers translocate to the nucleus to activate transcription of type II interferon signalling, whereas phosphorylated *STAT1* and *STAT2* homodimers together with interferon response factor 9 (*IRF9*) activate transcription of type I interferon signalling (46) (Figure 5.17). The Pattern recognition pathway was also down regulated with oligoadenylate synthetase genes *OAS1*, *OAS2* and *OAS3* as well as *TLR3* (Figure 5.18) also down regulated. In contrast, complement component, which signals through PI3K and the ERK1/2 pathway, were up regulated in encapsulated HLC compared to HLC (Figure 5.18). However, *FXR/RXR* pathway was activated with membrane transporter *ABCC2*, iron transporters *HPX* and *TF* showed significant up regulation in encapsulated HLC compared to HLC (Figure 5.19). More interestingly, there was increased expression of *LIPC* and *APOE* in encapsulated HLC which drive high-density lipoprotein (HDL) and cholesterol metabolism (Figure 5.19). There was increased expression of *MRP2*, involved in phospholipid secretion and *CYP27A1*, which catalyses the first step bile acid synthesis pathway (54) in encapsulated HLC relative to HLC (Figure 5.19). Acute phase response pathway was also activated with up regulation of complement component, *MAPK* and *SERPIN* genes (Figure 5.20). Phosphorylated *STAT3* homodimers activates *SERPINA3*; though *SERPINA3* was up regulated in encapsulated HLC, levels of *STAT3* remain unchanged (Figure 5.20). Upstream analysis showed up the regulation of mitogen-activated protein kinase *MAPK1* and *NKX2-3*, transcription factors involved in cell specification and maintenance of differentiation, whereas, interferon associated genes were down regulated.

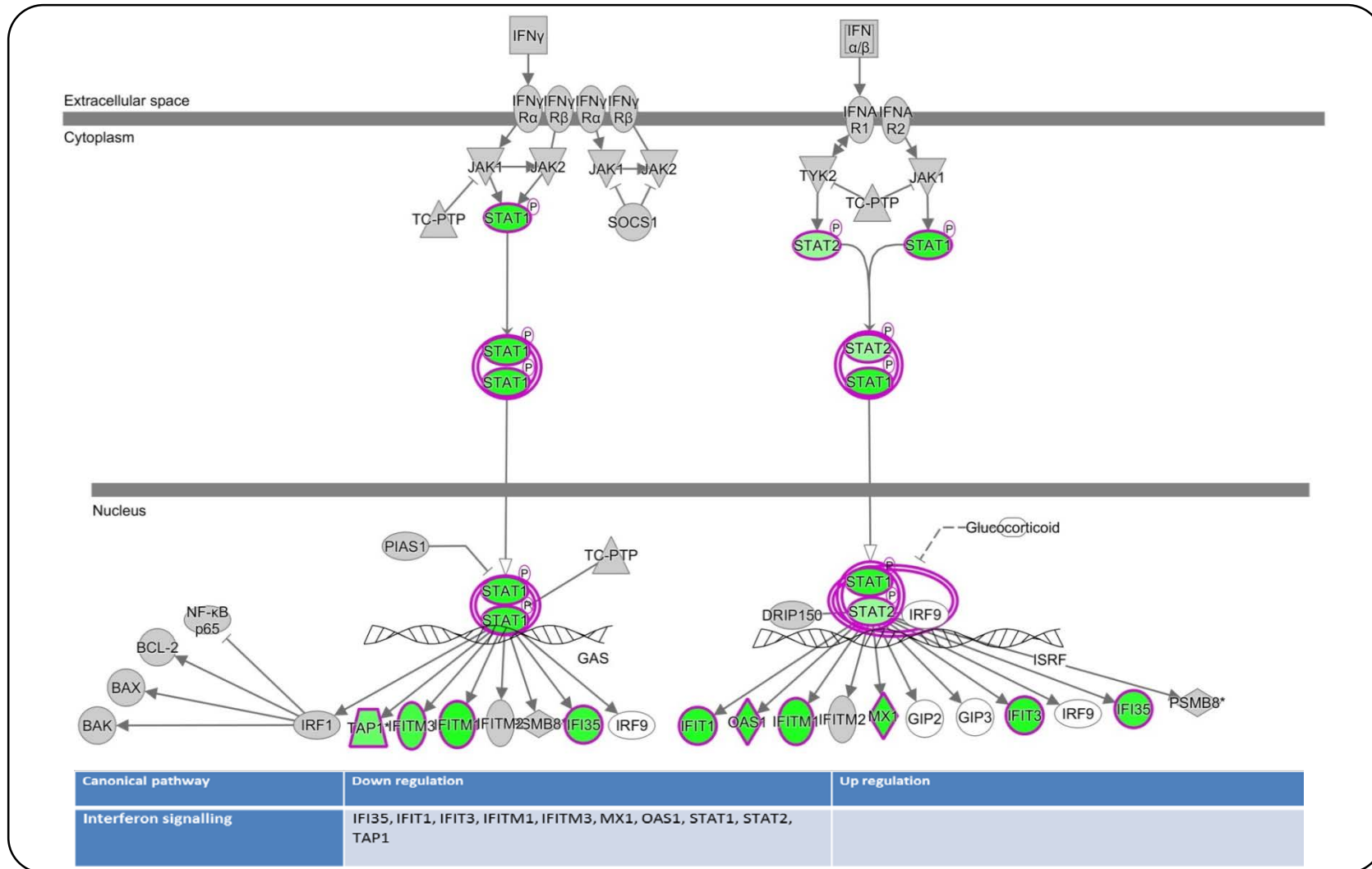


Figure 5.17. The interferon signalling pathway in encapsulated HLC. The top pathway affected in encapsulated HLC compared to hAEC was interferon signalling. The key regulators of the pathway, STAT1 and STAT2, were down regulated in encapsulated HLC compared to HLC. Phosphorylated STAT1 form homodimers and translocate to nucleus and activate type II interferon signalling (TAP1, IFIT3, IFITM1 and IFI35) were all down regulated in encapsulated HLC compared to HLC. Target genes of type I interferon signalling (IFIT1, OAS1, IFITM3, MX1, IFIT3 and IFI35), which is activated by phosphorylated heterodimer of STAT1 and STAT2, were also down regulated. Red indicates up regulation in encapsulated HLC and green indicates down regulation in encapsulated HLC with $P < 0.05$ and $Q < 0.05$ and fold change ≥ 2 from $n = 4$. 141

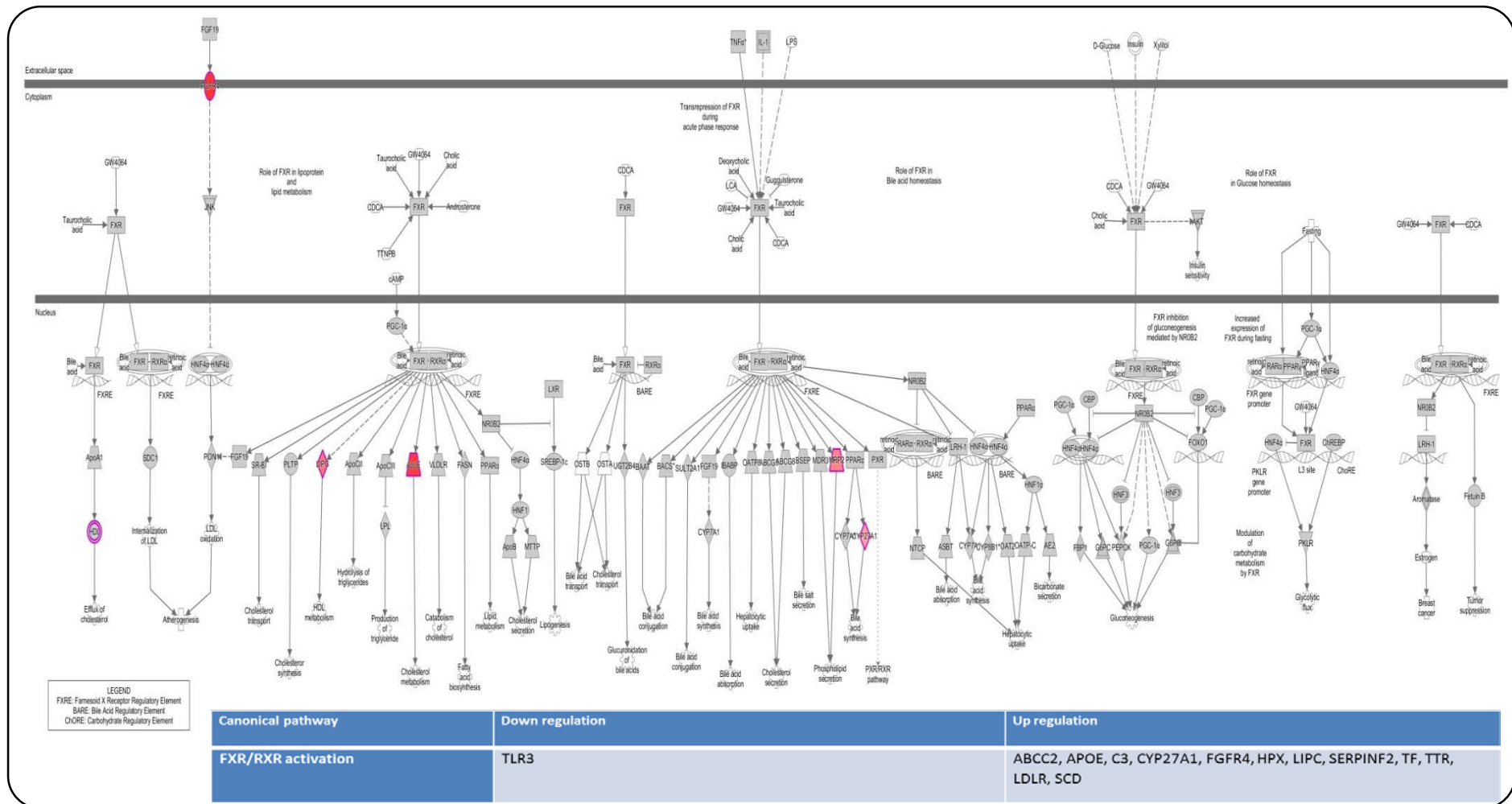


Figure 5.19. FXR/RXR activation in encapsulated HLC. The key network affected in encapsulated HLC compared to HLC was FXR/RXR activation. LIPC and APOE which leads to HDL and cholesterol metabolism were highly upregulated in encapsulated HLC. Cytochrome enzyme CYP27A1, which is involved in bile acid synthesis, was also up regulated in encapsulated HLC compared to HLC. Red indicates up regulation in encapsulated HLC and green indicates down regulation in encapsulated HLC with $P < 0.05$ and $Q < 0.05$ and fold change ≥ 2 from $n = 4$.

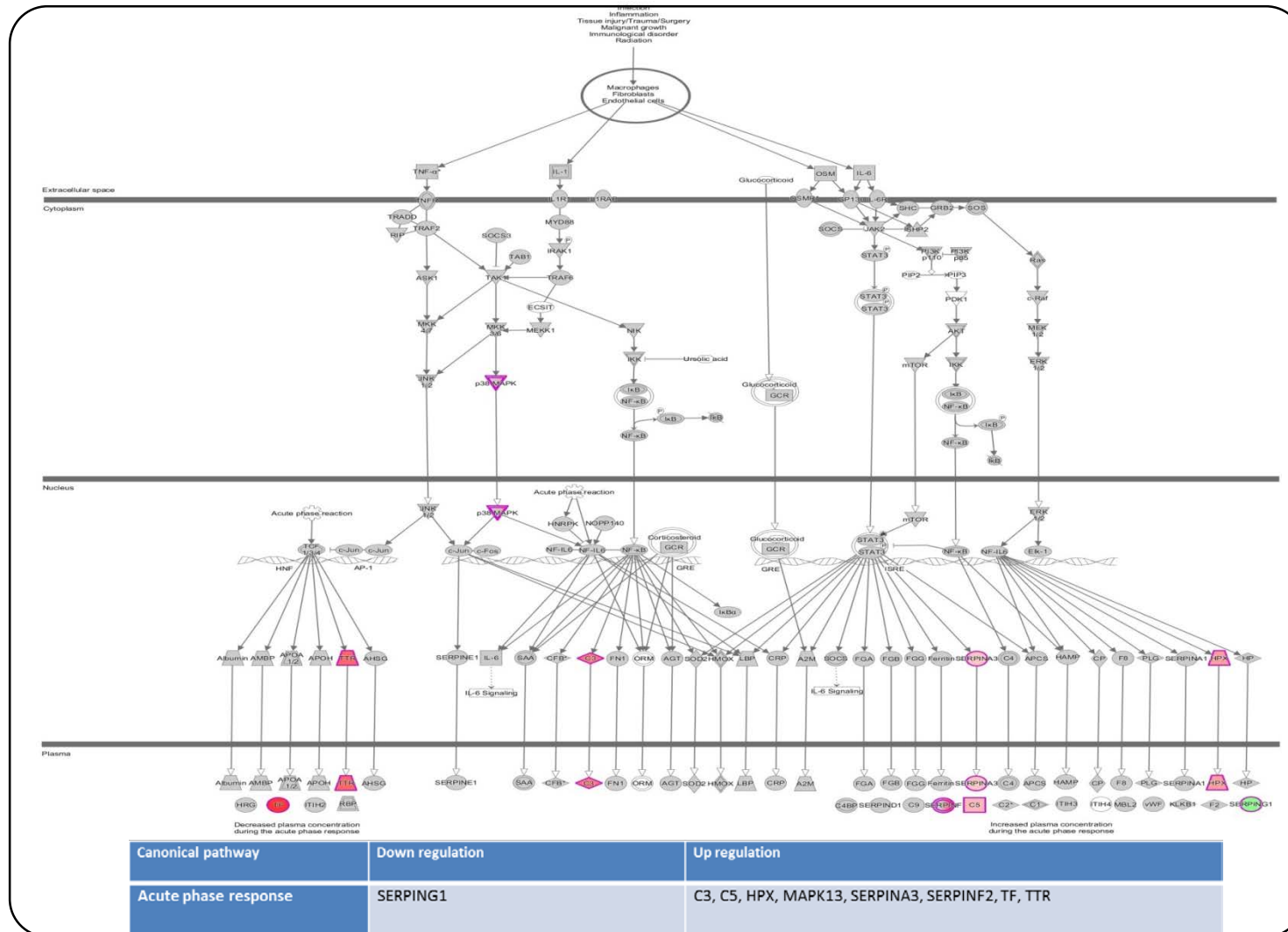


Figure 5.20. Acute phase response pathway in encapsulated HLC. Among the top networks affected in encapsulated HLC compared to HLC was acute phase response. There was major up regulation of TTR and TF, which are activated by TCF 1/2/3 in encapsulated HLC compared to HLC. NF- κ B activates complement 3 genes, which were up regulated and STAT3 downstream targets SERPINA3, SERPINF2, HPX and C5 were all up regulated in encapsulated HLC. Red indicates up regulation in encapsulated HLC and green indicates down regulation in encapsulated HLC with $P < 0.05$ and $Q < 0.05$ and fold change ≥ 2 from $n = 4$.

Network analysis showed organism injury and abnormalities as the top affected network with the majority of genes up regulated. Some of the genes upregulated in encapsulated HLC were involved in hepatocyte functions. These genes include urea cycle enzyme *ASS1*, epithelial cellular adhesion molecule *EPCAM*, amino acid metabolism and urea cycle enzyme *GOT1* and family members of pro-protein convertase *PCSK6* and *PCSK1N* (Figure 5.21A). Though *FSH* remains unchanged, its target genes *PCSK6*, *ENC1*, *GOT1*, *DHCR7*, *CARD10* and *AKAP12* were highly elevated in encapsulated HLC compared to HLC (Figure 5.21A). *EPCAM*, *OSGIN1* and *CDC6* were up regulated; they did not regulate expression of *cyclin A* (Figure 5.21A). The inflammatory response network was significantly down regulated with major down regulation of interferon and oligoadenylate synthetase (*OAS*) genes (Figure 5.21B). Down regulation of *STAT2* remained central to the network and interferon induced genes were all down regulated in encapsulated HLC compared to HLC (Figure 5.21B). There was increased expression of genes associated with organism development network (Figure 5.22A). In particular, cell matrix associated collagen genes were up regulated in encapsulated HLC. Although there was no change in *TGFβ* expression, *LIF* expression increased significantly (Figure 5.22A).

The family of poly (ADP-ribose) polymerase genes were also down regulated in the cell signalling network (Figure 5.22B). Down regulation of *STAT1* was central to the network which led to down regulation of interferon induced genes (Figure 5.22B). However, there was upregulation of the cell death and survival network in encapsulated HLC. Genes impacting the *AKT* pathway and collagen type IV were all up regulated in encapsulated HLC (Figure 5.23A). Encapsulated HLC also showed increased gene expression of basal cell adhesion molecule (*BCAM*), complement component *C5* and *C8G* and solute carrier *SLC20A1* and *SLC29A1* (Figure 5.23A).

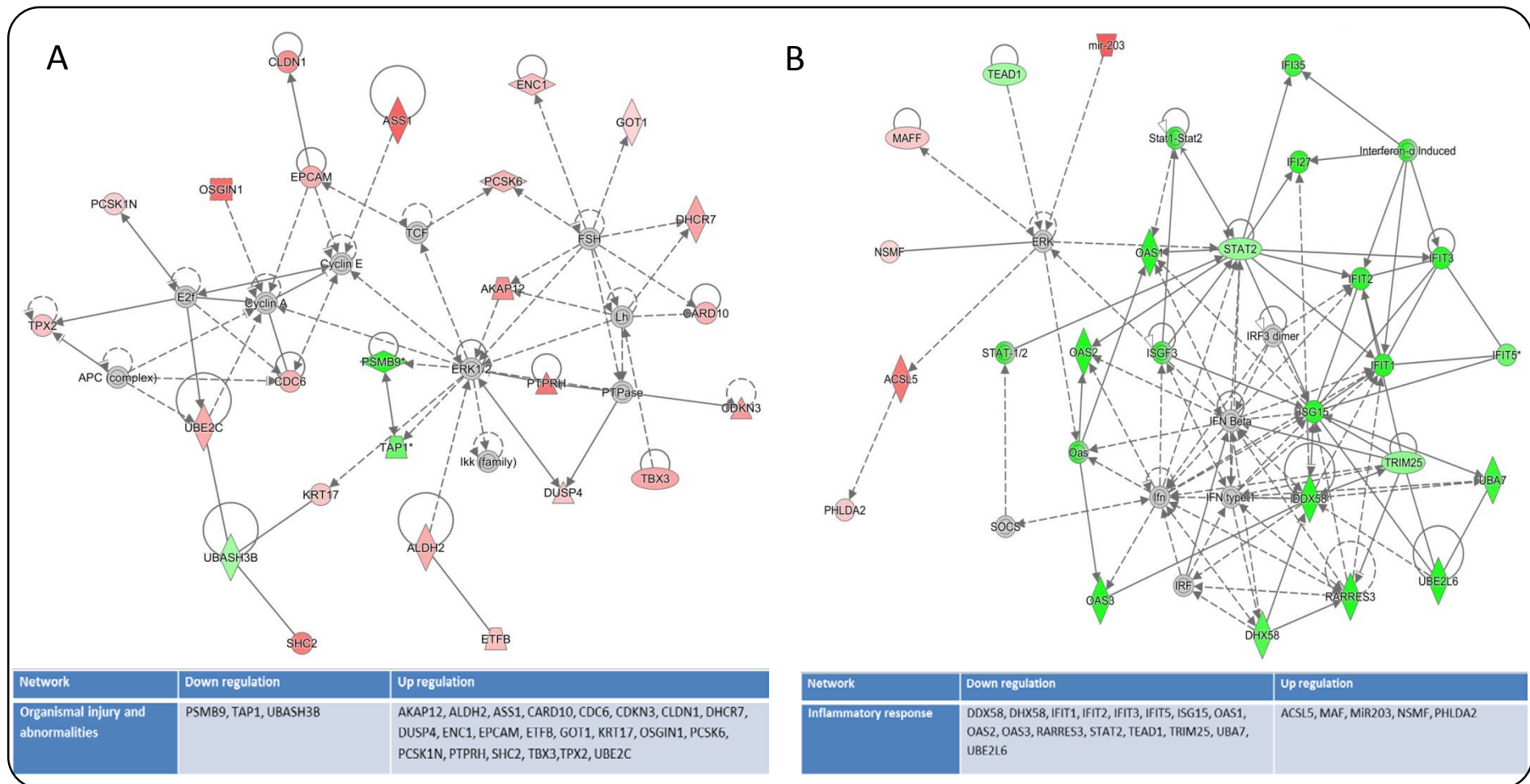


Figure 5.21. The organism injury and inflammatory response networks in encapsulated HLC. The top networks affected in encapsulated HLC compared to HLC were (A) Organism injury and abnormalities and (B) Inflammatory response. (A) The majority of the genes in the organism injury network were up regulated in encapsulated HLC compared to HLC. The central molecules in the pathway were ERK1, FSH and Cyclin E remained unchanged; however, their target genes were all up regulated in encapsulated HLC compared to HLC. (B) The inflammatory response network showed major down regulation of genes in encapsulated HLC compared to hAEC. In particular, STAT2 was down regulated which led to down regulation of the target genes. Although there was no change in expression of IFN, IFN Beta and IFN type I, their target genes were down regulated in the network in encapsulated HLC compared to HLC. Red indicates up regulation in encapsulated HLC and green indicates down regulation in encapsulated HLC with $P < 0.05$ and $Q < 0.05$ and fold change ≥ 2 from $n = 4$.

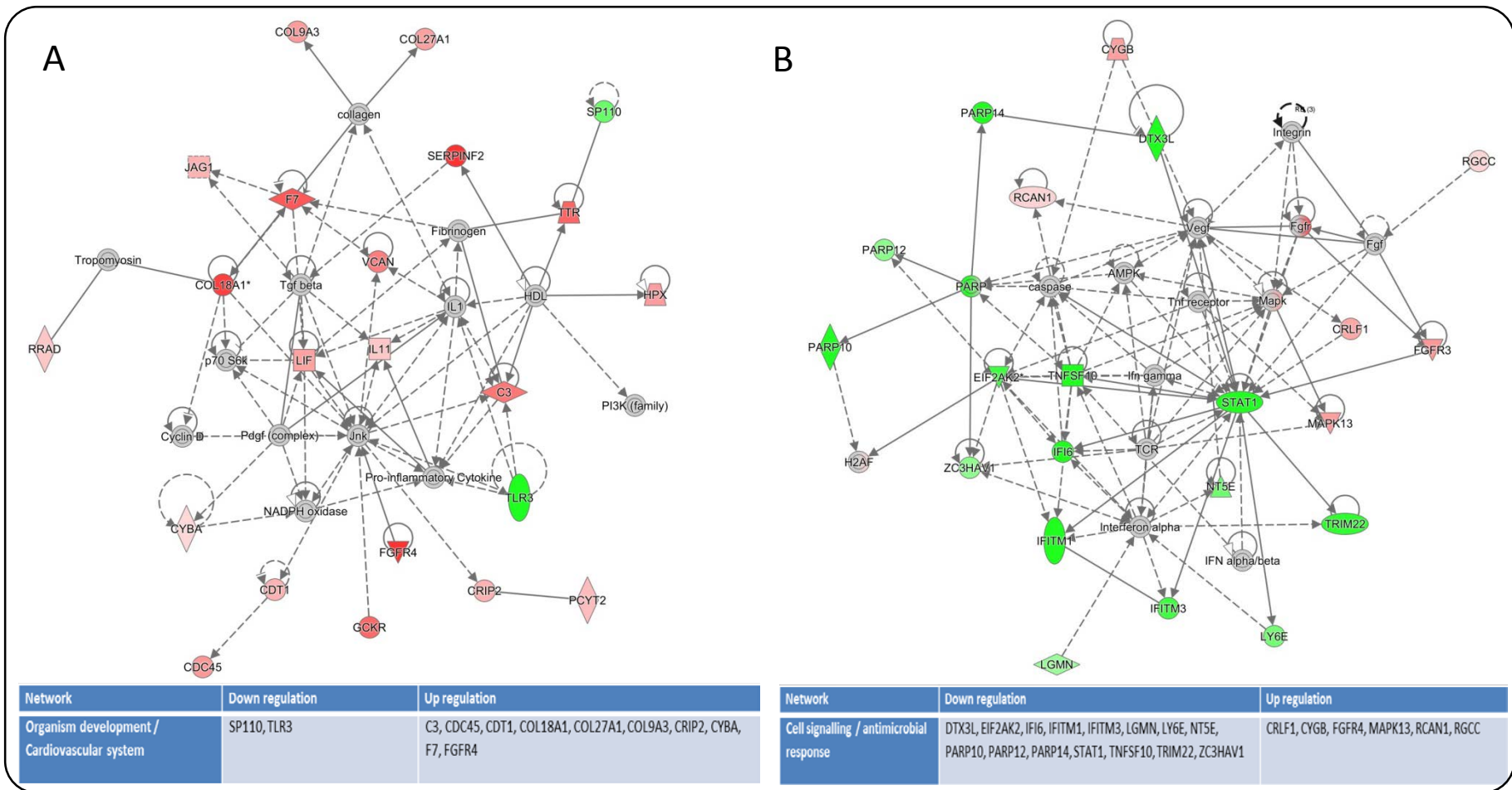


Figure 5.22. The organism development and cell signalling networks in encapsulated HLC. The top networks affected in encapsulated HLC compared to HLC were (A) Organism development / cardiovascular system and (B) Cell signalling / antimicrobial response. (A) The majority of the genes in the organism injury network were up regulated in encapsulated HLC compared to HLC. The Key molecules in the pathway (IL-1, JNK and TGF- β) remained all unchanged; their target genes were all up regulated in encapsulated HLC compared to HLC. In particular collagen genes (COL18A1, COL27A1 and COL9A3) were highly expressed in encapsulated HLC. (B) The cell signalling network showed major down regulation of genes in encapsulated HLC compared to hAEC. Down regulation of STAT1 was central to the network and the target genes of STAT1 were down regulated in encapsulated HLC compared to HLC. Red indicates up regulation in encapsulated HLC and green indicates down regulation in encapsulated HLC with $P < 0.05$ and $Q < 0.05$ and fold change ≥ 2 from $n = 4$.

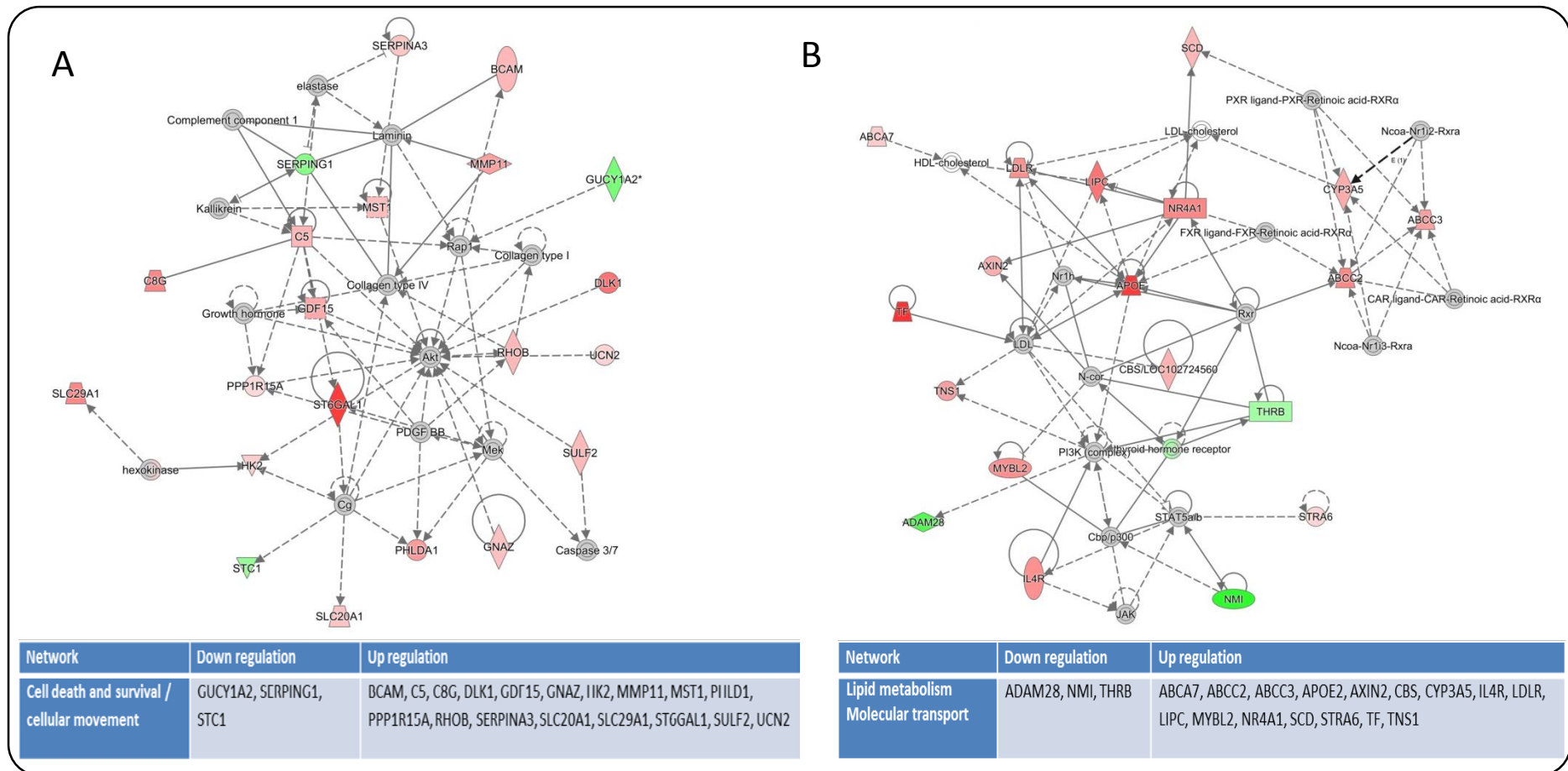


Figure 5.23. The cell death and survival and lipid metabolism networks in encapsulated HLC. Among the top networks affected in encapsulated HLC compared to HLC were (A) Cell death and survival and (B) Lipid metabolism. (A) The majority of the genes in the cell death and survival network were up regulated with the exception of GUCY1A2, SERPING1 and STC1 in encapsulated HLC compared to HLC. AKT remained central to the network and the target genes were all up regulated in encapsulated HLC compared to HLC. (B) The lipid metabolism network showed major up regulation of genes in encapsulated HLC compared to hAEC. APOE, TF and membrane transporters ABC (ABCC2, ABCC3 and ABCA7) were highly up regulated in encapsulated HLC compared to HLC. Red indicates up regulation in encapsulated HLC and green indicates down regulation in encapsulated HLC with $P < 0.05$ and $Q < 0.05$ and fold change ≥ 2 from $n = 4$.

The lipid metabolism network was the key network up regulated in encapsulated HLC. *APOE* was the key gene up regulated, with *LDLR*, *LIPC* and *NR4A1*, which are all associated with *APOE*, being up regulated in the pathway (Figure 5.23B). Cytochrome enzyme *CYP3A5* and membrane transporters *ABCC2* and *ABCC3*, which are involved in cholesterol breakdown, were also up regulated in encapsulated HLC compared to HLC (Figure 5.23B). Overall, these data suggest that encapsulated HLC are less immunogenic and have higher expression of hepatocyte specific genes. Thus encapsulation may enhance HLC function and provide a superior way of deriving hepatocytes.

5.4 Discussion

Cell encapsulation represents a novel way of immuno-protection by creating a 3D cell culture system. My data show that the average size of 600 μm is the optimal size for maintaining the viability of encapsulated cells and allows for diffusion of oxygen and nutrients to the core of the capsule. Other studies using human hepatocytes (55) and islet cells (56) have reported similar findings. Depletion of mtDNA by 20% and 50% prior to encapsulation did not affect the viability of encapsulated cells up to day 28 post differentiation. Maintenance of HLC viability and function at more than 90% increases the therapeutic potential of the encapsulated cell for liver disease.

My previous results show that mtDNA copy number does not increase when hAEC were induced to differentiate into HLC, which was due to DNA methylation at exon 2 of POLGA. Differentiation of encapsulated HLC resulted in reduced mtDNA copy number in 2wk encapsulated HLC and HLC. This may be due to the fact that encapsulation creates a 3D environment and with limited supply of nutrients and oxygen to the core of the capsule. A low oxygen and nutrient environment may promote differentiated HLC that rely on glycolysis for ATP production (38). However, low mtDNA copy number did not correlate with high methylation at exon 2 of POLGA. It was quite the opposite, the ratio of 5mC to 5hmC was lower but mtDNA copy number did not increase. Encapsulated 2wk HLC depleted of mtDNA (both 20 and 50% depletion) showed reduced mtDNA copy number with increased mtDNA copy number in HLC. These were correlated with a low DNA methylation ratio of 5mC to 5hmC at exon 2 of POLGA. These data suggest that hAEC are not able to modulate their mtDNA copy number either in 2D or 3D; neither with depletion of mtDNA nor without depletion. In addition, there is an inherent block in replication of mtDNA, which appears to be independent of POLGA.

I explored changes in gene expression HLC by comparing them to undifferentiated hAEC. My results indicate significant changes in differential gene expression, particularly KDR and VEGF, which are known to promote proliferation and tubular morphology, suggesting hepatic lineage commitment (41). Up regulation of DKK1, which an inhibitor of WNT-2 signalling suggests suppressed WNT-2 signalling. WNT/ β -catenin signalling acts in a gradient to establish metabolic zonation in human liver that drives different functional aspects of portal and perivenous hepatocytes (57, 58). These findings suggest a single phenotype and lack of metabolic zonation in differentiated HLC. MIR-122 is the most abundant miRNA present in liver (59), however, we did not find any differential expression of MIR-122. In addition, two other miRNA, MIR3936 and MIR612, which are implicated in inhibition of hepatocellular carcinoma proliferation were highly expressed in HLC. The exact role of expression of these miRNA is not clear in differentiation, but may be advantageous for cell therapies. There is increased evidence for hepatic differentiation with expression of GGT5, compliment factor B and CYP1B1, suggesting lineage commitment. Interestingly, differentiated HLC expressed OASL, which activates cytokine mediated signalling (43), suggests HLC are more immunogenic. I previously found that differentiation of HLC increased T-cell response *in-vitro* (60).

Cell adhesion associated genes L1CAM and PODXL were down regulated in HLC due to cell culture conditions and substrates. Surprisingly, LDLR and LIPG were also down regulated in differentiated HLC. LDLR, which is involved in endocytosis of cholesterol on the sinusoidal membrane of hepatocytes, may reduce hepatic functions (37). Down regulation of hepatic bile duct expressed SOX9 (61) and solute carrier gene SLCO2A1 suggests differentiated HLC are hepatocytes rather than biliary cells with reduced transport capacity.

Down regulation of ATM signalling, which is implicated as a cell-cycle checkpoint, suggests exit from proliferation (62). In addition, up regulation of CDK1 and Cyclin B, inhibits G2/M

transition suggesting lineage commitment and differentiation. More importantly, upregulation of anchored membrane proteins and WNT genes complements differentiation of HLC. Differentiation of cells is initially driven by reorganisation of the cytoplasmic machinery to adapt cell functions (63). Analysis of axonal guidance pathways showed up regulation of KALRN and SDC2, which control cytoskeletal reorganisation indicative of HLC differentiation. My data show that HLC down regulate genes involved in DNA replication machinery, particularly ORC and CDC45, which are indicative of exit from cell cycle.

Interestingly, differentiated HLC were more immunogenic relative to hAEC. There have been methods described to isolate hAEC in accordance with good manufacturing practise (GMP) (64), however, differentiation presents a challenge for the use of HLC in cell therapies. Activation of JAK1 and JAK2 leads to up regulation of STAT1; where phosphorylated STAT1 form homodimers to activate type II interferon signalling. Whereas phosphorylated heterodimers of STAT1 and STAT2 activate type I interferon signalling (46), activation of STAT genes leads to activation of interferon genes, resulting in an inflammatory state. Though JAK1 and STAT2 are required for early myogenic differentiation (65), their role in HLC remains undefined. In addition, there are reports of increased immunogenic responses to HLC (60), however, involvement of interferon signalling in HLC has not been reported.

Networks involved in differentiated HLC indicated differential expression of genes associated with cellular assembly and organisation. Involvement of genes associated with chromosomal segregation during mitosis (AURKB and NDC80) (66), and during cell division (BUB1 and SGOL1) (67) suggested exit from proliferation to differentiation. In addition, differentiated HLC show differential expression of genes associated with DNA replication and repair, suggesting constant DNA turnover and repair. The proliferation markers BARD1 and PCNA (68, 69) were down regulated in differentiated HLC suggestive of reduced proliferation. Expression of genes involved in the hepatic system development

network suggested true differentiation of HLC. NF κ B, which is central to the hepatic system network, can be activated by growth factors or free radical species to promote inflammatory events. Activation of NF κ B can be attributed to a pro-inflammatory environment induced by interferon signalling (70). Furthermore, differentiated HLC expressed genes associated with lipid, vitamin and mineral metabolism indicate functional aspects of HLC. A zinc metalloenzyme CA12 that catalyse hydration of carbon dioxide is associated with retinal dehydrogenase RDH11. NADP-retinol dehydrogenase and two associated genes RDH10 and DHRS3, which are involved in retinoid homeostasis (71), confer functional aspects to HLC at a transcriptional level.

When hAEC are encapsulated and differentiated into HLC, it had dramatic impact on gene expression of differentiated HLC. When we compared differentiation in encapsulated hAEC to naïve hAEC, I found more than 1325 differentially regulated genes. Micro RNAs are small noncoding RNAs that regulate post-transcriptional gene expression. Expression of MIR203 has been shown to be expressed in differentiating cells (72). MIR203 acts in conjunction with MIR302; where higher levels of expression of MIR302 promote pluripotency while MIR203 promotes differentiation (73). Higher levels of expression of MIR 203, which directly targets CDK6, Vimentin and SET (48) in encapsulated HLC, suggest that they have committed to hepatic differentiation. Encapsulation creates a 3D environment which has effects on cell adhesion and extracellular matrix genes COL18A1 and CD248. Cell-to-cell contact allows for deposition of collagen and cell-to-matrix interactions. Encapsulation and differentiation are enhanced by increased expression of Follistatin, which acts on the TGF- β superfamily that is known to inhibit adipogenesis and myogenesis while it promotes epithelial cell differentiation (74). A transcription factor FOXA3 is required in early embryogenesis and is expressed in liver primordium and in adult liver (75) and plays a crucial role in regeneration

of liver in FAH knockout mice (76). Higher expression of FOXA3 in encapsulated HLC suggests differentiation of HLC.

Unlike HLC differentiated in normal 2D culture, differentiation of encapsulated HLC creates an anti-inflammatory environment. Down regulation of TNFSF15, a tumour necrosis factor super family member, mediates activation of NF κ B, which suggests that encapsulated HLC down regulated inflammatory responses associated with NF κ B signalling. However, there were changes in expression of membrane proteins and components of tight junction Claudin 11 (CLDN11) and cell adhesion molecule PODXL, suggesting changes in cell-to-cell and cell-to-matrix interactions. CLDN11 has been associated with tumour metastasis and cell migration (77), though its down regulation in encapsulated HLC suggests otherwise. Moreover, reduction in lipid metabolism gene LIPG can be attributed to reduced lipoprotein metabolism in HLC while SEMA3D, which encodes semaphoring proteins, primarily functions as an axonal guide. These data suggest that encapsulated HLC have down regulated neuronal associated genes. Surprisingly, we observed down regulation of *Integrin- β 4* and *Inhibin- β A* in encapsulated HLC, suggesting a dynamic micro-environment within the capsule in regards to cell-to-cell and cell-to-matrix interactions.

Pathway analysis of encapsulated HLC compared to naïve hAEC suggests strong involvement of stellate cell activation. Large number of collagen genes, which are associated with extracellular matrix, and vascular endothelial growth factor were up regulated in encapsulated HLC. Increased deposition of collagen as extracellular matrix in 3D has been observed in cancer cells (78) and is known to promote functional aspects of hepatocytes. Moreover, VEGF acts via VEGF receptor to promote proliferation of encapsulated HLC. Increased collagen synthesis was complemented with reduced expression of MMP and TIMPS, which breakdown extracellular matrix. These findings suggest increased deposition of extracellular matrix and inhibition of their degradation. We observed down regulation of

Cyclins involved in centromere separation suggesting minimal proliferation of HLC in capsules. Interestingly, encapsulated HLC showed IL-1 mediated activation of RXR, which is known to maintain glucose and lipid homeostasis. Genes associated with lipid metabolism (APOE, APOC1 and SCARB1) and phase III transporters (MRP2 and MRP3) that facilitate xenobiotics and cytotoxin transport on the apical membrane (37) showed increased expression. Up regulation of lipid and xenobiotic metabolism suggests functional activity of the encapsulated HLC. Moreover, fatty acid metabolism associated genes were also highly elevated in encapsulated HLC, suggesting increased ATP production. I also observed activation of PTEN and P53 pathways, which are involved in cancer; however we did not observe any tumour forming capacity of hAEC.

My analysis of the networks affected in encapsulated HLC compared to naïve hAEC were DNA repair and replication, cellular assembly, free radical scavenging and drug metabolism. Encapsulated HLC showed up regulation of WNT2 that acts and down regulates GSK3B, a protein kinase that phosphorylates the rate limiting enzyme of glycogen synthesis (49). WNT2 signalling is also crucial during development for specification of hepatic progenitor cells (79). Interestingly, there was increased expression of zinc finger proteins ZNF133 and ZNF76, macrophage stimulating 1 (MST1) and natural killer cell triggering receptor, whilst there was no change in expression of its effector gene CD3. This suggested activation of immune cell associated genes, albeit their expression was low.

Encapsulated HLC showed increased capacity for free radical scavenging and cell-to-cell signalling. TNF receptor-associated factor 1 (TRAF1) showed activation of genes in the network. MIR210 is highly activated in the presence of hypoxia inducible factor 1-alpha (HIF1 α) (80) indicative of the capsule micro-environment led to suppression of MIR210 targets PTPB3 and BHLHE41. Encapsulation of HLC enhanced drug metabolism functions by increased expression of cytochrome enzyme CYP1B1, CYP2D6 and CYP2E1. Alpha

actin, catenin and cadherins, cytoskeletal and extracellular genes, are involved in drug metabolism networks; though their expression was not differentially regulated. Increased expression of cytochrome enzymes not only confers enhanced drug metabolism function of the encapsulated HLC but also represent a tool for *in vitro* drug screening assays. My data suggest that encapsulation of HLC achieves better hepatocyte differentiation with increased function and immune tolerance.

The effects of 3D HLC differentiation on gene expression

Comparing 3D encapsulated HLC against non-encapsulated HLC revealed a large number of genes upregulated in 3D encapsulated HLC. Iron is transported to dividing cells by serum protein transferrin (TF) (81), which showed highest upregulation in encapsulated HLC. Low oxygen concentration within the capsule increases hepatocyte iron uptake and also increases intracellular NADH and ROS activity (82). I observed increases in SERPINF2, a plasmin inhibitor that regulates cell-to-cell adhesion via cadherins and COL18A1, involved in cell adhesion and extracellular matrix reorganisation in the liver (52). Growth factor activator HGFAC and FGFR4 that act in a cascade to promote differentiation were also upregulated in encapsulated HLC. These allow for activation of HGF and FGF signalling to initiate differentiation. MIR203 was highly expressed while we did not detect differential expression of MIR302. MIR 203 acts to promote differentiation and activates ATP-binding cassette genes whereas MIR302 promotes pluripotency (73). Functional aspects of cholesterol metabolism were observed via increased expression of APOE, and catabolism of triglyceride-rich lipoproteins in encapsulated HLC.

In contrast, there was significant down regulation of OAS1, a gene associated with innate immune response to viral infection (53) and MX1, which participates in cellular antiviral response. Additionally, interferon signalling genes were down regulated in encapsulated HLC

suggesting inhibition of inflammatory response. STAT1, which acts upstream in conjunction with STAT2 to activate type I and II interferon signalling was also down regulated. Inhibition of inflammatory genes may play a pivotal role in use of encapsulated HLC to suppress the inflammatory micro-environment at a transplant site. Moreover, encapsulated HLC down regulated MIR612, which has been suggested to play a role in suppressing stemness in HCC and impede tumorigenesis (83). These findings suggest that MIR612 promotes differentiation and inhibits pluripotency.

Analysis of canonical pathways showed major down regulation of interferon signalling. Interferon gamma signalling activates phosphorylated homodimers of STAT1, which results in activation of inflammatory genes (84). However, interferon alpha / beta signalling activates phosphorylated heterodimers of STAT1 and STAT2 to activate inflammatory genes in conjunction with interferon regulatory factor 9 (85). Nevertheless, STAT1, STAT2 and their target genes were all down regulated in encapsulated HLC, indicative of inhibition of inflammatory pathways. In contrast, signalling in the complement component via PI3K and ERK 1/2 pathway were up regulated in encapsulated HLC. Activation of PI3K and ERK signalling is associated with a hypoxic environment (86) as well as invasion and migration of HCC (87) implicating the micro-environment of encapsulated HLC as initiators of the signalling pathway.

Functional aspects of encapsulated HLC were enhanced through activation of the FXR/RXR pathway. The FXR pathway is implicated in various metabolic pathways, along with RXR, it regulates glucose, lipid and lipoprotein metabolism (88). FXR/RXR also activate downstream target genes ABCA2, iron transporter HPX and TF. It also activates the drug metabolism enzyme CYP27A1, the cytochrome enzyme that catalyses the first step in bile acid synthesis (54) and lipoprotein metabolism associated genes APOE, LIPC and LDLR, which showed upregulation in encapsulated HLC. Encapsulated HLC showed increased expression of

MAPK1 and NKX2-3, which are involved in cell specification and differentiation. Pathway analysis of encapsulated HLC suggest that they are metabolically functional and anti-inflammatory.

Network analysis of encapsulated HLC showed increased capacity for urea metabolism. In particular, ASS1, catalyses the penultimate step of arginine biosynthesis in the urea cycle (89), the urea cycle enzyme GOT1 and Protein convertase PCSK6 and PCSK1N. Increased expression of urea cycle genes can be attributed to increased expression of the cell adhesion molecule EPCAM, which is known to affect hepatocyte polarisation thus resulting in increased functional output (90). Besides the expression of OSGIN1 and CDC6, which are implicated in oxidative stress induced growth inhibition and DNA replication, they did not affect expression of Cyclin A. Encapsulated HLC exhibited an anti-inflammatory profile by down regulating interferon inducible genes as well as STAT1, suggesting down regulation of its target genes. Due to a low oxygen and nutrient environment within the core of the capsule, cell death may result as a consequence. Encapsulated HLC showed up regulation of genes in cell death and survival, particularly ST6GAL1 and GDF15. However, genes involved in AKT signalling and type IV collagen were upregulated suggesting increased glycogen synthesis by blocking GSK3 and deposition of the extracellular matrix in encapsulated HLC (91).

Solute carriers are responsible for transport across the hepatocyte cell membranes. Encapsulating HLC increases cell-to-cell interaction by increasing BCAM and increased expression of solute carrier SLC20A1 and SLC29A1, which are phosphate and nucleoside transporters (92, 93). Complement proteins are synthesised in the liver and participate in innate immune responses (94-97) which were also highly expressed in encapsulated HLC indicating increased functional capacity. Lipid metabolism, bile acid synthesis and the cholesterol metabolism super-pathway are a key functional aspect of hepatocytes and plays a vital role in lipid homeostasis. Encapsulated HLC showed increased expression of LDLR,

LIPC and NR4A1 which are associated with APOE were all up regulated. The CYP3A family of cytochromes are most versatile biotransformation enzymes that catalyse a third of top 200 prescribed drugs (98). Encapsulated HLC showed increased expression of CYP3A5 and we have previously shown increased expression of CYP3A4 in encapsulated HLC. There was a concurrent increase in expression of ABCC2 (MRP2) and ABCC3 (MRP3), which are expressed on the apical cell membrane of hepatocytes, with increased expression of the CYP3A family in encapsulated HLC. ABCC2 and ABCC3 are responsible for export of potentially toxic exogenous and endogenous substrates (99). These data suggest that increases in expression of the drug metabolism enzyme is followed by an increase in membrane transporters responsible for elimination of breakdown products.

Encapsulation of HLC not only provides an alternative for cell transplantation but also creates an efficient 3D culture system for derivation of functional hepatocytes. Encapsulation creates a micro-environment with increased cell-to-cell and cell-to-matrix interaction that allows the native *in vivo* conditions to be mimicked. Encapsulated HLC are more versatile with increased lipid and drug metabolism capacity with suppressed immune response.

5.5 References

1. Schwartz RE, Reyes M, Koodie L, Jiang Y, Blackstad M, Lund T, et al. Multipotent adult progenitor cells from bone marrow differentiate into functional hepatocyte-like cells. *The Journal of clinical investigation*. 2002;109(10):1291-302.
2. Si-Tayeb K, Noto FK, Nagaoka M, Li J, Battle MA, Duris C, et al. Highly efficient generation of human hepatocyte-like cells from induced pluripotent stem cells. *Hepatology*. 2010;51(1):297-305.
3. Wang X, Ge S, McNamara G, Hao QL, Crooks GM, Nolte JA. Albumin-expressing hepatocyte-like cells develop in the livers of immune-deficient mice that received transplants of highly purified human hematopoietic stem cells. *Blood*. 2003;101(10):4201-8.
4. Vaghjiani V, Vaithilingam V, Saraswati I, Sali A, Murthi P, Kalionis B, et al. Hepatocyte-like cells derived from human amniotic epithelial cells can be encapsulated without loss of viability or function in vitro. *Stem cells and development*. 2014;23(8):866-76.
5. Pampaloni F, Reynaud EG, Stelzer EH. The third dimension bridges the gap between cell culture and live tissue. *Nature reviews Molecular cell biology*. 2007;8(10):839-45.
6. Rowley JA, Madlambayan G, Mooney DJ. Alginate hydrogels as synthetic extracellular matrix materials. *Biomaterials*. 1999;20(1):45-53.
7. Willerth SM, Sakiyama-Elbert SE. Combining stem cells and biomaterial scaffolds for constructing tissues and cell delivery. *StemBook*. Cambridge (MA)2008.
8. Augst AD, Kong HJ, Mooney DJ. Alginate hydrogels as biomaterials. *Macromolecular bioscience*. 2006;6(8):623-33.
9. Gerecht-Nir S, Cohen S, Ziskind A, Itskovitz-Eldor J. Three-dimensional porous alginate scaffolds provide a conducive environment for generation of well-vascularized embryoid bodies from human embryonic stem cells. *Biotechnology and bioengineering*. 2004;88(3):313-20.

10. Song K, Qiao M, Liu T, Jiang B, Macedo HM, Ma X, et al. Preparation, fabrication and biocompatibility of novel injectable temperature-sensitive chitosan/glycerophosphate/collagen hydrogels. *Journal of materials science Materials in medicine*. 2010;21(10):2835-42.
11. Cho CH, Eliason JF, Matthew HW. Application of porous glycosaminoglycan-based scaffolds for expansion of human cord blood stem cells in perfusion culture. *Journal of biomedical materials research Part A*. 2008;86(1):98-107.
12. Franzesi GT, Ni B, Ling Y, Khademhosseini A. A controlled-release strategy for the generation of cross-linked hydrogel microstructures. *Journal of the American Chemical Society*. 2006;128(47):15064-5.
13. Ashton RS, Banerjee A, Punyani S, Schaffer DV, Kane RS. Scaffolds based on degradable alginate hydrogels and poly(lactide-co-glycolide) microspheres for stem cell culture. *Biomaterials*. 2007;28(36):5518-25.
14. Buxton AN, Zhu J, Marchant R, West JL, Yoo JU, Johnstone B. Design and characterization of poly(ethylene glycol) photopolymerizable semi-interpenetrating networks for chondrogenesis of human mesenchymal stem cells. *Tissue engineering*. 2007;13(10):2549-60.
15. Maguire T, Novik E, Schloss R, Yarmush M. Alginate-PLL microencapsulation: effect on the differentiation of embryonic stem cells into hepatocytes. *Biotechnology and bioengineering*. 2006;93(3):581-91.
16. de Vos P, Faas MM, Strand B, Calafiore R. Alginate-based microcapsules for immunoisolation of pancreatic islets. *Biomaterials*. 2006;27(32):5603-17.
17. Zhang FT, Wan HJ, Li MH, Ye J, Yin MJ, Huang CQ, et al. Transplantation of microencapsulated umbilical-cord-blood-derived hepatic-like cells for treatment of hepatic failure. *World journal of gastroenterology*. 2011;17(7):938-45.

18. Vaithilingam V, Fung C, Ratnapala S, Foster J, Vaghjiani V, Manuelpillai U, et al. Characterisation of the xenogeneic immune response to microencapsulated fetal pig islet-like cell clusters transplanted into immunocompetent C57BL/6 mice. *PloS one*. 2013;8(3):e59120.
19. Orive G, Ponce S, Hernandez RM, Gascon AR, Igartua M, Pedraz JL. Biocompatibility of microcapsules for cell immobilization elaborated with different type of alginates. *Biomaterials*. 2002;23(18):3825-31.
20. Lim F, Sun AM. Microencapsulated islets as bioartificial endocrine pancreas. *Science*. 1980;210(4472):908-10.
21. Wilson JT, Chaikof EL. Challenges and emerging technologies in the immunoisolation of cells and tissues. *Adv Drug Deliv Rev*. 2008;60(2):124-45.
22. Hamazaki K, Doi Y, Koide N. Microencapsulated multicellular spheroid of rat hepatocytes transplanted intraperitoneally after 90% hepatectomy. *Hepatogastroenterology*. 2002;49(48):1514-6.
23. Mai G, Nguyen TH, Morel P, Mei J, Andres A, Bosco D, et al. Treatment of fulminant liver failure by transplantation of microencapsulated primary or immortalized xenogeneic hepatocytes. *Xenotransplantation*. 2005;12(6):457-64.
24. Chen AA, Thomas DK, Ong LL, Schwartz RE, Golub TR, Bhatia SN. Humanized mice with ectopic artificial liver tissues. *Proc Natl Acad Sci U S A*. 2011;108(29):11842-7.
25. Zhang RR, Takebe T, Miyazaki L, Takayama M, Koike H, Kimura M, et al. Efficient hepatic differentiation of human induced pluripotent stem cells in a three-dimensional microscale culture. *Methods in molecular biology*. 2014;1210:131-41.
26. Ishii T, Fukumitsu K, Yasuchika K, Adachi K, Kawase E, Suemori H, et al. Effects of extracellular matrixes and growth factors on the hepatic differentiation of human embryonic stem cells. *American journal of physiology Gastrointestinal and liver physiology*. 2008;295(2):G313-21.

27. Kelly RD, Mahmud A, McKenzie M, Trounce IA, St John JC. Mitochondrial DNA copy number is regulated in a tissue specific manner by DNA methylation of the nuclear-encoded DNA polymerase gamma A. *Nucleic acids research*. 2012;40(20):10124-38.
28. Lee W, Johnson J, Gough DJ, Donoghue J, Cagnone GL, Vaghjiani V, et al. Mitochondrial DNA copy number is regulated by DNA methylation and demethylation of POLGA in stem and cancer cells and their differentiated progeny. *Cell death & disease*. 2015;6:e1664.
29. Liu H, Lin J, Roy K. Effect of 3D scaffold and dynamic culture condition on the global gene expression profile of mouse embryonic stem cells. *Biomaterials*. 2006;27(36):5978-89.
30. Chang TT, Hughes-Fulford M. Molecular mechanisms underlying the enhanced functions of three-dimensional hepatocyte aggregates. *Biomaterials*. 2014;35(7):2162-71.
31. Chia SM, Leong KW, Li J, Xu X, Zeng K, Er PN, et al. Hepatocyte encapsulation for enhanced cellular functions. *Tissue engineering*. 2000;6(5):481-95.
32. Paszek MJ, Zahir N, Johnson KR, Lakins JN, Rozenberg GI, Gefen A, et al. Tensional homeostasis and the malignant phenotype. *Cancer cell*. 2005;8(3):241-54.
33. Li GN, Livi LL, Gourd CM, Deweerd ES, Hoffman-Kim D. Genomic and morphological changes of neuroblastoma cells in response to three-dimensional matrices. *Tissue engineering*. 2007;13(5):1035-47.
34. Miron-Mendoza M, Koppaka V, Zhou C, Petroll WM. Techniques for assessing 3-D cell-matrix mechanical interactions in vitro and in vivo. *Experimental cell research*. 2013;319(16):2470-80.
35. Li CL, Tian T, Nan KJ, Zhao N, Guo YH, Cui J, et al. Survival advantages of multicellular spheroids vs. monolayers of HepG2 cells in vitro. *Oncology reports*. 2008;20(6):1465-71.

36. Sainz B, Jr., TenCate V, Uprichard SL. Three-dimensional Huh7 cell culture system for the study of Hepatitis C virus infection. *Virology journal*. 2009;6:103.
37. Treyer A, Musch A. Hepatocyte polarity. *Comprehensive Physiology*. 2013;3(1):243-87.
38. Fu D, Mitra K, Sengupta P, Jarnik M, Lippincott-Schwartz J, Arias IM. Coordinated elevation of mitochondrial oxidative phosphorylation and autophagy help drive hepatocyte polarization. *Proceedings of the National Academy of Sciences of the United States of America*. 2013;110(18):7288-93.
39. Miranda JP, Rodrigues A, Tostoes RM, Leite S, Zimmerman H, Carrondo MJ, et al. Extending hepatocyte functionality for drug-testing applications using high-viscosity alginate-encapsulated three-dimensional cultures in bioreactors. *Tissue engineering Part C, Methods*. 2010;16(6):1223-32.
40. Tao ZH, Wan JL, Zeng LY, Xie L, Sun HC, Qin LX, et al. miR-612 suppresses the invasive-metastatic cascade in hepatocellular carcinoma. *The Journal of experimental medicine*. 2013;210(4):789-803.
41. Gogat K, Le Gat L, Van Den Berghe L, Marchant D, Kobetz A, Gadin S, et al. VEGF and KDR gene expression during human embryonic and fetal eye development. *Investigative ophthalmology & visual science*. 2004;45(1):7-14.
42. Fedi P, Bafico A, Nieto Soria A, Burgess WH, Miki T, Bottaro DP, et al. Isolation and biochemical characterization of the human Dkk-1 homologue, a novel inhibitor of mammalian Wnt signaling. *The Journal of biological chemistry*. 1999;274(27):19465-72.
43. Hartmann R, Olsen HS, Widder S, Jorgensen R, Justesen J. p59OASL, a 2'-5' oligoadenylate synthetase like protein: a novel human gene related to the 2'-5' oligoadenylate synthetase family. *Nucleic acids research*. 1998;26(18):4121-8.

44. Sutter TR, Tang YM, Hayes CL, Wo YY, Jabs EW, Li X, et al. Complete cDNA sequence of a human dioxin-inducible mRNA identifies a new gene subfamily of cytochrome P450 that maps to chromosome 2. *The Journal of biological chemistry*. 1994;269(18):13092-9.
45. Brown MS, Goldstein JL. Receptor-mediated endocytosis: insights from the lipoprotein receptor system. *Proceedings of the National Academy of Sciences of the United States of America*. 1979;76(7):3330-7.
46. Darnell JE, Jr., Kerr IM, Stark GR. Jak-STAT pathways and transcriptional activation in response to IFNs and other extracellular signaling proteins. *Science*. 1994;264(5164):1415-21.
47. Furuta M, Kozaki KI, Tanaka S, Arii S, Imoto I, Inazawa J. miR-124 and miR-203 are epigenetically silenced tumor-suppressive microRNAs in hepatocellular carcinoma. *Carcinogenesis*. 2010;31(5):766-76.
48. da Silva CG, Studer P, Skroch M, Mahiou J, Minussi DC, Peterson CR, et al. A20 promotes liver regeneration by decreasing SOCS3 expression to enhance IL-6/STAT3 proliferative signals. *Hepatology*. 2013;57(5):2014-25.
49. Ali A, Hoeflich KP, Woodgett JR. Glycogen synthase kinase-3: properties, functions, and regulation. *Chemical reviews*. 2001;101(8):2527-40.
50. Segref A, Sharma K, Doye V, Hellwig A, Huber J, Luhrmann R, et al. Mex67p, a novel factor for nuclear mRNA export, binds to both poly(A)⁺ RNA and nuclear pores. *The EMBO journal*. 1997;16(11):3256-71.
51. Takai S, Long JE, Yamada K, Miki T. Chromosomal localization of the human ECT2 proto-oncogene to 3q26.1-->q26.2 by somatic cell analysis and fluorescence in situ hybridization. *Genomics*. 1995;27(1):220-2.

52. Oh SP, Kamagata Y, Muragaki Y, Timmons S, Ooshima A, Olsen BR. Isolation and sequencing of cDNAs for proteins with multiple domains of Gly-Xaa-Yaa repeats identify a distinct family of collagenous proteins. *Proceedings of the National Academy of Sciences of the United States of America*. 1994;91(10):4229-33.
53. Hovnanian A, Rebouillat D, Mattei MG, Levy ER, Marie I, Monaco AP, et al. The human 2',5'-oligoadenylate synthetase locus is composed of three distinct genes clustered on chromosome 12q24.2 encoding the 100-, 69-, and 40-kDa forms. *Genomics*. 1998;52(3):267-77.
54. Cali JJ, Russell DW. Characterization of human sterol 27-hydroxylase. A mitochondrial cytochrome P-450 that catalyzes multiple oxidation reaction in bile acid biosynthesis. *The Journal of biological chemistry*. 1991;266(12):7774-8.
55. Jitraruch S, Dhawan A, Hughes RD, Filippi C, Soong D, Philippeos C, et al. Alginate microencapsulated hepatocytes optimised for transplantation in acute liver failure. *PloS one*. 2014;9(12):e113609.
56. Tuch BE, Keogh GW, Williams LJ, Wu W, Foster JL, Vaithilingam V, et al. Safety and viability of microencapsulated human islets transplanted into diabetic humans. *Diabetes care*. 2009;32(10):1887-9.
57. Benhamouche S, Decaens T, Godard C, Chambrey R, Rickman DS, Moinard C, et al. Apc tumor suppressor gene is the "zonation-keeper" of mouse liver. *Developmental cell*. 2006;10(6):759-70.
58. Loeppen S, Koehle C, Buchmann A, Schwarz M. A beta-catenin-dependent pathway regulates expression of cytochrome P450 isoforms in mouse liver tumors. *Carcinogenesis*. 2005;26(1):239-48.

59. Chang J, Nicolas E, Marks D, Sander C, Lerro A, Buendia MA, et al. miR-122, a mammalian liver-specific microRNA, is processed from hcr mRNA and may downregulate the high affinity cationic amino acid transporter CAT-1. *RNA biology*. 2004;1(2):106-13.
60. Tee JY, Vaghjiani V, Liu YH, Murthi P, Chan J, Manuelpillai U. Immunogenicity and immunomodulatory properties of hepatocyte-like cells derived from human amniotic epithelial cells. *Current stem cell research & therapy*. 2013;8(1):91-9.
61. Furuyama K, Kawaguchi Y, Akiyama H, Horiguchi M, Kodama S, Kuhara T, et al. Continuous cell supply from a Sox9-expressing progenitor zone in adult liver, exocrine pancreas and intestine. *Nature genetics*. 2011;43(1):34-41.
62. Abraham RT. Cell cycle checkpoint signaling through the ATM and ATR kinases. *Genes & development*. 2001;15(17):2177-96.
63. Kawaguchi N, Sundberg C, Kveiborg M, Moghadaszadeh B, Asmar M, Dietrich N, et al. ADAM12 induces actin cytoskeleton and extracellular matrix reorganization during early adipocyte differentiation by regulating beta1 integrin function. *Journal of cell science*. 2003;116(Pt 19):3893-904.
64. Murphy S, Rosli S, Acharya R, Mathias L, Lim R, Wallace E, et al. Amnion epithelial cell isolation and characterization for clinical use. *Current protocols in stem cell biology*. 2010;Chapter 1:Unit 1E 6.
65. Wang K, Wang C, Xiao F, Wang H, Wu Z. JAK2/STAT2/STAT3 are required for myogenic differentiation. *The Journal of biological chemistry*. 2008;283(49):34029-36.
66. Lampson MA, Renduchitala K, Khodjakov A, Kapoor TM. Correcting improper chromosome-spindle attachments during cell division. *Nature cell biology*. 2004;6(3):232-7.
67. Tang Z, Sun Y, Harley SE, Zou H, Yu H. Human Bub1 protects centromeric sister-chromatid cohesion through Shugoshin during mitosis. *Proceedings of the National Academy of Sciences of the United States of America*. 2004;101(52):18012-7.

68. Bravo R. Synthesis of the nuclear protein cyclin (PCNA) and its relationship with DNA replication. *Experimental cell research*. 1986;163(2):287-93.
69. Jin Y, Xu XL, Yang MC, Wei F, Aji TC, Bowcock AM, et al. Cell cycle-dependent colocalization of BARD1 and BRCA1 proteins in discrete nuclear domains. *Proceedings of the National Academy of Sciences of the United States of America*. 1997;94(22):12075-80.
70. Pauli EK, Schmolke M, Wolff T, Viemann D, Roth J, Bode JG, et al. Influenza A virus inhibits type I IFN signaling via NF-kappaB-dependent induction of SOCS-3 expression. *PLoS pathogens*. 2008;4(11):e1000196.
71. Adams MK, Belyaeva OV, Wu L, Kedishvili NY. The retinaldehyde reductase activity of DHRS3 is reciprocally activated by retinol dehydrogenase 10 to control retinoid homeostasis. *The Journal of biological chemistry*. 2014;289(21):14868-80.
72. Yi R, Poy MN, Stoffel M, Fuchs E. A skin microRNA promotes differentiation by repressing 'stemness'. *Nature*. 2008;452(7184):225-9.
73. Volinia S, Nuovo G, Drusco A, Costinean S, Abujarour R, Despons C, et al. Pluripotent stem cell miRNAs and metastasis in invasive breast cancer. *Journal of the National Cancer Institute*. 2014;106(12).
74. Massague J. The TGF-beta family of growth and differentiation factors. *Cell*. 1987;49(4):437-8.
75. Le Lay J, Kaestner KH. The Fox genes in the liver: from organogenesis to functional integration. *Physiological reviews*. 2010;90(1):1-22.
76. Wangenstein KJ, Zhang S, Greenbaum LE, Kaestner KH. A genetic screen reveals Foxa3 and TNFR1 as key regulators of liver repopulation. *Genes & development*. 2015;29(9):904-9.

77. Karagiannis GS, Schaeffer DF, Cho CK, Musrap N, Saraon P, Batruch I, et al. Collective migration of cancer-associated fibroblasts is enhanced by overexpression of tight junction-associated proteins claudin-11 and occludin. *Molecular oncology*. 2014;8(2):178-95.
78. Horning JL, Sahoo SK, Vijayaraghavalu S, Dimitrijevic S, Vasir JK, Jain TK, et al. 3-D tumor model for in vitro evaluation of anticancer drugs. *Molecular pharmaceutics*. 2008;5(5):849-62.
79. Si-Tayeb K, Lemaigre FP, Duncan SA. Organogenesis and development of the liver. *Developmental cell*. 2010;18(2):175-89.
80. Wang H, Flach H, Onizawa M, Wei L, McManus MT, Weiss A. Negative regulation of Hif1a expression and TH17 differentiation by the hypoxia-regulated microRNA miR-210. *Nature immunology*. 2014;15(4):393-401.
81. Hershberger CL, Larson JL, Arnold B, Rosteck PR, Jr., Williams P, DeHoff B, et al. A cloned gene for human transferrin. *Annals of the New York Academy of Sciences*. 1991;646:140-54.
82. Thorstensen K, Romslo I. The role of transferrin in the mechanism of cellular iron uptake. *The Biochemical journal*. 1990;271(1):1-9.
83. Tang J, Tao ZH, Wen D, Wan JL, Liu DL, Zhang S, et al. MiR-612 suppresses the stemness of liver cancer via Wnt/beta-catenin signaling. *Biochemical and biophysical research communications*. 2014;447(1):210-5.
84. Hartman SE, Bertone P, Nath AK, Royce TE, Gerstein M, Weissman S, et al. Global changes in STAT target selection and transcription regulation upon interferon treatments. *Genes & development*. 2005;19(24):2953-68.
85. Reich NC. Nuclear/cytoplasmic localization of IRFs in response to viral infection or interferon stimulation. *Journal of interferon & cytokine research : the official journal of the International Society for Interferon and Cytokine Research*. 2002;22(1):103-9.

86. Risbud MV, Fertala J, Vresilovic EJ, Albert TJ, Shapiro IM. Nucleus pulposus cells upregulate PI3K/Akt and MEK/ERK signaling pathways under hypoxic conditions and resist apoptosis induced by serum withdrawal. *Spine*. 2005;30(8):882-9.
87. Saxena NK, Sharma D, Ding X, Lin S, Marra F, Merlin D, et al. Concomitant activation of the JAK/STAT, PI3K/AKT, and ERK signaling is involved in leptin-mediated promotion of invasion and migration of hepatocellular carcinoma cells. *Cancer research*. 2007;67(6):2497-507.
88. Claudel T, Staels B, Kuipers F. The Farnesoid X receptor: a molecular link between bile acid and lipid and glucose metabolism. *Arteriosclerosis, thrombosis, and vascular biology*. 2005;25(10):2020-30.
89. Engel K, Hohne W, Haberle J. Mutations and polymorphisms in the human argininosuccinate synthetase (ASS1) gene. *Human mutation*. 2009;30(3):300-7.
90. Giepmans BN, van Ijzendoorn SC. Epithelial cell-cell junctions and plasma membrane domains. *Biochimica et biophysica acta*. 2009;1788(4):820-31.
91. Friedl P, Brocker EB. The biology of cell locomotion within three-dimensional extracellular matrix. *Cellular and molecular life sciences : CMLS*. 2000;57(1):41-64.
92. Griffiths M, Beaumont N, Yao SY, Sundaram M, Boumah CE, Davies A, et al. Cloning of a human nucleoside transporter implicated in the cellular uptake of adenosine and chemotherapeutic drugs. *Nature medicine*. 1997;3(1):89-93.
93. Kavanaugh MP, Miller DG, Zhang W, Law W, Kozak SL, Kabat D, et al. Cell-surface receptors for gibbon ape leukemia virus and amphotropic murine retrovirus are inducible sodium-dependent phosphate symporters. *Proceedings of the National Academy of Sciences of the United States of America*. 1994;91(15):7071-5.
94. Ruddy S, Gigli I, Austen KF. The complement system of man. 4. *The New England journal of medicine*. 1972;287(13):642-6.

95. Ruddy S, Gigli I, Austen KF. The complement system of man. 3. The New England journal of medicine. 1972;287(12):592-6.
96. Ruddy S, Gigli I, Austen KF. The complement system of man (second of four parts). The New England journal of medicine. 1972;287(11):545-9.
97. Ruddy S, Gigli I, Austen KF. The complement system of man. I. The New England journal of medicine. 1972;287(10):489-95.
98. Zanger UM, Turpeinen M, Klein K, Schwab M. Functional pharmacogenetics/genomics of human cytochromes P450 involved in drug biotransformation. Analytical and bioanalytical chemistry. 2008;392(6):1093-108.
99. Vlaming ML, van Esch A, Pala Z, Wagenaar E, van de Wetering K, van Tellingen O, et al. Abcc2 (Mrp2), Abcc3 (Mrp3), and Abcg2 (Bcrp1) are the main determinants for rapid elimination of methotrexate and its toxic metabolite 7-hydroxymethotrexate in vivo. Molecular cancer therapeutics. 2009;8(12):3350-9.

Chapter 6

Summary, Implications and Future Perspectives.

6.1 Summary

Using stem cells for differentiation of hepatocyte-like cells may overcome the shortage resulting from the lack of available human hepatocytes and livers for transplantation purposes. My findings show that functional hepatocyte-like cells can be derived from human amniotic epithelial cells. Using hAEC has key advantages of accessing a readily available source of stem cells which is ethically accepted. HAEC are derived from the embryonic epiblast and possess anti-inflammatory (1-5) and the immuno-modulatory properties (6-8). In addition, hAEC express some of the pluripotency markers (9-11) as well as some hepatic progenitor (7, 12, 13) and mature markers (7, 10, 11, 14, 15). Differentiation of hAEC using growth factors induces expression of a key hepatic transcription factor HNF4 α ; whilst serum protein albumin continued to be expressed; and there was increased glycogen storage.

HLC differentiation increased gene expression of drug / membrane transporter ABCA2, cholesterol metabolism cytochrome CYP7A1 (16) and bile acid transporter ABCB11 (17), suggesting an active cholesterol metabolism / bile acid synthesis pathway in differentiated HLC. Moreover, HLC expressed low density lipoprotein (LDL) receptor and showed uptake and accumulation of LDL in the cytoplasm. HLC showed remarkable functional capacity for drug metabolism through expression of CYP3A4 and functional CYP3A4 activity. I also observed increased urea synthesis and increased expression of genes in the urea cycle. Furthermore, HLC showed the capacity to uptake and efflux indocyanine green (ICG), a dye used to evaluate hepatic function (18). HLC also had high levels of total and oxidised glutathione that are responsible for eliminating reactive oxygen species (ROS) (19).

Encapsulated HLC maintain their viability and expression of transcription factor HNF4 α ; serum protein albumin and increased glycogen storage. Encapsulation of HLC creates a 3D environment which enhances functional aspects of hepatocytes. Encapsulated HLC showed

uptake of LDL and ICG with increases in oxidised glutathiones. These finding suggest increased functional output of hepatocytes and effective elimination of ROS via oxidation of glutathiones suggesting increased ROS generation due to increased function. Moreover, increased gene expression of CYP3A4 and functional CYP3A4 activity were observed in encapsulated HLC. The increased expression of CYP3A4 was due to increased expression of HNF4 α which binds to the promoter and drives expression of CYP3A4 (20). Additionally, there was increased gene expression of the urea cycle enzyme CPS1 as well as increased urea production in encapsulated HLC. However, the functional aspects of differentiated HLC were reduced compared to the hepatocellular carcinoma cell line HepG2. Summary of the findings is illustrated in figure 6.1.

During differentiation, there is increased demand for cellular energy for functional output and to attain polarization (21). Mitochondrial DNA (mtDNA) copy number is synchronously increased during differentiation, which in turn is regulated by DNA methylation at exon 2 of POLGA (22, 23). During HLC differentiation, mtDNA copy number did not increase and DNA methylation at exon 2 of POLGA remained high (Summary Fig 6.1). Though there was gene expression of hepatocyte markers, pluripotency markers also continued to be expressed alongside. DNA methylation can be modulated by 5-azacytidine (5aza) treatment of cells. Treatment with 5aza during HLC differentiation increased mtDNA copy number and reduced DNA methylation at exon 2 of POLGA. However, 5aza treatment during HLC differentiation also resulted in aberrant expression of hepatocyte genes and increased gene expression of pluripotency markers.

Depletion of mtDNA re-establishes the pluripotent state with increased expression of pluripotency genes that allows cells to fully progress through differentiation. Depletion of mtDNA in hAEC for 3 and 7 days significantly reduced mtDNA copy number and reduced DNA methylation at exon 2 of POLGA. However, when depleted hAEC were allowed to

differentiate after mtDNA depletion, mtDNA copy number did not increase and this was marked by increased DNA methylation at exon 2 of POLGA. Increased hepatic gene expression was observed after 7 days of differentiation. Pluripotency genes continued to be expressed in differentiated HLC which were mtDNA depleted and peaked at 14 days of differentiation. Oncogene cMYC and proliferation marker hTERT were also highly expressed in hAEC and mtDNA depleted hAEC. I evaluated the tumorigenic capacity of mtDNA depleted hAEC because of high expression of cMYC and hTERT. However, I found that both mtDNA depleted hAEC and non-depleted hAEC did not form tumours.

Since hAEC are unable to modulate their mtDNA copy number during HLC differentiation, I sought to create a 3D culture environment by encapsulation. Encapsulation and differentiation of HLC did not increase mtDNA copy number beyond their original mtDNA copy number levels. However, DNA methylation at exon 2 of POLGA was significantly reduced in encapsulated HLC. As hAEC are unable to modulate mtDNA copy number but have low DNA methylation in encapsulated HLC, I performed transcriptome analysis of hAEC, HLC and encapsulated HLC through RNAseq. Comparing differentiated HLC to naïve hAEC showed that HLC expressed hepatocyte specific genes as well as pro-inflammatory genes. HLC showed significant levels of expression of STAT1 and STAT2, which activate type I and II interferon signalling. In addition, gene regulating proliferation and cell cycle control were also affected. The top pathways affected were ATM signalling, cell cycle control and interferon signalling. The top networks affected were cell cycle and cellular assembly, DNA replication and repair, developmental disorders, hepatic system development and lipid, vitamin and mineral metabolism. The implications of the involvement of these pathways and networks not only demonstrate differentiation but the immunogenic profile of HLC (Summary Fig 6.1).

To assess if HLC differentiation is better achieved in encapsulated HLC, I compared encapsulated HLC with naïve hAEC. There were 1325 differentially regulated genes with 705 genes up regulated and 620 genes down regulated. Encapsulated HLC showed up regulation of genes involved with micro RNA, cell adhesion molecules, extracellular matrix and liver specific transcription factors. These that were down regulated include pro-inflammatory transcription factor NFκB, TNFα and cell adhesion molecules. The top canonical pathways affected were stellate cell activation, which showed significant increases in collagen genes, matrix metalloproteinase and tissue inhibitors of matrix metalloproteinase. Other pathways affected include the mitotic role of polo-like kinase, IL-1 mediated inhibition of RXR, P53 and PTEN pathways. The top networks affected were the cell cycle and DNA repair network, cellular assembly and cell cycle network, free radical scavenging and cell-to-cell signalling network.

Evaluation of encapsulated HLC against HLC revealed 286 differentially regulated genes with 210 genes up regulated and 76 genes down regulated. Highly up regulated genes were associated with cell adhesion, extracellular matrix reorganisation and cholesterol metabolism. These that were down regulated were primarily pro-inflammatory associated genes including interferon inducible genes, STAT transcription factors and OAS. The top canonical pathway affected was interferon signalling, which was down regulated. However, the PI3K and ERK1/2 pathway and FXR/RXR pathway were highly activated and play important roles in functional aspects of hepatocytes. The top networks affected were the organism injury, the inflammatory response network, and the cell signalling and lipid metabolism networks.

Overall, my findings show that functional HLC can be derived from hAEC, however, they also become more immunogenic. In contrast, they are unable to modulate their mtDNA copy number due to increased DNA methylation at exon 2 of POLGA. MtDNA copy number can partially be modulated with 5aza treatment but not with depletion of mtDNA copy number, as

has been shown for tumour cells. Nevertheless, partial depletion normally promotes synchrony between the nuclear and mitochondrial genomes (24). The pro-inflammatory state can be overcome by encapsulation of HLC; which suppresses pro-inflammatory response and enhances hepatic differentiation and function.

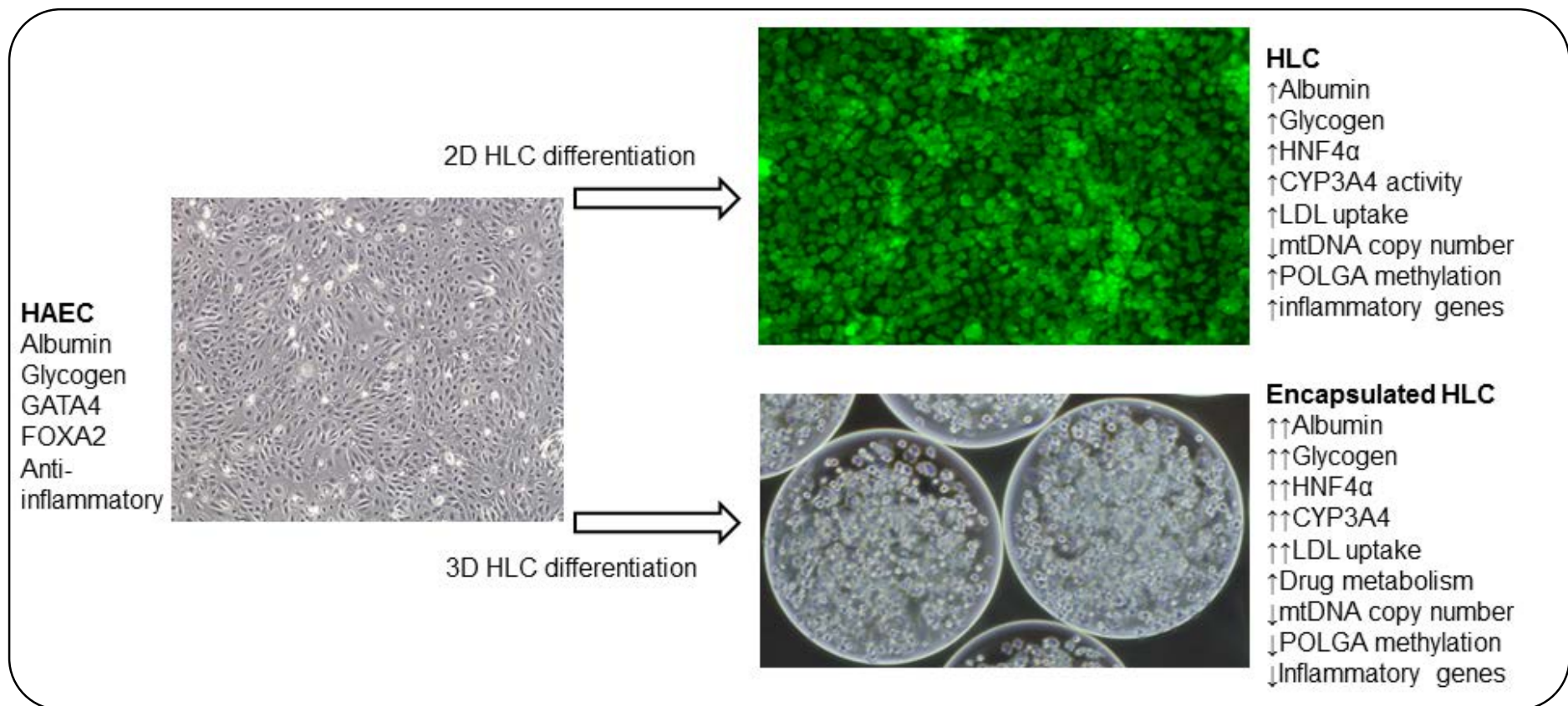


Figure 6.1. Summary of HLC differentiation compared to encapsulated HLC. Naïve hAEC express some hepatic markers such as Albumin, Glycogen storage, GATA4, FOXA2 and have an anti-inflammatory profile. When hAEC are differentiated into HLC, they express hepatic transcription factor HNF4 α , have drug metabolism capacity and uptake LDL. However they fail to regulate their mtDNA copy number, increase DNA methylation of POLGA at exon 2 and become more immunogenic. On the other hand, encapsulated HLC have enhanced expression of Albumin, glycogen storage, HNF4 α , CYP3A4, LDL uptake and increased drug metabolism capacity. They also fail to regulate their mtDNA copy number but have low DNA methylation at exon 2 of POLGA and down regulate inflammatory genes.

6.2 Implications

My study demonstrates that functional HLC can be derived from differentiation of hAEC. Differentiated HLC have characteristics of human hepatocytes at gene expression and partial metabolic function levels. HLC can be used as cell therapy in lieu of human hepatocytes for both chronic and metabolic liver diseases. There are various studies that have evaluated the use of hAEC for liver regeneration in disease models (14, 25, 26), however, use of differentiated HLC as cell therapy has been limited. My findings show that differentiation of HLC creates an inflammatory environment which may not be permissive for use of HLC as they would elicit an immune response. This has been a key challenge in using HLC in cell therapies; thus hAEC have been favoured instead of HLC. Encapsulated HLC are far more functionally adept and their gene expression profile similar to hepatocytes relative to non-encapsulated HLC.

Encapsulation of HLC creates a 3D environment that enhances gene expression and metabolic functions. Encapsulated HLC could be used for drug screening assays *in-vitro*, which could be used in high throughput drug discovery and toxicity assays (27). This would make it cost effective and speed up new drug discoveries. Encapsulation of HLC also creates an immunological barrier that prevents the host immune system from attacking the HLC. Thus, encapsulated HLC could be used as cell therapy for acute and chronic liver diseases where they would perform some hepatic functions. Encapsulated HLC can be transplanted into the extra peritoneal cavity which is well vascularised to nourish encapsulated HLC with oxygen and nutrients. The drugs and toxins are able to enter the capsule and metabolic waste can be excreted from the pores of the capsules. Using encapsulated HLC for cell transplantation is a realistic approach for patients that need liver support. The encapsulated HLC can be injected into the body using a 14 gauge catheter. In a pilot study, encapsulated HLC could be transplanted into the peritoneal cavity of mice and survive for up to 10 days.

Transplantation of encapsulated islet cells has been trialled in humans as a way of immune protection from the host immune system (28).

Differentiated HLC are unable to modulate their mtDNA copy number due to high DNA methylation at exon 2 of POLGA. Besides expressing high levels of genes associated with pluripotency and oncogenicity, hAEC did not form tumours. This may be advantageous from a clinical perspective, that transplantation of these cells does not risk induction of tumours. Analysis of RNAseq data provides a gene signature of differentiated HLC and shows how closely aligned they are to hepatocytes. In addition, network and pathways analysis of encapsulated HLC shows significant improvement in metabolic function and the gene expression. RNAseq data provides the blue print for comparison of different cell types into the hepatic lineage and provides a direct comparisons tool. My studies lay the foundations for use of HLC for both the basic understanding of cell fate and lineage commitment as well as their use in the clinical setting.

6.3 Future Perspectives

I evaluated functional characteristics of HLC and showed they could breakdown cholesterol, bile acid synthesis, drug metabolism and urea synthesis. However, when I compared functional aspects of HLC to the hepatocellular carcinoma cell line HepG2, the functional output was significantly lower. Functional aspects of HLC need to be compared to human hepatocytes for their true indication of functional output. The metabolic functional capacity of hAEC derived HLC does not quite reach those observed in human hepatocytes as previously reported. Evaluation of the drug metabolism capacity could also be expanded further than CYP3A4. A better guide might be to compare metabolic functions and gene expression levels to human hepatocytes. This may give a true indication of their capacity to perform hepatic functions and their suitability for use in cell transplantation.

Alternate ways need to be explored to modulate mtDNA copy number in differentiated HLC. Increased mtDNA copy number is critical to ATP generation and has an eventual significant impact on metabolic function and cell polarity. If mtDNA can be modulated in HLC, this may result in increased function and hepatic gene expression. Modulation of mtDNA is critical in differentiation of any cell type to reach maximum capacity for energy generation. If mtDNA copy number can be reached at levels observed *in vivo*, that would result in efficient cell function. Use of 5-aza as a demethylation agent causes genome wide demethylation. Though 5-aza targets and demethylates CpG islands (29), Vitamin C targets CpG shores (30); however, there are no compounds available to target specific genes. Demethylation of specific gene regions (POLGA) may prove to be the key turning point for modulation of mtDNA copy number.

Encapsulation is a novel way of immune protection for the transplanted cells from the host immune system. Barium alginate encapsulation is widely used; however, the capsule material

produces a foreign body response that results in over growth of host cells around the capsule. The result is lack of nutrients and oxygen to the cells within the capsule resulting in cell death. The foreign body response can be significantly reduced by using a purer grade of alginate (31). Addition of other materials can also be trialled to evaluate if that results in reduced foreign body response. More recently, addition of growth factors and cell surface molecules onto biomaterial scaffolds has been achieved (32). Addition of growth factors such as HGF to the capsules may enhance their HLC differentiation potential and improve functional parameters.

In vitro cell culture often tries to mimic *in vivo* conditions to derive functional cells. Due to the complexity of the liver, there are various other supporting cell types besides hepatocytes. The critical supporting cell types are Kupffer cells, endothelial cells and stellate cells. These cells secrete factors and extracellular matrix that provide appropriate signalling for hepatocyte functions. Recent studies demonstrated enhanced HLC differentiation and hepatic function of embryonic stem cells when co-cultured with endothelial / stellate cells (33, 34). Co-culture and differentiation of HLC with supporting cells in different combinations and ratios may enhance their metabolic functions. Encapsulation of stellate cells with HLC may also increase deposition of the extracellular matrix, which is known to enhance hepatic functions.

My study demonstrates that functional HLC can be derived from hAEC, however, they fail to regulate their mtDNA copy number and become immunogenic. HLC can be encapsulated and exhibit enhanced functional characteristics and less immunogenic gene signature. Thus, HLC differentiation can be enhanced with encapsulation, which also provides immuno-isolation.

6.4 References

1. Moodley Y, Ilancheran S, Samuel C, Vaghjiani V, Atienza D, Williams ED, et al. Human amnion epithelial cell transplantation abrogates lung fibrosis and augments repair. *American journal of respiratory and critical care medicine*. 2010;182(5):643-51.
2. Pratama G, Vaghjiani V, Tee JY, Liu YH, Chan J, Tan C, et al. Changes in culture expanded human amniotic epithelial cells: implications for potential therapeutic applications. *PloS one*. 2011;6(11):e26136.
3. Cargnoni A, Gibelli L, Tosini A, Signoroni PB, Nassuato C, Arienti D, et al. Transplantation of allogeneic and xenogeneic placenta-derived cells reduces bleomycin-induced lung fibrosis. *Cell transplantation*. 2009;18(4):405-22.
4. Hodges RJ, Jenkin G, Hooper SB, Allison B, Lim R, Dickinson H, et al. Human amnion epithelial cells reduce ventilation-induced preterm lung injury in fetal sheep. *American journal of obstetrics and gynecology*. 2012;206(5):448 e8-15.
5. Murphy S, Lim R, Dickinson H, Acharya R, Rosli S, Jenkin G, et al. Human amnion epithelial cells prevent bleomycin-induced lung injury and preserve lung function. *Cell transplantation*. 2011;20(6):909-23.
6. Banas RA, Trumpower C, Bentejewski C, Marshall V, Sing G, Zeevi A. Immunogenicity and immunomodulatory effects of amnion-derived multipotent progenitor cells. *Human immunology*. 2008;69(6):321-8.
7. Tee JY, Vaghjiani V, Liu YH, Murthi P, Chan J, Manuelpillai U. Immunogenicity and immunomodulatory properties of hepatocyte-like cells derived from human amniotic epithelial cells. *Current stem cell research & therapy*. 2013;8(1):91-9.
8. Wolbank S, Peterbauer A, Fahrner M, Hennerbichler S, van Griensven M, Stadler G, et al. Dose-dependent immunomodulatory effect of human stem cells from amniotic

membrane: a comparison with human mesenchymal stem cells from adipose tissue. *Tissue engineering*. 2007;13(6):1173-83.

9. Ilancheran S, Moodley Y, Manuelpillai U. Human fetal membranes: a source of stem cells for tissue regeneration and repair? *Placenta*. 2009;30(1):2-10.

10. Ilancheran S, Michalska A, Peh G, Wallace EM, Pera M, Manuelpillai U. Stem cells derived from human fetal membranes display multilineage differentiation potential. *Biology of reproduction*. 2007;77(3):577-88.

11. Miki T, Lehmann T, Cai H, Stolz DB, Strom SC. Stem cell characteristics of amniotic epithelial cells. *Stem cells*. 2005;23(10):1549-59.

12. Parolini O, Alviano F, Bagnara GP, Bilic G, Buhring HJ, Evangelista M, et al. Concise review: isolation and characterization of cells from human term placenta: outcome of the first international Workshop on Placenta Derived Stem Cells. *Stem cells*. 2008;26(2):300-11.

13. Takashima S, Ise H, Zhao P, Akaike T, Nikaido T. Human amniotic epithelial cells possess hepatocyte-like characteristics and functions. *Cell structure and function*. 2004;29(3):73-84.

14. Marongiu F, Gramignoli R, Dorko K, Miki T, Ranade AR, Paola Serra M, et al. Hepatic differentiation of amniotic epithelial cells. *Hepatology*. 2011;53(5):1719-29.

15. Miki T, Marongiu F, Ellis EC, Dorko K, Mitamura K, Ranade A, et al. Production of hepatocyte-like cells from human amnion. *Methods in molecular biology*. 2009;481:155-68.

16. Nitta M, Ku S, Brown C, Okamoto AY, Shan B. CPF: an orphan nuclear receptor that regulates liver-specific expression of the human cholesterol 7 α -hydroxylase gene. *Proceedings of the National Academy of Sciences of the United States of America*. 1999;96(12):6660-5.

17. Strautnieks SS, Bull LN, Knisely AS, Kocoshis SA, Dahl N, Arnell H, et al. A gene encoding a liver-specific ABC transporter is mutated in progressive familial intrahepatic cholestasis. *Nature genetics*. 1998;20(3):233-8.
18. El-Desoky A, Seifalian AM, Cope M, Delpy DT, Davidson BR. Experimental study of liver dysfunction evaluated by direct indocyanine green clearance using near infrared spectroscopy. *The British journal of surgery*. 1999;86(8):1005-11.
19. Simon HU, Haj-Yehia A, Levi-Schaffer F. Role of reactive oxygen species (ROS) in apoptosis induction. *Apoptosis : an international journal on programmed cell death*. 2000;5(5):415-8.
20. Tirona RG, Lee W, Leake BF, Lan LB, Cline CB, Lamba V, et al. The orphan nuclear receptor HNF4alpha determines PXR- and CAR-mediated xenobiotic induction of CYP3A4. *Nature medicine*. 2003;9(2):220-4.
21. Treyer A, Musch A. Hepatocyte polarity. *Comprehensive Physiology*. 2013;3(1):243-87.
22. Kelly RD, Mahmud A, McKenzie M, Trounce IA, St John JC. Mitochondrial DNA copy number is regulated in a tissue specific manner by DNA methylation of the nuclear-encoded DNA polymerase gamma A. *Nucleic acids research*. 2012;40(20):10124-38.
23. Lee W, Johnson J, Gough DJ, Donoghue J, Cagnone GL, Vaghjiani V, et al. Mitochondrial DNA copy number is regulated by DNA methylation and demethylation of POLGA in stem and cancer cells and their differentiated progeny. *Cell death & disease*. 2015;6:e1664.
24. Lee WT, John JS. The control of mitochondrial DNA replication during development and tumorigenesis. *Annals of the New York Academy of Sciences*. 2015;1350(1):95-106.

25. Manuelpillai U, Lourensz D, Vaghjiani V, Tchongue J, Lacey D, Tee JY, et al. Human amniotic epithelial cell transplantation induces markers of alternative macrophage activation and reduces established hepatic fibrosis. *PloS one*. 2012;7(6):e38631.
26. Manuelpillai U, Tchongue J, Lourensz D, Vaghjiani V, Samuel CS, Liu A, et al. Transplantation of human amnion epithelial cells reduces hepatic fibrosis in immunocompetent CCl(4)-treated mice. *Cell transplantation*. 2010;19(9):1157-68.
27. Persidis A. High-throughput screening. *Advances in robotics and miniturization continue to accelerate drug lead identification. Nature biotechnology*. 1998;16(5):488-9.
28. Tuch BE, Keogh GW, Williams LJ, Wu W, Foster JL, Vaithilingam V, et al. Safety and viability of microencapsulated human islets transplanted into diabetic humans. *Diabetes care*. 2009;32(10):1887-9.
29. Mossman D, Kim KT, Scott RJ. Demethylation by 5-aza-2'-deoxycytidine in colorectal cancer cells targets genomic DNA whilst promoter CpG island methylation persists. *BMC cancer*. 2010;10:366.
30. Chung TL, Brena RM, Kolle G, Grimmond SM, Berman BP, Laird PW, et al. Vitamin C promotes widespread yet specific DNA demethylation of the epigenome in human embryonic stem cells. *Stem cells*. 2010;28(10):1848-55.
31. Orive G, Ponce S, Hernandez RM, Gascon AR, Igartua M, Pedraz JL. Biocompatibility of microcapsules for cell immobilization elaborated with different type of alginates. *Biomaterials*. 2002;23(18):3825-31.
32. Drury JL, Mooney DJ. Hydrogels for tissue engineering: scaffold design variables and applications. *Biomaterials*. 2003;24(24):4337-51.
33. Soto-Gutierrez A, Navarro-Alvarez N, Zhao D, Rivas-Carrillo JD, Lebkowski J, Tanaka N, et al. Differentiation of mouse embryonic stem cells to hepatocyte-like cells by co-culture with human liver nonparenchymal cell lines. *Nature protocols*. 2007;2(2):347-56.

34. Bhandari RN, Riccalton LA, Lewis AL, Fry JR, Hammond AH, Tandler SJ, et al. Liver tissue engineering: a role for co-culture systems in modifying hepatocyte function and viability. *Tissue engineering*. 2001;7(3):345-57.